AFWAL-TR-87-2049

AD-A200 442

MEGAWATT SPACE POWER CONDITIONING, DISTRIBUTION, AND CONTROL STUDY

TRW Space & Technology Group
One Space Park
Redondo Beach, Ca 90278

March 1988

Final Report for Period September 1985 to September 1987

Aero Propulsion Laboratory
Air Force Wright Aeronautical Laboratories
Air Force Systems Command
Wright-Patterson Air Force Base, Ohio 45433-6563

UNCLASSIFIED
SECURITY CLASSIFICATION OF THIS PAGE

REPORT DOCUMENTATION PAGE

Form Approved OMB No. 0704-0188

1a. REPORT SECURITY CLASSIFICATION UNCLASSIFIED	1b. RESTRICTIVE MARKINGS
2a. SECURITY CLASSIFICATION AUTHORITY	3. DISTRIBUTION/AVAILABILITY OF REPORT Approved for public release; distribution unlimited
2b. DECLASSIFICATION/DOWNGRADING SCHEDULE	
4. PERFORMING ORGANIZATION REPORT NUMBER(S) TRW Report Number: 46568-912	5. MONITORING ORGANIZATION REPORT NUMBER(S) AFWAL-TR-87-2049
6a. NAME OF PERFORMING ORGANIZATION TRW Space & Technology Group 6b. OFFICE SYMBOL (If applicable)	7a. NAME OF MONITORING ORGANIZATION Aero Propulsion Laboratory (AFWAL/POOC)
6c. ADDRESS (City, State, and ZIP Code) One Space Park Redondo Beach, CA 90278	7b. ADDRESS (City, State, and ZIP Code) Air Force Wright Aeronautical Laboratories Wright-Patterson AFB, OH 45433-6563
8a. NAME OF FUNDING/SPONSORING ORGANIZATION Aero Propulsion Laboratory 8b. OFFICE SYMBOL (If applicable) AFWAL/POOA	9. PROCUREMENT INSTRUMENT IDENTIFICATION NUMBER F33615-85-C-2571
8c. ADDRESS (City, State, and ZIP Code) Air Force Wright Aeronautical Laboratories Air Force Systems Command Wright-Patterson AFB, OH 45433	10. SOURCE OF FUNDING NUMBERS PROGRAM ELEMENT NO: 62203F; PROJECT NO: 3145; TASK NO: 23; WORK UNIT ACCESSION NO: 02

11. TITLE (Include Security Classification)

Megawatt Space Power Conditioning, Distribution, and Control Study.

12. PERSONAL AUTHOR(S)
W. T. Morgan

13a. TYPE OF REPORT	13b. TIME COVERED	14. DATE OF REPORT (Year, Month, Day)	15. PAGE COUNT
Final	FROM 9/85 TO 9/87	March 1988	189

16. SUPPLEMENTARY NOTATION
This research was partially funded by the inhouse independent research fund.

17. COSATI CODES			18. SUBJECT TERMS (Continue on reverse if necessary and identify by block number)	
FIELD	GROUP	SUB-GROUP	Power conditioning	Pulsed power
09	05		Megawatt space power	Space power
			Power processing	Spacecraft power distribution

19. ABSTRACT (Continue on reverse if necessary and identify by block number)

This study defined appropriate methodologies for conditioning, distribution, and controlling prime electrical power for megawatt level directed and kinetic energy weapons and identified mission critical and mission enabling technologies. The methodology used was:

a. Identify candidate payloads,
b. Identify candidate power sources,
c. Create a system to interconnect the source and load.
d. Estimate the weight of the system,
e. Evaluate the selected system against other candidate systems.

The key issue identified is the necessity to match the generator to the load with minimum power conditioning equipment. Every additional piece of equipment placed in the power transmission chain adds substantially to the weight. High-voltage transmission is clearly desirable, even though any terminations or exposed parts must be isolated from the space
(continued)

20. DISTRIBUTION/AVAILABILITY OF ABSTRACT	21. ABSTRACT SECURITY CLASSIFICATION
☒ UNCLASSIFIED/UNLIMITED ☐ SAME AS RPT ☐ OTIC USERS	UNCLASSIFIED
22a. NAME OF RESPONSIBLE INDIVIDUAL Mr. Jerrell M. Turner, Chief, Power Conversion Project Office	22b. TELEPHONE (Include Area Code) (513) 255-6235
	22c. OFFICE SYMBOL AFWAL/POOA

DD Form 1473, JUN 86 — Previous editions are obsolete

SECURITY CLASSIFICATION OF THIS PAGE
UNCLASSIFIED

19. Abstract Continued

plasma. Only low current (a few hundred amps or less) transmission/distribution lines lend themselves to being uncooled. Everything higher in current probably requires at least some cooling.

Development needs include either a high-voltage generator or an efficient generator/transformer combination that can produce high voltage. This latter combination requires either a high frequency generator, or a light-weight transformer, or both. All of the systems require either ac/dc converters (rectifiers) or dc/dc converters (inverter/rectifiers). Both require efficient high voltage/high current semiconductors, currently under development as MOS/bipolar devices. The thermal interfaces require substantial further study. Finally, there is a need to demonstrate such high voltage systems in an actual space environment to examine all the interaction problems that may not be evident in a paper study.

CONTENTS

CONTENTS (Continued)

CONTENTS (Continued)

FIGURES

FIGURES (Continued)

FIGURES (Continued)

TABLES

1. INTRODUCTION

Megawatt Power Conditioning, Distribution and Control (MPCDC) Systems for Directed and Kinetic Energy Weapons represent a radical departure from present space based power systems. The MPCDC systems represent a power level growth of three orders of magnitude over other space power systems that are now planned and which might be flown in this century. On the other hand, the very short operating times associated with these missions, and the possibility for synergistic thermal management involving the payload, the MPCDC system, and the power source, create opportunities, that, if pursued, might make the weight and size of the operating systems, as well as associated development tasks, much more practical. Different and improved technologies will be used to store energy aboard the spacecraft and to generate and distribute power at the multimegawatt level. The continuously operated, and massive generation and distribution equipment normally associated with ground-based systems will give way to lightweight, compact designs for space based in part on technology development only now beginning to be envisioned.

In a previous study conducted by TRW for the Air Force (Reference 1), energy storage/power generation system options were identified and studied at the conceptual level for several candidate directed energy weapon systems. The work has, to date, demonstrated that much state-of-the-art technology can, with further development, be adapted to meet these new mission requirements, and to help demonstrate their feasibility.

It has not been possible in the previous study to develop design concepts for power processing (conditioning and distribution) and control systems and components. Nevertheless, data and information from many sources indicate that this important link between the power source and the weapon payload may contribute unacceptable weight and size penalties, as well as significant development risk. This study defines appropriate procedures for conditioning, distributing, and controlling prime electrical power to help us better understand and identify critical mission enabling technologies.

The results of the study will directly benefit Air Force advanced technology planning efforts. See Section 6 for a suggested Megawatt Power Processing Technology Development Program plan.

Our earlier work demonstrated the benefits of taking an integrated systems approach to the development of conceptual designs for weapon energy storage and power generation. We have continued that approach for this study by applying our understanding of power source/weapon system concepts to the initial trades and definitions of candidate power distribution concepts. The study team examined major issues that arose, each specialist from his own perspective. During the study we were assisted by Professor A. Scott Gilmour, Jr. of the State University of New York at Buffalo. Dr. Gilmour is a nationally recognized expert in high peak and pulse power spacecraft power system applications, microwave device technology, and high power component and switch technology.

2. METHODOLOGY

The methodology used in this study was:

a. Identify candidate payloads

b. Identify candidate power sources

c. Create a system to interconnect the source and load

d. Estimate the weight of the system

e. Evaluate the selected system against other candidate systems.

2.1 Payloads. Candidate payloads have been identified in a number of reports (e.g., Ref 2). Generically, these can be summarized as follows:

2.1.1 High Voltage RF. These payloads include the Free Electron Lasers (FELs), Neutral Particle Beams, (NPBs), and High Power Microwaves (HPM), and similar devices that use RF to drive an accelerator. The tubes that produce the RF can be klystrons, klystrodes, crossed-field devices, etc. At the moment, the leading candidate is the advanced klystrode, which currently appears to be the smallest and lightest device, and is used as the reference case in this study. This does not imply an endorsement of this particular device, but simply a selection of convenience for the

study. Anticipated operating voltages range from tens of kilovolts to over 100 kV with currents in the kiloampere range.

2.1.2 Medium Voltage Capacitor Storage. The typical payload is an Electromagnetic Launcher (EML) which uses capacitor storage. Typical voltages are 8 to 12 kVdc, with currents at the kiloamp level.

2.1.3 Low Voltage Inductor Storage. This is also an EML, but with inductor storage. This is a monopulse system, with voltages in 100 to 2000 range, with currents at the megamp level.

2.1.4 Low Voltage RF. These are similar to the payloads in 1, above, but using solid-state devices instead of tubes to produce the RF. Voltages are at the 50 to 300 V level with modest currents at the block level, but with aggregate system current at the megamp level.

2.2 Power Sources. There are a number of candidate power sources (Reference 3), but generically they can be categorized as follows:

2.2.1 Alternating Current (ac) Devices. These are all turbine-generator machines, which can be driven by any number of systems ranging from straight combustion devices to nuclear reactors. In this study, the system starts at the generator, and ignores the heat source and the prime mover. Generator types range from conventional to superconducting rotor, disk generator, homopolar, compulsator, etc. This study focuses on the desired output characteristics, not the mechanization of the design to achieve the end results. The results of the study indicate the need for development of at least one of the following:

a. A very high voltage unit (~60kV line-to-neutral), 3-phase, with frequency in the 1000 to 2000 Hz range. Such a generator would permit going directly to 140 kV dc to run the high-voltage tubes described in Paragraph 2.1.1 without the need for transformers.

b. A very high frequency unit (~10kHz), 3 phase, with voltage in the 5 to 15 kV level. This would permit generating the high voltage for the tubes described in Paragraph 2.1.1 with only a modest penalty for transformation.

2.2.2 Direct Current (dc) Devices. These include magneto-hydrodynamic (MHD) systems, thermionic systems, fuel cells, and batteries. The first two, MHD and thermionic, tend to run at 3 to 10kV (dc) levels.

The batteries and fuel cells are inherently low-voltage devices, but can be series-connected to achieve voltage levels from 100 to 2000 volts. MHD and thermionic devices are likely to be centrally located and of large size, while fuel cells and batteries can be locally mounted and grouped to fit individual smaller loads.

2.3 Systems. Table 2-1 summarizes the above listing of payloads and sources. This study demonstrates the various ways that the source and payload can be connected together, and evaluates the candidate systems thus designed. Figure 2-1 shows such a source-payload topology map, using the payloads described in Paragraph 2.1 in the middle, and the sources described in Paragraph 2.2 on either side, the AC sources on the left, and the DC sources on the right. Figure 2-1 shows that there are only a limited number of interesting options, which are described in detail in Section V. Table 2-2 shows the most favorable systems, weight-wise, for the various loads. Each of these systems is shown in Figures 2-2 through 2-8, and they are briefly described in the following paragraphs.

2.3.1 Very High Voltage (VHF) Systems. Two very interesting systems emerged from the study. The first, shown in Figure 2-2, utilizes a very high voltage generator (about 60 kV line-to-neutral) to provide a transmission voltage of 105 kV line-to-line. When rectified in a three-phase full-wave rectifier, this becomes 140 kV dc (Eac = 0.74 Edc) (Reference 4). Note that very high voltage is critical to achieving high power output in klystrode-type devices (Section 2). The attraction of this system is that it eliminates a heavy step-up transformer, at the expense of designing a very high voltage generator, whose feasibility remains to be established. Also note that this system does not encompass elaborate regulation schemes. It assumes that the klystrode can be regulated by modulating the RF drive. Because of the high transmission voltage (thus low amperage), the transmission line can be uncooled copper or aluminum. The study also shows that it doesn't matter if the rectifier is put at the load end of the transmission line or placed at the generator end and the power transmitted as dc. Either way, the weights turn out about the same. Note that the generator must operate ungrounded since the system ground is

Table 2-1. Source Payload Comparison

Power Generation					Transmission and Distribution	Payloads	
Prime Energy	Power Conversion	Location	Type of Current	Maximum Voltage		Type	Type of Current	Voltage
Combustion								
Straight ($e.g., H_2$-O_2	Turbine-Generator	Central	ac/dc	~60 kV	TBD	RF Tubes Klystrodes, Klystrons, etc.	dc (kiloamps)	50-150 kV
Seeded	MHD	Central	dc	~10 kV	TBD			
Electro-chemical	Fuel cells	Central or distributed	dc	~1000 V	TBD	Capacitor Storage	dc (kiloamps)	5-12 kV
	Batteries	Central or distributed	dc	~300 V	TBD	Inductor Storage	Monopulse (megamps)	A/R
Nuclear	Turbine-generator	Central	ac/dc	~60 kV	TBD	Solid-State RF	dc (megamps)	50-300 V
	Thermionic Thermo-electric	Central	dc	~5 kV	TBD			

Table 2-2. Lowest-Weight Systems

Case	Generator			Pre-Trans	Transmission	Post-Trans	Payload	Sp. Wt	Remarks
	Type	V	F	Power Cond.		Power Cond.		kg/kw	
VHV-4	Disk	9kV AC	10kHz	Transformer	104kV 3ϕ AC 10kHz	140kV DC Rectifier-Filter	Klystrode	0.38	Weight includes fuel and tankage for t_1 seconds burst time
VHV-5	Super-Con	60kV AC	<1kHz	None	104kV 3ϕ AC <1kHz	140 kV DC Rectifier-Filter	Klystrode	0.40	Weight includes fuel and tankage for t_1 seconds burst time
MHV-2	Super-Con	17.1kV	400Hz	None	30kV 3ϕ AC 400Hz	40kV DC Rectifier-Filter	Crossed-Fired Amplifier	0.37	Weight includes fuel and tankage for t_1 seconds burst time
EML-1	Homo-Polar	~300V	Pulsed	None	300-1000V ~1 megamp	Opening switch	Inductor-Storage EML	0.60	Weight includes fuel and tankage for t_1 seconds burst time
EML-2	MHD/ Thermal	5kV DC	-	None	5kV DC 10kA	DC-DC Converter W/tap CAGR	Capacitor-Storage EML	0.44	Weight includes fuel and tankage for t_1 seconds burst time
EML-3	T-G	10kV	TBD	None	10kV AC 3ϕ	Transformer (w/tap CAGR) Rectifier	Capacitor Storage EML	0.37	Weight includes fuel and tankage for t_1 seconds burst time
LV-2	T-G	15kV AC	<1kHz	None	15kV AC 3ϕ	Transformer Rectifier 15 KV AC/ 500 VDC	Low-Voltage RF	0.42	Weight includes fuel and tankage for t_1 seconds burst time
LV-3	Fuel Cell	500V	DC	None	None	None	Low-Voltage RF	0.26	Weight includes fuel * and tankage for t_1 seconds burst time

*(Weight does not include extra fuel and oxidizer lines instead of trans)

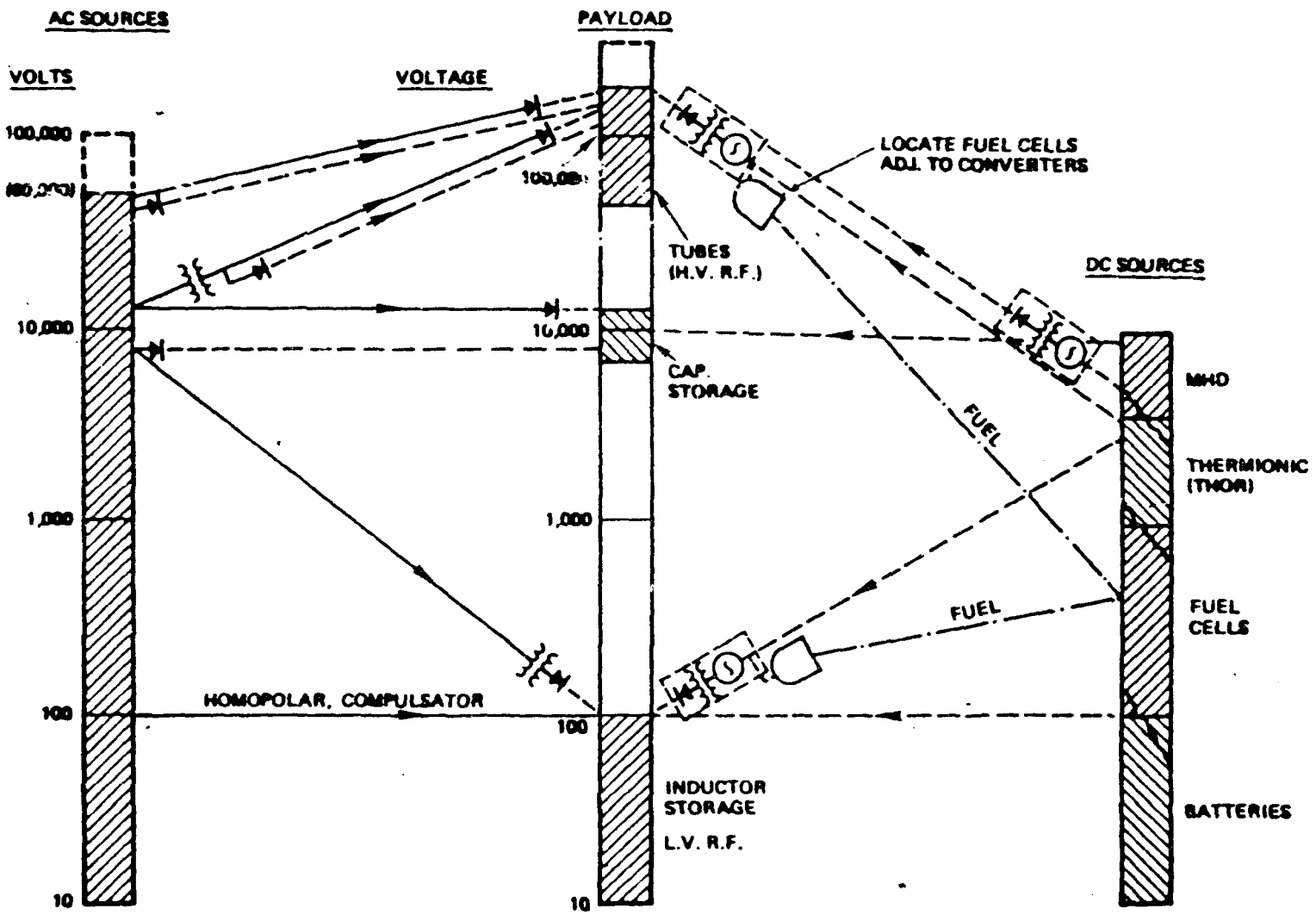

Figure 2-1. Source Payload Topology

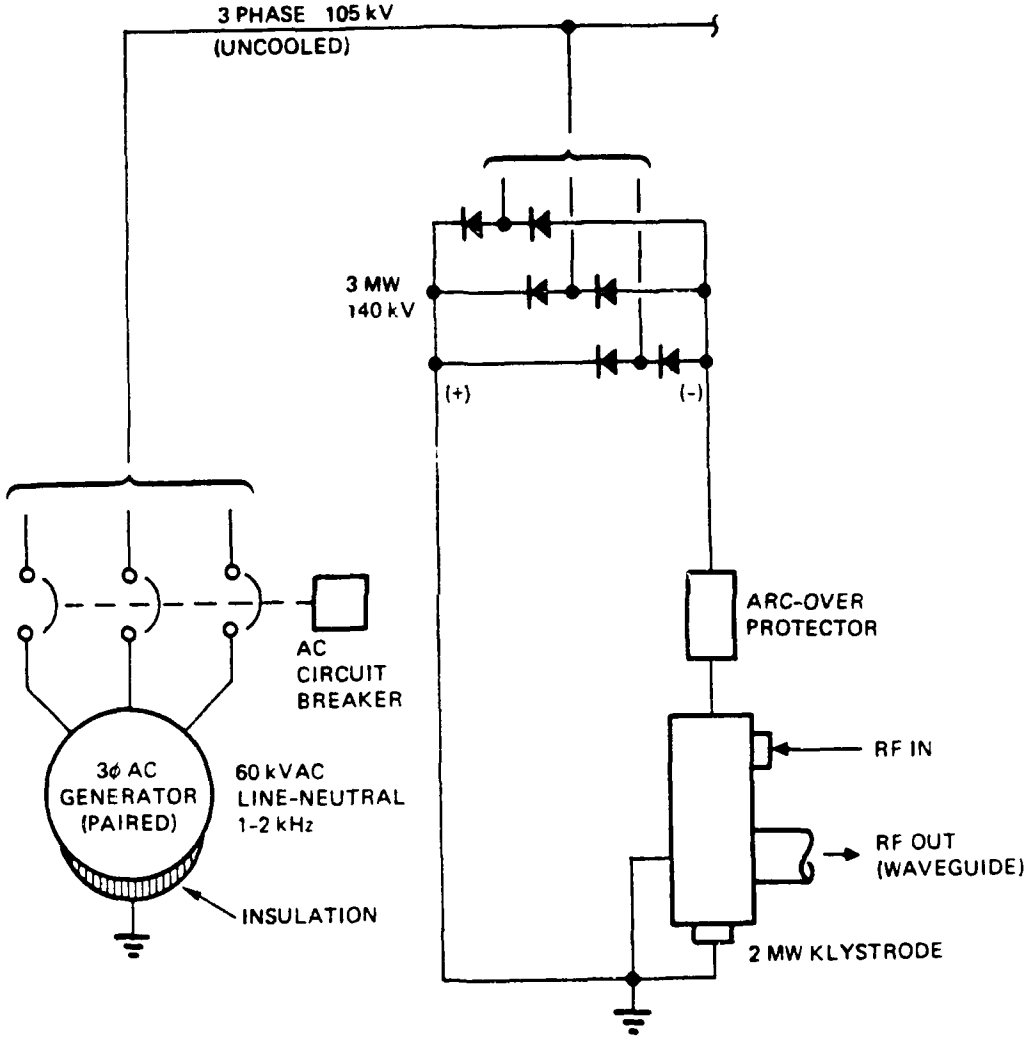

Figure 2-2. Generator-VHV RF System (A)

on the negative dc bus. The generator frequency is not critical, but should be as high as convenient (say 1.5 kHz) to minimize dc ripple.

Figure 2-3 shows an alternate system for providing the VHV dc. It assumes that the VHV generator shown above may be difficult to develop, thus requiring a transformer in the system. Although such a system could be fielded today using state-of-the-art components, the most attractive way to keep the weight down is by increasing system generated frequency. As discussed in Section 3-2, at least one vendor has expressed some confidence that a 10 kHz generator could be developed, thus reducing the transformer weight.

Consideration also must be given to the design of an ac transmission line for this relatively high frequency.

2.3.2 Medium High Voltage Systems. Figure 2-4 shows a medium high voltage system that represents state-of the-art generator technology (similar, but scaled up from the superconducting rotor machine designed by GE for AFWAL). The key to making this system really interesting for MMW systems is the development of an RF tube that will handle substantial power at these lower operating voltages. As described in Appendix A, there is some indication that newer crossed-field amplifiers (CFA or magnetrons) may fit this niche. The development of such a device would simplify generator development, while still retaining most of the advantages of high-voltage systems.

2.3.3 Capacitor Storage Electromagnetic Launch (EML) Systems. Figure 2-5 shows a typical capacitor-storage EML system (courtesy Maxwell Laboratories, Reference 5). The problem here is not to match maximum generator voltage and payload voltage, which is easily done in this case, but to match a capacitor which requires variable voltage (preferably constant current) charging with a generator that provides relatively constant output voltage. There are several ways to do such matching: Figure 2-5 shows the use of a tap-changing transformer to provide variable voltage from a constant-voltage ac transmission line. A smoothing inductor helps match the input to the load. The transformer, tap changer, and inductor add substantial weight to the system. The firing sequence is to:

1. Close circuit breaker 1 to energize all capacitor banks
2. Close c.b. number 2 to discharge capacitor number 1 through its inductor to initiate the railgun

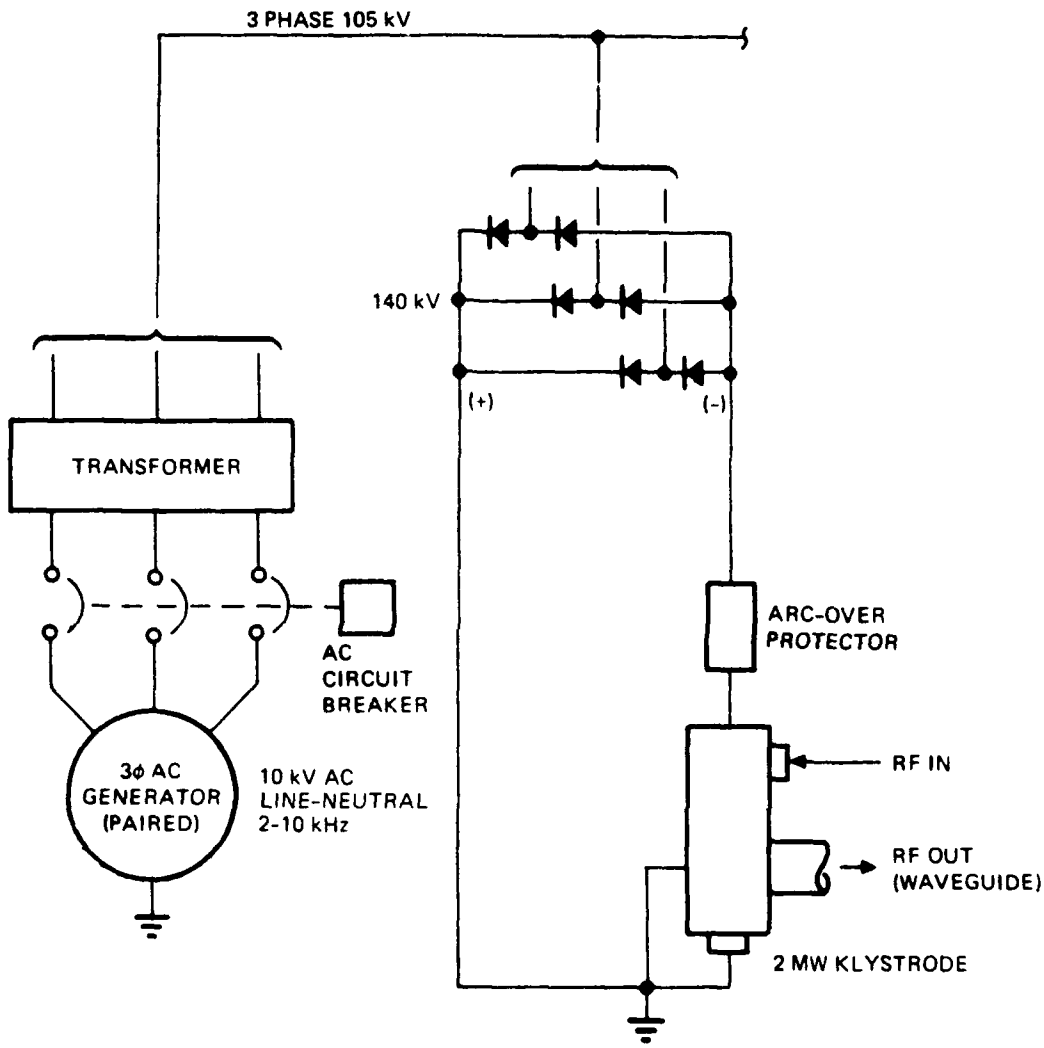

Figure 2-3. Generator VHV RF System (B)

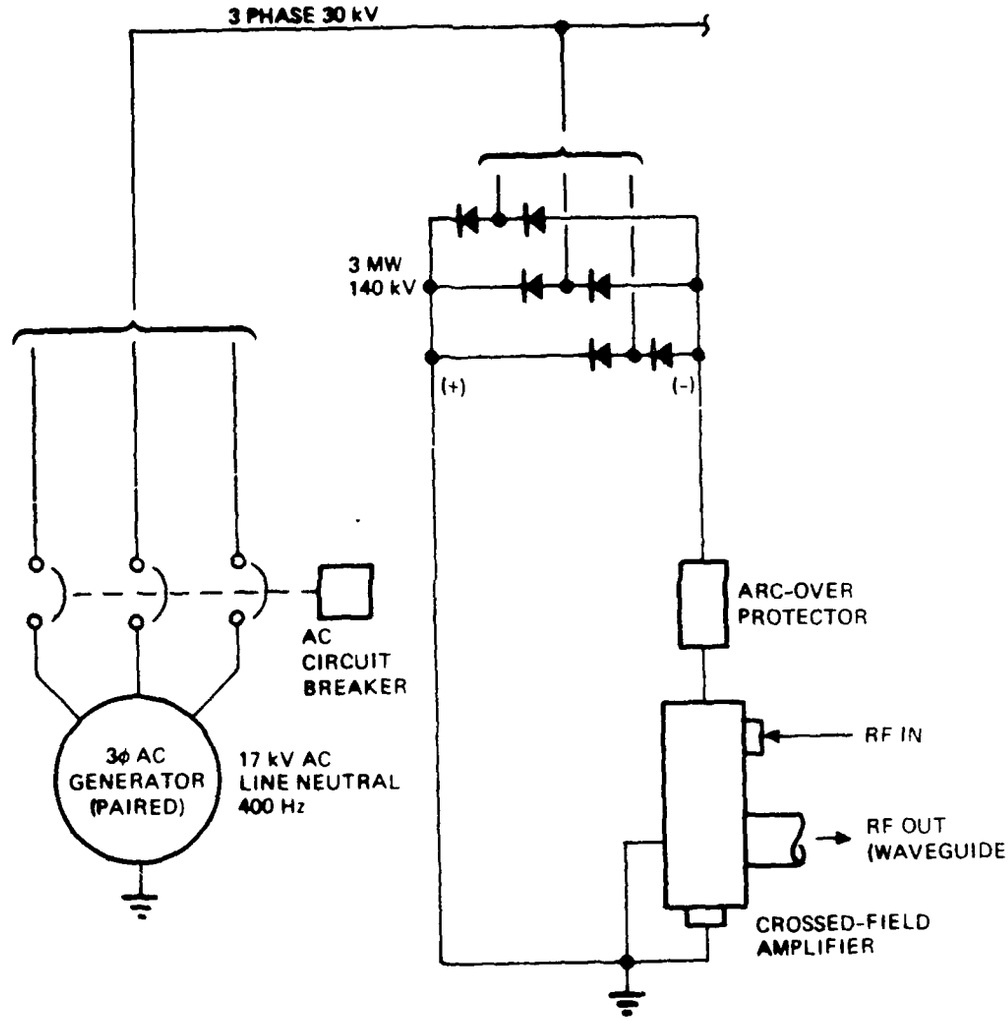

Figure 2-4. Generator MHV RF System

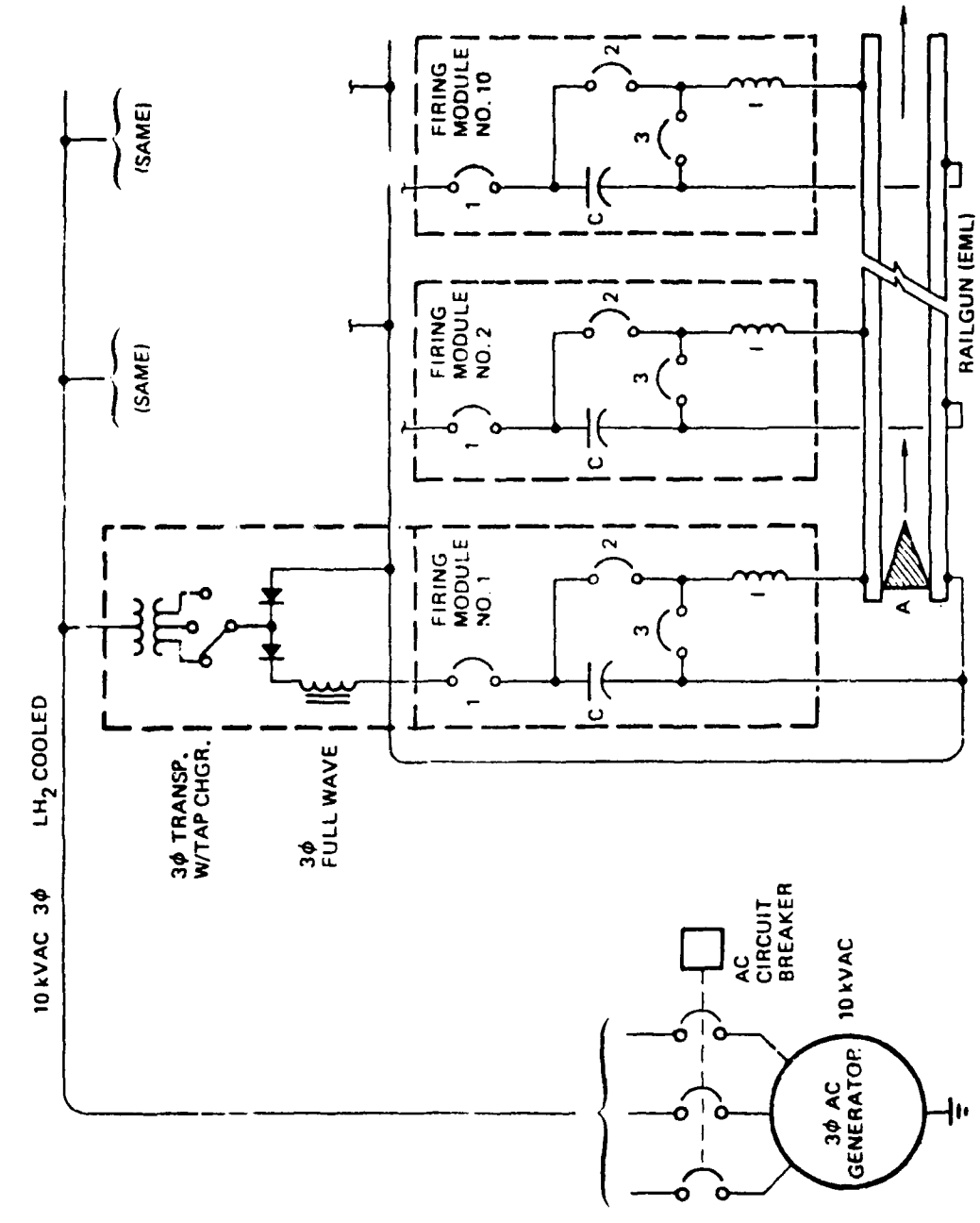

Figure 2-5. Turbogenerator-EML System

3. Close c.b. number 3 in module 1 to discharge inductor-stored energy into the railgun

4. Sequentially discharge modules 2 through n as the projectile moves down the barrel.

Figure 2-6 shows the dc version of the same system, using either a MHD generator or a thermionic generator (such as the THOR reactor, Reference 6) to provide system power. In this case, the source/load match is done with a dc/dc converter utilizing internal tap-changing on the transformer. This is even heavier than the ac system described above. There is the possibility with this system that the entire load matching device could be eliminated, since the output V-I characteristic of the generator essentially matches the capacitor charging voltage. While saving electrical system weight, this also penalizes the generator, since the entire system operates at a lower efficiency. A further trade study could be made to compare the weight of such a simple but larger system with the more complex but more efficient system.

2.3.4 Low Voltage EML Systems. Figure 2-7 shows a typical inductor-storage EML system powered by a compulsator (Courtesy University of Texas, Reference 7). A system powered by a homopolar generator would be essentially the same, except that an opening switch is required instead of a closing switch. In this system, voltage and frequency are not issues; the voltage is whatever it takes, from a few hundred to a few thousand volts, but the currents number in the megamp range. The key to this system is either to mount the generator very close to the load, or to provide a transmission line capable of handling megamp current levels.

2.3.5 Low Voltage RF Systems. RF systems have been proposed utilizing solid-state amplifiers which operate at the 50 to 300 volt dc level. Such a system requires many modules, whose aggregate current is extremely large. The fuel cell concept (Figure 2-8) looks attractive here, as the cells can be connected to provide the desired output voltage, and the cell banks can be locally mounted to reduce the current handling

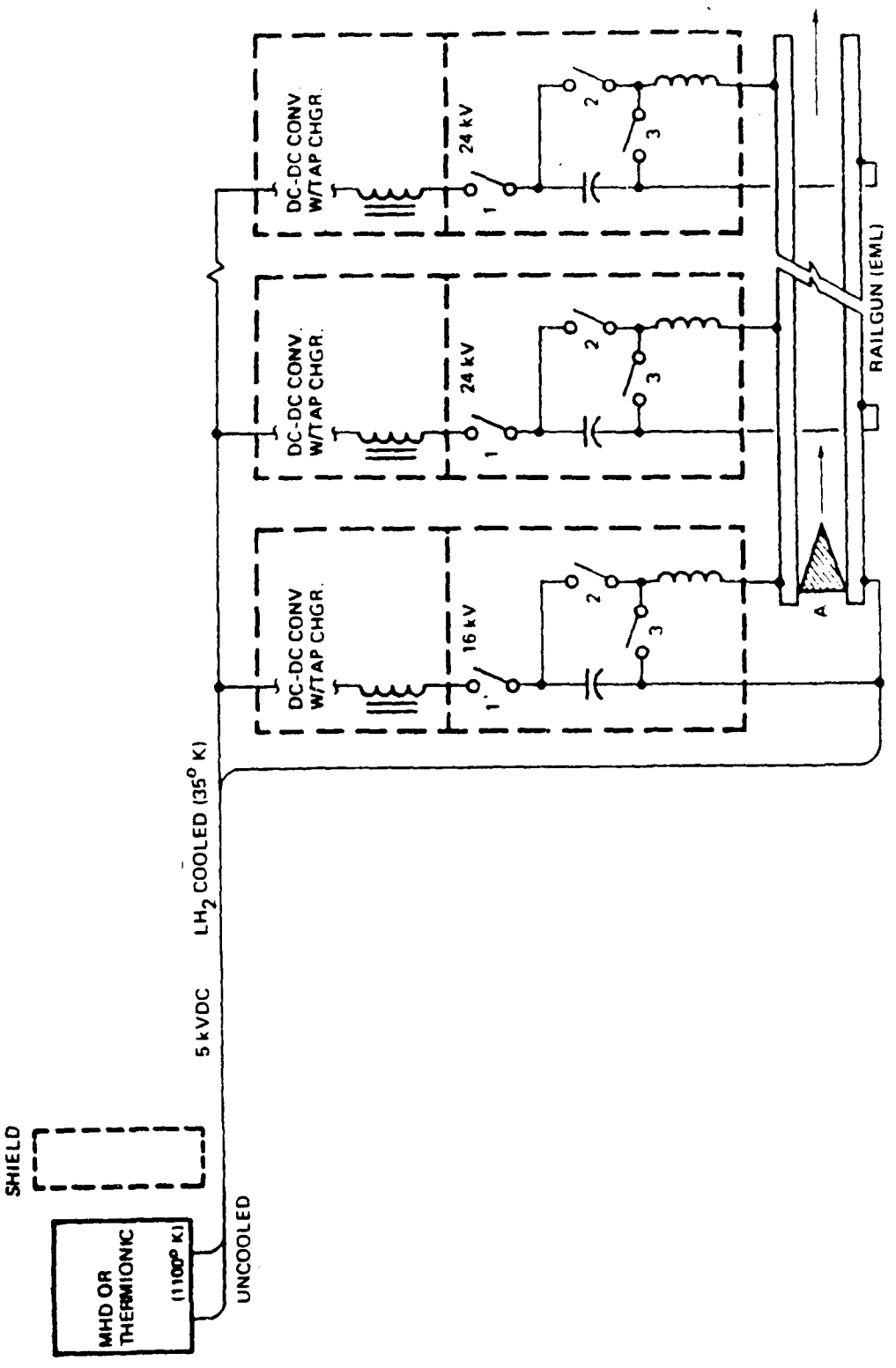

Figure 2-6. MHD/Thermionic-EML System

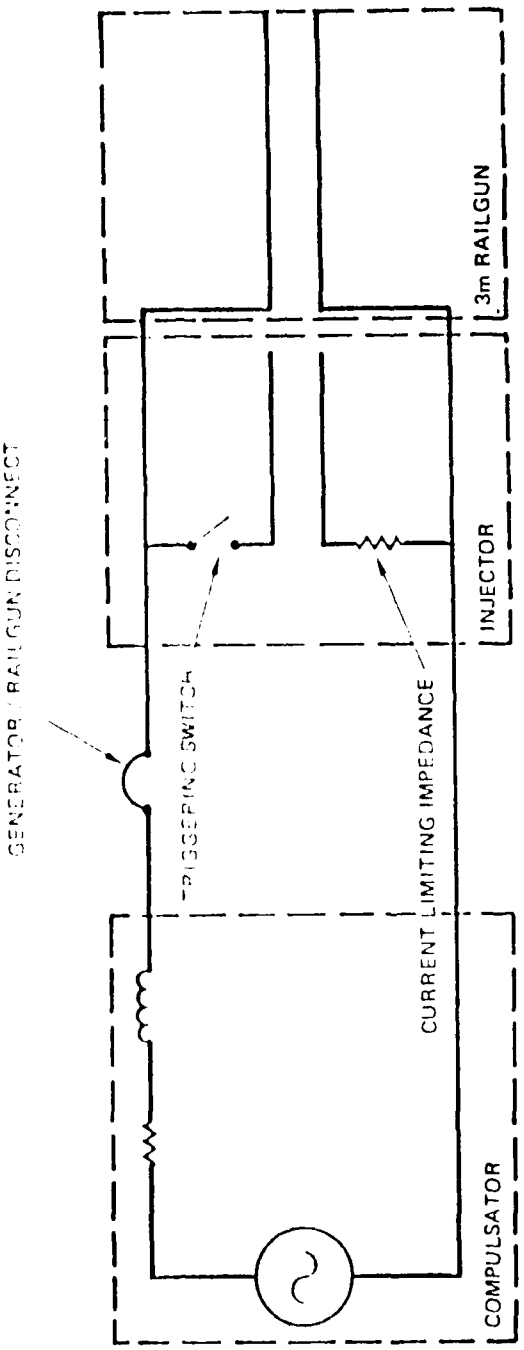

Figure 2-7. Compulsator-Driven Railgun System

problem. Note that in the high-voltage RF case described in Paragraph 2.3.1 above, although fuel cells are not the lightest weight system, they are very attractive from a redundance standpoint, since they lend themselves to easy subdivisions and replication.)

2.4 Thermal Interfaces. While the dissipation of waste heat in space vehicles has been extensively examined, this study concludes that the subject of thermal gradients at the system interfaces is a major issue also to be addressed. Figure 2-9 shows the most extreme of the cases examined, that of a THOR-type nuclear reactor driving a superconducting accelerator/FEL payload. There are three major thermal interfaces, which are discussed below:

2.4.1 Reactor Transmision Interface. The thermionic diodes of the THOR reactor are at a temperature level of about 1100 K, although the edge temperature of the mounting plates is reduced to perhaps 900 to 1000 K. This is connected by massive copper pipes to an aluminum transmission line cooled to about 35 to 50 K with liquid hydrogen for transmission efficiency. In order to prevent the system temperatures from wandering around, the concept of a "thermal anchor" is introduced. This would be an actively controlled interface device (as yet unspecified) to provide a reasonably constant temperature at some point in the interface, shown as 400 K in Figure 2-9. Initial examination of the thermal losses indicates that they are not unreasonable.

2.4.2 Transmission Converter Interface. As noted above, the desirable transmission temperature is about 50 K, while the semiconductors in the dc/dc converters prefer to remain near "room temperature," or about 350 K. This interface has not been extensively examined.

2.4.3 Klystrode Accelerator Interface. This could be a major problem, both during burst operation and during standby. During burst operation, the collector of the Klystrode is dumping approximately 20 percent of the total generated power, and will be very hot. The waveguide, connected to the klystrode output cavity (and very near the collector) connects directly to the superconducting accelerator cavity, operating at perhaps 5 to 6 K (perhaps higher in the future as new superconducting materials are developed). The waveguide, which is the size of a small air

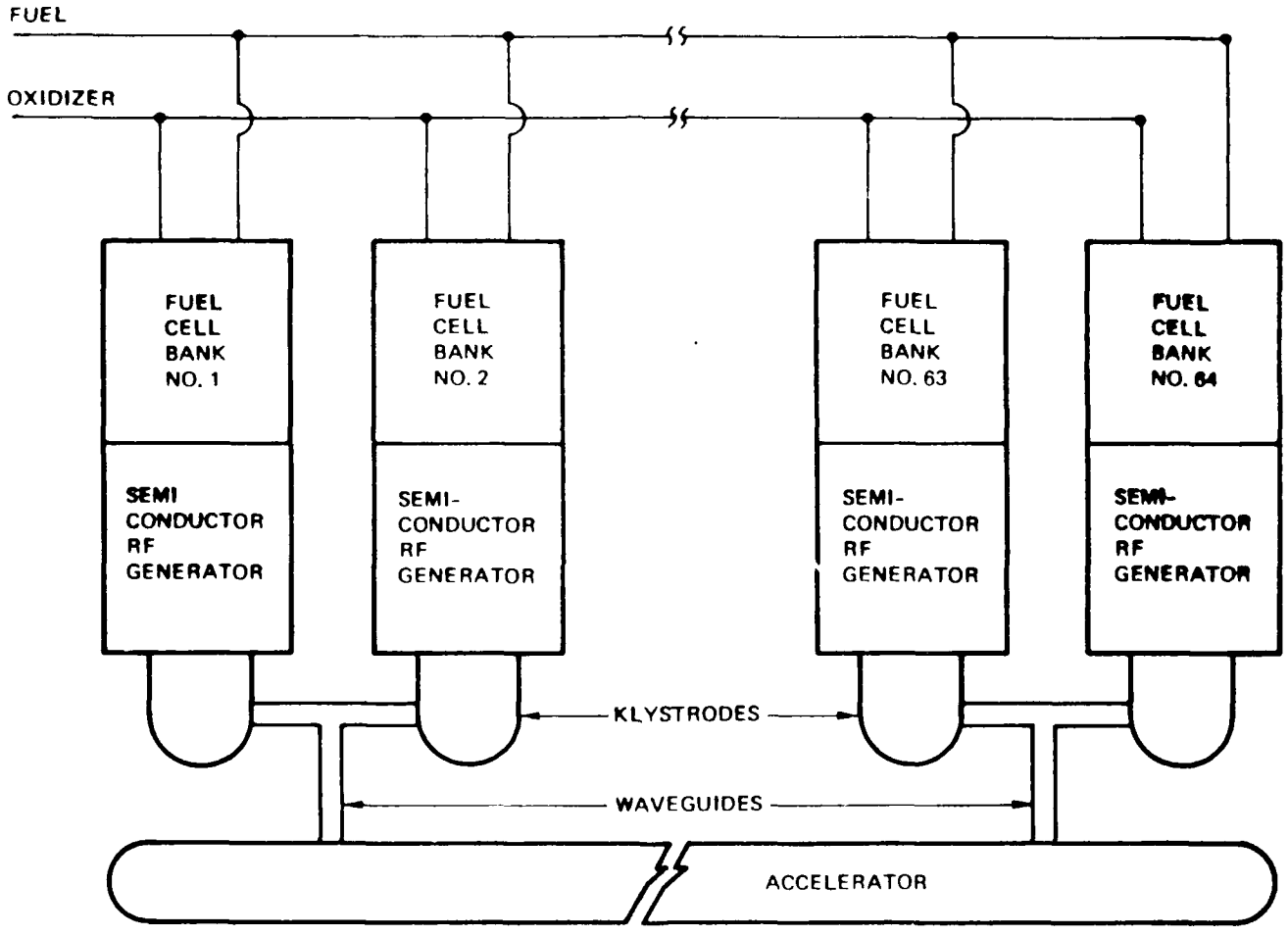

Figure 2-8. Fuel Cell - Low-Voltage RF Schematic

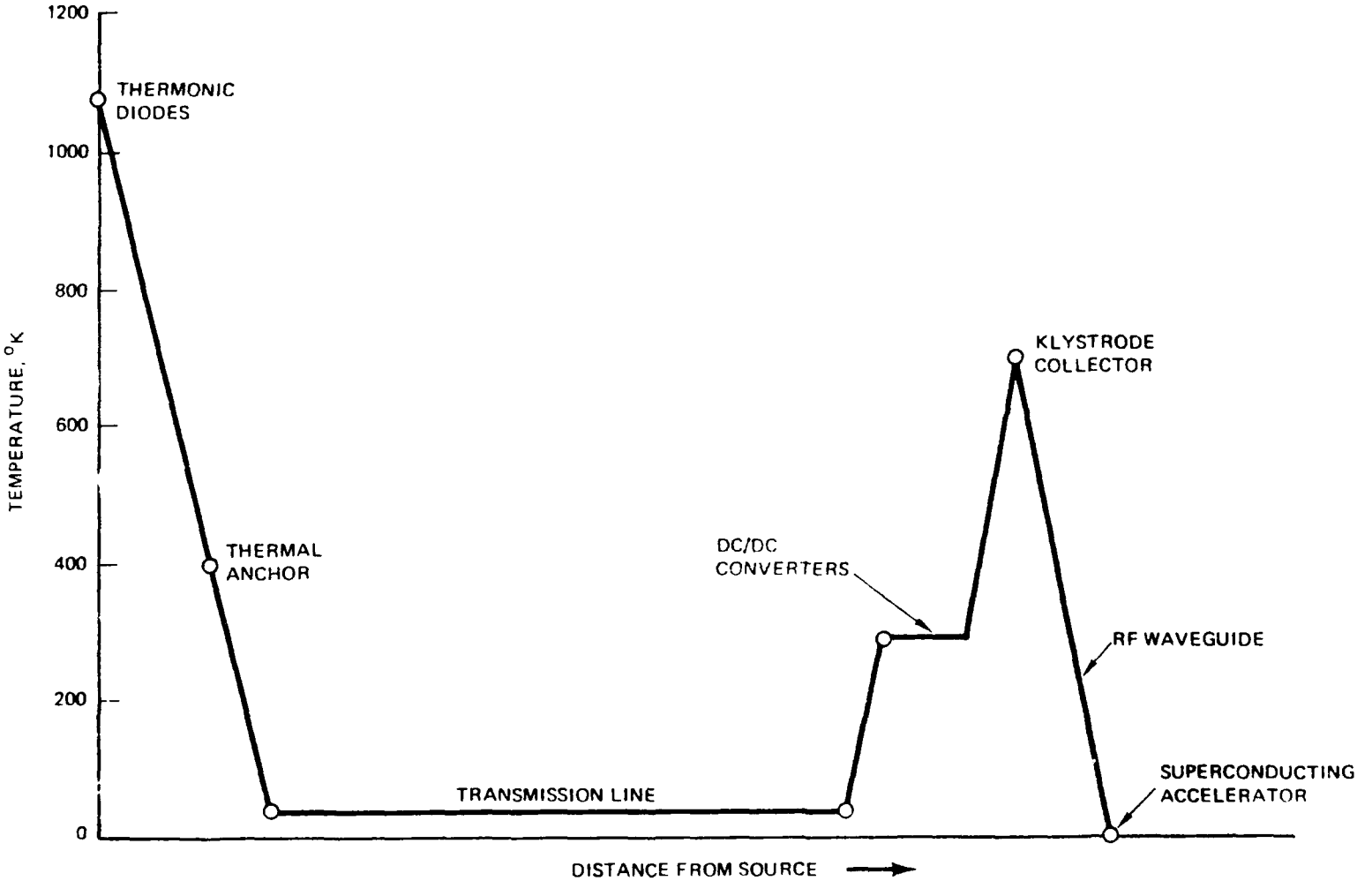

Figure 2-9. Typical Thermal Gradients (Thermionic System)

conditioning duct, represents a substantial conductive and radiative thermal path. During standby mode, with the accelerator maintained at its low temperature, thermal leaks through the waveguide may constitute an unacceptable heat loss that must be handled by the helium cryostat.

Figure 2-10 shows one method of handling the thermal loads and interfaces of such a system. Liquid hydrogen is used to buffer the helium-cooled accelerator, with the effluent hydrogen cooling the dc/dc converters. Liquid hydrogen is also used to cool the transmission line, which is envisioned to be a coaxial pipeline, with hydrogen flowing down the inside pipe, and back through the outside pipe. Since one of the major advantages of the THOR reactor system is that it has no effluents, the hydrogen is dumped into a lithium absorber after it has been used. Figure 2-10 assumes that both the klystrode collector and the "thermal anchor" are radiation-cooled. This concept is further discussed in Section 4.

Figure 2-11 shows a similar profile for a turbine-generator system. We generally assume that such a generator would be cryo-cooled, which simplifies the interface with the transmission line. The converter/klystrode/accelerator interface remains as discussed earlier.

Figure 2-12 shows the mechanization of the system shown in Figure 2-11. Since the major hydrogen user is the combustor for the turbine, the hydrogen tank is shown near the generator, where it can be pumped from a shaft-mounted pump. The hydrogen flows through/alongside the transmission line, cools the accelerator, the converters, and the klystrode collectors, and is returned to the combustor at whatever temperature is achieved during the collector cooling. This system assumes that all effluent is discharged overboard.

2.5 Summary and Development Needs. Table 2-3 summarizes the key issues, of which matching generation to load with minimum conditioning is the primary one. Every additional piece of equipment placed in the power transmission chain adds substantially to the weight. A corollary to this is that loads requiring minimal voltage regulation are highly preferred over those requiring close regulation, even at some efficiency sacrifice. High-voltage transmission is clearly desirable, even though any terminations or exposed parts must be isolated from the space plasma. The issue of cooled vs. uncooled transmission/distribution lines is clear: only

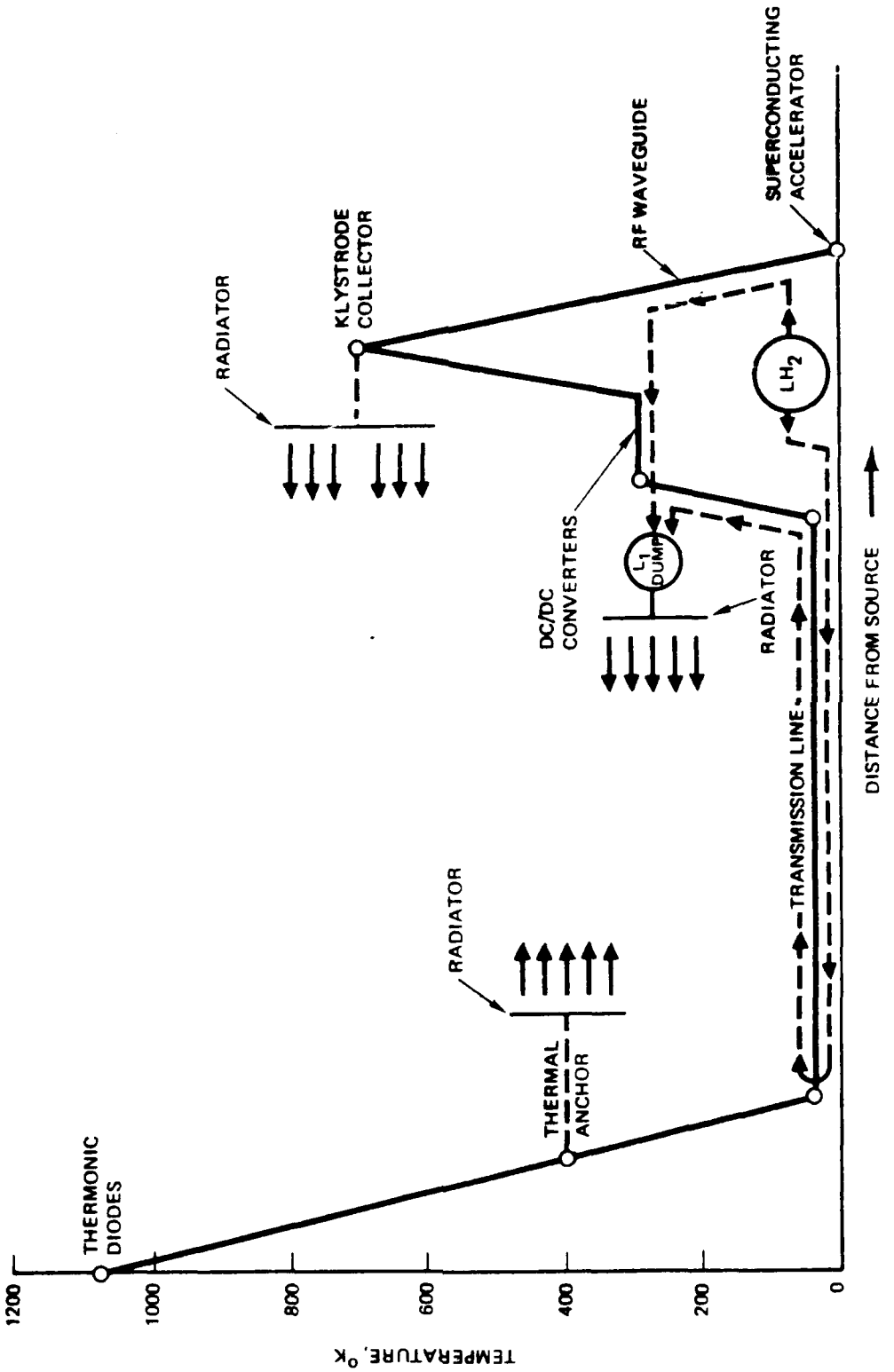

Figure 2-10. Control of Thermal Gradient (Thermionic System)

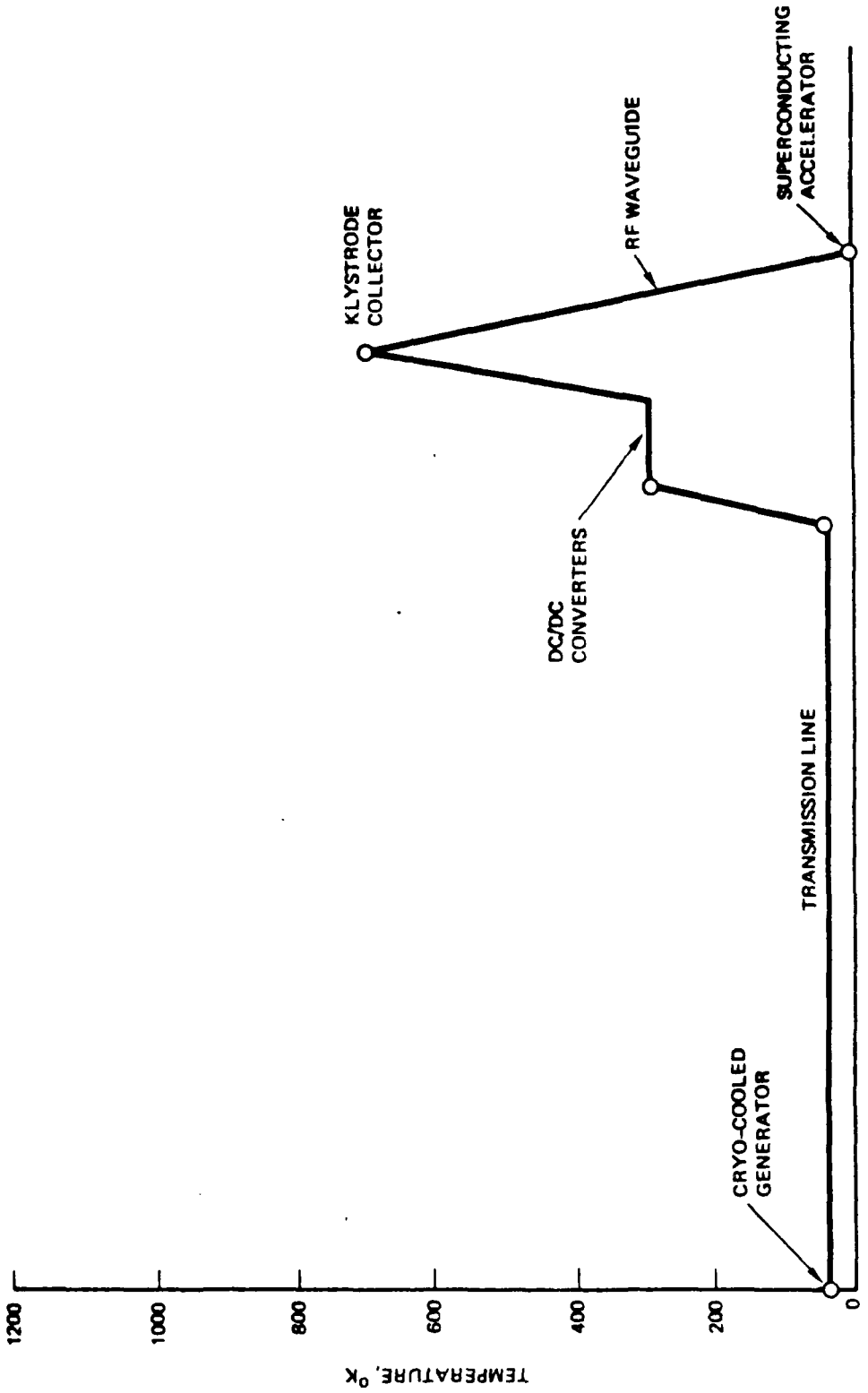

Figure 2-11. Typical Thermal Gradients (Turbine Generator System)

M2-011-88

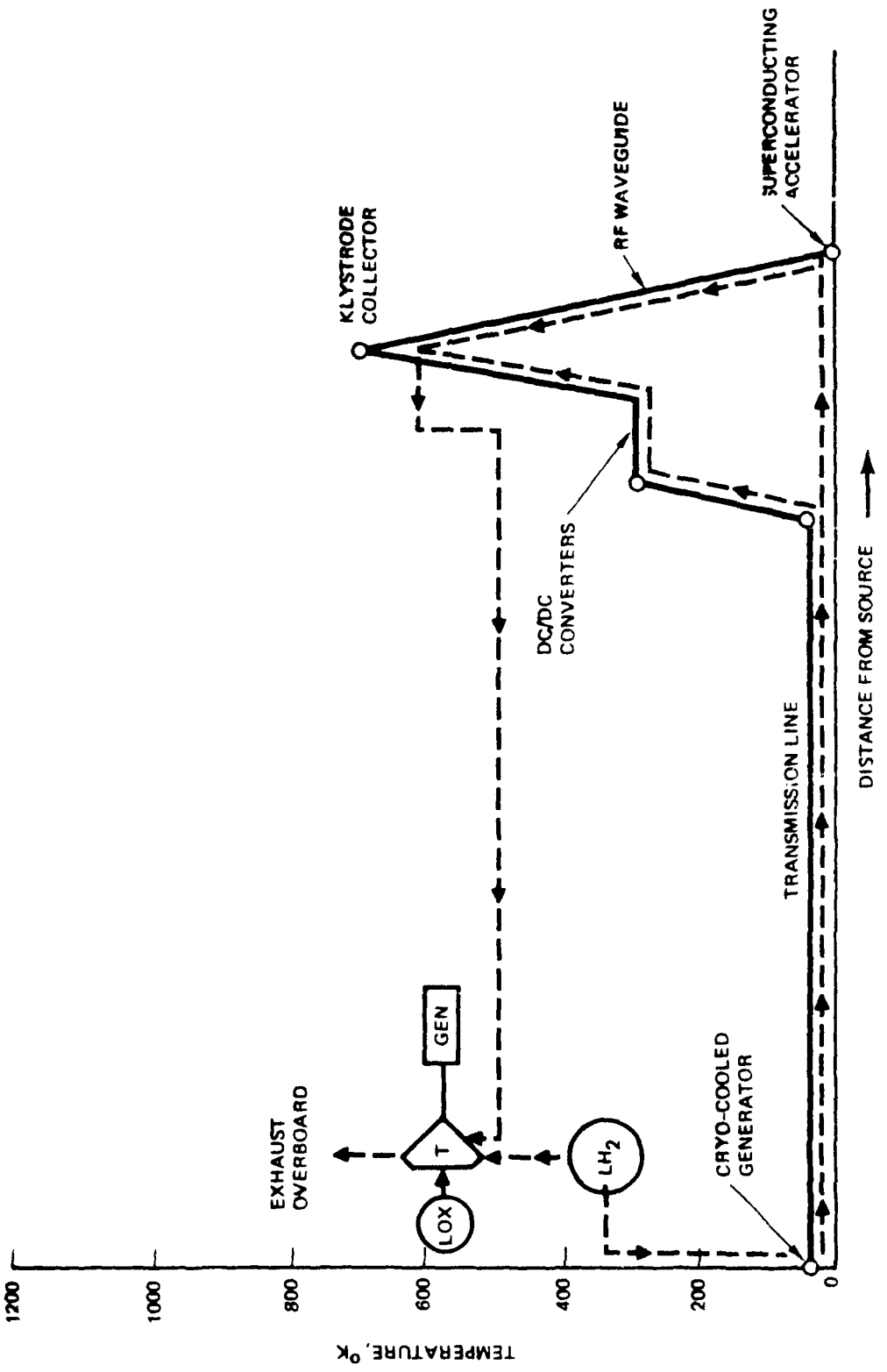

Figure 2-12. Control of Thermal Gradients (Turbine Generator System)

Table 2-3. Summary/Issues

Match generation to load with minimum conditioning
High voltage (>5 kV) desirable for transmission
Transformers undesirable (weight)
Cooled transmission lines above ~200 amps
Terminations or bare conductors must be isolated or protected from space plasma

low current lines (a few hundred amps or less) lend themselves to being uncooled. Everything higher in current probably requires at least some cooling.

Table 2-4 summarizes the principal development needs. For high voltage loads we need either a generator that can deliver very high voltage directly, or an efficient generator/transformer combination that can do the same. This latter combination requires either a high frequency generator, or a light-weight transformer, or both. All of the systems require either ac/dc converters (rectifiers) or dc/dc converters (inverter/rectifiers). Both of these require efficient high voltage/high current semiconductors, currently under development as MOS/bipolar devices. The thermal interfaces, described in Paragraph 2.4 above, require substantial further study. Finally, there is a need to demonstrate such high voltage systems in an actual space environment to examine all the interaction problems that may not be evident in a paper study.

Table 2-4. Multimegawatt Development Needs

Generators	High voltage (70 kV ℓ-n and up), high frequency (1000-2000 Hz) or Medium voltage (10-20 kV) and very high frequency (~10 kHz)
Transformers	Lower mass, high efficiency
Rectifiers/converters	Optically-switched MOS/bipolar technology
Thermal interfaces	High temperature to cryogenic transitions (power and RF)
Demonstration	Test high voltage configurations in space environment

3. STUDY VARIABLES

3.1 Payloads.

3.1.1 Radio Frequency (RF) Driven Devices. A major category of directed energy weapons (DEW), including free-electron lasers (FEL), neutral particle beams (NPB), and high power microwaves (HPM) utilize RF energy as their principal input. The FEL shown in Figure 3-1 utilizes RF at about 500 MHz to drive a LINAC-type accelerator, whose output is converted to light through a wiggler and optical resonator structure.

A neutral particle beam device is shown in Figure 3-2. Again, this device uses RF energy to drive the debuncher and DT Linac.

High power microwave devices (no figure) use RF directly, usually in the pulsed mode, as the weapon output.

Although these devices can operate in either the pulsed or continuous mode (CW), in the interest of conserving study time, only the CW mode was further considered. Also, since the technique of deriving the RF from the prime power is identical for the several weapons, they have all been lumped together in this study.

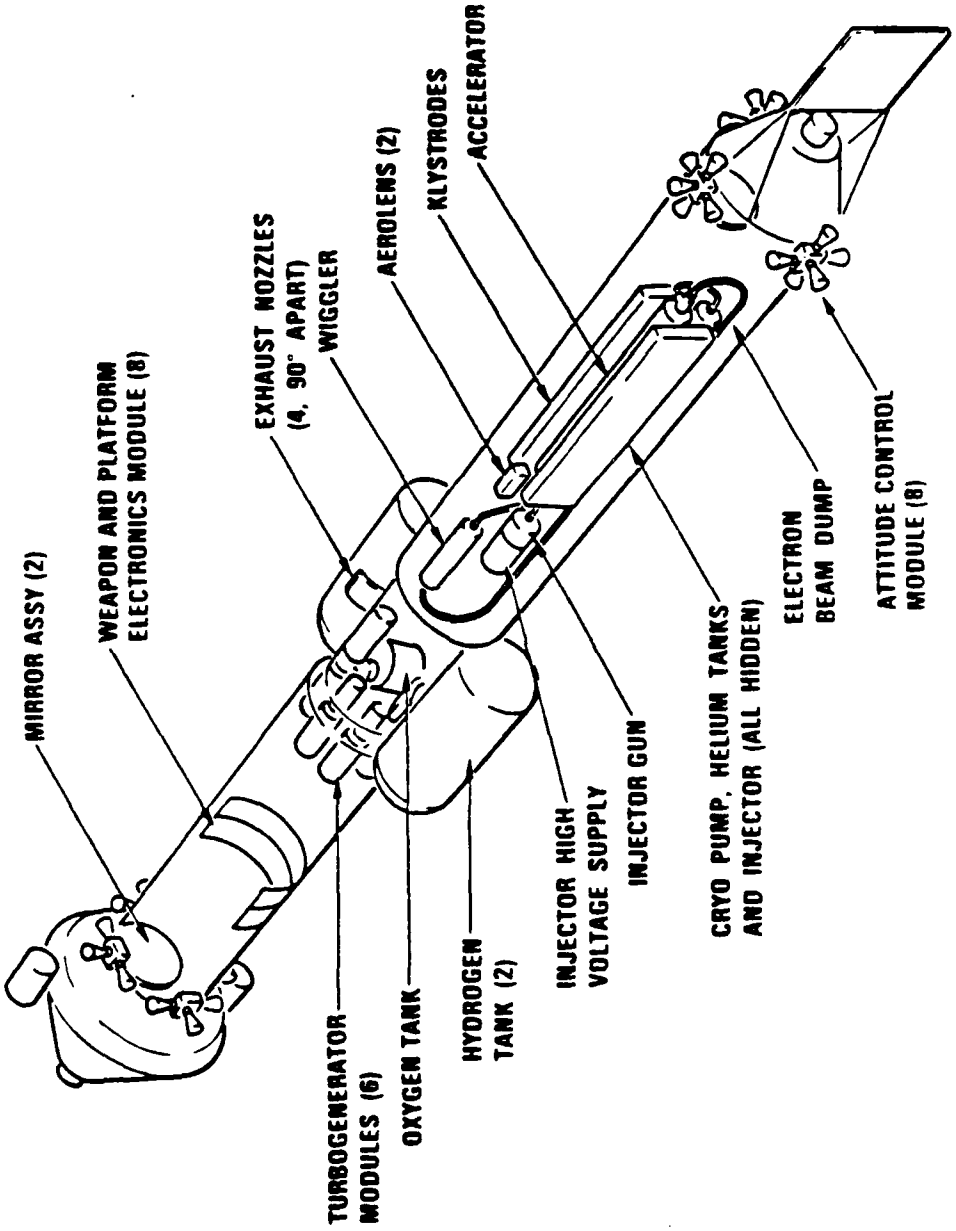

Figure 3-1. FEL Application

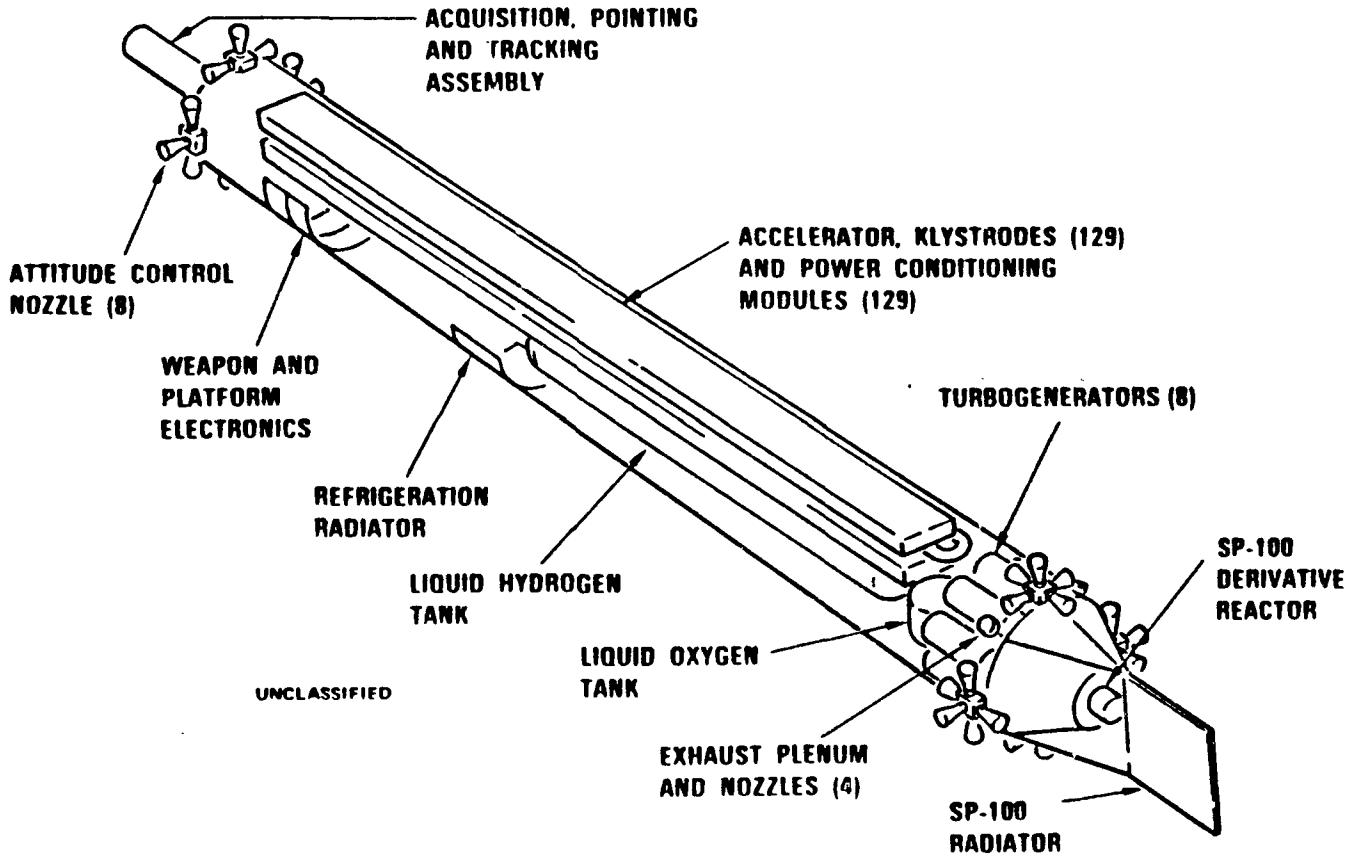

Figure 3-2. NPB Application

3.1.2 Power Distribution for DEWs. Directed energy weapons convert prime electrical power into RF power (in the 400 to 1500 megahertz range) to operate particle accelerators. There are a number of devices used to produce multimegawatt RF power, e.g., klystrons, klystrodes, crossed-field devices and semiconductors. Each of these devices convert direct current (as prime power) into RF power. Candidate power distribution approaches for these devices are illustrated in Figure 3-3.

3.1.2.1 Klystrons. (Figure 3-4) Klystrons may require multiple depressed collectors to attain high efficiency (80 percent, or more). Five to seven voltages may be required (in steps to 100 kilovolts, or so). Typical regulation for these collectors voltages is modest (perhaps 5 percent), but the acceleration electrode requires very precise regulation (a fraction of one percent) to maintain RF phase and amplitude stability in the klystron. Alternatively, phase and amplitude stability may be able to be achieved with control of the RF input signal which would permit a relaxation of the anode voltage regulation.

There are two principal approaches to power distribution for klystrons:

1a. Distribute three-phase alternating current at high voltage (in the rank of 5 to 20 kilovolts) and transform and rectify this pow er to produce direct current at multiple high voltages.

1b. Generate multiphase high voltage alternating current, tap the generator, and rectify the outputs to produce the desired direct current at the various voltages.

Approach 1a is heavy as it includes transformers at full power. However, individual rectification at each klystron provides an opportunity for fault protection with controlled rectifiers for individual klystron isolation. Approach 1b avoids the heavy transformers but entails complex generator windings (and taps) and distributes direct current at the multiple high voltage levels required by the klystron collectors. This provides simpler distribution circuitry than distributing alternating current. (Three or six alternating current conductors are required for each direct current voltage.) However, fault protection for individual klystrons will require additional very high voltage switchgear. Alternatively, it may be possible

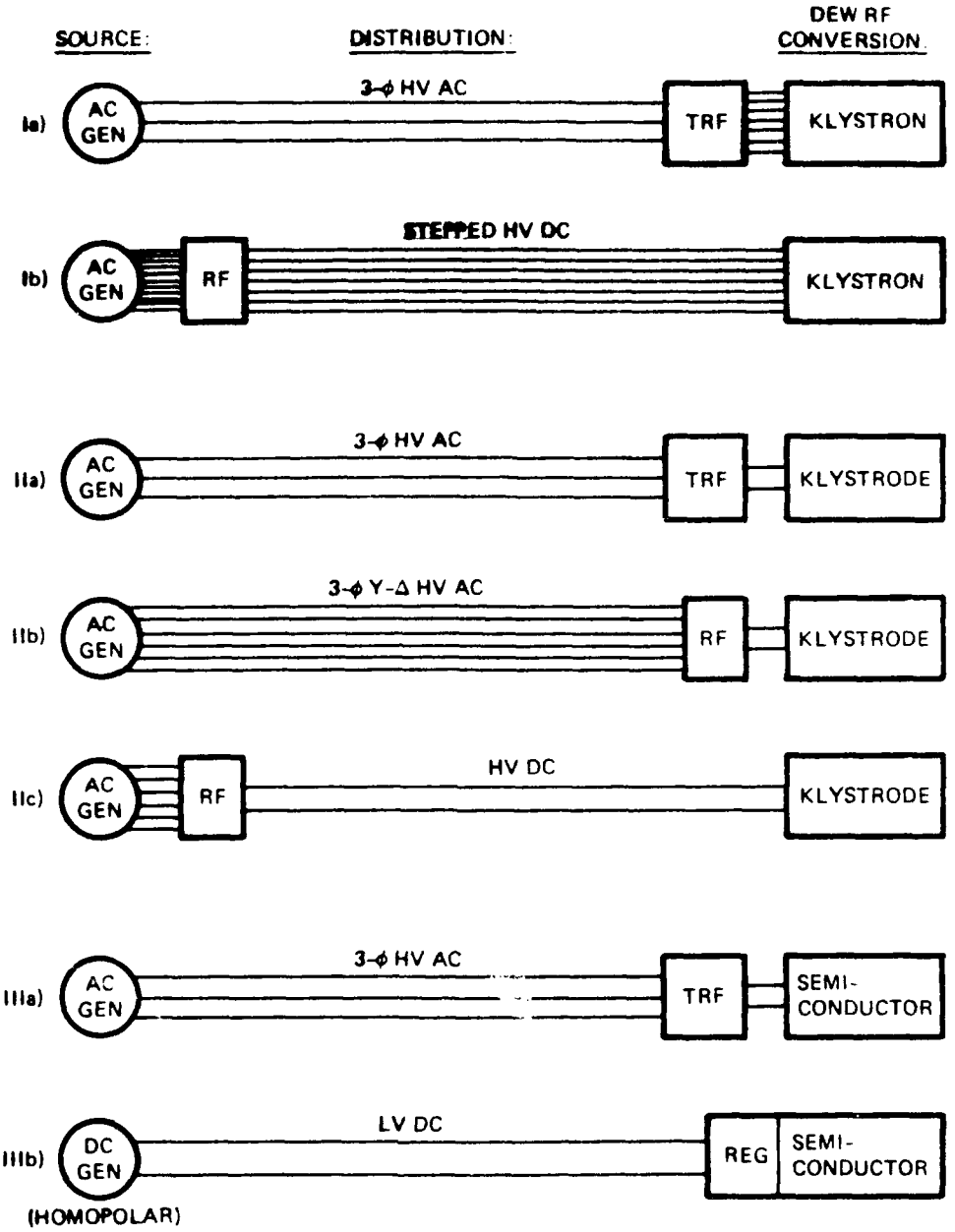

Figure 3-3. DEW Distribution Concepts

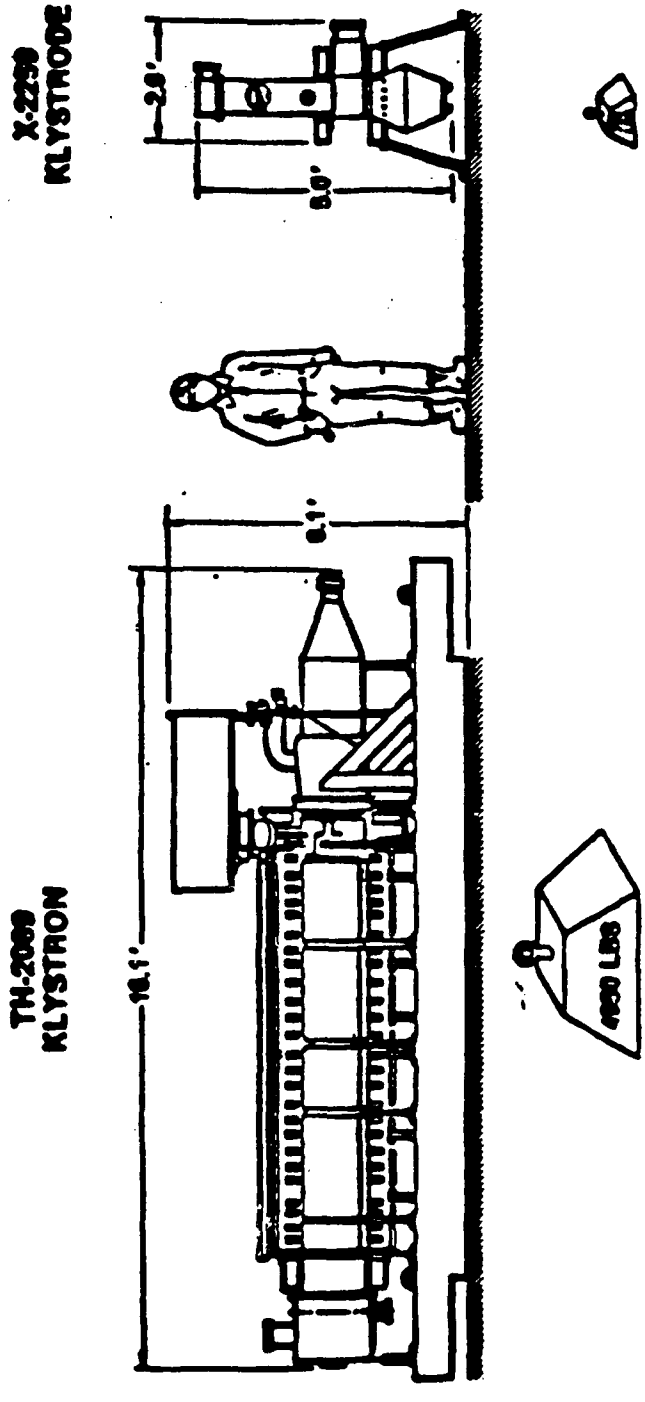

Figure 3-4. Particle Accelerator RF Energy Sources

to provide fault protection with modulating anodes in the klystrons (or in klystrodes), thus eliminating the need for much of the switchgear.

3.1.2.2 Klystrodes. (Figure 3-5), to date, have used only one collector electrode and no attempt has been made, nor has there been a detailed analysis of the possible benefits of using multistage depressed collectors. It is probable that an efficiency of at least 75 percent will be achieved with a single electrode collector. It may be possible to increase this efficiency to the 80 to 85 percent range with a multistage depressed collector, just as is the case for the klystron. Phase and amplitude stabilization may be accomplished either by precisely regulating the anode voltage or by controlling the RF drive signal.

Three candidate distribution approaches are identified in Figure 3-5. Approach 2a is similar to 1a for klystrons, includes a transformer, and is therefore heavy. Approach 2b avoids the transformer by transmitting three-phase alternating current at a very high voltage (about 50 kilovolts) with wye and delta generator output configurations. This provides good regulation upon rectification (only 3.6 percent ripple), but it requires high voltage rectifier devices (or series connected devices). Approach 2c moves the rectifiers to the generation location and distributes direct current at the klystrode collector voltage (approximately 100 kilovolts). However, fault protection for individual klystrodes may require additional very high voltage switchgear.

3.1.2.3 Semiconductors. For RF generation (~500 megahertz) semiconductors presently utilize direct current at 30 to 40 volts. Devices are being developed to utilize higher voltages, and RF semiconductors utilizing 80 to 100 volts may become practical in a decade or so. Hence, direct current at very low voltages (relatively) is required for semiconductor RF generation.

Two candidate distribution approaches are identified in Figure 3-3 for semiconductor RF generation. Approach 3a is similar to 1a and 2a; a substantial transformer-rectifier-filter (TRF) is required to change high voltage alternating current to low voltage direct current with appropriate regulation. A more appropriate generation source is the homopolar generator which provides direct current at low voltage. This approach (3b)

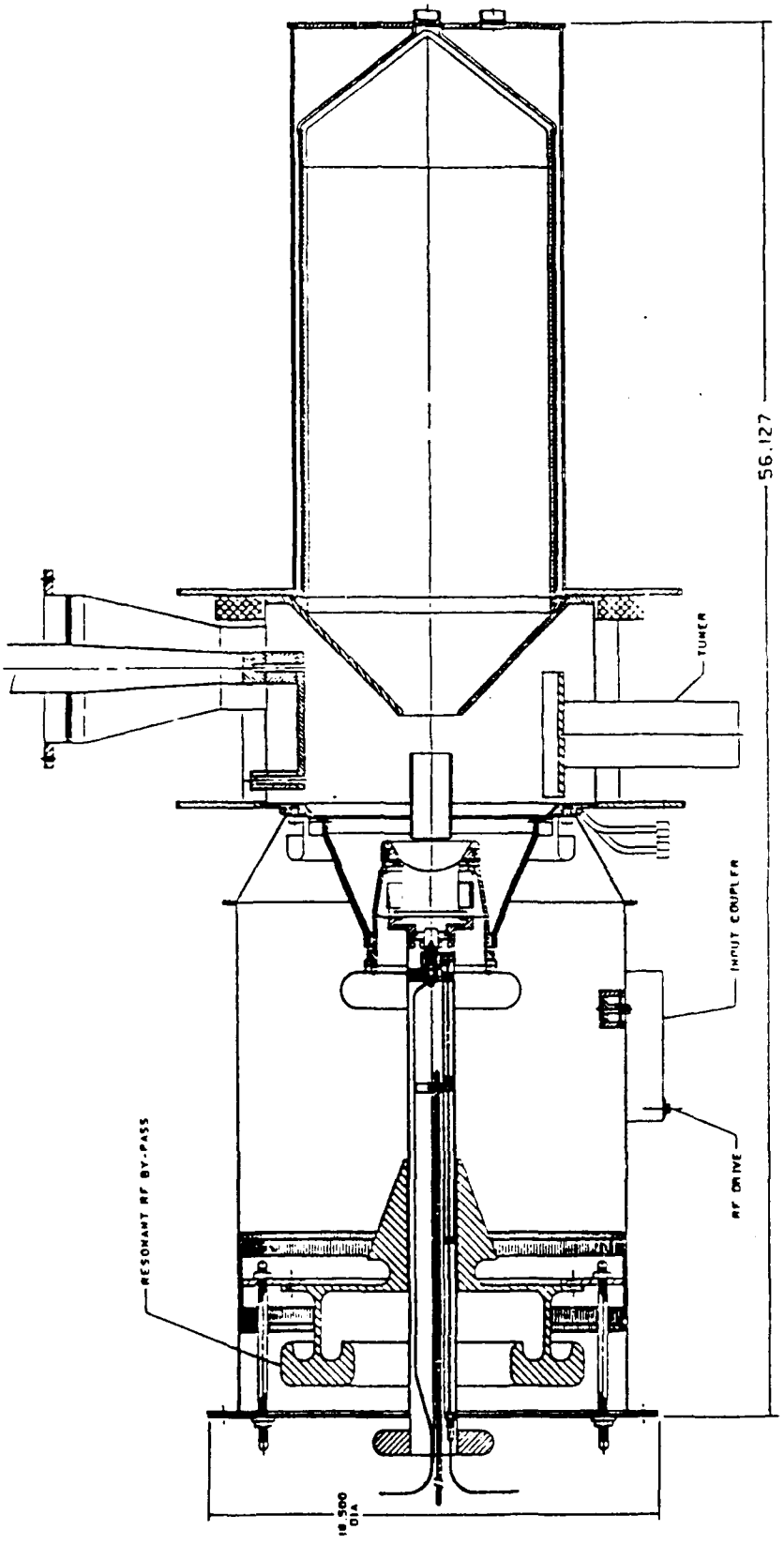

Figure 3-5. Klystrode Conceptual Design
(Courtesy Eimac Division of Varian)

provides a match of the source power form and utilization power form. However, direct current distribution at these low voltages entails multimegampere currents for multihundred megawatt power transfer. Conductor mass, losses and cooling voltage regulation and power quality, and distribution implementation to hundreds of thousands of semiconductor devices become major considerations for this approach. Fault isolation, however, may be more easily attained at local modules.

3.1.2.4 Super Audio Frequency. (10 to 40 kilohertz) will also be considered for power distribution. This approach converts the generation source power form to relatively high frequency alternating current for subsequent transformation and rectification at the utilization equipment (load). This approach may be suitable and appropriate for static generation sources that produce direct current such as thermionics, fuel cells, batteries, and magnetohydrodynamic generators.

3.1.3 Pulse-Driven Devices. The kinetic energy weapons (KEW) are driven by extremely large pulses of current, delivered from either capacitor-type storage, or inductor storage. Figure 3-6 shows a generic block diagram, while Figure 3-7 shows an inductor-storage scheme, and Figure 3-8 shows a capacitor-storage scheme. From a generation/ distribution viewpoint, these two schemes are very different; the inductor method requires high current at relatively low voltage (usually from a homopolar generator or compulsator), while the capacitor storage requires constant voltage (in the 10 kV level) with variable current during the charging cycle.

3.1.4 Kinetic Energy Projectiles. The kinetic energy weapon (KEW) hits the target with a very high velocity projectile. This energy (E) is determined by the projectile mass (Mp) and the closing velocity of the projectile onto the target (Vp -Vt, projectile velocity-target velocity):

$$E = 1/2mv^2 = 1/2\ Mp\ (Vp-Vt)^2$$

A "smart projectile" is envisioned to provide minor trajectory corrections and to home onto the target. A kilogram projectile has been estimated as the minimum mass to package this homing mechanization. In addition, up to another kilogram of propulsion consumables may be required

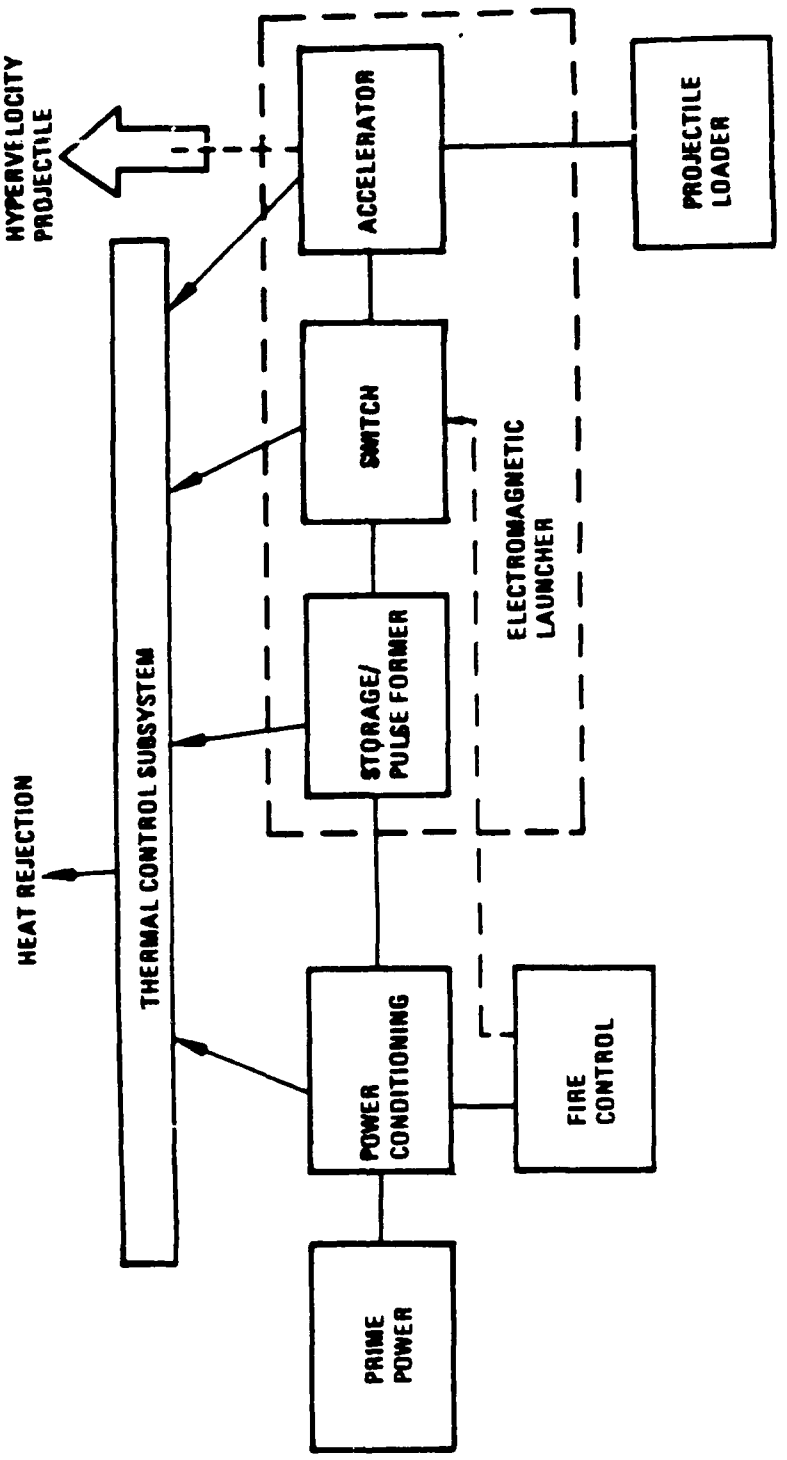

Figure 3-6. Block Diagram of EML

OPERATION OF DC EM LAUNCHER

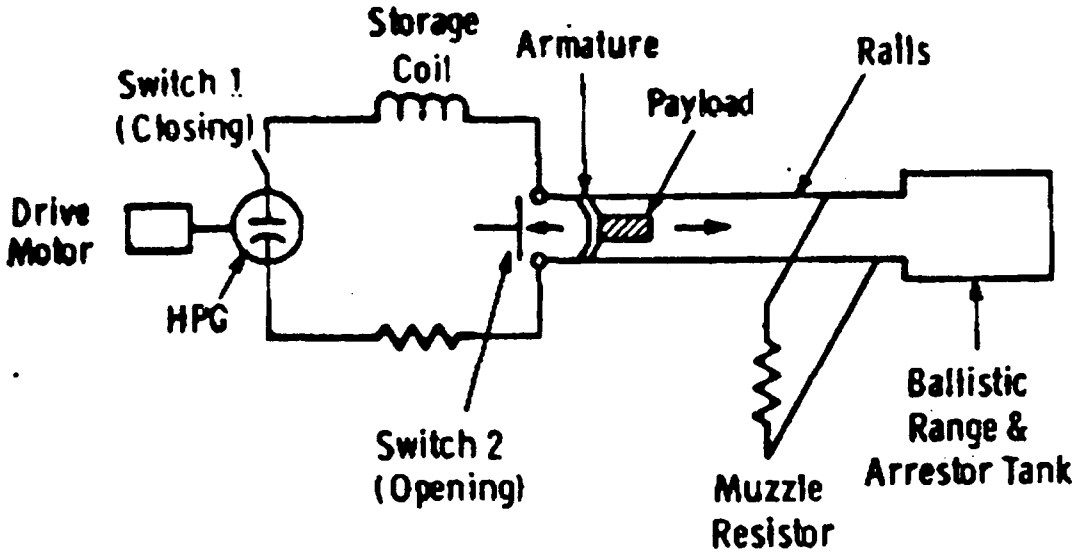

Features

- Inertial Energy Storage in HPG From Prime Mover
- Energy Compression Into Inductor During Charging By Closing Switch 1
- Opening Switch 2 Transfers Inductive Energy Into Armature and Launches Projectile
- Muzzle Resistor Dissipates Unused Stored Energy

Figure 3-7. Operation of DC EM Launcher

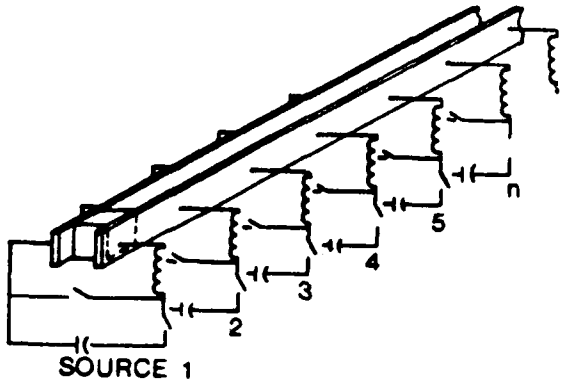

PHYSICAL ARRANGEMENT

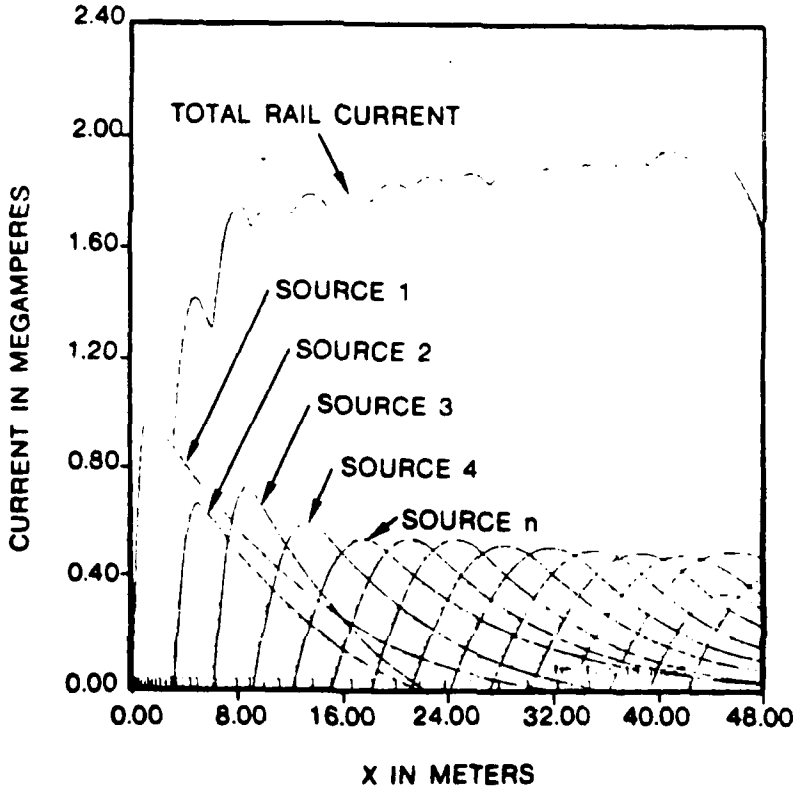

Figure 3-8. Individual Source Currents and Total Rail Current for Distributed Energy System. (Maxwell Laboratories, Inc., computer simulation)

to supply an adequate range of trajectory correction. Hence, projectiles of 1 to 2 kilograms are envisioned.

Initial projectile velocities of 10 to 20 kilometers per second are envisioned to provide adequate target closing velocities (to assure a high probability of hitting the target). These velocities typically provide more than adequate energy for target destruction (penetration of an inch or more of steel with explosive effects). The resulting initial kinetic energy imparted to a projectile is in the range of 50 to 400 megajoules (Figure 3-9).

The efficiency of a rail gun (electromagnetic launcher, EML) is projected in the range of 25 to 40 percent, with the greater efficiencies attained with the larger guns. Hence, the requirement for stored energy is the range of 150 megajoules to 1 gigajoule, or more (Figure 3-10). This energy must be imparted to the projectile in only a few milliseconds:

Velocity = acceleration x time

t = v/a = 10,000/500,000 Gs = 0.002 seconds

t = v/a = 20,000/100,000 Gs = 0.020 seconds

This rapid energy release represents a peak power pulse on the order of 50 gigawatts (or more):

150 MJ/0.002 sec = 75 GW

1000 MJ/0.020 sec = 50 GW

Very rapid discharge of electrically stored energy is required to provide this power pulse.

Maxwell Laboratories have a classified contract to develop capacitors suitable for KEW applications. One of the goals of this effort is to produce sample capacitors providing 2,000 joules per kilogram performance during 1986. Capacitor performance of 5,000 to 10,000 joules per kilogram is projected by year 2000 based on the development knowledge and insight acquired from this contract. These energy storage densities project capacitive storage mass on the order of 100,000 kilograms (Figure 3-11) both for large storage applications circa 2,000 and for more modest applications near term.

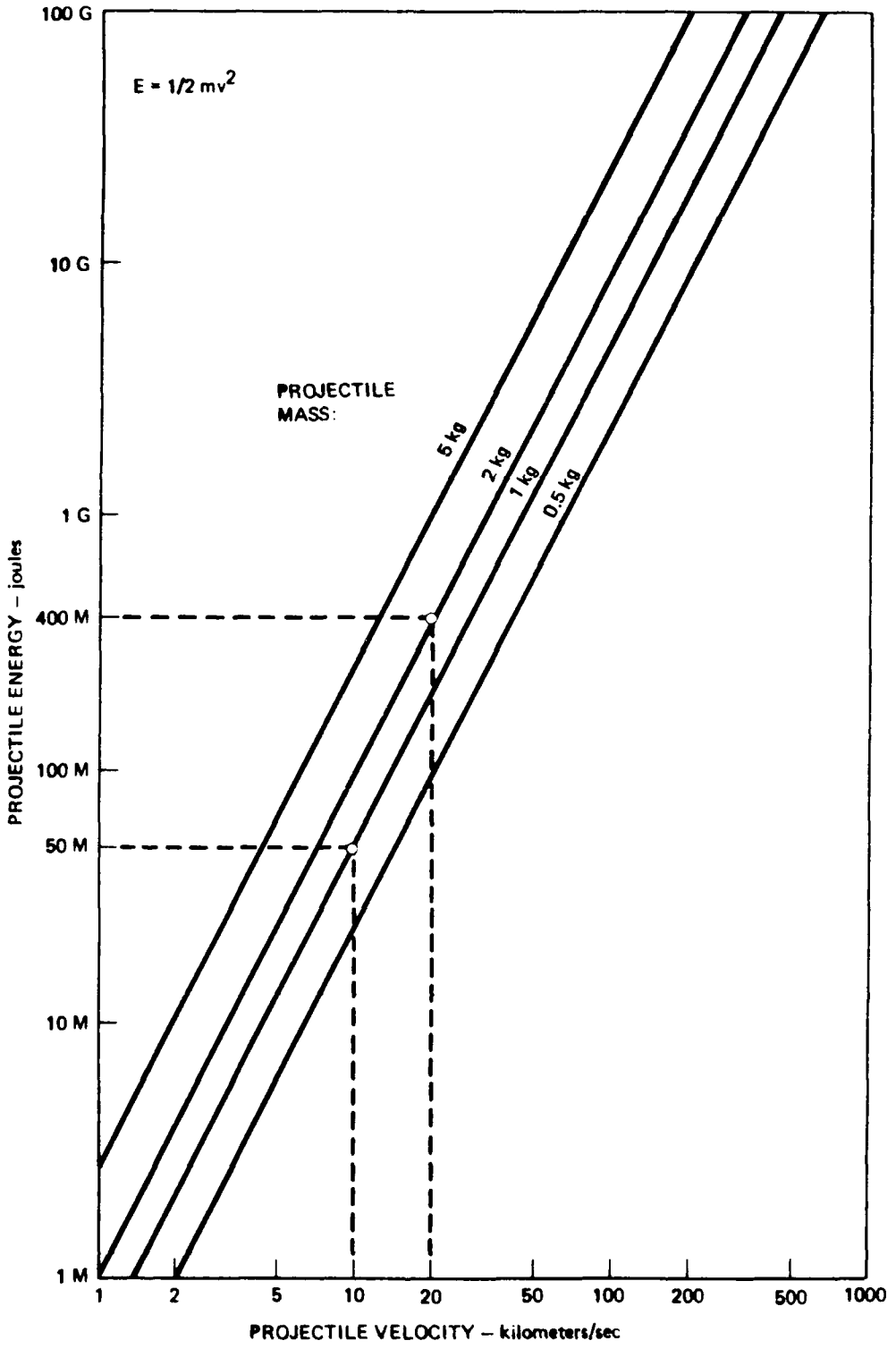

Figure 3-9. Energy Requirements

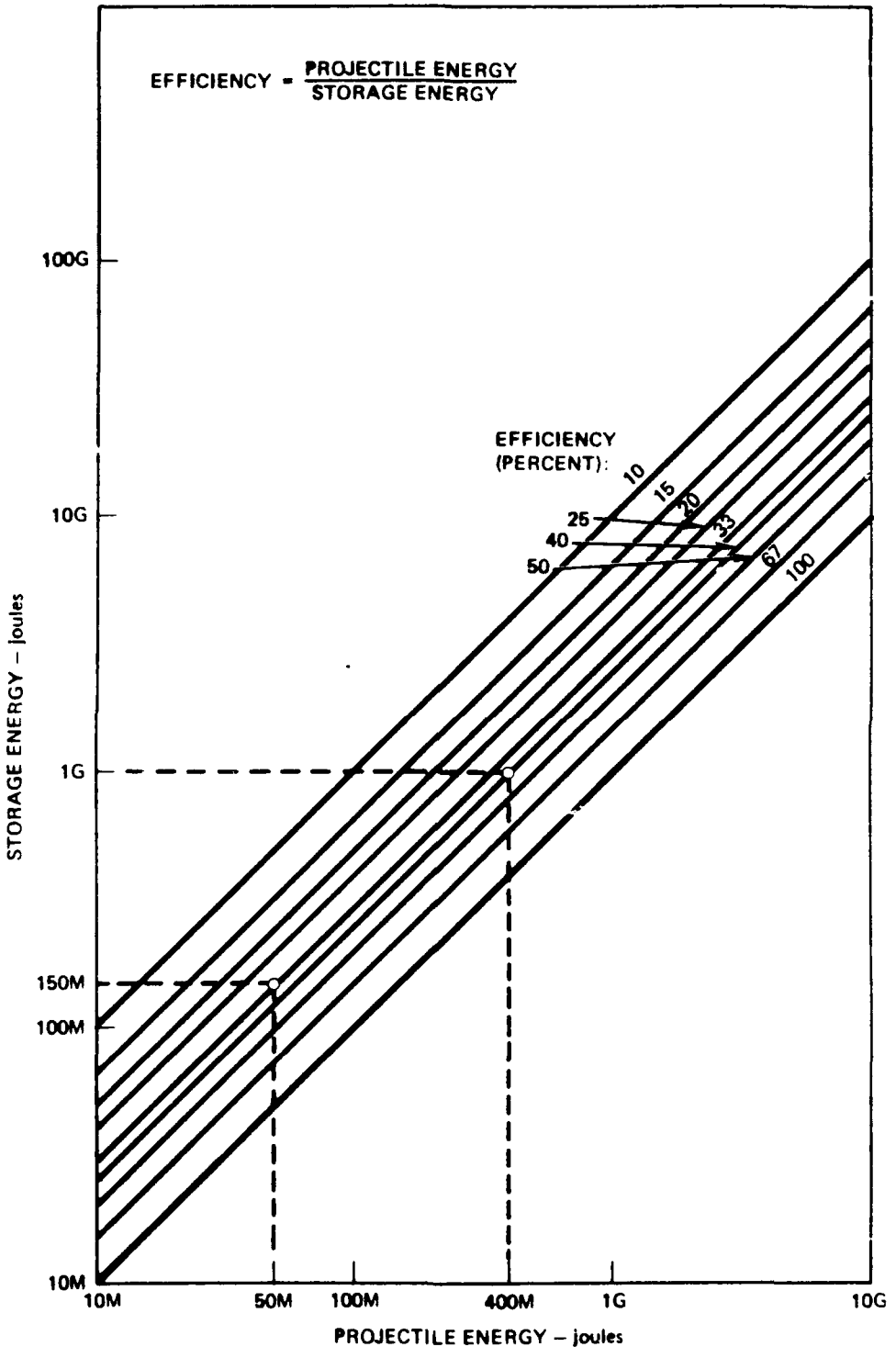

Figure 3-10. Energy Storage Requirements

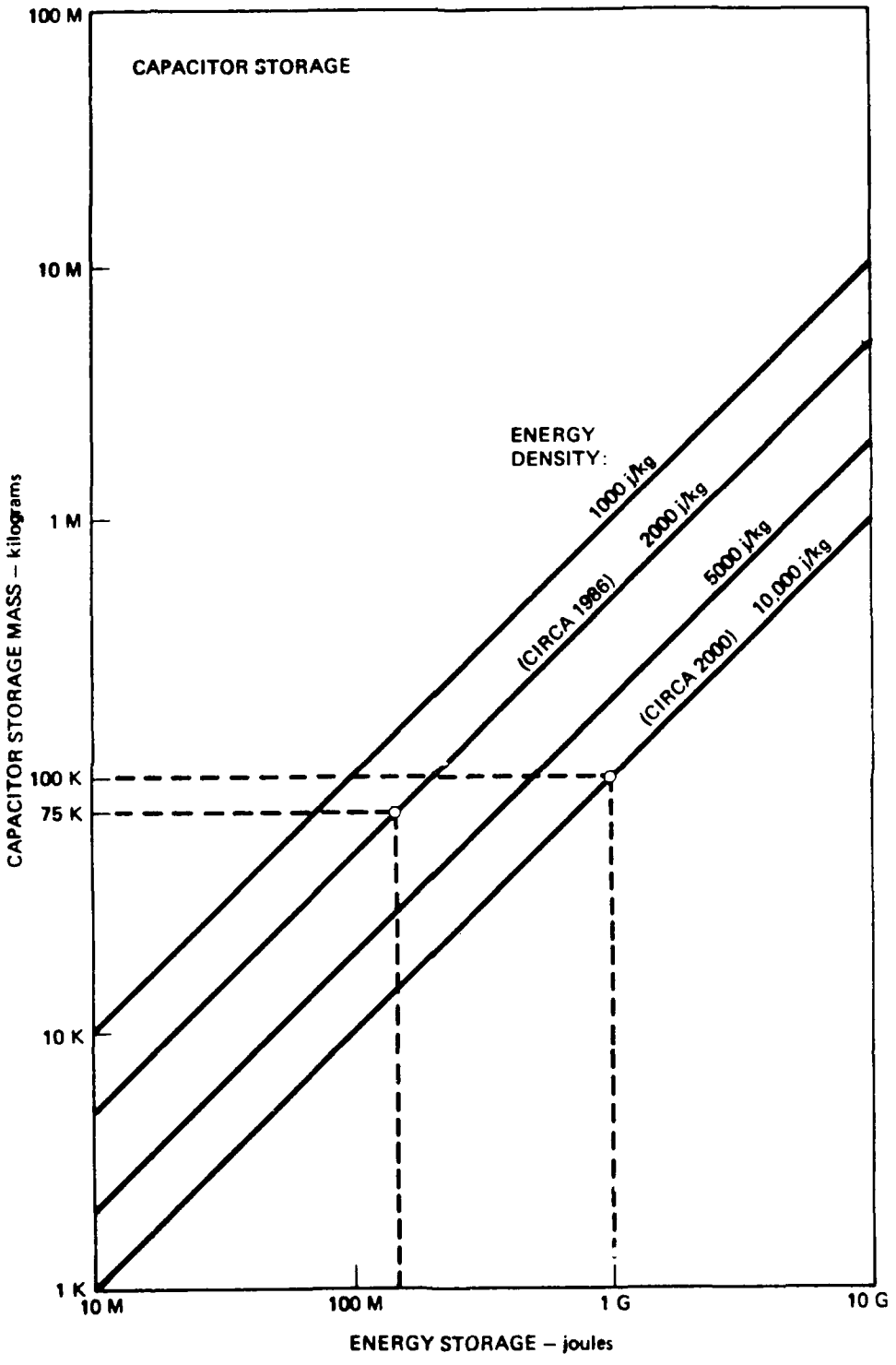

Figure 3-11. Capacitor Storage Mass Projections

The power requirements to charge the energy storage elements (Figure 3-12) are dependent upon the energy storage capacity and the firing rate (charge/discharge repetition rate). Rapid rates (considerably more than 1 per second, e.g., 10 shots per second) require charging power levels into the multigigawatt range. This implies a formidable power source in physical size and mass for space platform deployment. Considerably more moderate firing rates (e.g., one shot every 10 seconds) mitigate the power requirements to multimegawatt levels.

Operating scenarios typically assume rapid charge and immediate discharge (rail gun firing) upon attaining full charge of the energy storage elements (Figure 3-13a). Charging power is large and sustained during the rapid, uniform firing engagement (Figure 3-13b). However, this scenario seems idealistic and requires further system level studies.

Actual operation is more likely erratic firing as targets are available. The energy storage elements are charged rapidly to provide quick response, but targets are not evenly and uniformly available as full charge is attained (Figure 3-13c). This produces an erratic, pulsed charge requirement (Figure 3-13d). Meeting this requirement will require multimegawatt or even multigigawatt power sources. Turbodynamic machinery at MMW or MGW power levels cannot be operated in fractional second pulses. Several seconds may be required for each startup and shutdown. Consequently, electrical load is required regardless of energy storage state of change. This implies a parasitic load whenever the energy storage elements are fully charged.

Alternatively, an electrochemical source may be considered. The pulse limitation with these sources are the maximum current densities for the electrochemical source and the rate of change of current flow to provide the pulse. However, electrochemical sources are unduly massive for even multimegawatt operation and inordinately massive for multigigawatt operation.

A weapons-system trade is required to evaluate a large platform and power system that provides several shots per second versus a group of smaller platforms, each incorporating a rail gun, energy storage, and a modest power source to recharge the weapon in 10 seconds (or longer).

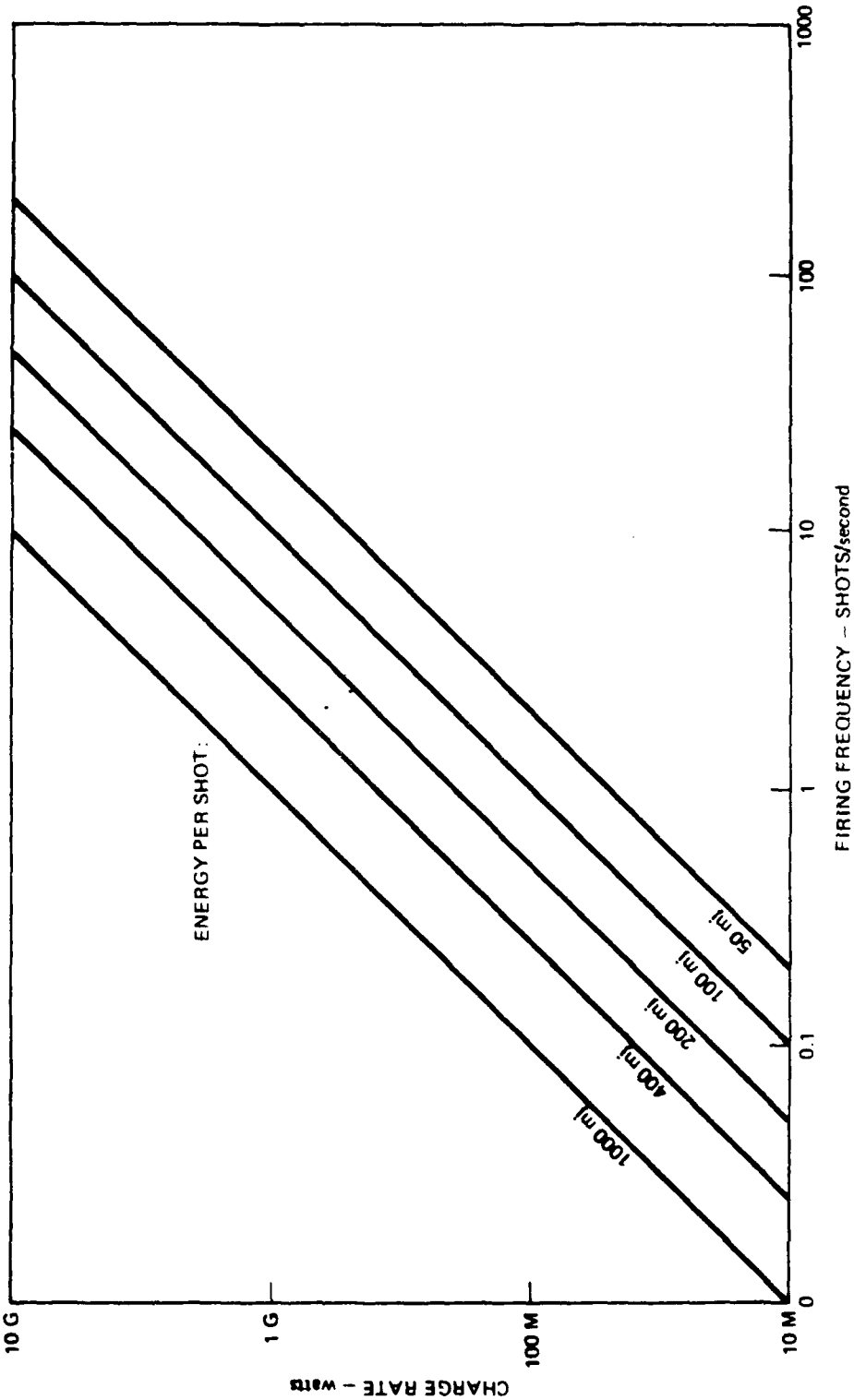

Figure 3-12. Power Requirements Projections

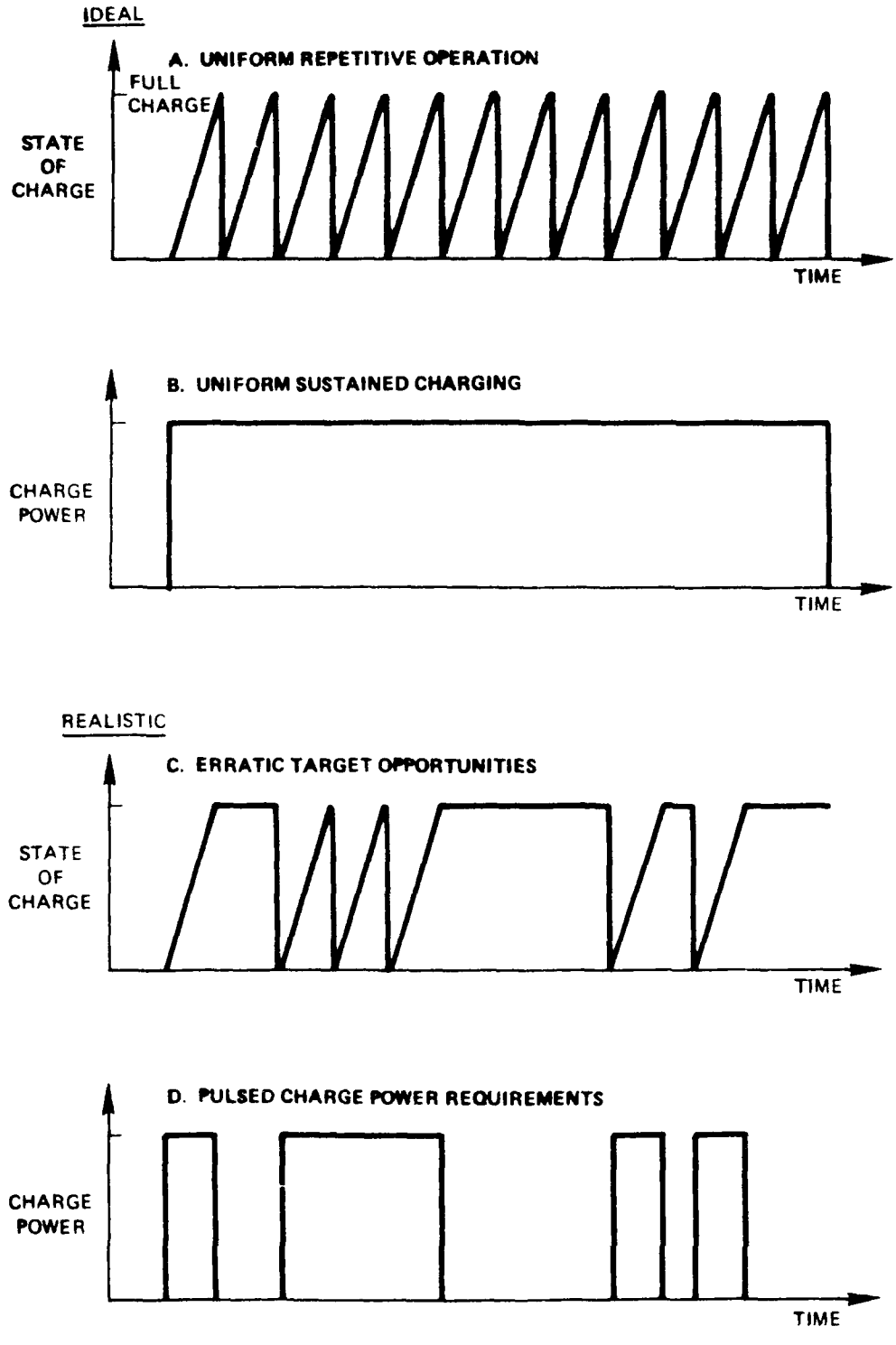

Figure 3-13. Recharge Requirements

The launching of a KEW projectile produces a reaction on the space platform similar to the recoil of a field artillery cannon. However, the space platform has no "earth mass" to absorb or react this recoil. Hence, the platform incurs acceleration, velocity change, and displacement. The magnitude of the platform reaction is dependent upon the mass ratio of the projectile to the platform and upon the acceleration of the projectile:

$$F = m1 \cdot a1 = m2 \cdot a2$$

$$\text{Platform acceleration} = \frac{\text{projectile mass}}{\text{platform mass}} \times \frac{\text{projectile}}{\text{acceleration}}$$

The range of platform accelerations are 0.2 to 20g, with durations of a few milliseconds. (This is more typical of a shock impulse.) Platform shocks of one g or less are more typical unless heavy projectiles are fired from light platforms with large accelerations (Figure 3-14). Platform equipment must withstand multiple (repetitive) shocks of this magnitude.

The above analysis assumes the rail gun is "bore sighted" through the center of mass of the platform. Any other alignment geometry allows the recoil to produce a torque on the platform, imparts angular momentum to the platform, and introduces an angular velocity component to the projectile trajectory.

3.2 Power Sources.

3.2.1 Prime Power. A large number of prime power sources have been considered for providing the large quantities of burst power required for space weapons. The Space Power Architecture Study (SPAS), now being conducted by TRW for AFSTC (References 2 and 3) has analyzed the systems shown in Tables 3-1 and 3-2. For the purposes of this study, however, the prime power source is not a consideration, as we begin with the electrical source, or generator. The large number of systems listed on the two tables cited can be broken down into the following basic categories:

Rotating Machines	Static Conversion
1. Alternators	1. Magnetohydrodynamic (MHD)
2. Homopolar generators	2. Thermionic (usually nuclear-driven)
3. Compulsators	3. Fuel Cells

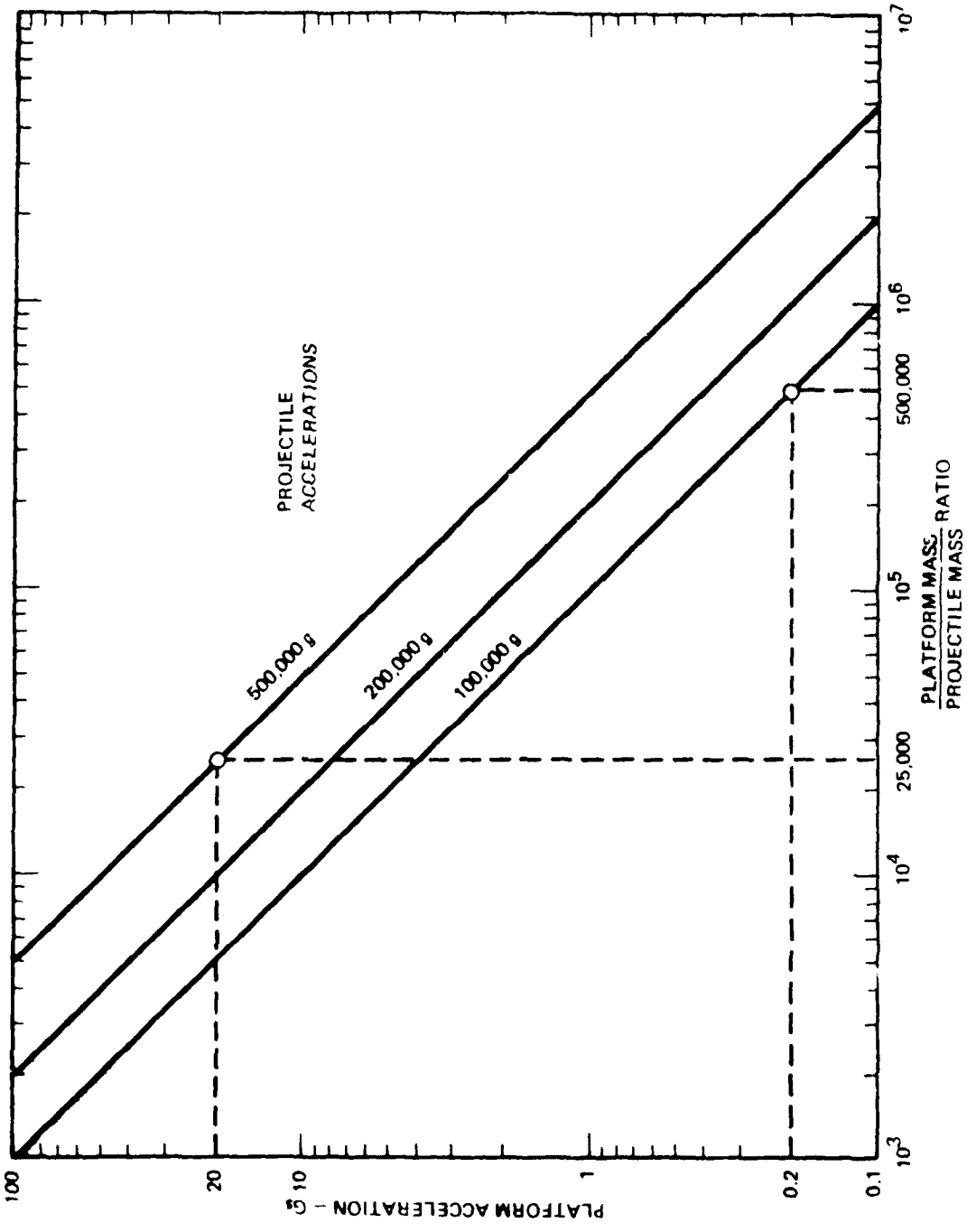

Figure 3-14. Platform Reaction Acceleration

Table 3-1. Burst Power Concepts (100-2000 MW)

Effluents Allowed

Symbol	Concept Description	Effluents
NDR/TG	NERVA derivative nuclear reactor/turbogeneration	Hydrogen
NDR/MHD	NERVA derivative nuclear reactor/magnetohydrodynamics	Hydrogen, Cesium
PBR/TG	Particle bed nuclear reactor/turbogeneration	Hydrogen Fission products Bed particles
PBR/MHD	Particle bed nuclear reactor/magnetohydrodynamics	Hydrogen, Cesium Fission products Bed particles
H + O/TG	Hydrogen + oxygen combustion/turbogeneration	Steam Hydrogen
H + O + Ti/TG	Hydrogen + oxygen combustion/turbogeneration; titanium water removal	Hydrogen
H + O/FC	Hydrogen + oxygen catalytic combustion/fuel cell; product water condensed and contained with hydrogen cooling	Hydrogen
H + O/MHD	Hydrogen + oxygen combustion/megnetohydrodynamics	Steam Cesium hydroxide Hydrogen
Gel/MHD	Beryllium + IRFNA as gels/magnetohydrodynamics; reactants stored as gels IRFNA - inhibited red fuming nitric acid	Beryllium oxide Steam, nitrogen Nitrogen oxides Cesium hydroxide Potassium oxide
Li + H/TG(O)	Lithium + hydrogen reaction/turbogeneration; open cycle (80 percent hydrogen effluent)	Hydrogen

No Effluents

Table 3-2. Burst Power Concepts (100-2000 MW)

Symbol	Concept Description	Waste Heat Management
THOR	Fold-up in-core thermionics	Storage/radiator (unfold)
NDR/B	NERVA derivative reactor/closed Brayton cycle	Storage/radiator
PBR/B	Particle bed reactor/closed Brayton cycle	Storage/radiator
Ti + O/KR	Titanium-oxygen combustion/closed cycle potassium Rankine cycle	Radiator
Ti + O/B	Titanium-oxygen combustion/closed Brayton cycle	Water/radiator
Be + O/B	Beryllium-oxygen combustion/closed Brayton cycle	Water/radiator
HC + O/SB	Hydrocarbon-oxygen combustion/closed supercritical cycle	Water heatsink
Li + H/TG	Lithium-hydrogen reaction/turbogeneration	Radiator
Li + SDF/R	Lithium-sulfur hexafluoride reaction/steam Rankine cycle	Ammonia heatsink
H + O/TG(CC)	Stiochiometric hydrogen-oxygen combustion/turbogeneration Steam cooled, condensed, and contained	Ammonia heatsink
H + O/FC(CC)	Catalytic hydrogen-oxygen reaction/fuel cell	Ice heatsink
H + O/MHD(CC)	Hydro-oxygen combustion/magnetohydrodynamics Steam cooled, condensed, and contained	Ammonia heatsink

Thermoelectric devices and batteries are not further considered in this study as it appears unlikely that they will be built in the sizes of interest for burst power systems.

Throughout the remainder of this study, we have selected 50 MW electrical as the reference source size, for the following reasons:

1. It is large enough to be of interest
2. It represents a reasonable scale-up from the state of the art
3. Since space weapons will probably require redundant generators, it represents a reasonable unit size that can be replicated to provide larger power levels.

The length of the power burst is not specifically considered, as it does not have a major bearing on conditioning, distribution, and control, the major elements of this study. Rather, it impacts primarily the quantity of fuel and the tankage, which are critical variables in the overall scheme of things, but which can be ignored here. In the few instances where total weight is of interest, the burst time is identified only as "t", to maintain the unclassified status of this report. The value of "t" will be communicated separately to the customer.

3.2.2 Rotating Machines.

3.2.2.1 Alternators. The current state of the art in standard alternators is the GE superconducting rotor unit now being readied for test at Wright-Patterson AFB. This is a 20 MW lightweight unit that provides 17.1 kV 3 phase, 200 Hz ac, which is rectified to provide 40kV dc. Highlights of the unit's design are shown in Figure 3-15. Considerable optimism has been expressed that the unit can be scaled up to 50 MW, and to 100 kV dc output. It seems unlikely, however, that the frequency can be scaled up very much.

A conceptual design of a disk-type generator is shown in Figure 3-16. At the present time, a contract is in place between AFWAL and Kaman Aerospace to design a 20 MW, 1.5 kHz machine. Kaman is also designing a 20 to 40 MJ pulsed unit for DARPA-ARDEC. Conversations with Kaman indicates that their proposed units will be cryo-cooled (not superconducting), and that voltages of 1200 volts per stator phase are reasonable. This would

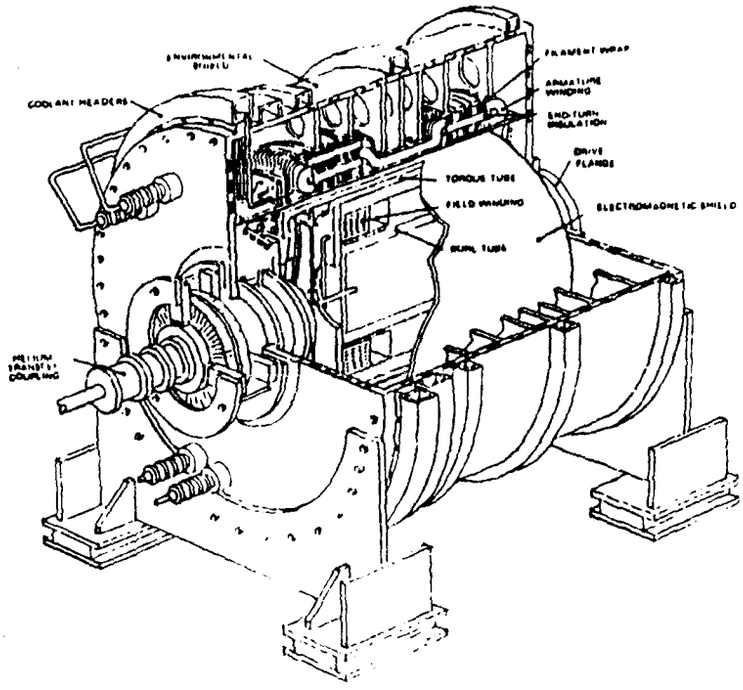

Power	20 MW (into a rectifier)
Number of Poles	4
Number of Phases	3
Frequency	200 Hz
Rotor	
Speed	6000 rpm
Bearing Span	32 in.
Outer Diameter	21.1 in.
Field Winding Outer Radius	9.0 in.
Modules/Pole	1
Module Cross-Section	2.85 x 2.94 in.
Straight Length	6 in.
Turns/Pole	881
Module Current Density	15,000 A/cm^2
Design Current	921 A
Inductance	0.61 H
Armature	
Annular Region	11.0 to 12.0 in. radius
Straight Length	6 in.
Annular Current Density	1760 A/cm^2
Coils/Phase	56
Turns/Coil	5-1/2 and 6-1/2 (average of 6)
Shield Radius	20.5 in.
Design and Base Current	408 A
Design Voltage	17.1 kV rms
Open Circuit Voltage	22.3 kV rms (design excitation)
Base Voltage for Reactances	19.1 kV rms
Reactances	
(46.8 Ω Base, 23.4 MVA)	
Synchronous	0.56 p.u.
Transient	0.50 p.u.
Subtransient	0.26 p.u.
Losses	
Armature Joule Heating	990 kW
Armature Eddy Current	440 kW
Case Eddy Current	488 kW

Figure 3-15. 20 MW Superconducting Generator

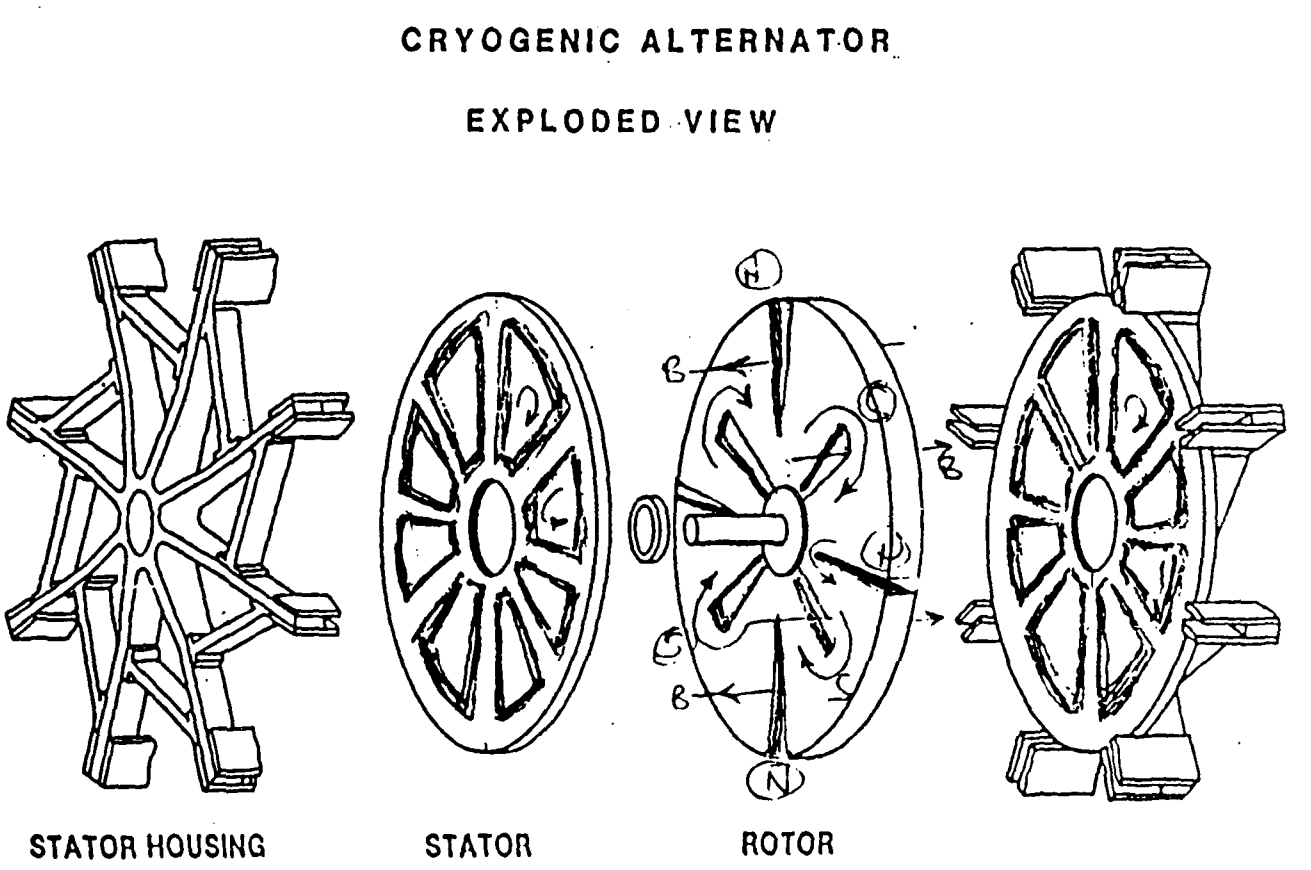

Figure 3-16. High Performance Alternators
(Courtesy Kaman Aerospace)

lead to an output voltage of 8 to 9 kV. Although the current design is for 1.5 kHz, optimism is expressed that the design could produce up to about 10 kHz.

Figure 3-17 shows one design of a homopolar generator. This, and the compulsator, are actively under design by the University of Texas Center for Electromechanicsal Laboratory, and have been extensively described in the literature.

3.2.3 Static Power Conversion. Three types of static power converters were considered in this study. They are

1. MHD devices
2. Thermionic devices
3. Fuel cells.

Figure 3-18 shows the design of a disk-type MHD unit designed by TRW in response to the Department of Energy's proposal DE-RP22-86PC90270. In general, MHD generators are expected to be capable of providing about 2 to 10 kV dc, at power levels up to about 100 MW. Some are expected to be capable of pulsed operation by programming the combustors.

Figure 3-19, shows a thermionic reactor designed by GA Technology called THOR. It produces power and stores waste heat in the folded-up mode, then dissipates the stored heat by unfolding its radiators and preparing for the next engagement. Because of the large number of individual thermionic modules, the unit can be connected in various series-parallel modes to generate a wide variety of dc voltages and currents. The design shown was configured for 5 kV dc output, which was used for the remainder of this study.

Figure 3-20 shows a typical fuel cell configuration. Like the thermionic module, individual cells can be connected in various series-parallel modes to yield a variety of dc outputs. The fuel cell also has one major advantage: all of the previously described generators are large, centrally located devices; the fuel cells can be arranged in smaller, dispersed units mounted adjacent to the unit loads they serve. This provides additional redundancy, and sharply reduces the length of the

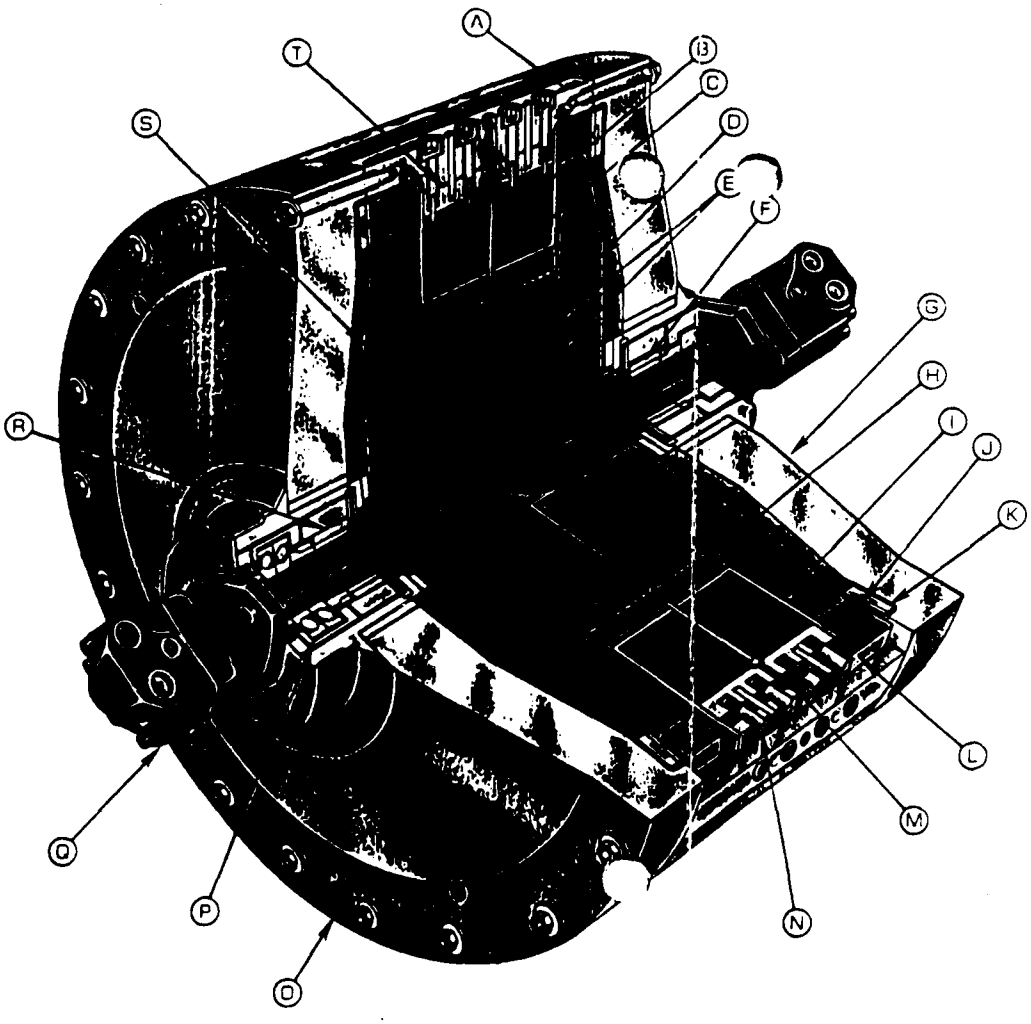

Figure 3-17. Homopolar Generator
(Courtesy OIME, Inc)

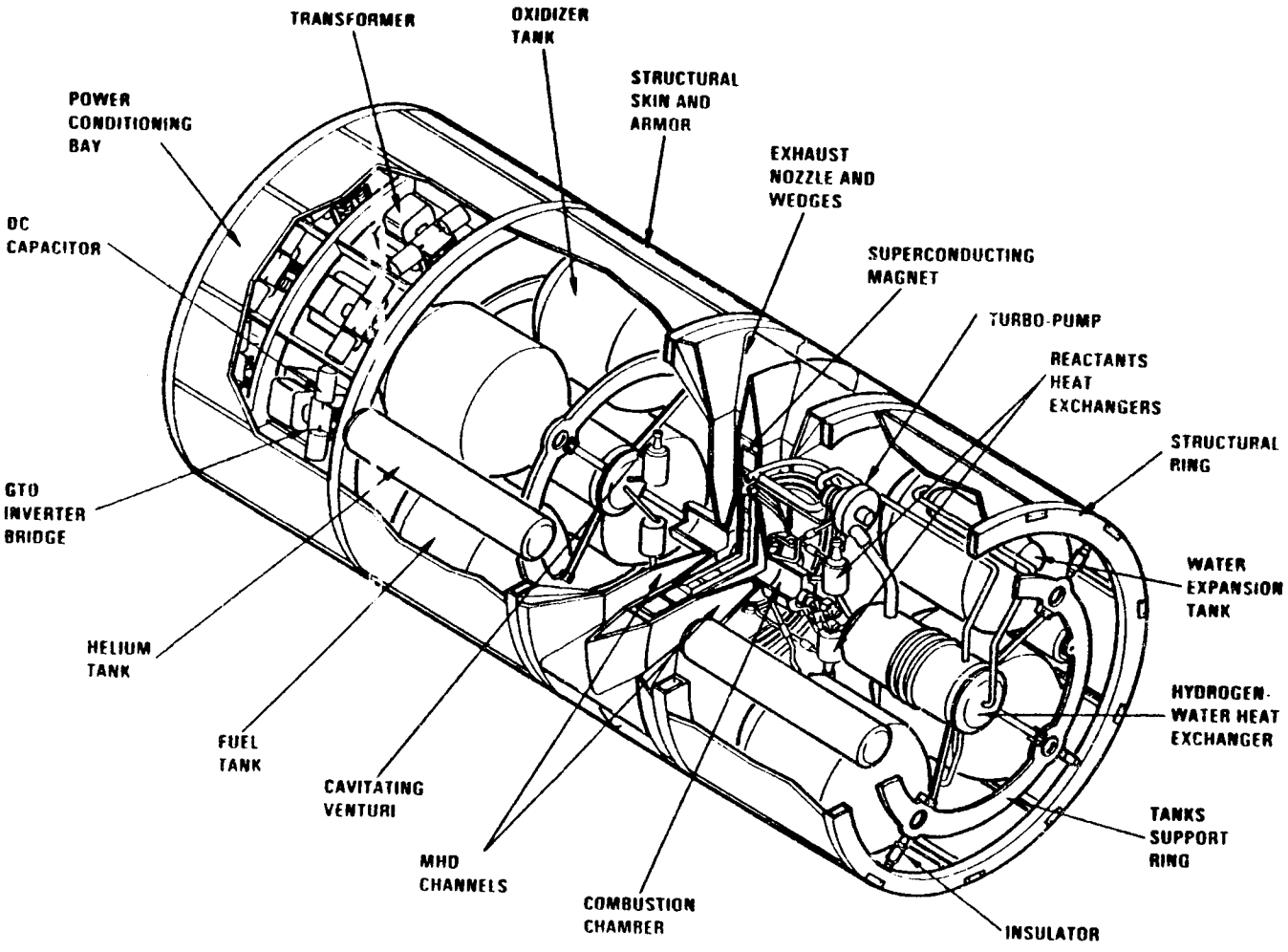

Figure 3-18. Isometric View of 100 MW MHD System

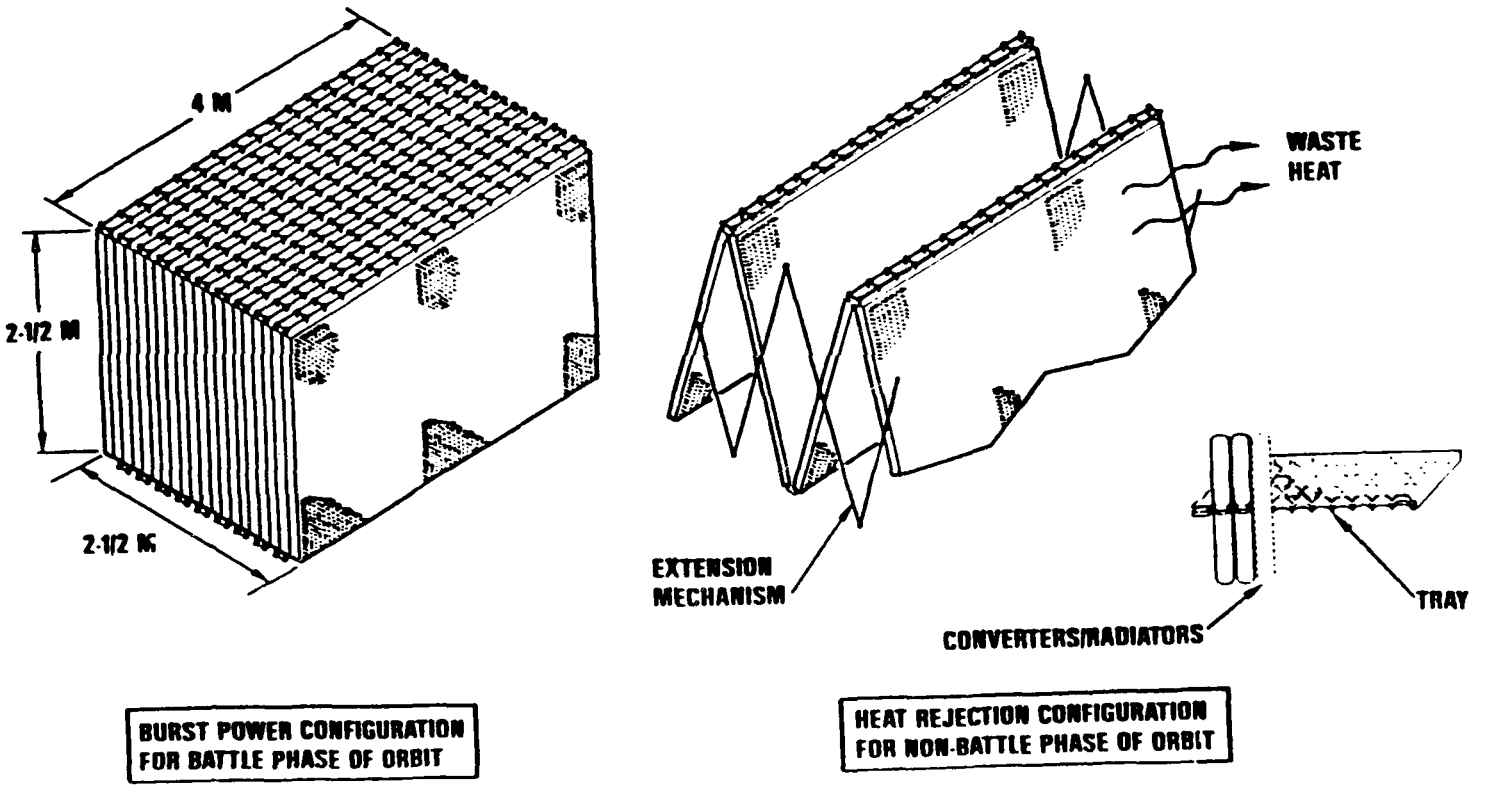

Figure 3-19. THOR Geometry at Power and When Radiating
(Courtesy GA Technology)

(U) Hydrogen-Oxygen Fuel Cell (Closed)

Conceptual Arrangement*

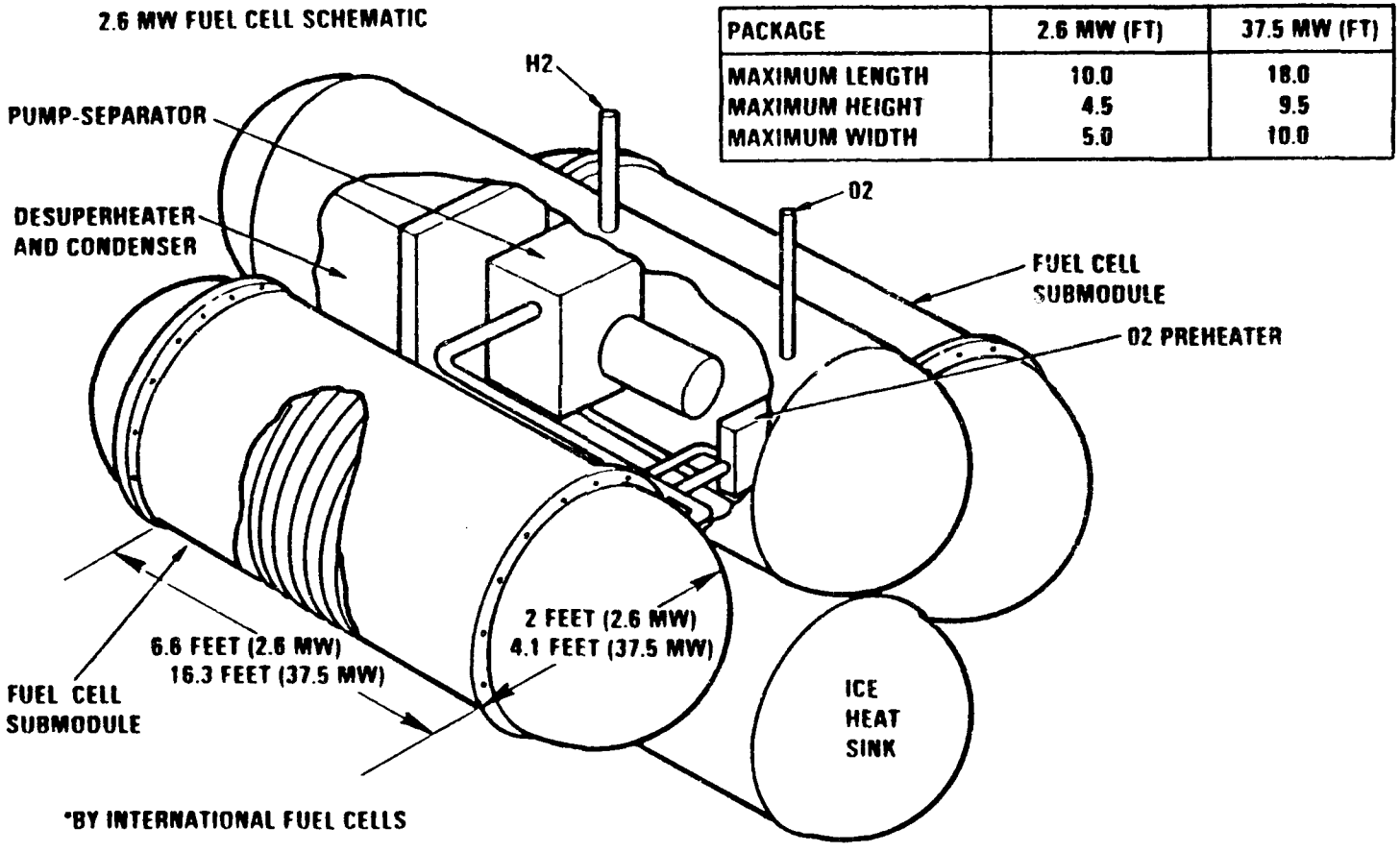

PACKAGE	2.6 MW (FT)	37.5 MW (FT)
MAXIMUM LENGTH	10.0	18.0
MAXIMUM HEIGHT	4.5	9.5
MAXIMUM WIDTH	5.0	10.0

Figure 3-20. Typical Fuel Cell
(Courtesy International Fuel Cells)

cables between the generator and the load. The trade-off is the extra amount of piping required to distribute the fuel and oxidizer.

3.3 Power Conditioning. Power conditioning (PC) is defined as the circuits which condition prime power to the appropriate voltage levels and waveforms necessary to meet the weapon interfaces. Power conditioning systems can be divided into two subsystems; slow power conditioning and fast power conditioning as shown in Figure 3-21.

Slow power conditioning (SPC) encompasses the conversion of prime power to the appropriate voltage, frequency, and current to facilitate power transmission to the loads and for input to fast power conditioning subsystem loads. Components within a slow power conditioning system are solid state switching devices, capacitors, inductors, transformers, rectifiers, inverters, converters, filters, regulators, etc. Fast power conditioning (FPC) encompasses:

1. Networks for delivery of short, repetitive, high energy pulses to the weapon and
2. The conversion of electrical energy into RF power for delivery to accelerator loads.

Pulse forming networks and high energy pulse generators are components of the first category and high power, high frequency tubes or solid state devices are components of the second.

3.3.1 Slow Power Conditioning. As used in this study, slow power conditioning includes the following:

1. Power transformers
2. Rectifiers
3. dc to ac inverters
4. Charge control networks (for capacitors)
5. Circuit breakers and switches

Multimegawatt power transformers have been built for the utilities and industrial applications at 60 Hz and for the military at 400 Hz. These devices are designed for ground and long life applications where reliability, efficiency, and costs (procurement and operating) are design

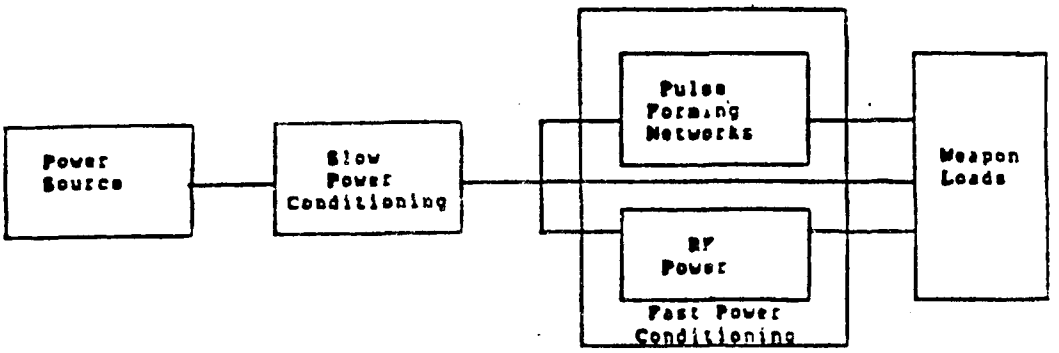

Figure 3-21. Power Conditioning Subsystems

drivers and there is no constraint for size and weight. The military does place a constraint for size with the operating frequency changed to 400 Hz. With the SDI space weapon system, the design drivers are changed to short operational lifetimes, and minimum size and weight. High efficiency is not presently a design driver since there is usually a surplus cooling capability due to the hydrogen used for the power source. There is no power conditioning data base that can be used to establish a bogey, due to the lack of operational multimegawatt experience for space applications. Power conditioning equipment characteristics have been projected to the year 1993 with new component technology development as applied to the utility/industrial/military hardware experience. The projected new power conditioning advancements are:

- High frequency (2 kHz to 10 kHz) alternators
- High speed, high voltage, high current power semiconductors utilizing hybrid semiconductor processing
- Advanced magnetic materials
- Advanced capacitor film technologies.

Figure 3-22 shows power transformer weight plotted against power output, with operating frequency as a parameter. The efficiency of the power transformers are projected at 98 percent due to high current density of the transformer winding (100 cm/amp) and due to high flux density of the transformer core material. These curves are for short operational life units, i.e., 100 to 1000 hours. (Storage/standby life is 10 years).

Table 3-3 shows the current state of the art in power control devices suitable for rectifiers and inverters. Integrated MOS/bipolar technology shows promise on elements rated at 250 C and radiation hard. Based on preliminary development data from General Electric Research Laboratory, projections of future semiconductor technology can be made. Figures 3-23 and 3-24 tabulate weights vs. power level for rectifiers and dc to ac inverters using the new semiconductor technology.

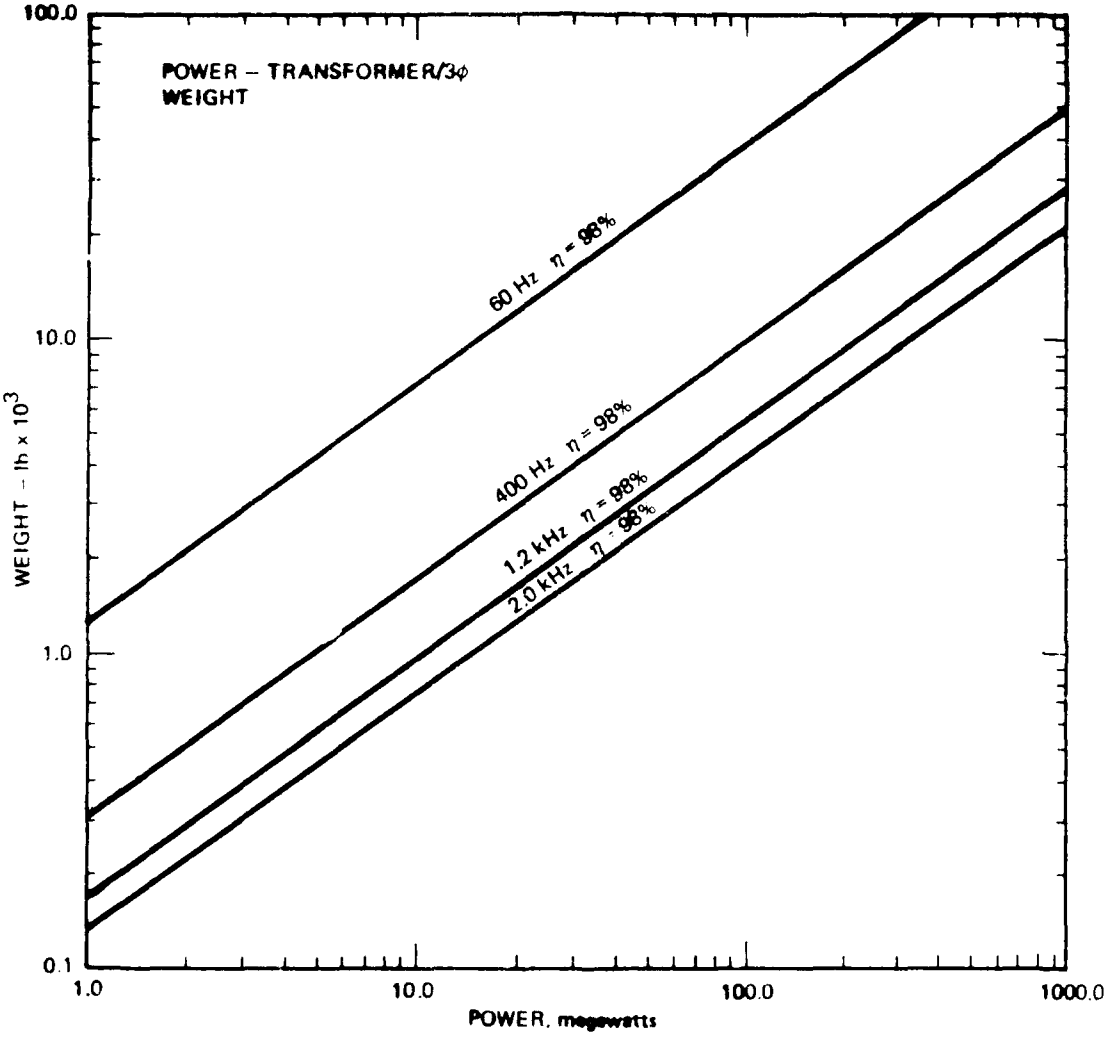

Figure 3-22. Power Transformer Weight

Table 3-3. State-of-the-Art Power Control Devices

Switch Type	Rating	Status
Thyristor	5 kV, 2200 A (light-triggered)	Commercial
Thyristor	0.5 kV, 3500 A (light-triggered)	Under active development
GTOs	5 kV, 200 A (self-contained)	Available in 6 months
MOS/Thyristors	1.2 kV, 150 A	Technology
MOS/Thyristors	5 kV, 2500 A	Maybe in 5 years

There are three basic techniques that can be utilized to charge up the pulse forming network.

- Ac-dc Converters
- Dc-dc Converters
- Resonant Charger

Both the ac/dc converter and dc/dc converter use pulse width modulation technique to control the current charging rate and/or charging power into the pulse forming network. Figure 3-25 illustrates a resonant charging network. In this configuration, the dc voltage source is switched to the charging inductor and PFN capacitance through switch SCR. The current through the SCR is a sine current. The period of charging is determined by the charging inductor and its PFN capacitance. The value of this PFN charging voltage is approximately two times the dc input source. When the PFN is charged, the power switch is turned on and this PFN energy is transferred to the load through the pulse transformer. The length of the output pulse period is determined by the PFN inductance, pulse transformer inductance and the PFN capacitance. Ideally the pulse transformer inductance is minimized so the total output pulse characteristic is determined by the PFN characteristics.

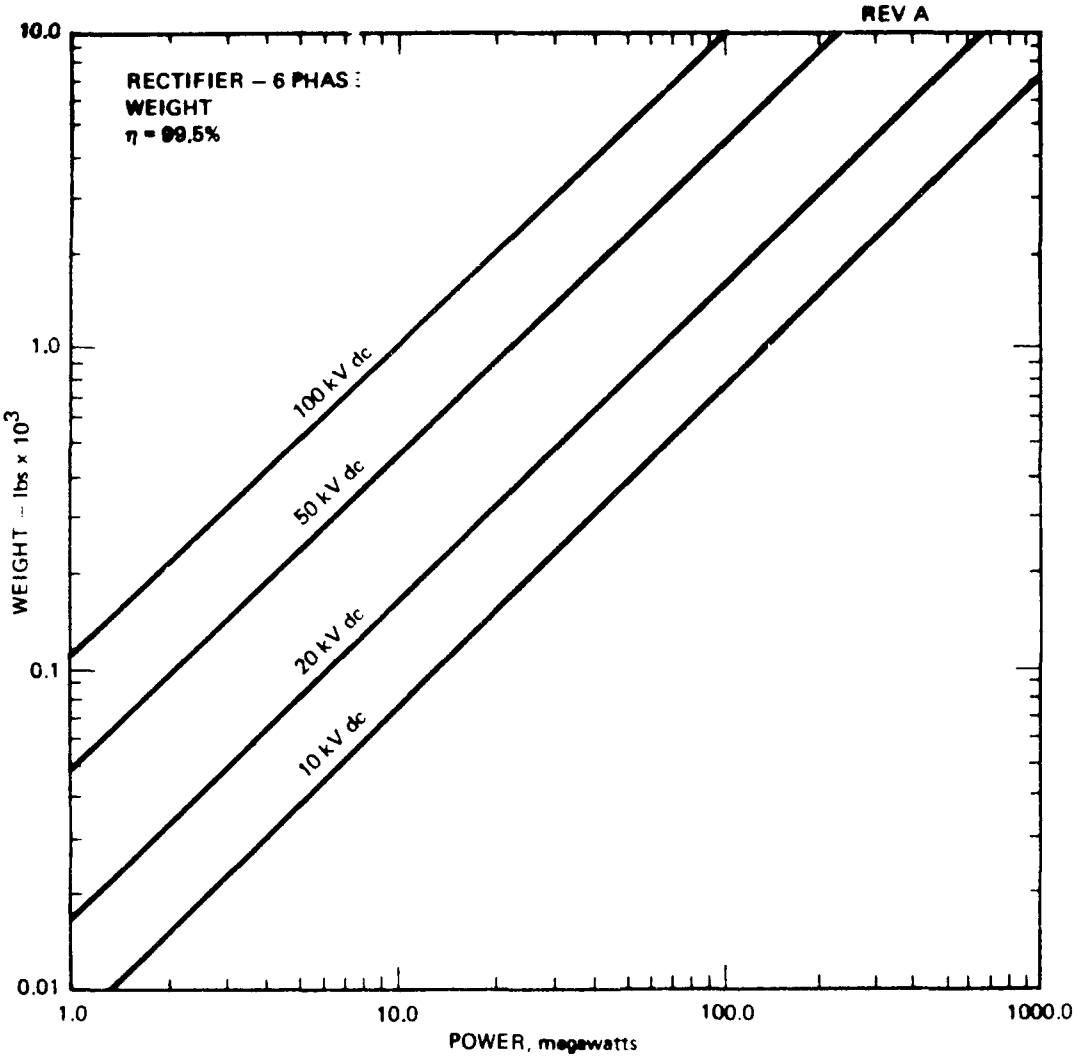

Figure 3-23. Rectifier Weight

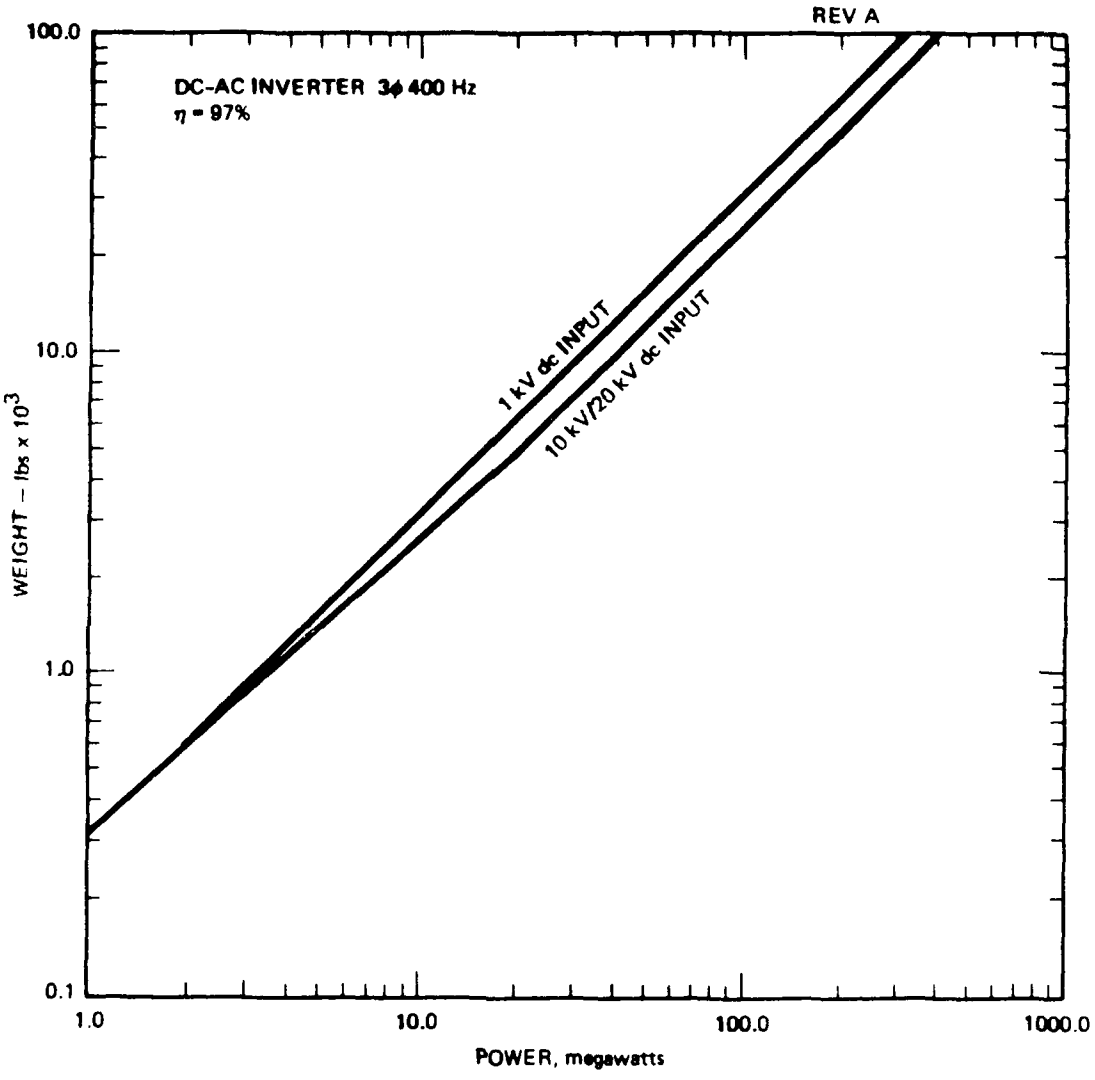

Figure 3-24. Inverter Weight

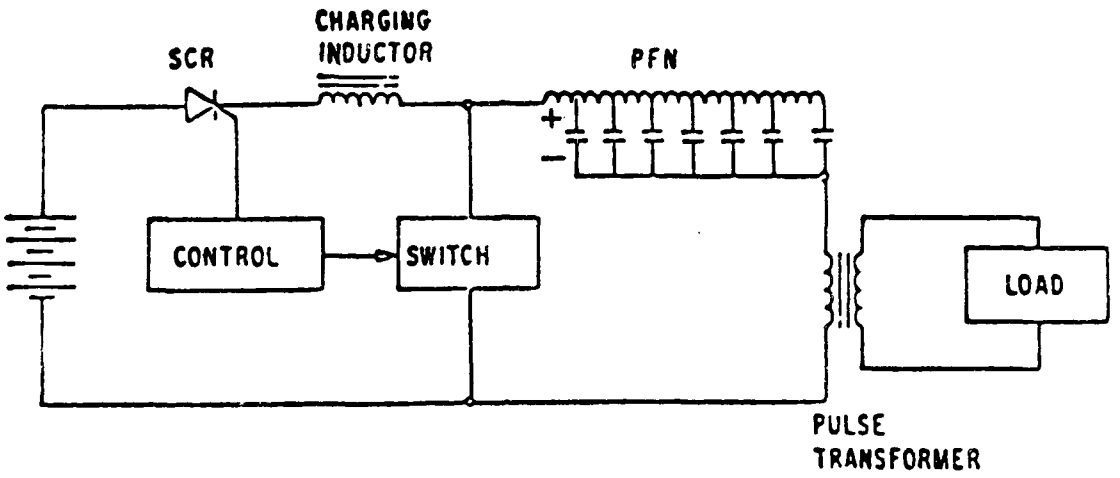

Figure 3-25. Resonant Charging Schematic

The state of the art in vacuum interrupters, the most likely candidate for high power switchgear in space, is shown in Figure 3-26. The design of the interrupter unit itself can probably be adapted as is for space work. However, the externalities of ground-based units (e.g., mounting, insulation, closing mechanisms) are clearly not applicable. Use of such devices in spacecraft would require a complete redesign of the external mechanisms. Figure 3-27 shows predicted weights vs. load for ac circuit breakers. For dc breakers, it is estimated that they will weigh 50 percent more than their ac counterparts because of the need for additional commutating devices to force a current zero in the dc circuit.

3.4 Transmission Lines. For most of the power sources discussed in Section 3.2, the power conversion device, e.g., turbogenerator, is located perhaps 50 meters from the center of the load. Thus, some type of transmission line is required between the generation center and the load center, where further distribution is made to the individual load groups. The selection of the type of transmission line depends principally on the following parameters:

1. Current carrying capacity required
2. Material selection
3. Temperature of operation.

From studies conducted to date it appears that voltage level is not a serious factor in the selection. All voltages of interest must be totally insulated and/or shielded from the space plasma, and insulation does not appear to be a major weight problem. The selection of ac or dc likewise does not appear critical; in most cases, comparative ac and dc weights are approximately a push.

3.4.1 Optimum Conductor Sizing. The mass for electrical power transmission is composed of the conductor mass plus the incremental mass of power generation and energy storage to supply the transmission losses and the thermal management mass to dissipate these losses. In addition, any power conditioning equipment at the power generation source must be increased to handle the incremental power due to these losses. As the transmission conductor size (cross section) is increased, thermal

The basic design of vacuum interrupters for contactors and circuit-breakers is similar. The arcing chamber with the two stem-connected contacts is located between two ceramic insulators. One contact is fixed to the housing, the other is a moving contact connected to the housing via vacuum tight bellows.

The arcing chamber acts as a vapour shield. On opening, a metal vapour arc is drawn between the contacts and is extinguished at current zero. The small amount of metal vapour that is not redistributed over the contacts condenses on the arcing chamber wall. This protects the inside of the ceramic insulators against condensed metal vapour, which could reduce the insulation. The metal bellows enables the moving contact to carry out its stroke. This varies according to the rated voltage of the vacuum interrupter and is only 8 mm for 24 kV. A metal bellows must be able to withstand the movement corresponding to 30,000 make/break operations without failing. This was confirmed in long-term tests; fractures did not occur until after more than 200,000 such operations.

The insulators are made of metallized aluminium oxide ceramics, which permits them to be brazed to metal so that there is no need to use conventional seals.

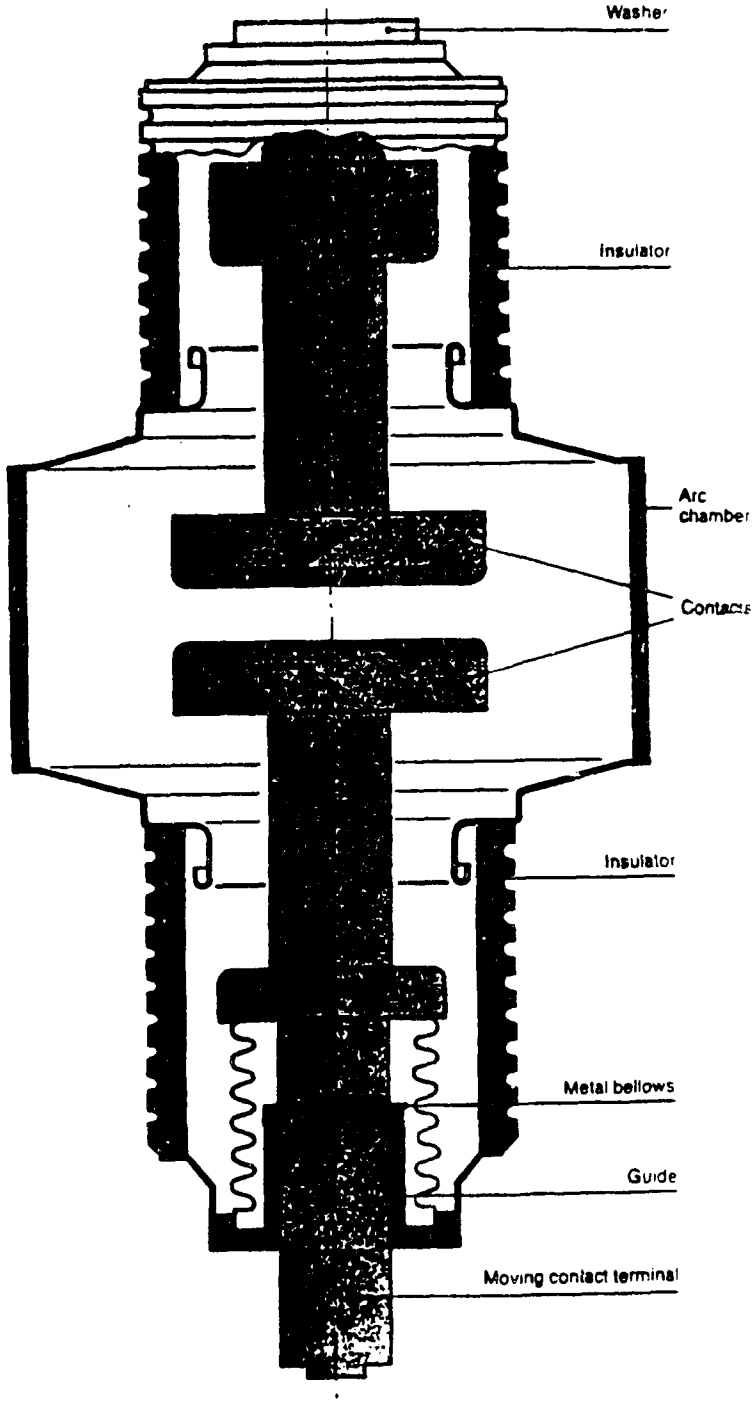

Figure 3-26. Construction of a Vacuum Interrupter
(Courtesy Siemens Aktiengesellshaft)

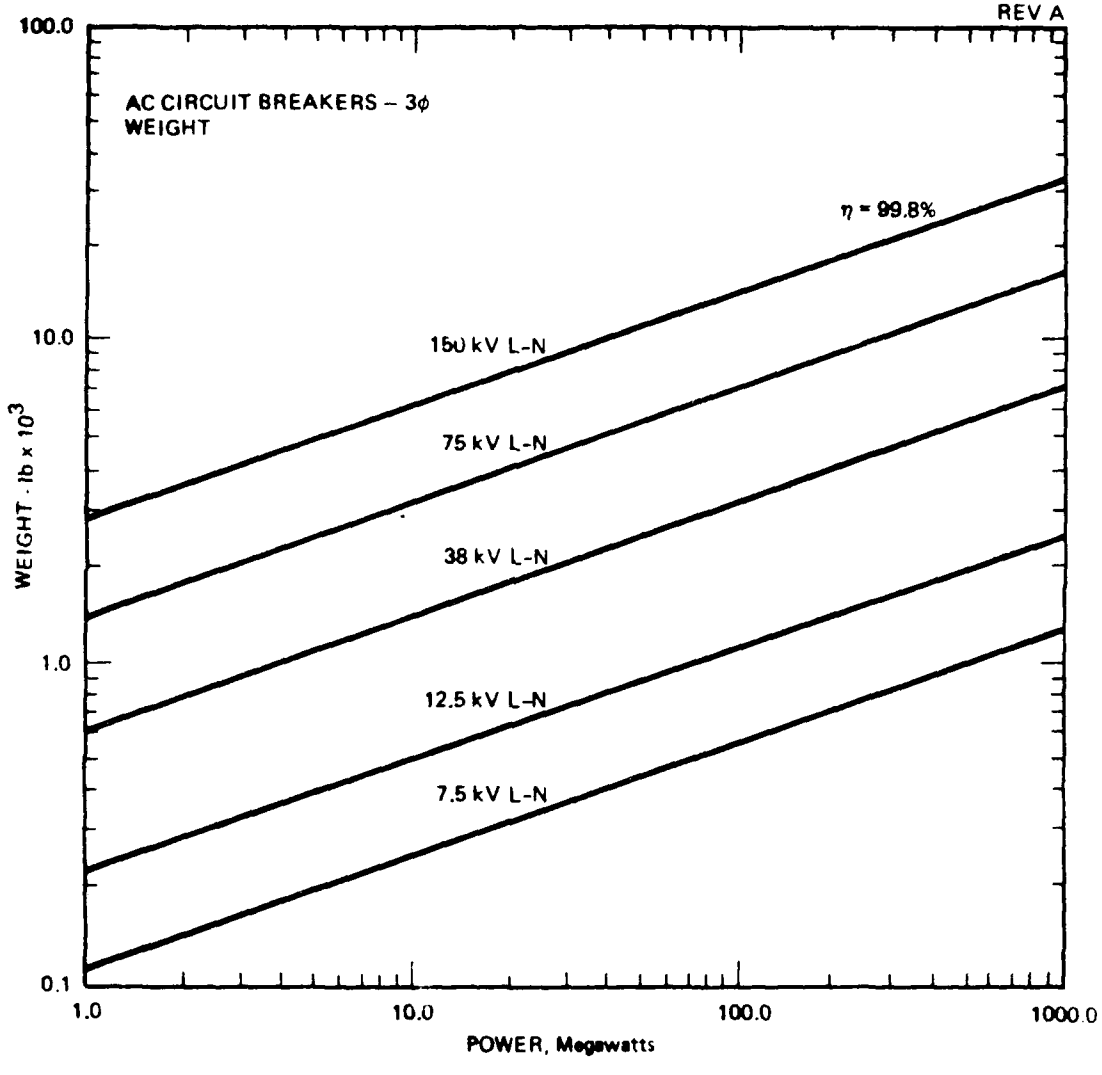

Figure 3-27. Circuit Breaker Weights

management, and power conditioning requirements decrease. Consequently, a mass optimization exists.

The system mass for electrical power transmission is the sum of five relatable terms:

$$M_{trans} = M_{wire} + M_{power\Delta} + M_{energy\Delta} + M_{thermal\Delta} + M_{power\ conv\Delta}$$

where:

- M_{wire} = the mass of the electrical transmission conductors (M_w).
- $M_{power\Delta}$ = the mass of the incremental increase in the electrical power generation source to supply the transmission losses (M_p).
- $M_{energy\Delta}$ = the mass of the incremental increase in energy storage capacity to supply the transmission losses (M_e).
- $M_{thermal\Delta}$ = the mass of the incremental increase in the thermal control equipment (radiators, pumps, plumbing, cryogenics, etc.) to dissipate the electrical transmission loss and the associated support losses (power generation and conversion) and the incremental increase in power to support the thermal management increase (M_t).
- $M_{power\ conv\Delta}$ = the mass of the increase in power processing/ regulation equipment due to the increased load attributable to transmission conductor losses (M_c).

Each of these terms is complex but may be related to the parameters of the transmission conductor under consideration (Figure 3-28).

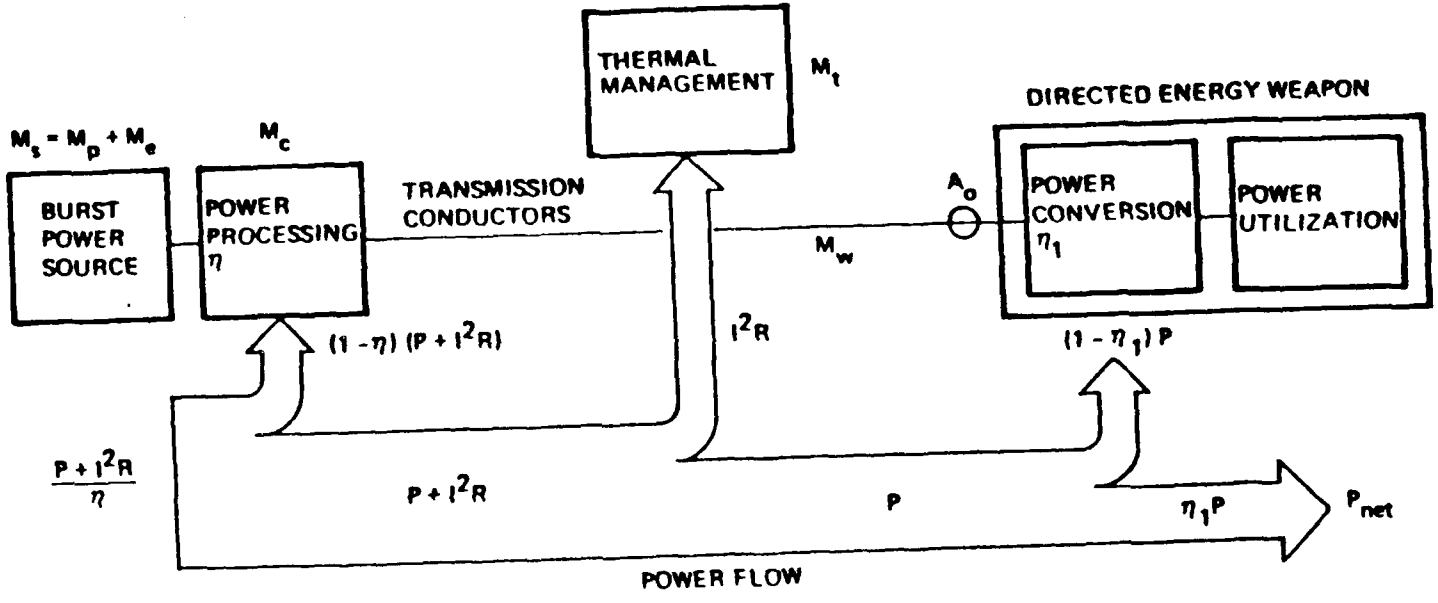

M trans = M wire + M source Δ + M power cond Δ + M thermal Δ

$$= M_w + \frac{I^2R}{\eta} K_s + I^2R\,K_c + I^2R\,K_t$$

$$= M_w + I^2R\left(\frac{K}{\eta} + K_c + K_t\right)$$

Where η and η_1 are efficiencies, Ks, Kc, and Kt are performance factor (mass/power), and P_1 Pnet are load.

Figure 3-28. Transmission Mass and Loss Relationship

The transmission conductor mass is easily expressed as the product of the conductor material density (σ) and volume, which in turn is the product of the conductor cross-sectional area (A) and circuit length (ℓ):

M wire = $\sigma A \ell$, lb, where:

σ = material density, lb/ft^3

A = conductor cross section, ft^2

ℓ = circuit length, * ft

---

*The circuit length considers the transmission conductor routing including the power return path.

The transmission conductor losses may be expressed as I^2R, where I is the transmission current, and R is the total conductor path resistance. The current is related to the transmitted power (P) and selected transmission voltage (V): I = P/V. The resistance is a function of the condutor parameters:

R = $\rho\ell/A$, ohms, where:

ρ = resistivity of conductor material, ohm-ft

ℓ = conductor circuit length, ft

A = conductor cross-sectional area, ft^2

The losses are therefore:

$$I^2R = \frac{P^2 \rho \ell}{V^2 A}, \text{ watts}$$

---

*The circuit length considers the transmission conductor routing including the power return path.

The incremental increase in power source, energy storage, thermal control, and power conversion mass due to transmission losses is obtained by multiplying these losses (I^2R) by the respective performance factors (K_p, K_e, K_t, K_c in pounds per watt):

$$M_p = I^2R \cdot K_p = \frac{P^2 \rho \ell}{V^2 A} \cdot K_p$$

$$M_e = I^2R \cdot K_e = \frac{P^2 \rho \ell}{V^2 A} \cdot K_e$$

$$M_t = I^2R \cdot K_t = \frac{P^2 \rho \ell}{V^2 A} \cdot K_t$$

$$M_c = I^2R \cdot K_c = \frac{P^2 \rho \ell}{V^2 A} \cdot K_c$$

Summing these terms for the total mass yields an interesting equation:

$$\begin{aligned} M \text{ trans} &= M_w + M_p + M_e + M_t + M_c \\ &= \sigma A \ell + I^2R \, (K_p + K_e + K_t + K_c) \\ &= \sigma A \ell + \frac{P^2 \rho \ell}{V^2 A} \, (k_p + K_e + K_t + K_c) \end{aligned}$$

Note that the factor $(K_p + K_e + K_t + K_c)$ is not a function of the transmission conductor area (A). Hence, differentiating with respect to A, setting the result equal to zero, and solving for A yields the optimum-mass cross-sectional area (A_o) for transmission conductors:

$$\frac{d \, (M \text{ trans})}{d \, A} = \sigma \ell - \frac{P^2}{V^2} \, \frac{\rho \ell}{A^2} \, (K_p + K_e + K_t + K_c) = 0$$

$$A_o = \frac{P}{V} \sqrt{\frac{\rho}{\sigma} \, (K_p + K_e + K_t + K_c)}$$

$$A_o = \frac{P}{V} \sqrt{\frac{\rho}{\sigma} \, (\text{factor})} = \frac{P}{V} \sqrt{\frac{\rho f}{\sigma}}$$

where "factor" (f) is the sum of the mass performance parameters (pounds/watt) for power loss support (power, energy, thermal, conversion). Note that the optimum conductor corss-section is dependent upon power level (P), transmission voltage (V), and conductor material (ρ,σ). Length (ℓ) does not enter into the solution for optimum conductor cross-sectional area!

A number of interesting relationships evolve from the optimum wire derivation. At optimum cross section (A_o):

1. the conductor mass is proportional to current and length:

$$M_w = \sigma A_o \ell = \frac{P\ell}{V}\sqrt{\rho\sigma f} = I\sqrt{\rho\sigma f}$$

2. the total system mass for power transmission is twice the conductor mass:

$$M\ \text{trans} = \sigma A_o \ell + \frac{P^2\rho\ell f}{V^2 A_o} = 2\frac{P\ell}{V}\sqrt{\rho\sigma f} = 2I\ell\sqrt{\rho\sigma f}$$

3. the voltage drop (ΔV) is independent of power or transmission voltage and is a constant per unit length:

$$\Delta V = IR = \frac{P}{V}\cdot\frac{\rho\ell}{A_o} = \ell\sqrt{\frac{\rho\sigma}{f}}$$

$$\Delta V/\ell = \sqrt{\frac{\rho\sigma}{f}}$$

4. the transmission conductor losses are proportional to current (I), not the square of the current:

$$I^2R = \frac{P}{V^2}\cdot\frac{\rho\ell}{A_o} = \frac{P\ell}{V}\sqrt{\frac{\rho\ell}{f}} = I\ell\sqrt{\frac{\rho\sigma}{f}}$$

The expression $\sqrt{\rho\sigma}$ occurs in the solutions for transmission conductor mass (M_w), total transmission mass (M_{trans}), regulation (Δv), and conductor losses (I^2R). These parameters, resistivity (ρ) and density (σ), are

material properties, and the product $\rho\sigma$ should be minimized* to improve transmission attributes (reduced mass, better regulation, lower losses).

Conductor Materials

A preliminary comparion of the $\sqrt{\rho\sigma}$ figure of merit shows six materials to be potentially superior to copper at 20 C (Table 3-4). However, sodium and lithium have low melting temperatures, and hence they are vulnerable to hostile threats (laser weapons). In addition, these are highly reactive elements and would require some protective sheath for fabrication and assembly in terrestrial humid environments. Sodium and lithium become molten at elevated temperatures (Table 3-4). Containing these liquid metals as electrical conductors, allowing for thermal expansion and contraction, and maintaining electrical continuity (precluding voids in the molten metals during cooling cycles) becomes difficult. Potential engineering solutions to these problems would cause a greater penalty than using aluminum conductors.

Aluminum, third ranked in $\sqrt{\rho\sigma}$ property, is very attractive. Cadmium sublimes in space vacuum environment, will subsequently deposit onto other surfaces, and hence is an undesirable spacecraft material. Magnesium is not as attractive as aluminum, ($\sqrt{\rho\sigma}$ value), is more difficult to fabricate and assemble than aluminum, and can be potential fire hazard. Beryllium is a difficult material to fabricate, is highly toxic, and is not as attractive as aluminum. Hence, aluminum is the material of principal interest.

At elevated temperatures (for example, 1000 R = 540 F = 556 K = 283 C), aluminum remains the desirable conductor material based upon its $\sqrt{\rho\sigma}$ characteristic (Table 3-5). The resistivity of beryllium increases faster than aluminum (Figure 3-29) and aluminum remains superior to beryllium in its $\sqrt{\rho\sigma}$ value (Table 3-6). The resistivities of silver and copper increase at lower rates than aluminum or beryllium (Figure 3-29),

*Other analyses have suggested $\sqrt{\sigma/\rho}$ as the figure of merit for material selection, (e.g., IECEC paper 869381). These analyses optimize conductor area, not total system mass.

Table 3-4. Conductor Material Comparison

Conductor Material	Melting Temp. °C	At 20°C			
		Resistivity ρ:μ·ohm·cm	Density σ: gm/cc	Figure of Merit $\sqrt{\rho\sigma}$	Relative Conductor Mass
Sodium	98	4.6	0.97	2.11	0.79
Lithium	180	9.3	0.53	2.22	0.83
Aluminum	660	2.67	2.7	2.66	1.00
Cadmium	320	7.5	8.67	2.74	1.03
Magnesium	650	4.46	1.74	2.79	1.05
Beryllium	1283	4.57	1.8	2.87	1.08
Copper	1083	1.69	8.92	3.88	1.46
Silver	900	1.62	10.5	4.12	1.55
Graphite	3500	1400	2.26	56.1	21.1

Source: Handbook of Chemistry, N.A. Lange, ed., Handbook Publishers, Inc., 1956

Table 3-5. Aluminum Remains Attractive at High Temperatures

	At 1000°R (540°F, 556°K, 283°C)			
Conductor Material	Resistivity ρ: μ ohm-cm	Density* σ: gm/cc	Figure of Merit $\sqrt{\rho\sigma}$	Relative Conductor Mass
Aluminum	5.6	2.7	3.9	1.00
Beryllium	10.0	1.8	4.2	1.08
Copper	3.2	8.92	5.3	1.36
Silver	3.3	10.5	5.9	1.51

*20°C

Source: Handbook of Thermophysical Properties of Solid Materials, Revised Edition, Volume 1, Elements, A. Goldsmith, et.al., The MacMillan Company, New York, 1961.

Table 3-6. Aluminum is Attractive at Cryogenic Temperatures

Conductor Material	Application Temp. °K	Resistivity ρ μ:ohm:cm	Density* σ gm/cc	Figure of Merit $\rho\sigma$	Relative Conductor Mass
Beryllium	50	0.007	1.8	0.11	0.69
Aluminum		0.01	2.7	0.16	1.00
Copper		0.01	8.92	0.30	1.88
Cadmium		1.00	8.65	2.9	18.1
Aluminum	20	0.002	2.7	0.07	1.00
Beryllium		0.006	1.8	0.10	1.43
Copper		0.008	8.92	0.27	3.86
Cadmium		0.2	8.65	0.93	13.3
Aluminum	4	0.0002	2.7	0.023	1.00
Cadmium		0.0001	8.65	0.03	1.30
Copper		0.0004	8.92	0.06	2.61
Beryllium		0.006	1.8	0.10	4.35

Extracted from Figure 5.

*at 20°C (293°K).

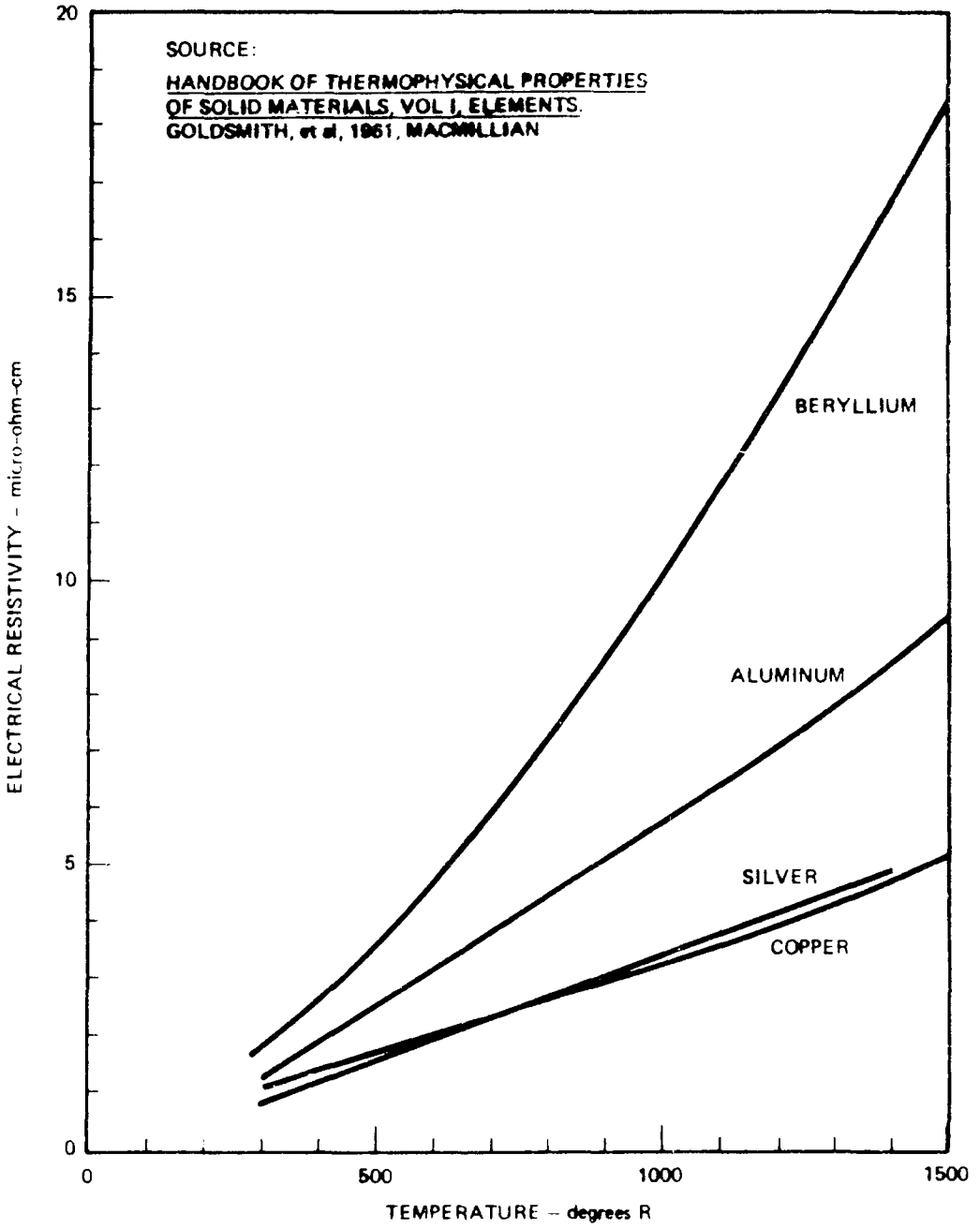

Figure 3-29. High Temperature Resistivity

but the high mass densities of silver and copper produce inferior values for their $\sqrt{\rho\sigma}$ characteristics. Other materials exhibiting negative resistivity properties, remain orders of magnitude above the resistivities of aluminum and beryllium (Figure 3-30), and their $\sqrt{\rho\sigma}$ characteristics are not attractive.

Four elements, aluminum, beryllium, cadmium, and copper, exhibit greatly reduced resistivities at cryogenic temperatures (Figure 3-31). For various DEW applications, cryogenic coolant (cold gaseous hydrogen) may be available in copious amounts. Cryogenic cooling of conductors then becomes attractive.

At these reduced temperatures, aluminum remains the more desirable material (Table 3-6), but it is somewhat dependent upon the material purity for best enhancement of conductivity (Figure 3-32).

3.4.2 Systems Study. A study of various systems was conducted to provide an estimating tool for calculating weights for the various systems discussed later in Section 5. Table 3-7 shows the algorithms used. The following were the assumptions made for each of the systems analyzed.

Assumptions and Comments

Pure Aluminum Conductors. This type of conductor is assumed to operate in the cryogenic temperature regime at about 50 K. The voltage is assumed to be on the order of 100 volts which indicates that the cryogenic hydrogen gas enveloping the conductor should serve as an adequate insulator. The resistivity of the material is assumed to be 5.6E-11 ohm-meters. This is the resistivity of the super-pure filaments plus matrix, and is the value given in the report "Cryogenic Aluminum-Wound Generator Concept for Nuclear Power Conversion." The density is assumed to be 2950 kg/cubic meter, which value is also taken from the report. It seems likely that continued development of this material should result in increased conductivity by increasing the portion of super-pure aluminum in the matrix. This development would decrease the slope of the curve of mass versus current, but would not lower the zero current initial point, which is fixed by the mass of the gas piping required, as shown in the second graph. This curve assumes two cryogenic

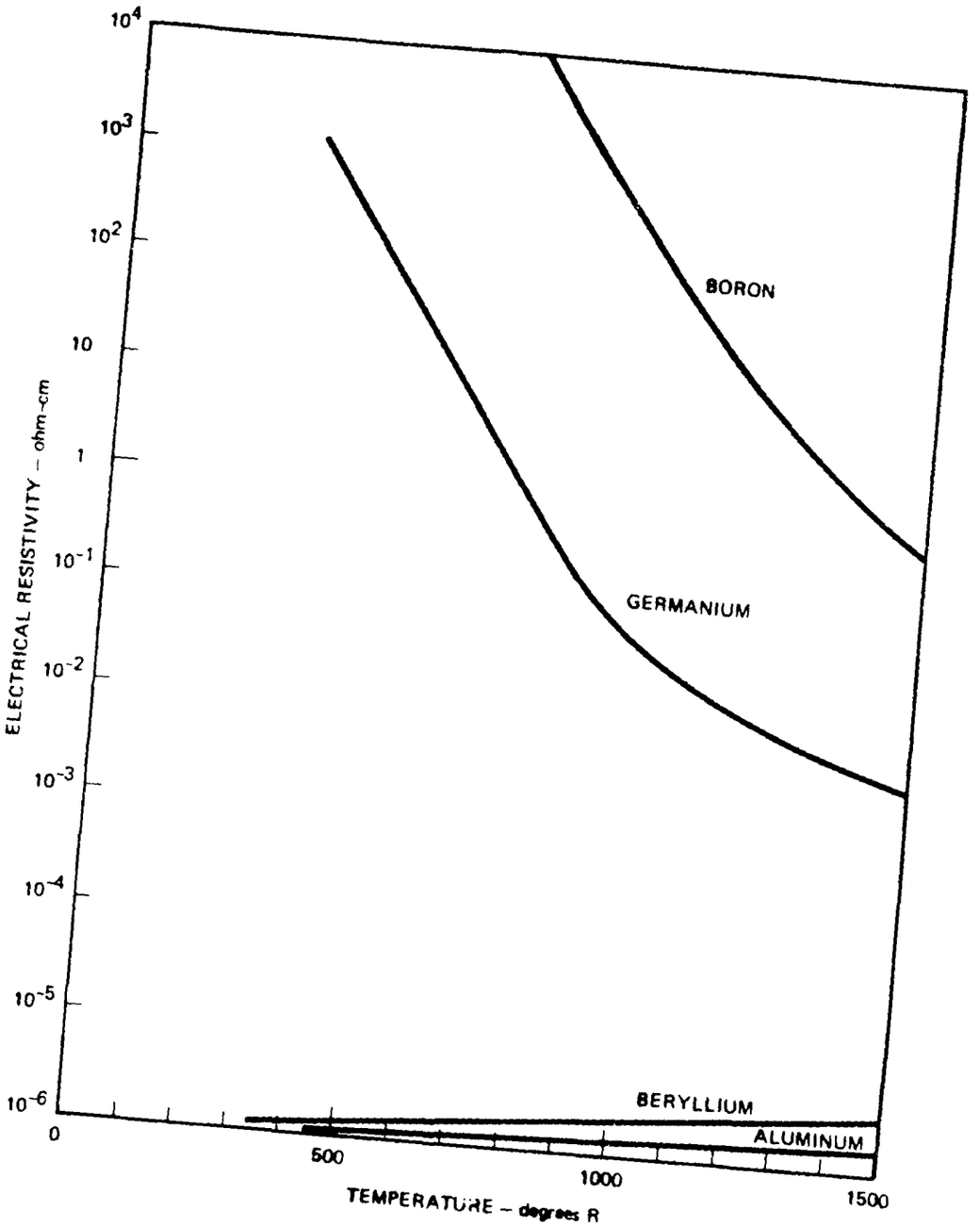

Figure 3-30. Negative Resistance Materials Have High Resistivity

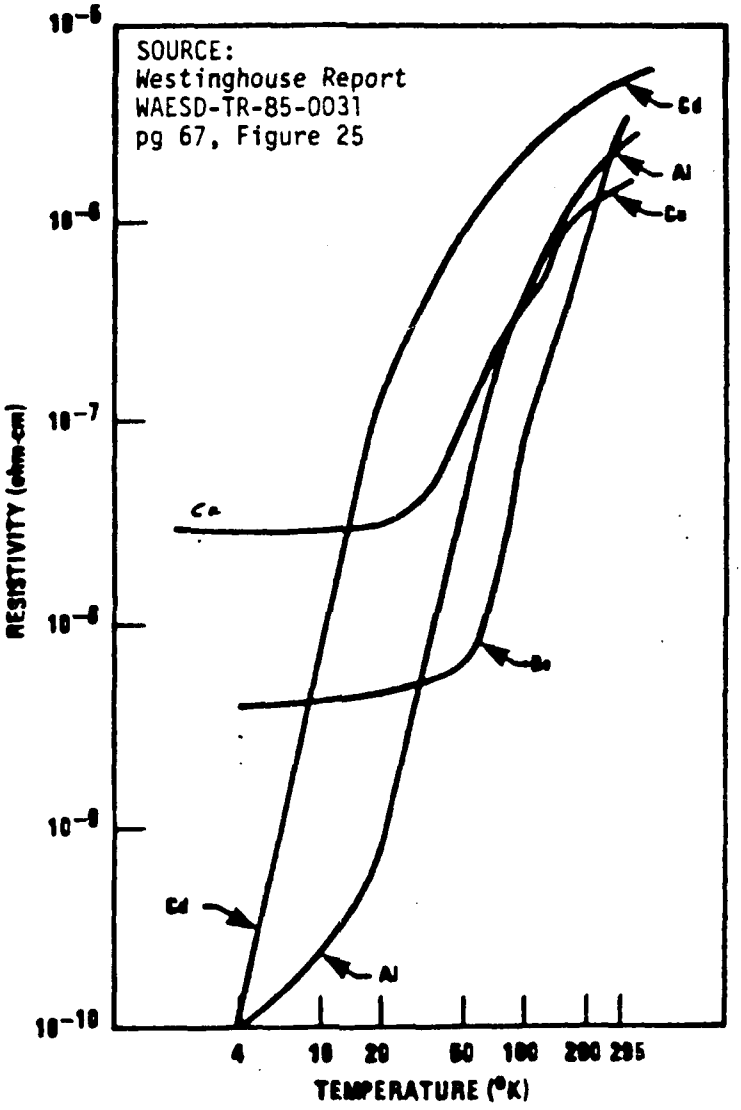

Figure 3-31. Cryogenic Temperatures Greatly Enhance Conductivity

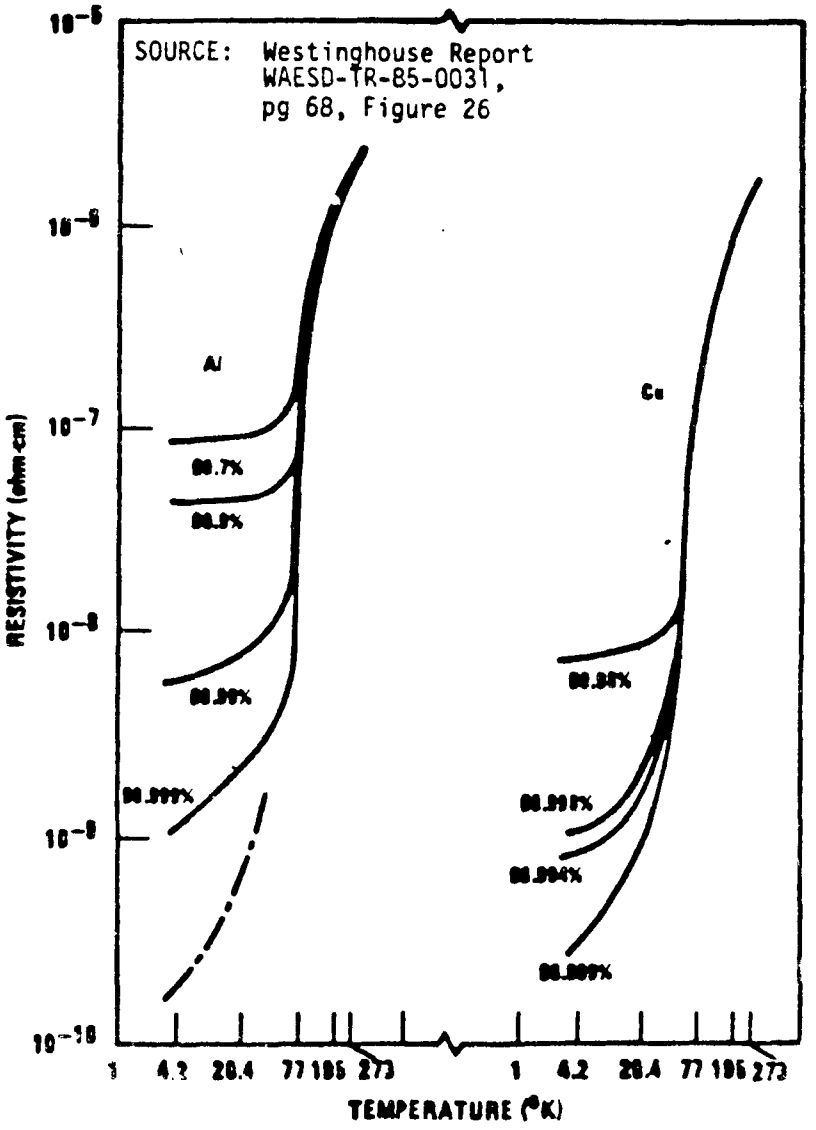

Figure 3-32. Conductivity at Cryogenic Temperatures is Enhanced by Very High Purity

Table 3-7. Algorithms for Transmission Line Study

Super-Pure A_C

$$\Delta M_T = A\rho\ell + \frac{I^2\sigma\ell f}{Ac}$$

Cooled Dc

$$\Delta M_T = 2\rho\ell\left(A_c + A_g\right)\left[\frac{2p}{S} - \left(\frac{P}{S}\right)^2\right] + \frac{I^2 f\sigma\ell}{A_c}$$

Cooled 3-c AC

$$\Delta M_T = \frac{3\rho\ell\ PA_c^{\ 2}}{2\pi\delta^2 S} + \frac{3A_c\rho\sigma\ell}{SI_{Nc}D_s} + \frac{I_{DC}^2\sigma\ell f}{A_c}$$

Uncooled AC

$$\Delta M_T = 3t\rho\ell\ \frac{\left(A_c + \pi\delta^2\right)}{\delta} + \frac{3\ P\alpha\ell\ \left(A_c + \pi\delta^2\right)}{\delta I_{Nc}D_s} + \frac{I_{DC}^2\sigma\ell f}{A_c}$$

Uncooled DC

$$\Delta M_T = 2\rho\ell A_c + 4\sqrt{\pi A_c}\ \frac{P\alpha\ell}{I_{Nc}D_s} + 2\ \frac{I_{DC}^2\sigma\ell f}{A_c}$$

ρ = density A P = power f = kg/watt factor

α = density Kapton p = pressure I = current

ℓ = 50 meter D_S = dielectric strength δ = skin depth

σ = conductivity S = material strength

gas pipes are used, one for each line of the dc circuit. These pipes are sized to withstand approximately 550 psi. Two pipes were assumed because it would require less structure inside the pipe, and hence less flow turbulence. It also decreases the chance of arcs between lines through the cryogenic hydrogen. This particular design WOULD NOT serve for ac systems due to skin effect. Plating the super-pure material onto the outside of a supporting material or imbedding it in a dielectric material will be necessary to apply this type of conductor to an ac system. Note that this curve assumes power is constant and varies the system voltage accordingly.

Cryogenic dc System. This system utilizes the walls of the cryogenic gas piping as the power conduction line. It assumes a density of 2700 kg/ cubic meter for aluminum. The resistivity is on the order of 1E-10 ohm-meter at the cryogenic operating temperature. A coaxial arrangement was assumed since this eliminates interactions of the system with the ambient magnetic field of the earth, and eliminates the need for insulation in addition to the hydrogen gas. This system is assumed to be operating in the neighborhood of 100 volts, which means no insulation of the inner conductor should be required since the gaseous hydrogen will be able to withstand that much voltage. This conclusion is based on the Paschen curve for gaseous hydrogen at room tempera- ture which indicates that hydrogen at the pressures to be used here (550 psi) should be capable of holding off 300 to 500 volts/millimeter easily. Also, we assume that the outer conductor can be system ground, which means that no insulation will be required for this system. Note that this curve assumes power is constant and varies the voltage of the system accordingly.

Uncooled dc System. This system is intended for high voltage, low current dc applications. It consists of two solid conductors that are assumed to have circular cross section. This provides the lowest surface area and hence the least insulator weight. It assumes the same material properties as the other systems, except the resistivity is 2.67E-8 ohm-meters. Note that this curve assumes power is constant.

Uncooled ac System. This system is intended for high voltage, low current applications. It assumes the conductor and insulator properties of the other systems, except the resistivity is now 2.67E-8 ohmmeters. The

conductors are configured as tubes with the thickness determined by structural needs rather than by electrical requirements since the skin depth is only about four millimeters. Five millimeters were assumed for this curve. This system is three phase ac and assumes one triplet of conductors with insulation on each line. Again, this curve assumes constant power with the voltage varied accordingly as a function of current.

Cooled ac System. This system is intended for high voltage, moderate current applications. It consists of a triplet of conducting pipes which carry cryogenic hydrogen coolant. Each pipe is insulated. The material parameters are the same as the other systems except the resistivity is the cryogenic value of 1E-10 ohm-meters. Since these pipes must carry the gaseous hydrogen for other purposes, there is a minimum material requirement in order to provide the gas transport. This minimum requirement determines the system weight up to a current of approximately 1000 amps. At this point, the required conducting surface for a mass-effective system drives the system weight. This system assumes constant power and varies the applied voltage accordingly as a function of the current.

Comments. The environmental effects problems of these systems are varied. The low voltage, high current systems should not require major new technologies to control the problems of plasma arcing and corona due to the low operating voltage. On the other hand, the enormous current flow could pose a major problem due to magnetic torque and interactions with other systems on the spacecraft. Though the system mass may be higher for a cooled coaxial conductor, it does have one significant advantage in that the magnetic effects of this configuration should be easily manageable, especially compared to the two conductor super-pure aluminum system. It may be advantageous to explore the possibility of producing super-pure material. Several points have not been examined so far for these two high current dc systems. The structure problems involved in pulsing these high

currents have not been examined. There may be an additional synergistic effect with the coaxial system in that the high currents will exert compressive forces on the pipe walls. If it were possible to somehow cool the walls and establish the high current flow before bringing the pipe up to full gas pressure, this compressive force may allow thinner pipe walls for a given diameter.

The high voltage systems should not have significant magnetic interaction problems, but we will need to solve major problems with arcing and corona. Also, the ac systems could experience losses due to energy coupling into the plasma environment. This occurs due to the existence of natural vibrational modes in the plasma that could be excited by the ac current flow and draw energy from the system. This phenomenon, like all other plasma associated problems, is orbit dependent. The best method of solving the arcing problem appears to be encasing the system in a conducting enclosure. This could cause other problems, however, due to outgassing of the system which could actually create a worse arcing environment than the ambient plasma. The best way of dealing with this problem is to pressurize the areas of concern such as switch gear, etc. This pressurization would probably not be done until the moment of operation since trying to keep a vessel under pressure for years would be difficult at best, and pressurizing and venting after an alert phase carries the problem of sizing the supply of pressurizing material for the number of alerts possible. Pumping of an enclosure to remove out-gassed material during operation is not deemed practical for several reasons. First of all, every high vacuum technology that I am familiar with is not reliable at startup. Most devices require some tinkering when first started to ensure proper operation. General laboratory practice is to leave the pump on once started and just close it off when the vacuum chamber is to be opened. Secondly, it may require an enormous pump to handle the possible outgassing during operation. Even a small hydrogen leak into an enclosure could overwhelm a good sized vacuum pump.

3.4.3 Study Results. Figure 3-33 shows the results for low-level values of current (less than a few thousand amperes). A key conclusion is that the break point between uncooled and cooled conductors is quite low,

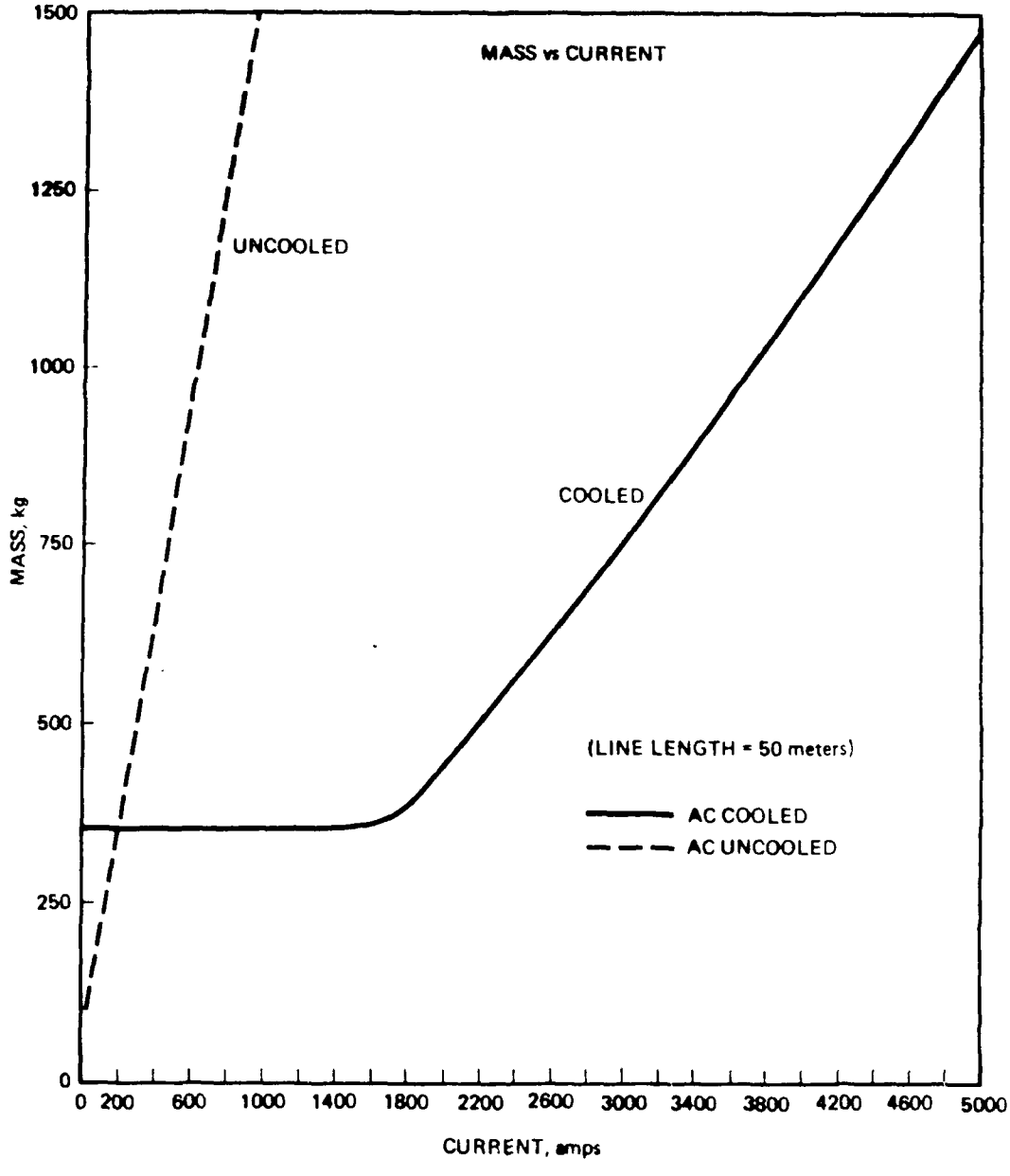

Figure 3-33. Transmission Line Weight (Low Current)

about 200 amperes in the figure cited. Note that the weight of the cooled line does not go to zero at zero amperes. This is because there is a minimum amount of piping, fluid connections, and accessories needed for any cooled line, regardless of current. This minimum weight line appears to hold up to about 1600 amps, where the weight starts to be proportional to current. Figure 3-34 shows typical cooling concepts. Figure 3-35 shows the results for large values of current, all for dc cooled lines. (There are no high current ac lines).

3.5 Control and Protection. Because of time limitations, study of system control problems was restricted. The following topics are of principal interest:

1. Voltage control and regulation
2. Transients and upset
3. Load subdivision and protection.

Voltage Control and Regulation. Throughout this study, it has been assumed that voltage can be controlled at the system (generation) level, and that extensive or precise regulation at the load level is not required. In fact, this suggests that payload implementation, e.g., selection of an RF supply, should be strongly guided by this requirement. Tubes that require minimal regulation should be selected over those requiring precise control, even at some price in efficiency, which could be traded off. Devices that require only a small portion of their feed to be regulated would be preferred over those requiring a large amount of regulated supply. In the case of the klystrode, the manufacturer states that the required regulation can probably be performed using the RF feed, thus nearly eliminating regulation of the bulk power.

Wherever rectifiers and inverters are shown in the systems of Section 5, it is assumed that these are gate turnoff devices, or equivalent, so that some regulation can be included without significant weight addition.

Transients and Upsets. Problems of this nature are usually design-specific, and have not been evaluated in this study, which is by nature more general than specific.

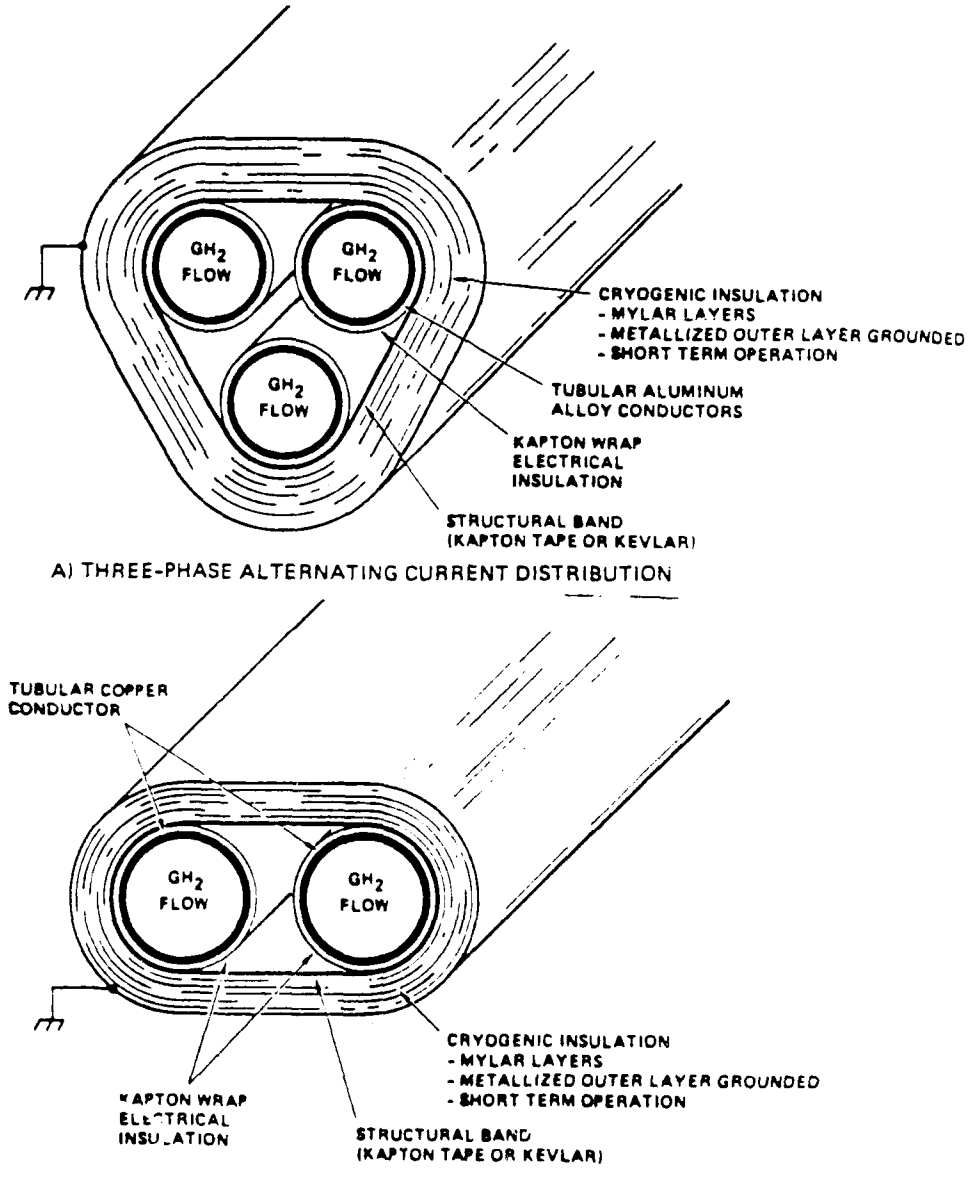

Figure 3-34. Transmission Conductor Concepts

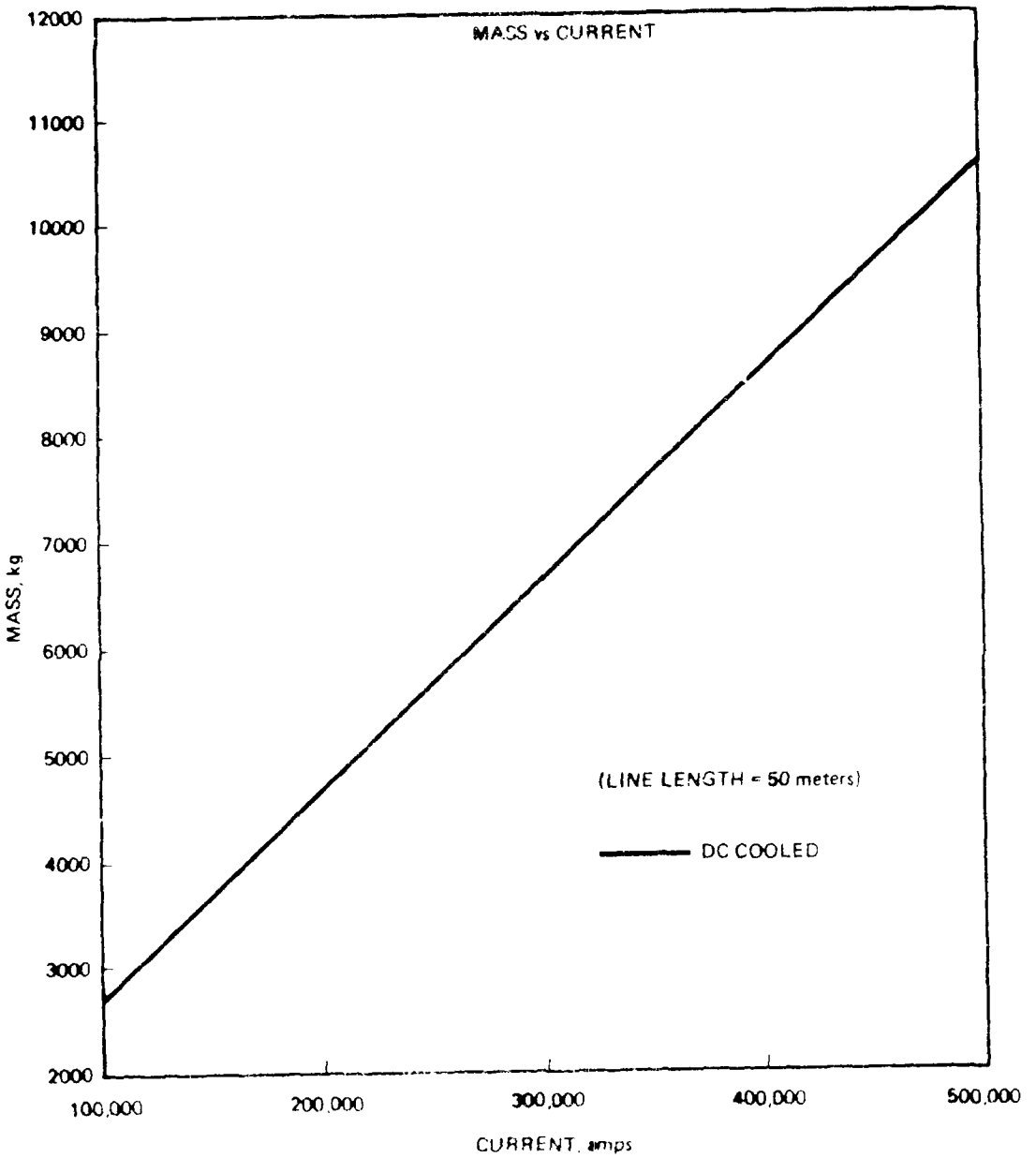

Figure 3.35. Transmission Line Weights (High Current)

Load Subdivision and Protection. Load subdivision also is somewhat design-specific, but generally we can conclude that all loads will be subdivided to some extent, and that all generation supplies will be subdivided, either from design constraints or the desire for redundancy. For example, all rotating machines will be configured in contra-rotating pairs to minimize torque unbalance on the space platform.

It is not clear how the various payloads will react to loss of part of their power supply. For some FELs their designers will accept some loss of RF power without unacceptable beam degradation. The weapon would be usable, although the target might have to be illuminated slightly longer to achieve the desired degree of damage. For kinetic energy weapons, loss of portions of the power supply or pulse-forming network might cause an unacceptable reduction in projectile range.

The directed energy weapons require direct current electrical power which is transformed into RF (~500 MHz) to drive the linear accelerators for FEL and NPB weapons. Klystrons, klystrodes, and crossed-field devices are typical candidates for this conversion. These devices use very high voltage (30,000 to > 100,000) for electron beam generation and control. Occasionally (perhaps often) these devices will arc. In this event, interruption of current flow is required to extinguish the arc, to save the device from destruction, and to protect the power source. Operational recovery is typically possible upon reapplication of power.

This phenomenon constrains power distribution designs to provide fault (arc over) detection and recovery either at the system level (at the power source) or at each device (klystron, klystrode, etc). Typically, this arc protection is designed into the individual power conditioners for traveling wave tube amplifiers on present satellites.

Protection is relatively easily accommodated by using gate controlled rectifiers and incorporating half cycle fault protection. That is, fault current may flow for only one-half cycle until reverse polarity causes interruption of rectification and extinction of the arc. Recovery by interrupting the high voltage direct current requires special design considerations and may lead to large or unreliable fault protection devices. Hence, fault protection is desirable at alternating current locations.

Fault protection can be incorporated at each RF device or centrally at the power generation source. Central rectification (incorporating fault protection) and distribution of 100,000 volt direct current for the RF devices will result in loss of whole groups of RF devices for one device fault and loss of significant DEW beam power.

The consideration of fault protection favors distributing alternating current to each RF device (klystron, klystrode, etc), rectifying at each RF device, and incorporating fault detection and isolation in the rectification devices for each RF device. This approach minimizes the effect on the DEW of an RF device failure (temporary or permanent), is consistent with rectification technology, and avoids the difficult technology needed to interrupt very high voltage and power direct current.

For systems using rectifiers or inverters, it is assumed that overload protection of the load segment downstream of the rectifier/inverter will be accomplished by using the turnoff features of the semiconductors selected. Thus, most of the systems shown in Section 5 do not include load switching circuit breakers or sectionalizing switches.

The use of circuit breakers or fuses in the system is much more controversial among power system designers. The principal investigator feels that a main generator circuit breaker will be inevitable, both for testing and for system restoration after a hit or a short circuit in one of the unit loads. It is envisioned that this circuit breaker would be of the reclosing type, opening only to permit clearing a shorted load, then reclosing rapidly to re-energize the remaining load. This, of course, presumes that the payload can still operate with a portion of the system shut down. Note that other investigators believe such circuit breakers can (and should) be eliminated from the design. Fuses are even more controversial because they are one-shot devices, and have a history of sometimes opening when least desired. Perhaps the judicial use of explosively-activated disconnects would provide an alternate to fuses or circuit breakers for isolating loads shorted or damaged beyond further use.

4. THERMAL AND ENVIRONMENTAL EFFECTS

4.1 Thermal Effects. Thermal effects can be categorized as follows:

1. Heat dissipation
2. Synergistic designs
3. Thermal interface control

Of the above three categories, the first, heat dissipation, has been studied in considerable detail. Information is available in the literature on radiators, heat pipes, heat exchangers, and all the other accoutrements of heat transfer in space vehicles.

The application of synergistic designs has received much less attention on the multimegawatt level. The ISTESA report (Ref. 1) suggested that onboard liquid hydrogen used for weapons cooling and/or fuel for a combustion turbine could also be used to cool the transmission lines and other ancillary equipment. This study continues that train of thought, since in most cases, synergistic use of hydrogen leads to a lower weight design than strict reliance on radiators.

One slightly surprising fallout of this study was that thermal interfaces may be very significant design problems in high powered spacecraft. In most cases, extreme thermal differences do not exist in terrestrial power systems. Most electrical systems operate at or slightly above ambient temperatures, and interface delta Ts are usually negligible. Interest in this problem evolved from the study of a system using the THOR reactor concept powering an FEL weapon. We suddenly realized that we were coupling a 1100 K generator to a 5 K accelerator, with several major swings in between. Figure 4-1 shows the situation. As the system design evolved, the major design choices involved the following:

1. A thermionic reactor operating in the 1100 K range.
2. A hydrogen-cooled transmission line, as the current was in the kiloampere range. This line would operate at perhaps 50 K.

3. A dc/dc converter to step the 5 kV dc supply to the 140 kV needed for the RF generator. This converter would prefer to operate in the 300 K range, although it could operate as lowas -60 C (213 K).

4. A klystrode RF amplifier that dumped 20 percent of its total input power to the collector. To remove this heat, either by hydrogen cooling or heat-pipe radiator, a collector temperature of 700 K is likely.

5. A superconducting accelerator cavity operating at liquid helium temperatures, 4 to 6 K. Moreover, the low temperature cavity is connected directly by waveguide to the hot klystrode. The size of the waveguide is about 7 x15 inches, the equivalent of a small air conditioning duct.

The design that evolved is shown in Figures 4-1 and 4-2. The exit electrical connectors (termed a "getaway" in terrestrial utility parlance) would be uncooled. They would be connected to the cryocooled transmission line through a "thermal anchor," a controlled heat leak that would be maintained at about 400 K and serve as a means of separating the very hot getaway from the very cool transmission line. On the other end, effluent hydrogen from the jacket around the helium-cooled accelerator would be used to cool the transmission line and the dc/dc converter. The klystrode collector would be radiation cooled, rather than hydrogen cooled, since the effluent hydrogen goes to a lithium tank in order to eliminate any effluents from the total system. Another concern is the loss of heat from the cavity through the waveguide during long standby periods.

The case of the turbogenerator powered FEL is a little less formidable, as shown in Figures 4-3 and 4-4. At the generator end, the interface is simple since the generator is assumed to be cryocooled also. At the klystrode, the collector can be hydrogen cooled, since all the hydrogen eventually goes to the turbine combustor, so temperatures and effluents are not an issue in this case.

4.2 Environmental Effects. Figure 4-5 summarizes the environmental effects surrounding any spacecraft. From a power distribution standpoint, the principal item of concern is the thermal plasma, which can cause arc-over of any exposed parts. While spacecraft are commonly operated at 28 vdc with exposed electrical terminals, most environmental experts predict problems in the 100 to 200 volt range. Since all the systems discussed or

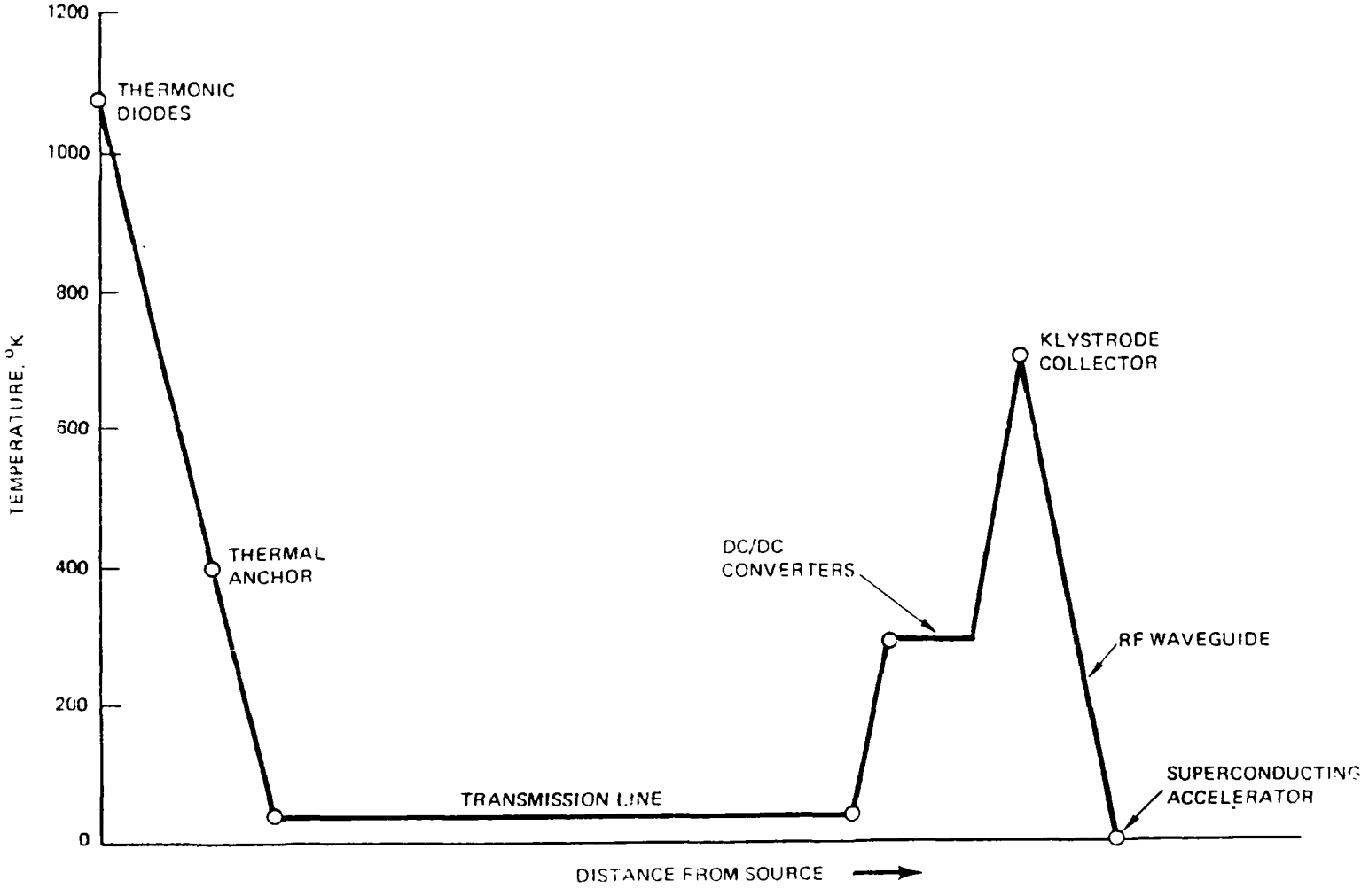

Figure 4-1. Thermal Gradients, THOR Concept

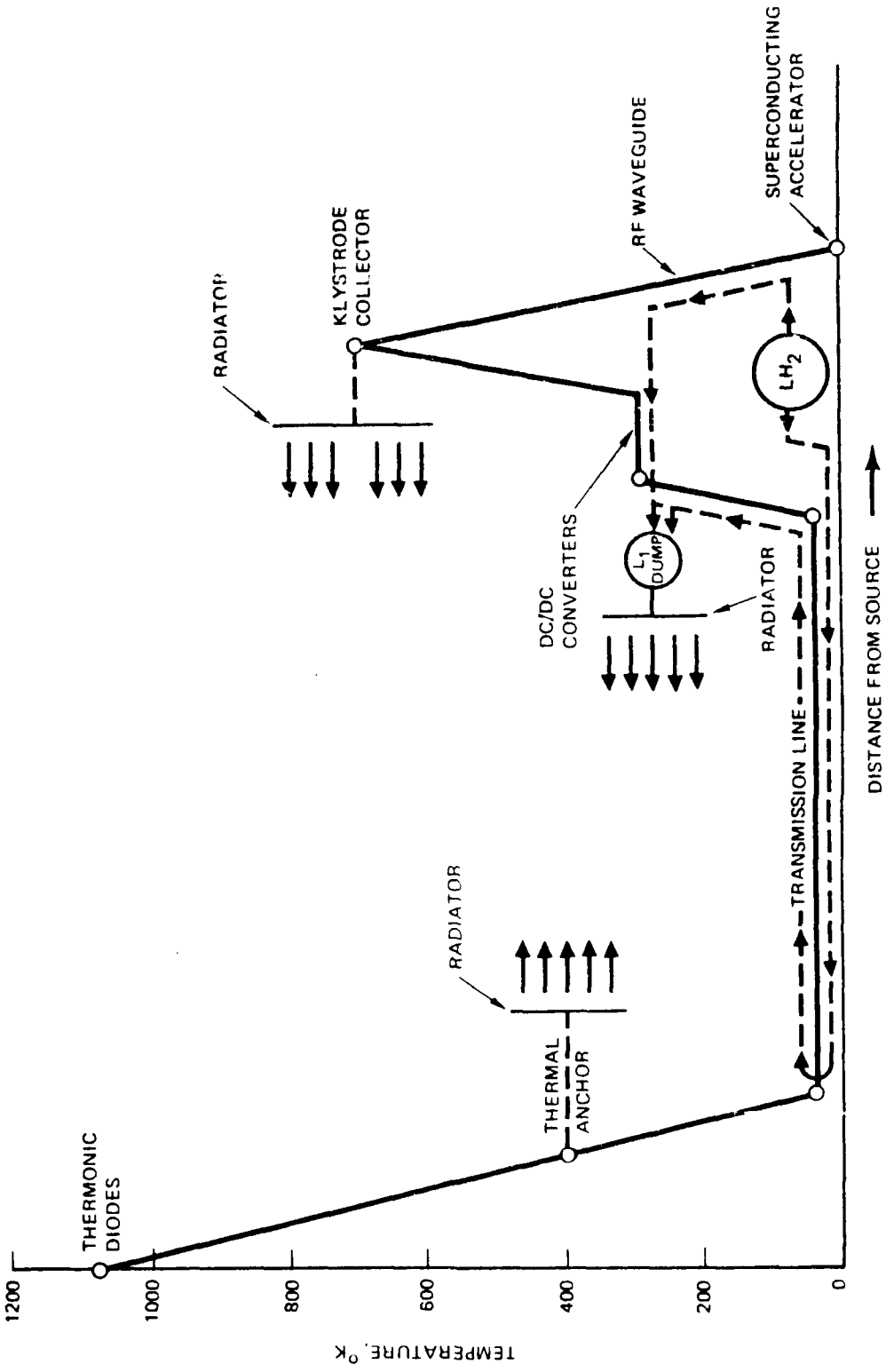

Figure 4-2. Thermal Gradients, THOR Concept, with Cooling

M2-011-88

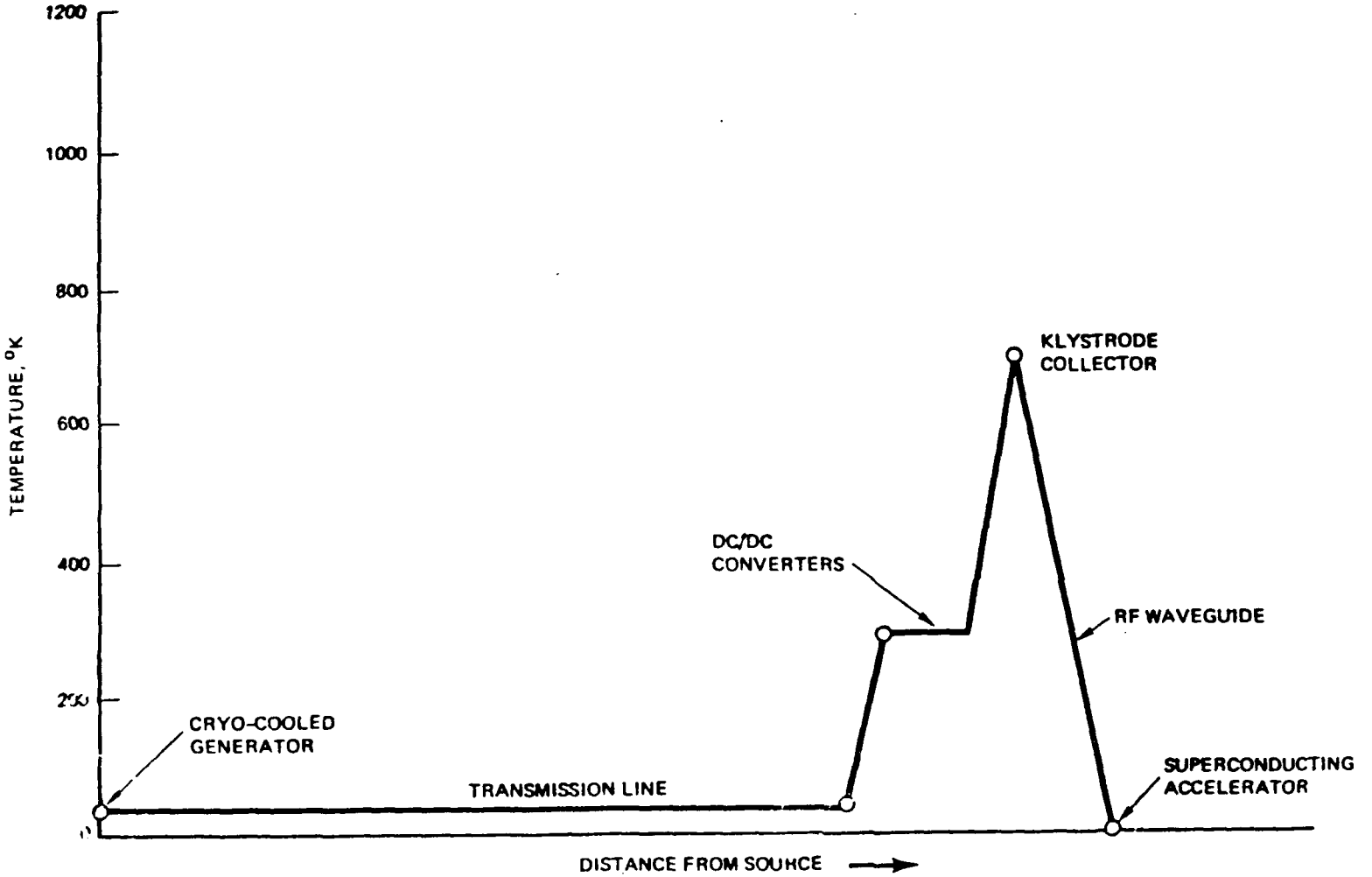

Figure 4-3. Thermal Gradients, Turbogenerator Concept

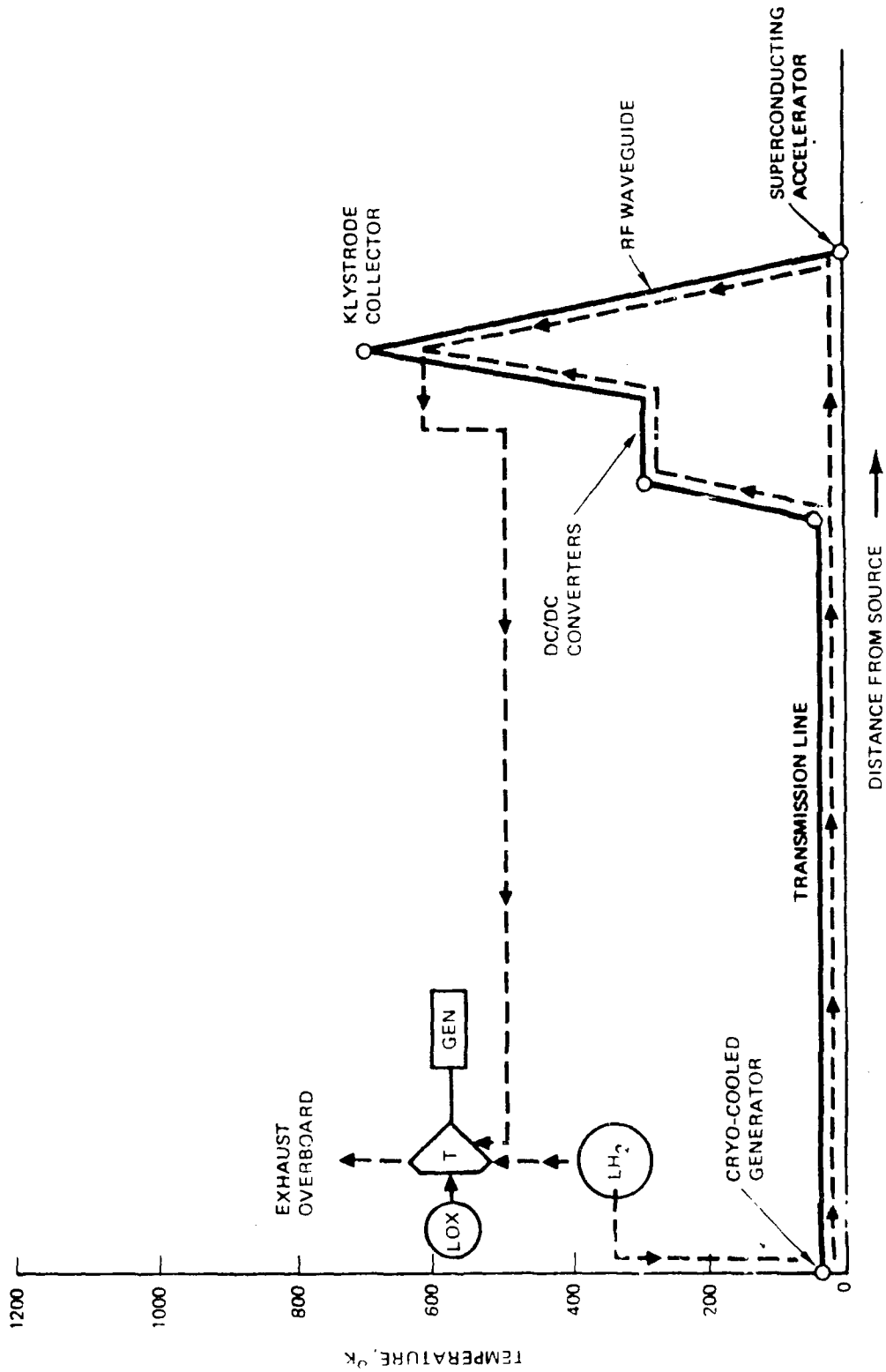

Figure 4-4. Thermal Gradients, Turbogenerator Concept, With Cooling

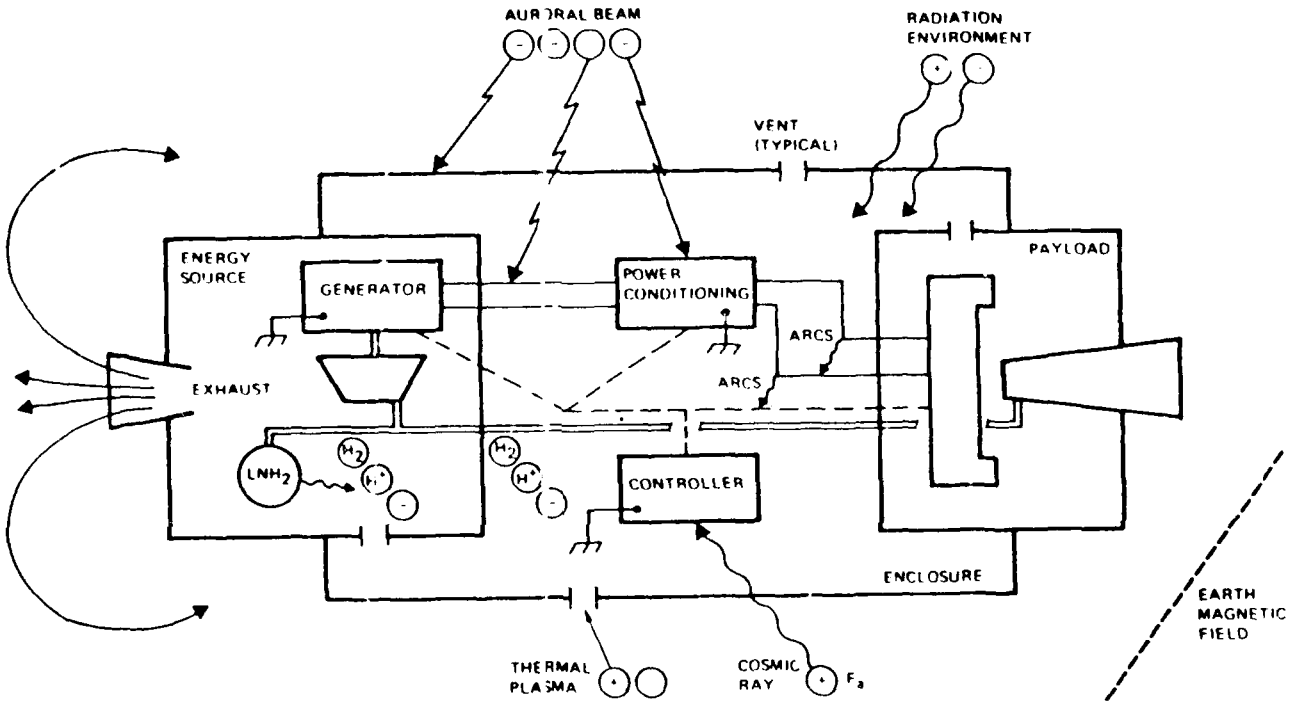

ENVIRONMENTAL PROBLEMS	SYSTEM EFFECTS	MITIGATION
THERMAL PLASMA	ARCING OF EXPOSED HV PARTS	FARADAY CAGES OR COMPLETE INSULATION
CHARGING PLASMA	SURFACE CHARGING, ARCS, COMPUTER UPSETS	CONDUCTIVE SURFACES, SHIELDING
ENERGETIC PLASMA	RADIATION DAMAGE	HARDENED COMPONENTS
EXHAUST	SURFACE CONTAMINATION WEAPON INTERFERENCE	CLOSED-CYCLE SYSTEMS

Figure 4-5. Environmental Effects

contemplated in this study are above (and some considerably above) this level, it appears to be a hard requirement that all exposed electrical leads be completely shielded from space plasma. This means fully insulated transmission and distribution lines, completely enclosed rectifiers, inverters, transformers, circuit breakers, and connection boxes. In addition, some of these devices may require insulating gas, e.g., SF6, within the enclosures to provide adequate insulation. The SPEAR test series (Space Power Experiments Aboard Rocket), initiated in late 1987, may provide useful data to address this problem.

For more information on space environmental effects, see Reference 5.

5. SYSTEMS STUDIED

The basic study matrix that was used in this effort is shown in Figure 5-1. As the figure shows, when using an alternating current generator as the source, there are basically three transmission options: 1. Transmit at generated voltage. 2. Step up the generated voltage using a transformer. 3. Convert the ac to dc and transmit as dc. With dc generation, the choices are more limited; practically, the only choice is to transmit at generated voltage since dc/ac or dc/dc converters are so heavy. The final selection in the study was to locate fuel cells in clusters directly at the load. Thus, the "transmission" becomes one of fuel and oxidizer rather than of electricity. This latter approach also has improved redundancy over the previous cases, since the fuel cell source lends itself to subdivision, while the other generators tend to be large and centrally located.

The interaction between the generation/transmission system and the loads is also shown in Figure 5-1. Note that certain loads can be served many ways, while others (notably the inductor storage EML system) are not as flexible. The following sections discuss the various cases in detail.

5.1 Very High Voltage (VHV) Systems. These systems are designed to exploit the use of 2 MW klystrode tubes (see Section 3.1) which require a dc voltage of about 140 kV. This high voltage can be achieved in a number of ways, and eight systems were studied.

Figure 5-2. This system uses a state-of-the-art ac generator similar to the GE superconducting rotor design now on test at AFWAL (Ref. 8). This study assumes that the GE unit can be scaled up from 20 to 50 MW, and the

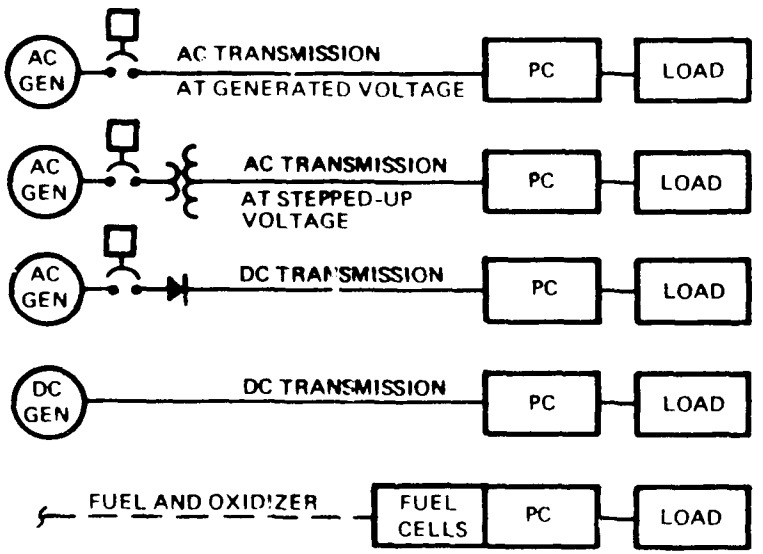

LOADS					CASES STUDIED
VHV TUBE	MHV TUBE	LV SEMICON-DUCTOR	EML-INDUC-TOR	EML CAPAC-ITOR	
X	X	X		X	VHV-1, 5 MHV-2 LVRF-2
X					VHV-2, 3, 4
X	X				VHV-6 MHV-1,3
X	X		X	X	VHV-7 EML-1, 2
X	X	X			VHV-8 LVRF-3

Figure 5-1. Study Matrix

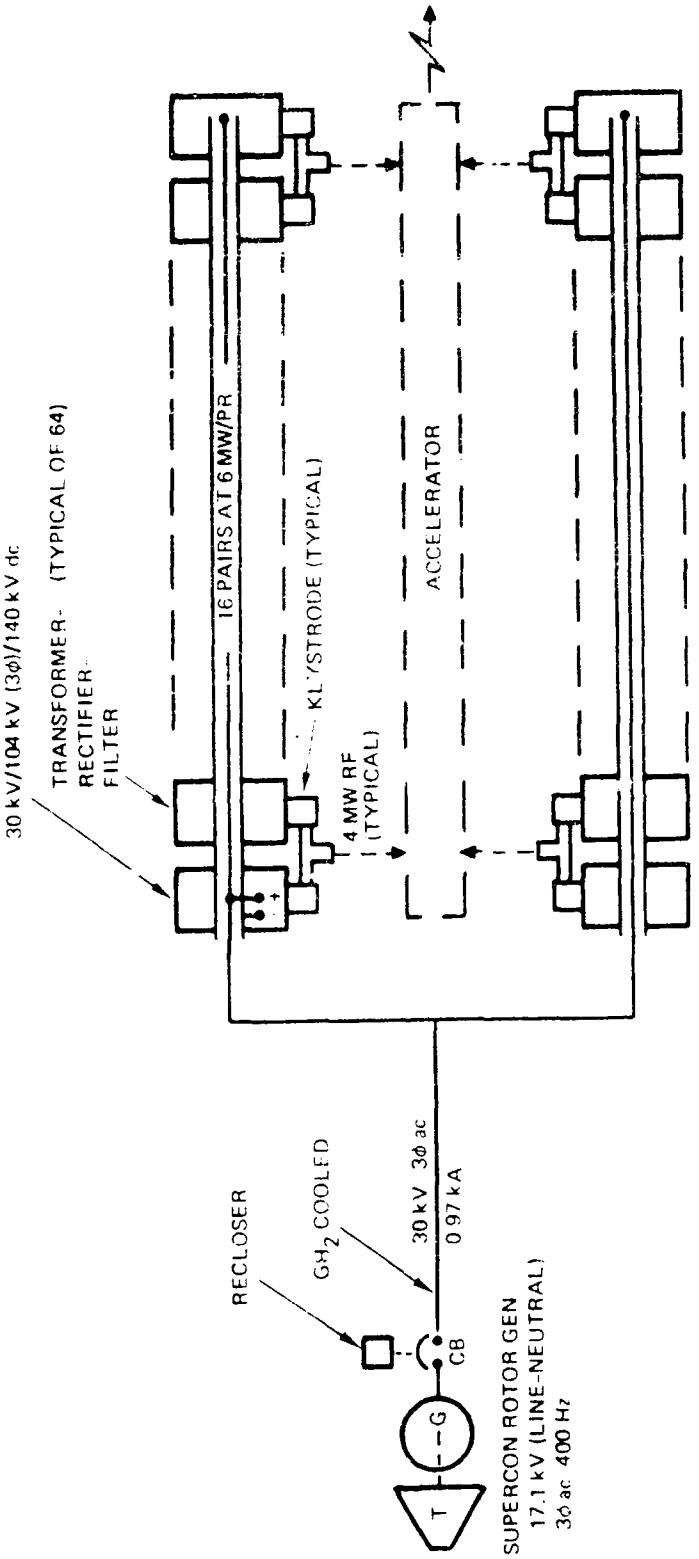

Figure 5-2. VHV Case 1

frequency raised from 200 to 400 Hz. Transmission is at generated voltage (17.1 kV line-neutral, 30 kV line-line) with a current just under a kiloamp. At this current level, a cooled (50 K) conductor is assumed (see Section 3.4). Conversion from the 30 kV transmission to the klystrode operating voltage is accomplished by unit transformer rectifier filter units housed together with the klystrode (see Figure 5-3). Thirty-two pairs of power conditiong units are required at about 3 MW (input) each. Each klystrode delivers about 2 MW RF, and they are paired to deliver 4 MW of RF energy to each port of the superconducting accelerator. As discussed in Section 3.5 regulation is minimal, and the RF output is controlled by programming the RF feed to the klystrodes. Although not shown in Figure 5-2, power for the RF feed is also taken off the main transmission line, but the klystrode accessories (e.g., ion pump, cathode heater, magnet power, etc. are assumed to be supplied by the platform's steady-state (housekeeping) power plant so that tne system can be warmed up during alert without energizing the main burst-power generators.

Figure 5-4. This system is similar to the one above, using the same generator, but the voltage is stepped up to 104 kV ac for tranmission. (104 kV is the ac input needed to produce 140 kV dc using a three-phase bridge rectifier; see Ref. 4). Since the current is considerably reduced, the transmission line can be uncooled (see Section 3). The remainder of the system is similar to the previous one.

Figure 5-5. This system assumes use of a disk generator, as discussed earlier in Section 3). The attraction of this design is that it can apparently operate at higher frequencies than the superconducting rotor machine, thus reducing the size of the transformer(s) involved. In fact, as shown later, the 10 kHz system is one of the more attractive combinations. One of the concerns is that to date there have been no three-phase high voltage, high frequency transmission lines designed.

Figure 5-6. While the previous cases have been predicated on state-of-the-art generators, this figure assumes the possibility of designing a generator that would produce at least 60 kV line-to-neutral voltage, which would provide the necessary 104 kV line-to-line voltage needed to obtain

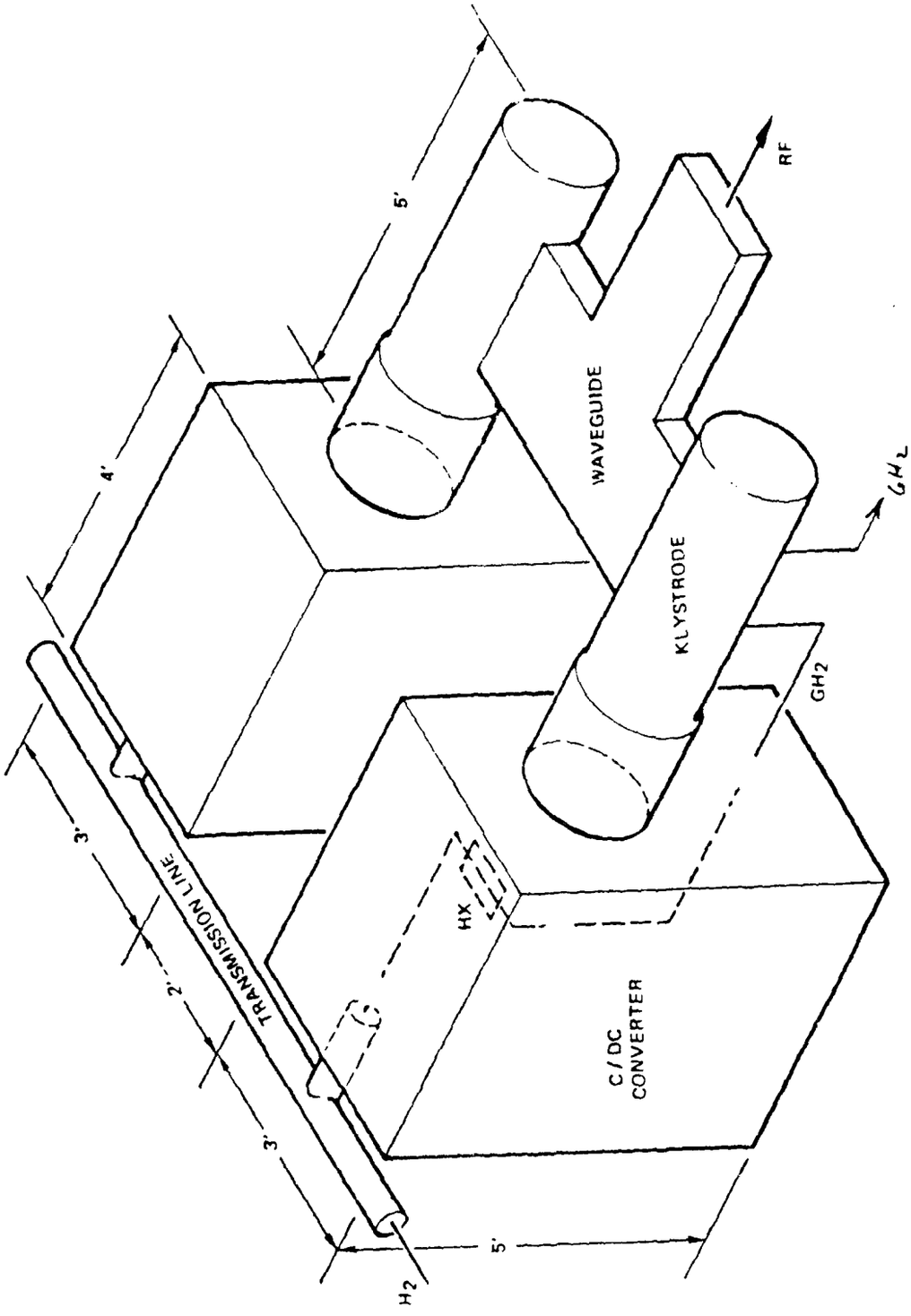

Figure 5-3. Converter-Klystrode Configuration

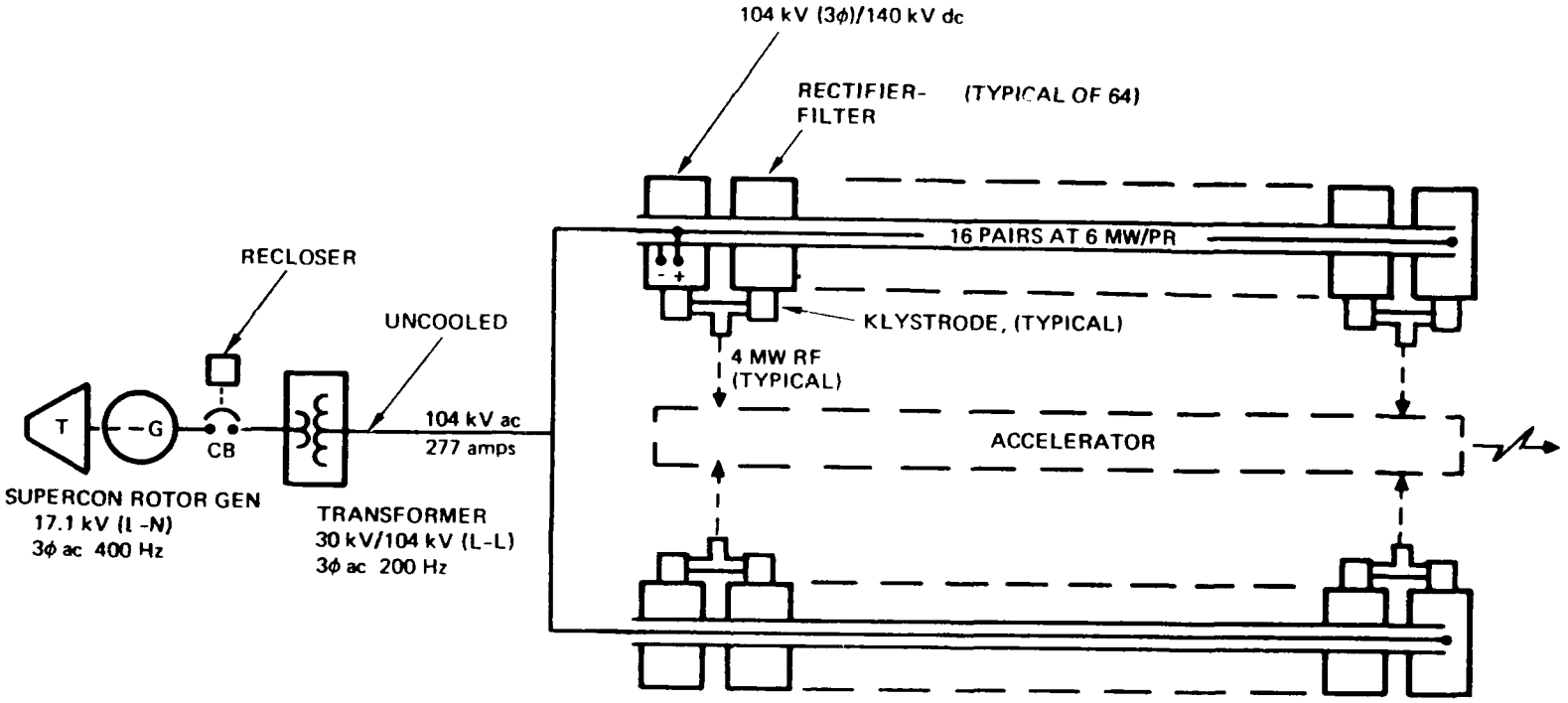

Figure 5-4. VHV Case 2

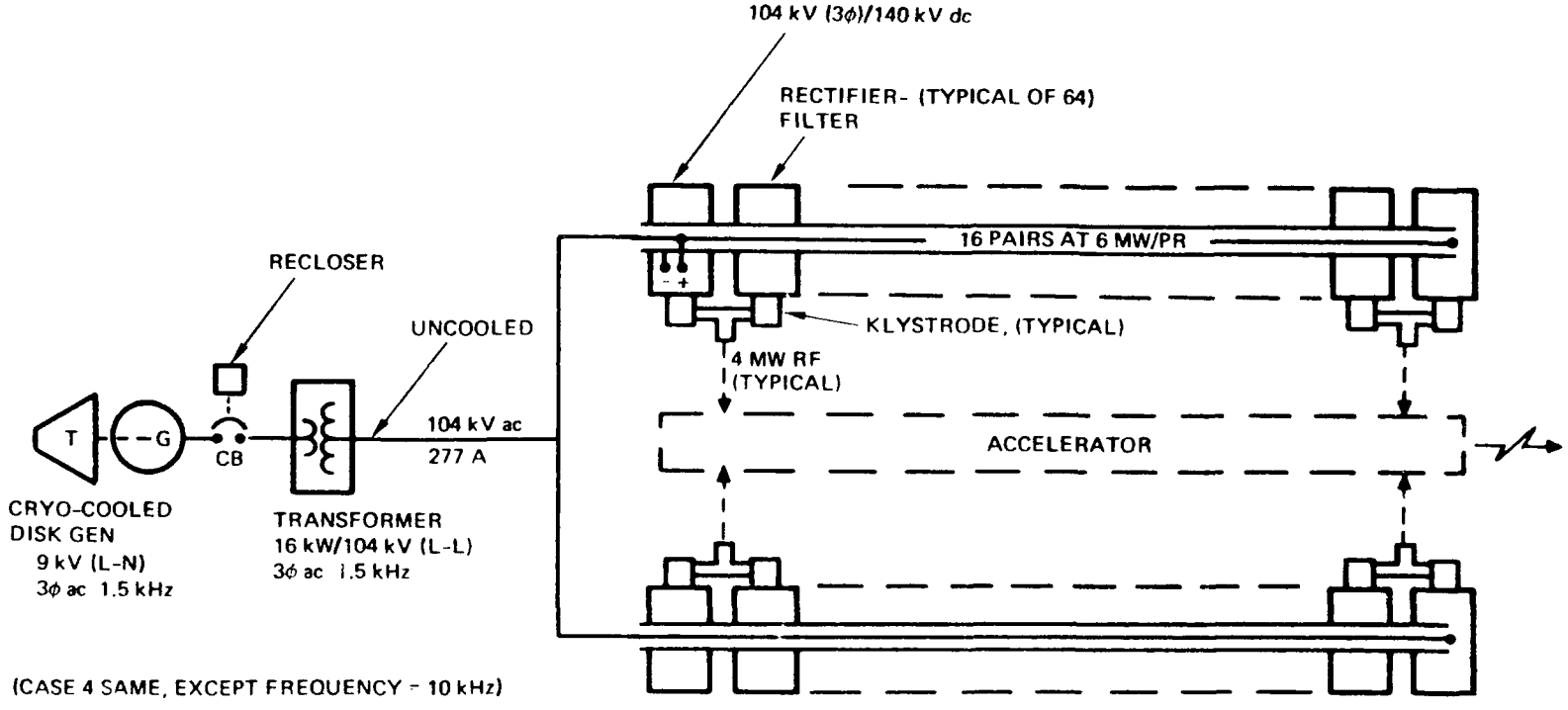

Figure 5-5. VHV Case 3 and 4

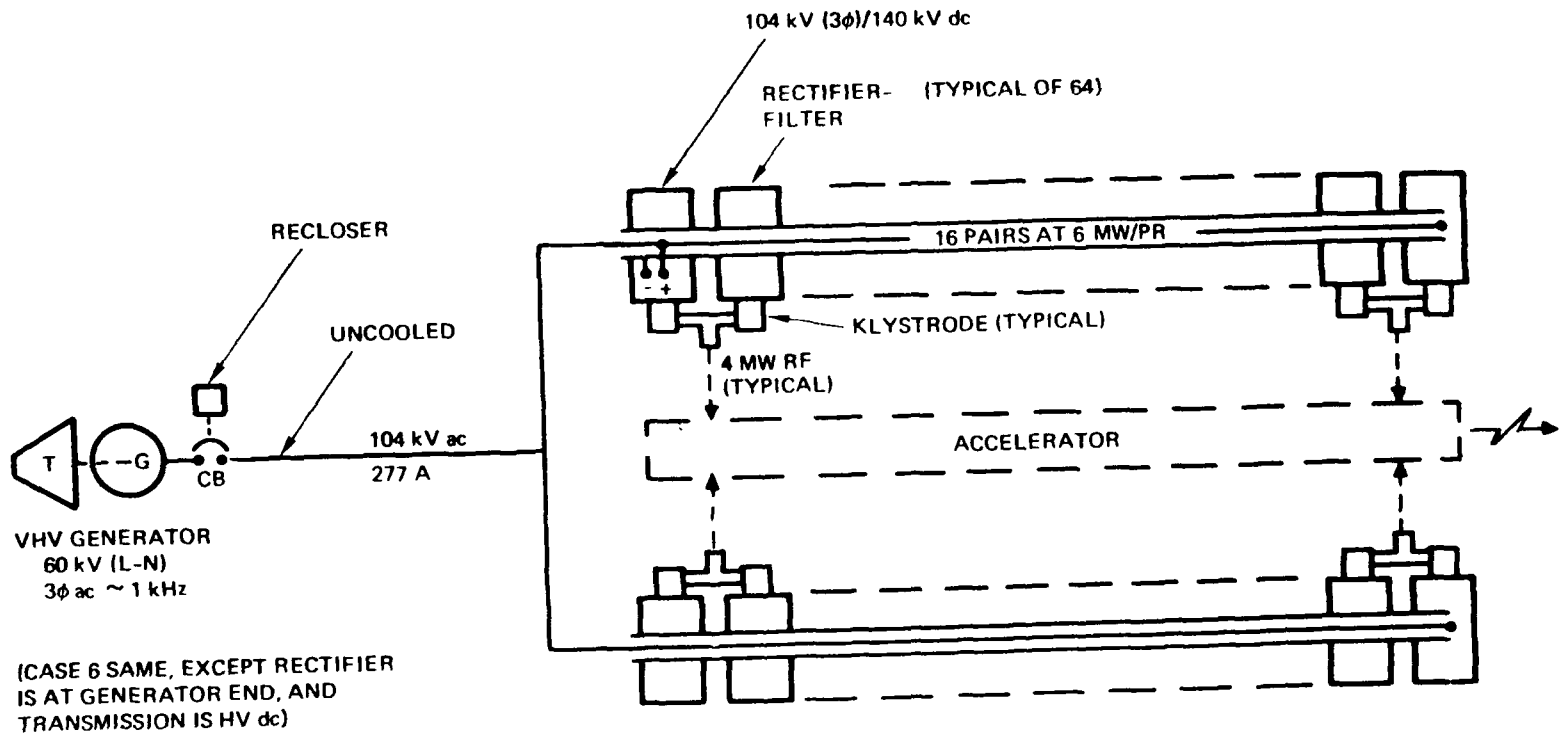

Figure 5-6. VHV Case 5 and 6

140 kV dc directly, without transformers. Although some optimism has been expressed regarding a 60 kV machine, this remains to be demonstrated.

Figure 5-7. This figure utilizes a THOR reactor (Ref. 6) which generates 5 kV dc directly using reactor-heated thermionic diodes. Power is transmitted at generated voltage, which requires cooled transmission lines at the 5 kiloamp level. Note that there are severe thermal interfaces, as discussed in Section 4.1. The system is further penalized by needing a dc/dc converter to provide the 140 kV to the klystrodes, as before. Note that although the electrical system is heavier than the previous examples, the attraction of this system is its no-effluent posture, as compared with the previous ones that exhaust vast quantities of burned hydrogen overboard).

Figure 5-8. This is the fuel cell case. Although it is somewhat penalized by the need for a dc/dc converter in the system, the attraction here is that the fuel cells can be co-located with the power conversion and klystrodes, thus minimize the length of transmission/distribution wiring, and maximize redundancy. If the accelerator can operate with part of the RF feed out, then this system offers the most flexibility and minimizes the loss of power if one of the generating units goes out.

5.2 Medium High Voltage (MHV) Systems. These systems are designed to exploit a lower voltage (approx 40 kV) high power RF amplifier such as the crossed-field amplifier described in Appendix A.

Figure 5-9. This system uses the present superconducting rotor design, upgraded to 50 MW. It is included here for reference. In practice, it would be replaced by one of the two following designs.

Figure 5-10. This system upgrades the previous one by adding a main circuit breaker, and distributing the power at ac rather than dc.

Figure 5-11. This is the same as the preceding figure, except with dc transmission.

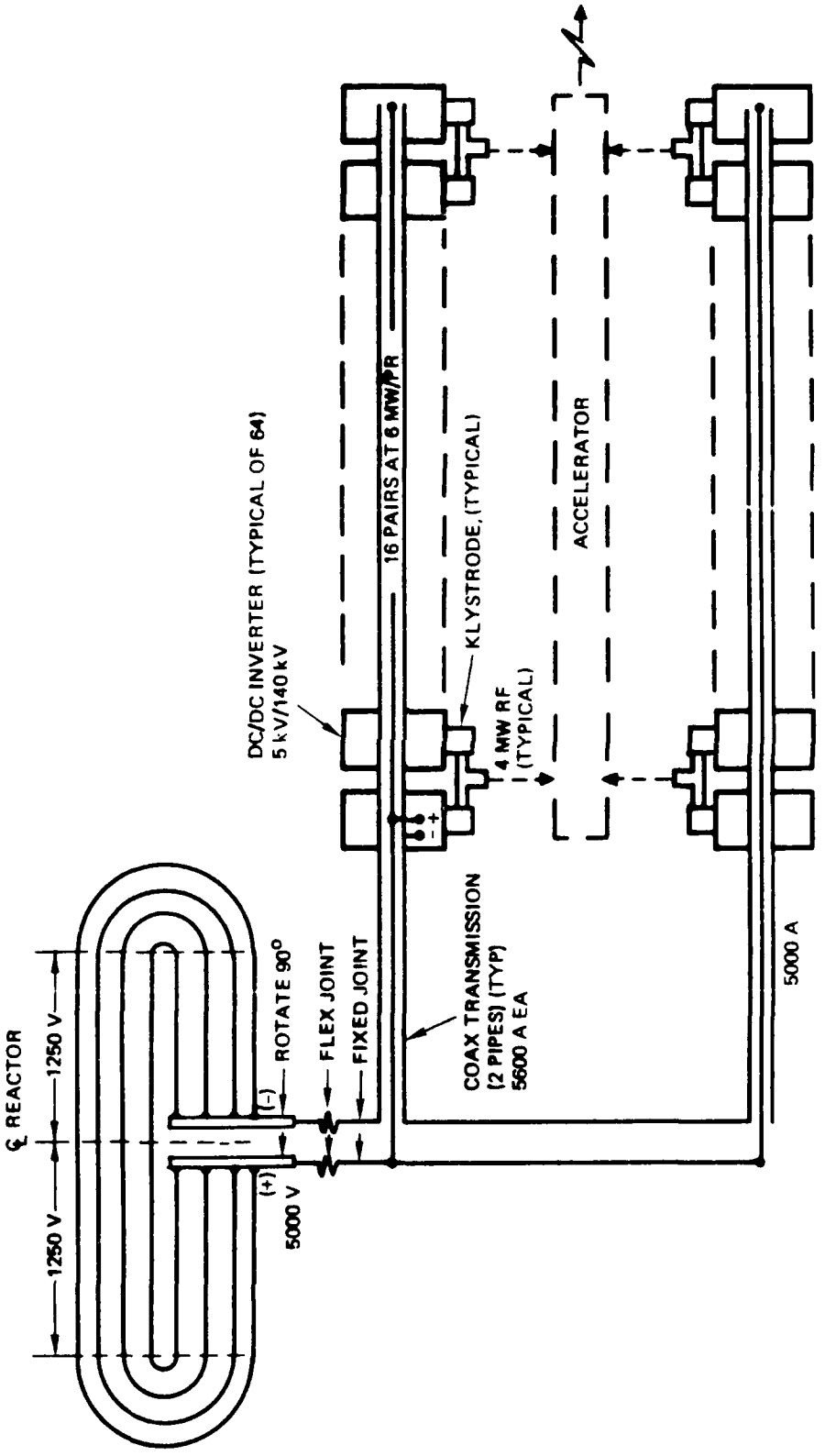

Figure 5-7. VHV Case 7

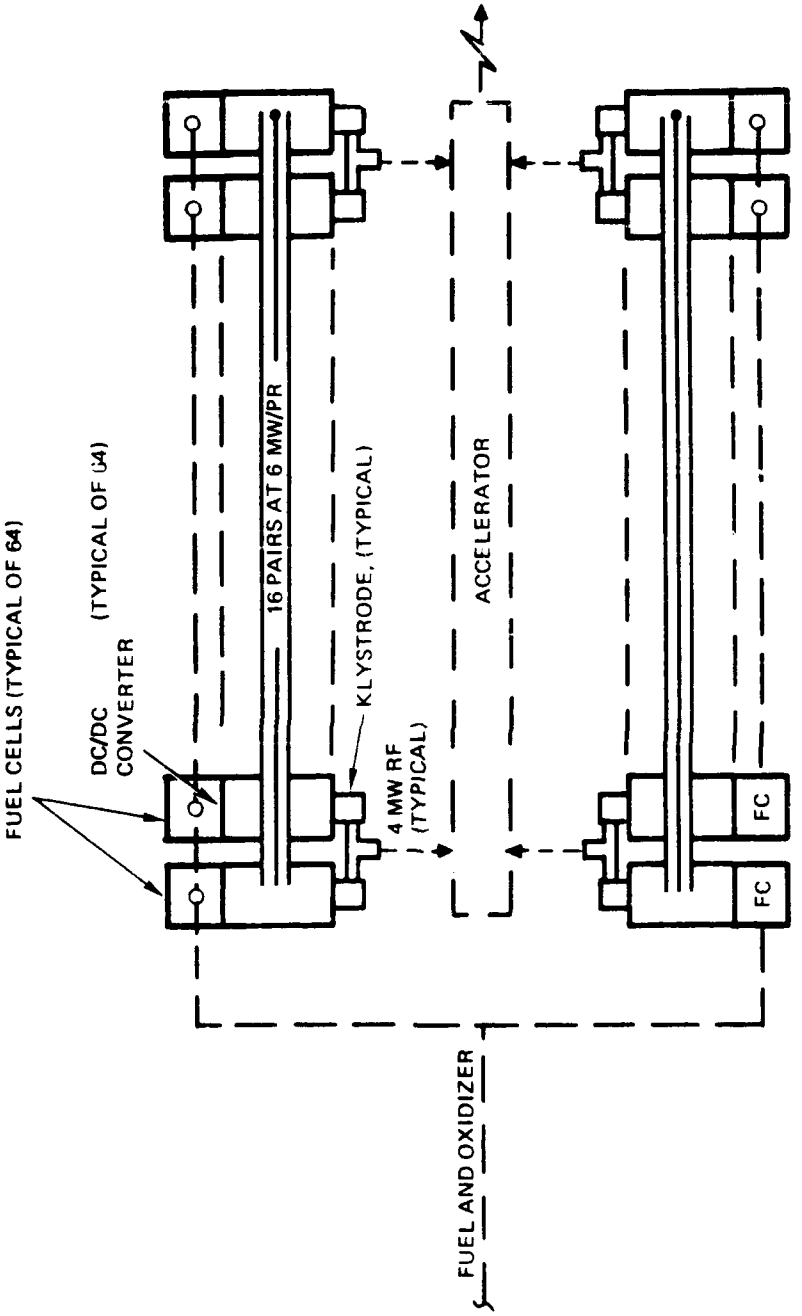

Figure 5-8. VHV Case 8

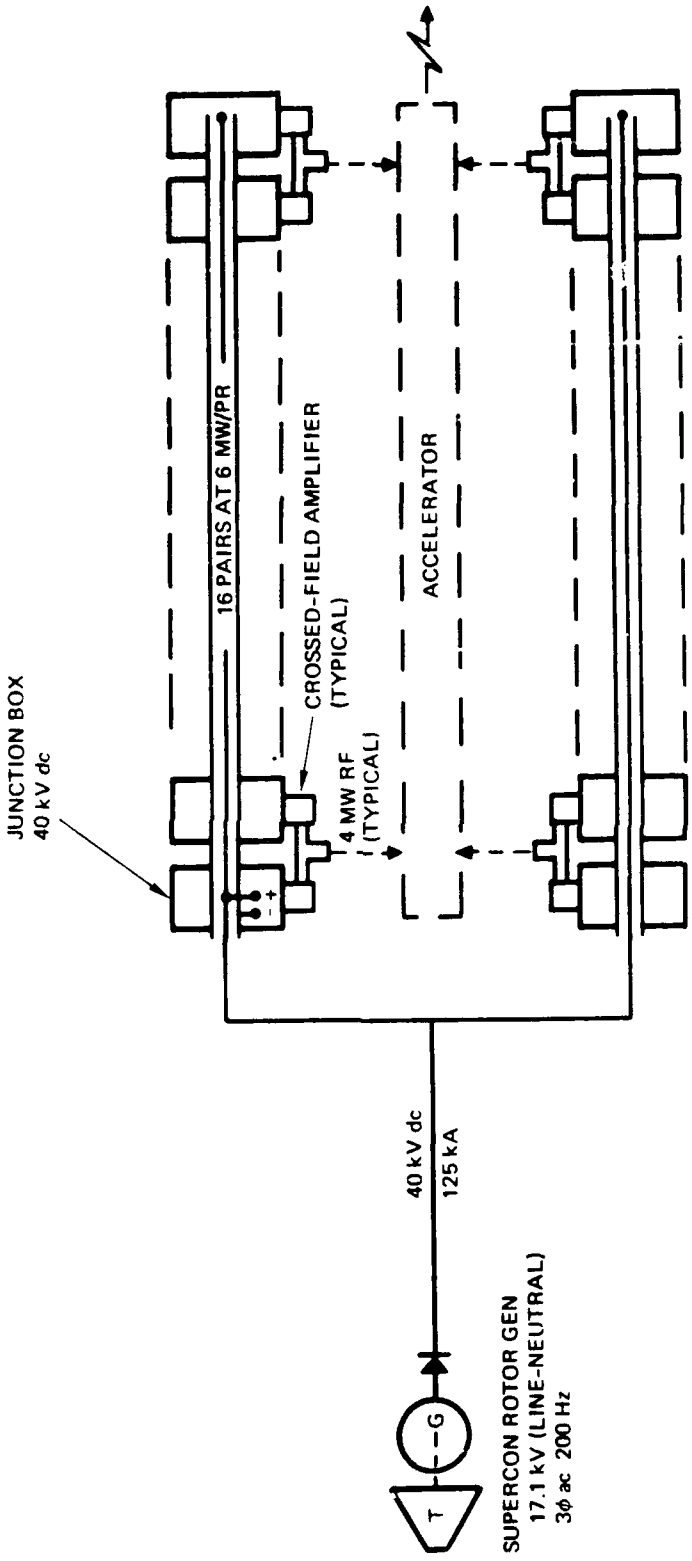

Figure 5-9. MHV Case 1

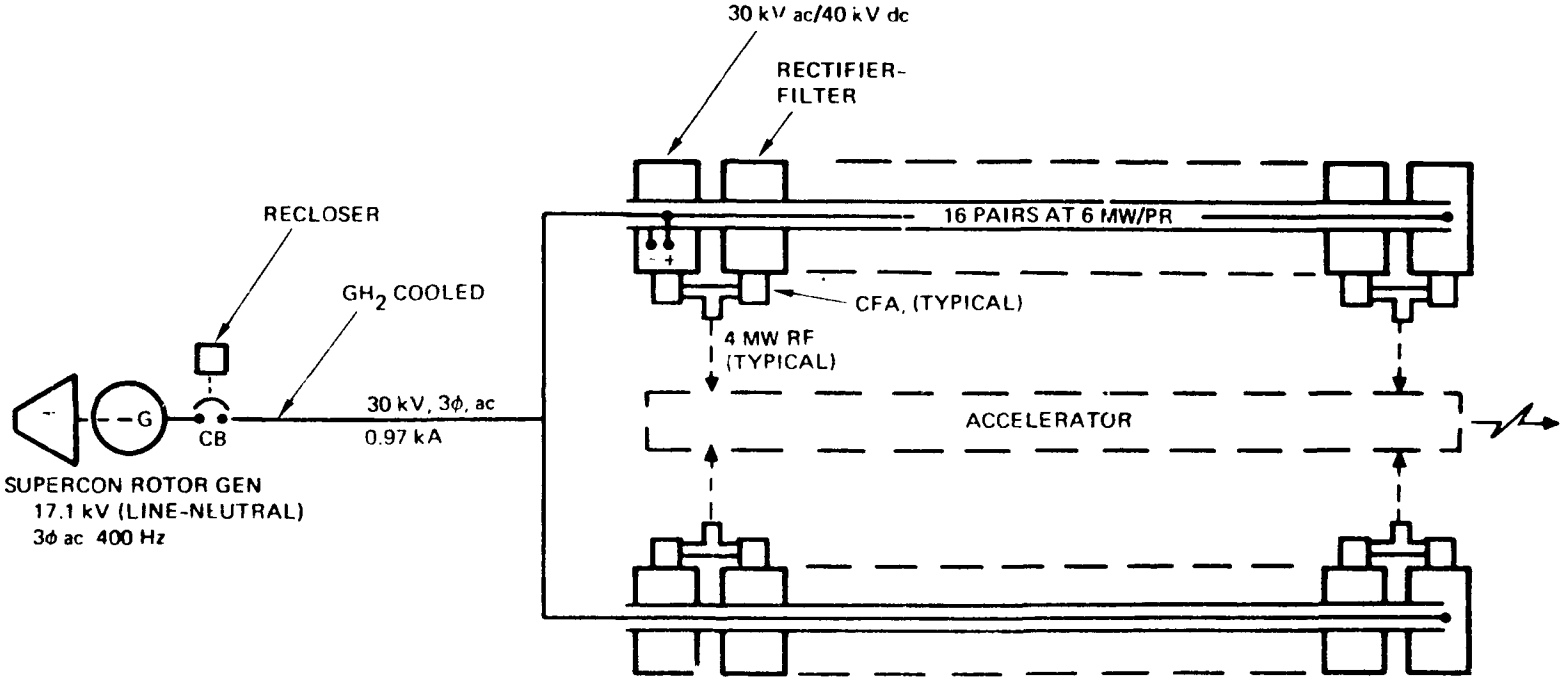

Figure 5-10. MHV Case 2

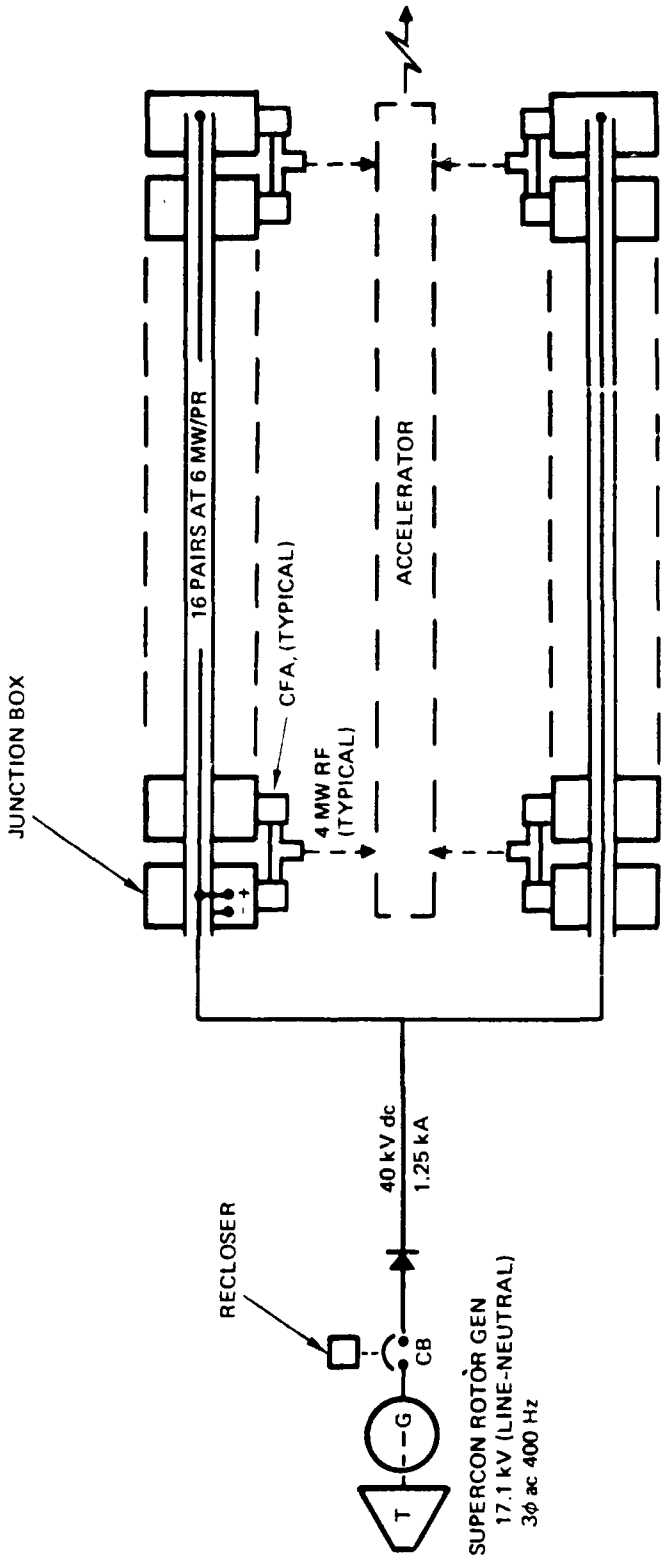

Figure 5-11. MHV Case 3

5.3 Medium Voltage Pulsed Systems. These systems are designed to supply the pulsed systems used to power electromagnetic railguns (EMLs). Railgun systems typically use either inductors or capacitors as their major storage medium, and the design of the power system differs markedly from one to the other.

Figure 5-12. This shows a compulsator-driven system, taken from Ref. 7. From a power conditioning and distribution standpoint, all of the key elements are included in the generator and in the weapon. The key design problem is to conduct very large pulses of current (megamps) between the generator and the weapon. This will require large conductors, even at cryo-cooled conditions. Key elements of the design include placing the generator as near the load as possible, depending on the design of the spacecraft. The case utilizing a homopolar generator is similar.

Figure 5-13. This circuit uses a MHD or thermionic system to charge a capacitor-storage railgun. Although the currents are modest, and the voltage available from the generator is in the right range, the problem is that the charging system prefers a variable voltage, constant current mode in order to operate at a reasonable efficiency. In Figure 5-13, we have shown a dc/dc converter incorporating a tap changer as the charge control device. Other systems are feasible, but no attempt was made to optimize the arrangements during the limited time available.

Figure 5-14. This is the ac equivalent of the previous scheme. Again, a tap-changing transformer is employed for matching the generator to the capacitor load.

5.4 Low Voltage RF (LVRF) Systems. These systems all use the low voltage (less than 500 volts) semiconductor modules discussed in Appendix A. The desgn problem is to arrange a large number of low power sources in a practical configuration and remove the excess heat efficiently. This is beyond the scope of this particular study. From a power distribution standpoint, three systems were evaluated.

Figure 5-15. This is an all dc system, but requires extremely large currents and probably is not a reasonable solution.

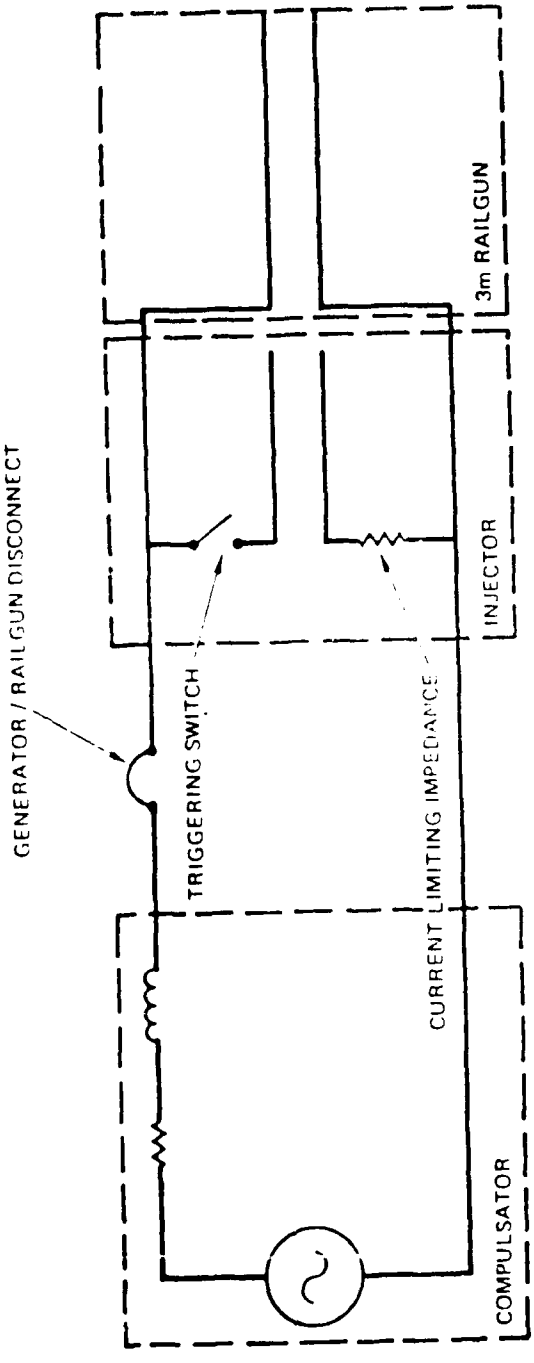

Figure 5-12. Compulsator-Driven Railgun System

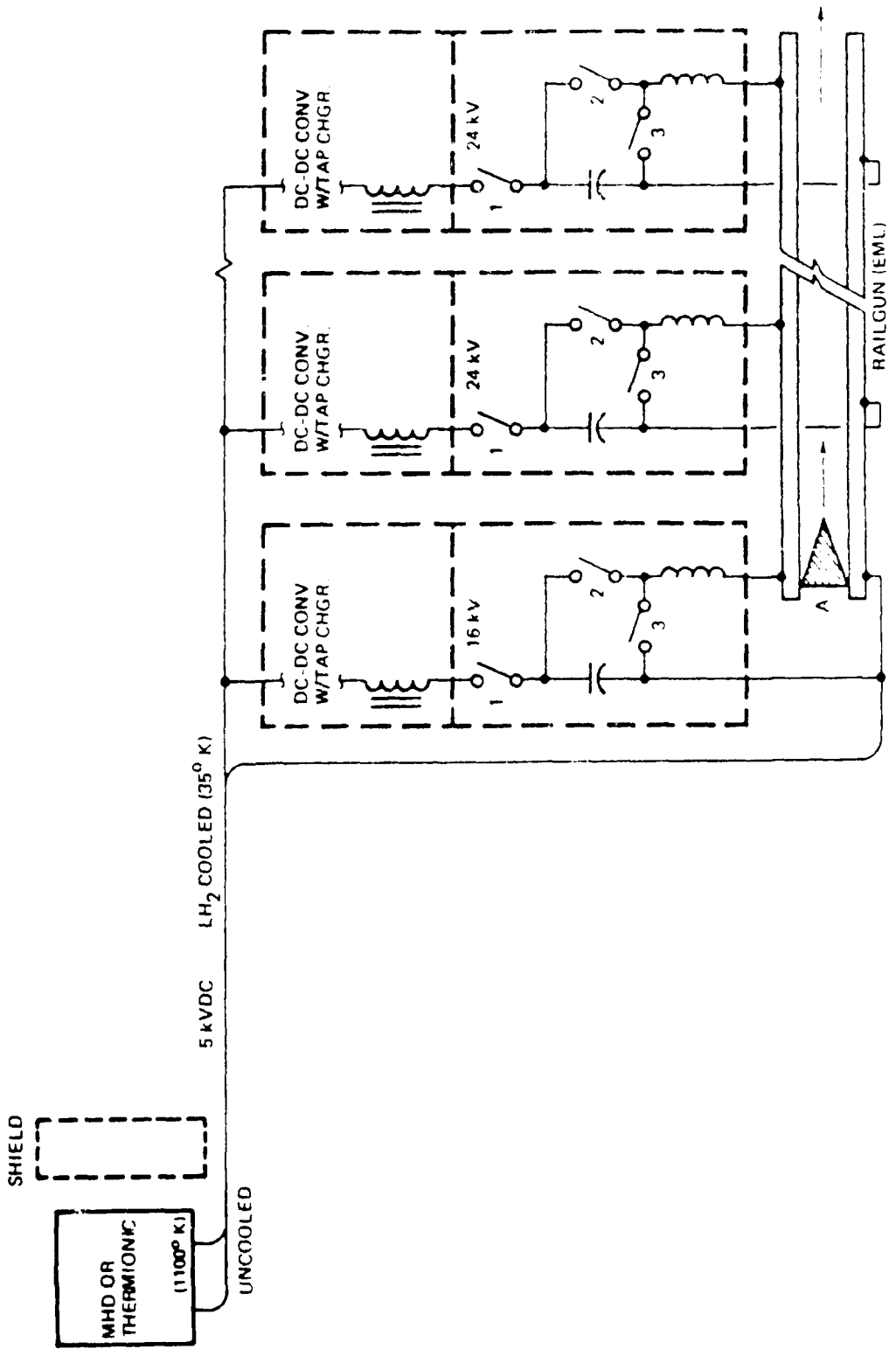

Figure 5-13. MHD/Thermionic-FML System

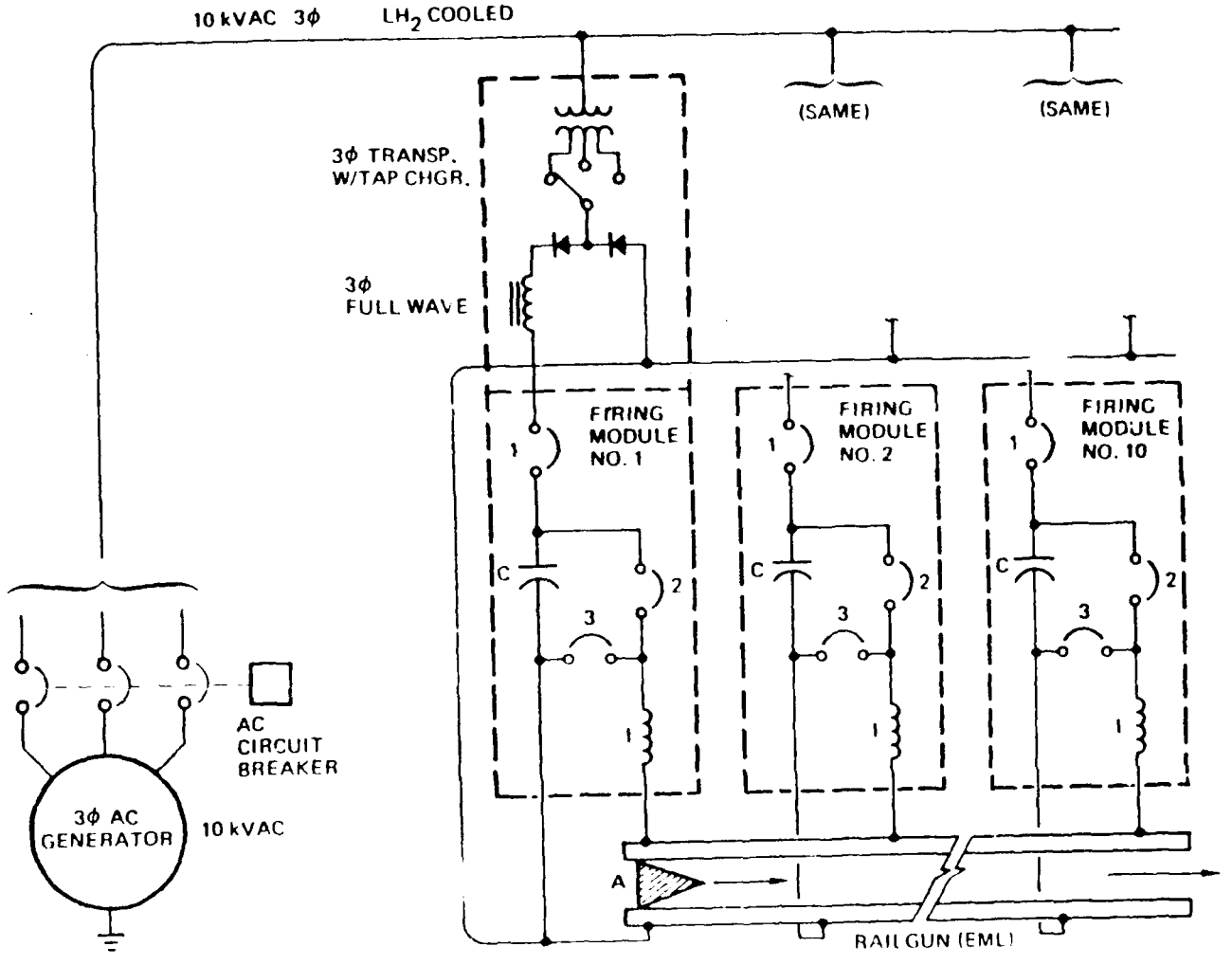

Figure 5-14. Turbogenerator-EML System

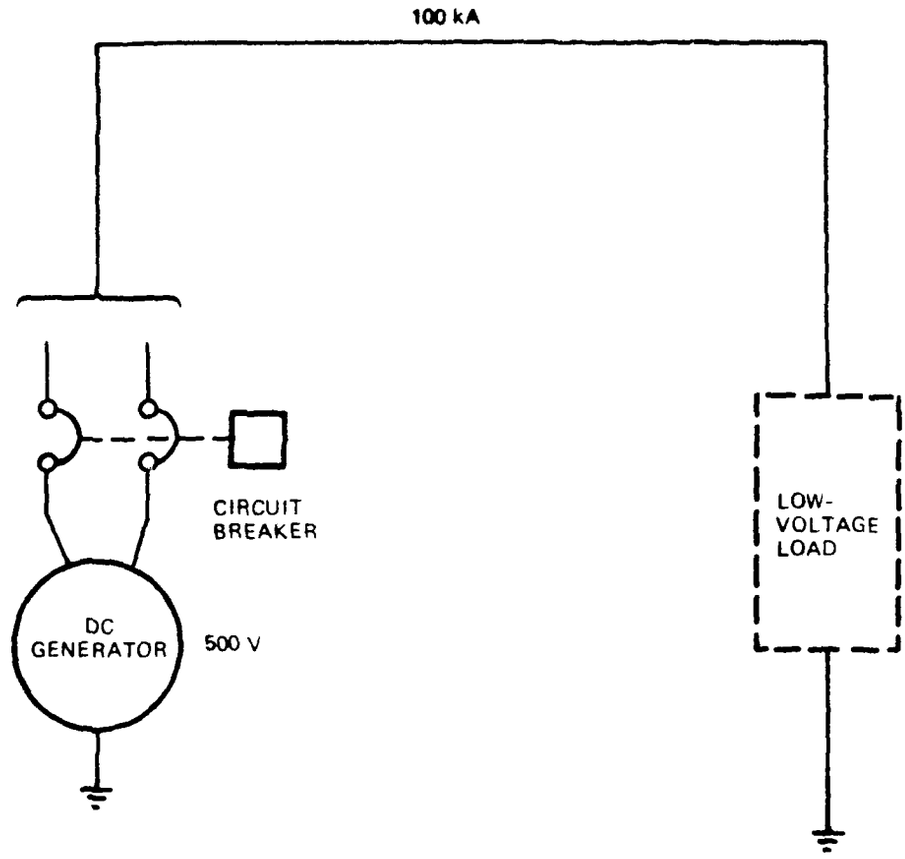

Figure 5-15. Generator LV RF System

Figure 5-16. This system uses an ac generator, transmitting power at a modest voltage, which is then stepped down to obtain the low voltage required for the semiconductors. The transformer/rectifiers would be located immediately adjacent to the groups of amplifiers being serviced. As noted before, use of the highest frequency generation available will minimize the transformer weights.

Figure 5-17. The use of fuel cells located immediately next to the RF generators represents an interesting configuration, since the fuel cells can be connected to deliver the desired output voltage without intermediate power conditioning. Since the fuel cells can be located next to the amplifiers, the high current interconnections can be minimized.

5.5 Evaluation. Table 5-1 tabulates the weights of the various systems described in this section (see Figure 5-18). From a weight standpoint, the most interesting systems are as follows:

5.5.1 VHV Systems. The two most interesting concepts are the very high voltage generators, and the very high frequency generators. The former has the advantage of eliminating any transformers in the system, but at the cost of requiring a VHF circuit breaker. The latter (VHF) systems benefit from easing the design constraints on the generated voltage, and using a medium voltage circuit breaker. However, the problem of transmitting high frequencies (up to 10 Khz) at three phases, remains to be demonstrated. The fuel cell concept, although not the lowest weight system, has the distinct advantage of redundancy over the centrally located turbogenerators.

5.5.2 MHV Systems. Although the first system, MHV-1 has the lowest weight, the lack of adequate system protection suggests that either MHV-2 or 3 would be more acceptable. To consider these systems, however, development has to proceed on a satisfactory medium voltage tube-type amplifier, such as the crossed-field amplifier, for the system to be successful.

5.5.3 EML Systems. Transmission and distribution considerations do not seem to dominate these selections, as the weight of the pulse forming networks probably govern the total. For the inductor type gun, either the

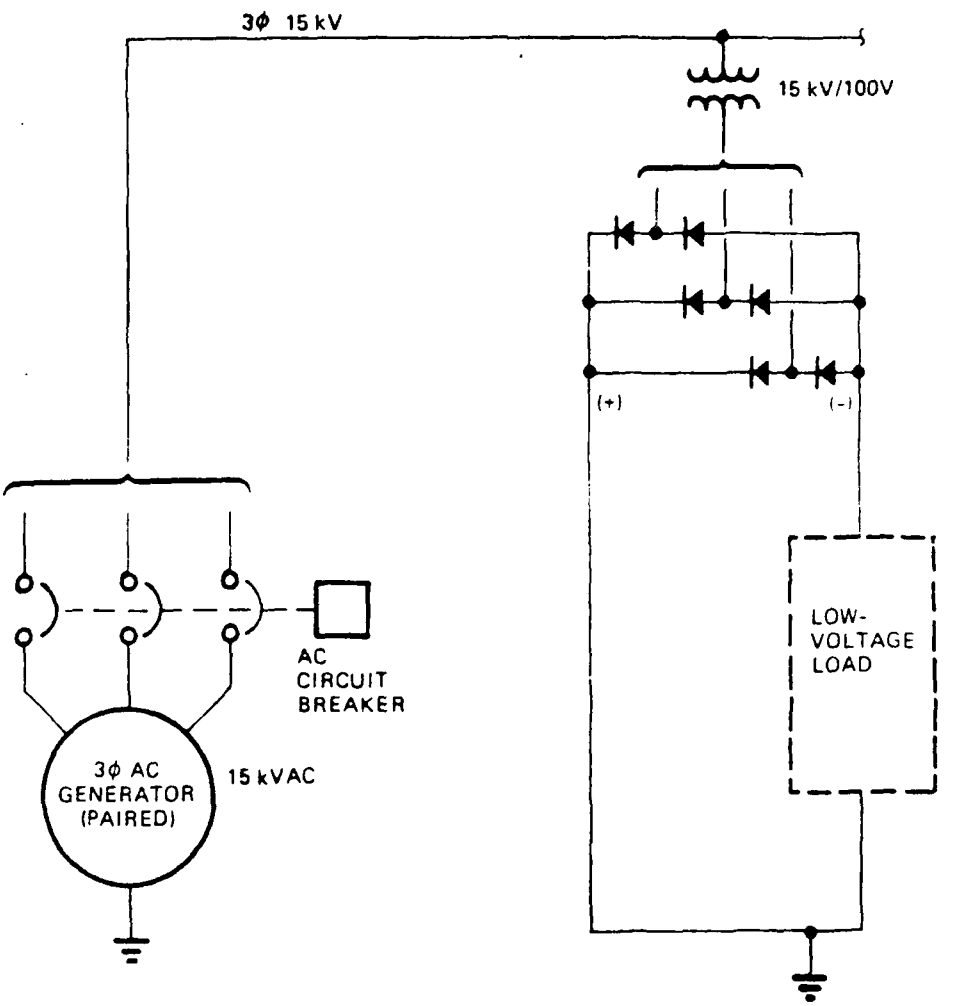

Figure 5-16.VLV Case 3

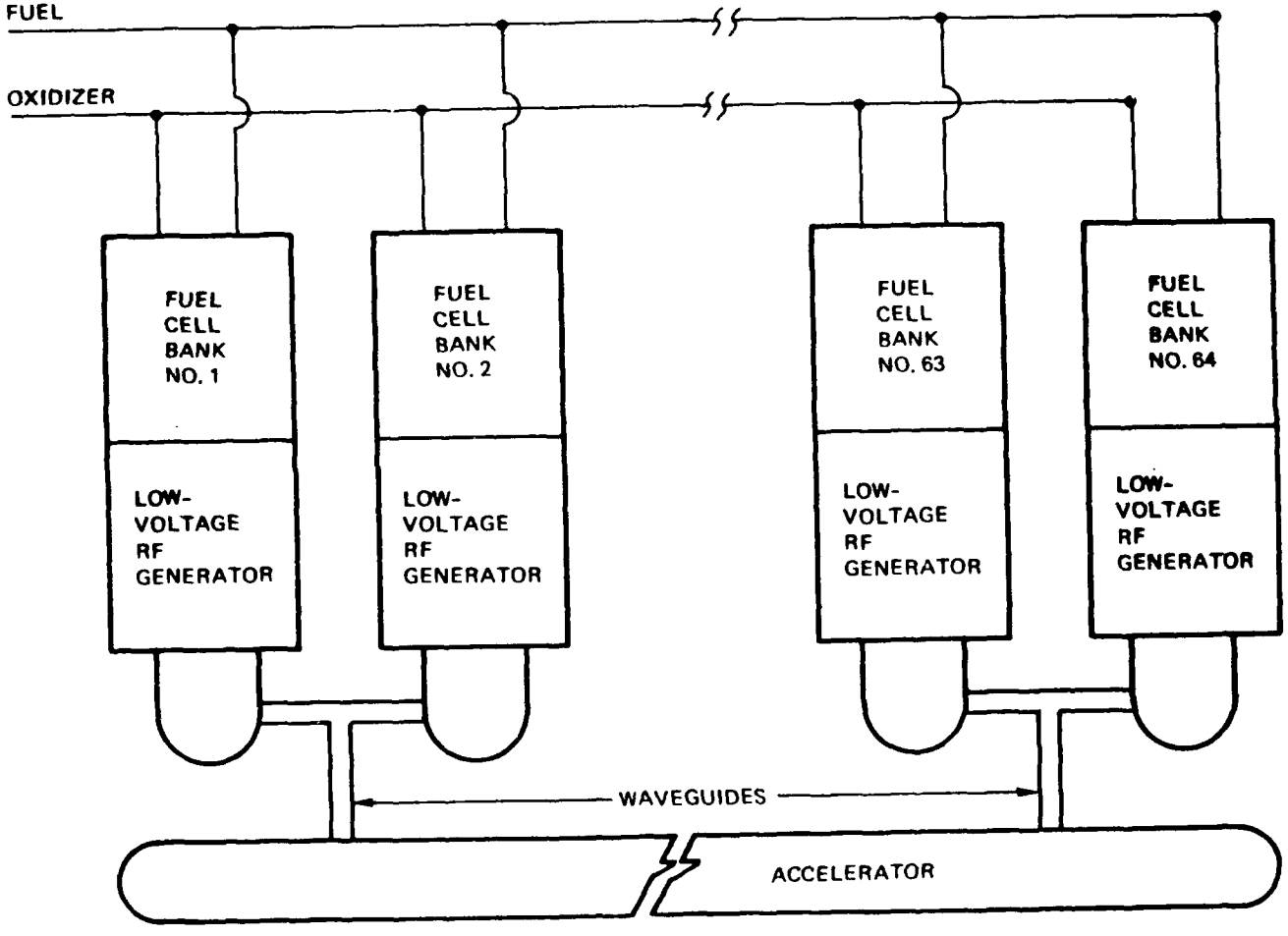

Figure 5-17. Fuel Cell-Low Voltage RF System

Table 5-1. Tabulation of System Weights*

Case No.	Prime Mover and Generator	Circuit Breaker	Pre-Trans. Power Cond.	Transmission	Post-Trans Power Cond.	Payload Conditioning	Payload	Total Weight	Specif. Wt. kW/kg
VHV-1	33000/15000	1500/700	-	900/400	5500/2500	5000/2300	NOT INCL.	45900/21000	2.38
VHV-2	33000/15000	1500/700	5500/2500	900/400	-	5000/2300	NOT INCL.	45900/21000	2.38
VHV-3	33000/15000	900/400	3000/1400	900/400	-	5000/2300	NOT INCL.	42800/19500	2.56
VHV-4	3300/1500	900/400	1500/700	1400/600	-	5000/2300	NOT INCL.	41800/19000	2.65
VHV-5	35000/16000	3000/1400	-	900/400	-	5000/2300	NOT INCL.	43900/20000	2.50
VHV-6	35000/16000	3000/1400	5000/2300	900/400	-	5000/2300	NOT INCL.	43900/20000	2.50
VHV-7	30000/1400	-	-	2000/900	-	17000/8000	NOT INCL.	49000/22500	2.22
VHV-8	28000/13000	-	-	-	-	17000/8000	NOT INCL.	45000/21000	2.38
MHV-1	33000/15000	-	5000/2300	900/400	-	-	NOT INCL.	38900/18000	2.78
MHV-2	33000/15000	1500/700	-	900/900	-	5000/2300	NOT INCL.	40400/18400	2.71
MHV-3	33000/15000	1500/700	5000/2300	900/400	-	-	NOT INCL.	40400/18400	2.71
EML-1	33000/15000	-	-	33000/15000	-	NOT INCL.	NOT INCL.	66000/30000	1.66
EML-2	30000/14000	-	-	2000/900	15000/7000	NOT INCL.	NOT INCL.	47000/22000	2.27
EML-3	33000/15000	1500/700	-	900/400	5000/2300	NOT INCL.	NOT INCL.	40400/18500	2.70
LV-1	33000/15000	-	-	33000/15000	-	NOT INCL.	NOT INCL.	66000/30000	1.66
LV-2	33000/15000	1500/700	-	900/400	5500/2500	5000/2300	NOT INCL.	45900/21000	2.38
LV-3	28000/13000	-	-	-	-	-	NOT INCL.	28000/13000**	3.84**

*Weights are in pounds/kilograms (rounded)
**Does not include extra fuel and oxidizer piping

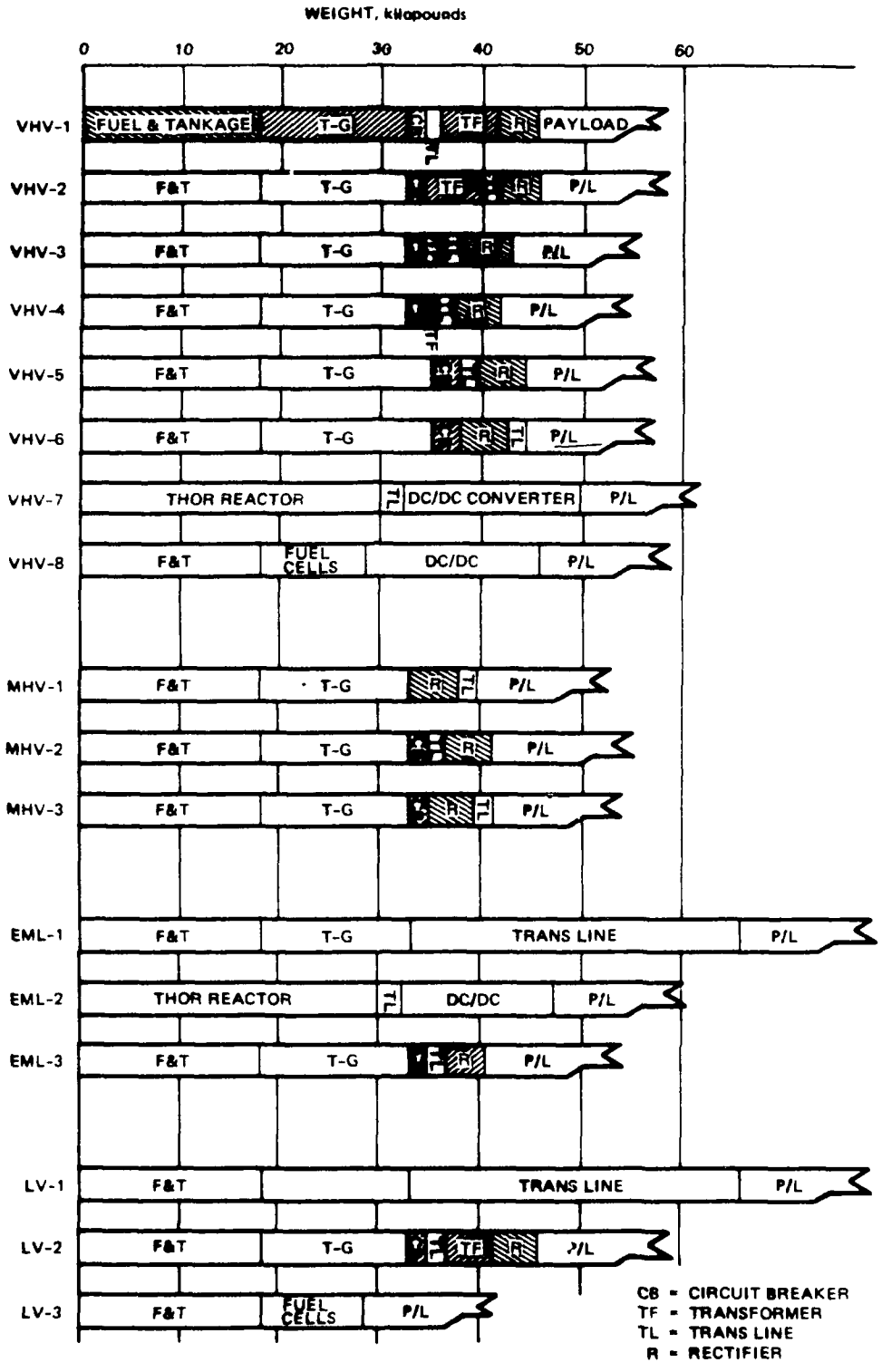

Figure 5-18. Weight of Various Systems

compulsator or the homopolar generator could be used. For the capacitor type gun, the medium voltage turbogenerator appears best.

5.5.4 LVRF Systems

The most attractive system here is the integrated fuel cell/RF generator approach, which minimizes any heavy power conditioning equipment. The second choice would be a medium voltage, high frequency ac system with low voltage transformers adjacent to the RF modules.

6. RECOMMENDED MEGAWATT POWER PROCESSING TECHNOLOGY PROGRAM

Based upon a preliminary review of existing power conditioning, distribution, and control technologies, apparently there are no insurmountable obstacles to the development of megawatt space power systems. Much of the power processing technology used by the national space program, used for high power industrial applications, and being developed for pulse-power applications can be readily adapted and extended by means of supporting technology development programs to meet the new mission requirements. We must use extensive planning, systems engineering, and advanced technology development to design and produce a high quality configuration. A preliminary plan is presented for an integrated Megawatt Space Power Processing Technology Development Program to help the Air Force structure their long range plans in support of future megawatt level missions. The results of this study will aid in further defining and refining these important technology development plans.

The Megawatt Space Power Processing Technology Development Program is envisioned in six basic categories:

1. Basic experiments
2. Device technology
3. Materials and processes
4. Technology demonstration breadboards
5. Prototype hardware
6. Subsystem planning and demonstration.

Table 6-1 contains a preliminary list of candidate programs that proceed in parallel in a coordinated manner so that technical data

Table 6-1. Recommended Megawatt Power Processing Technology Program

Item	Generators	Transformers	Transmission Lines	Power Conditioning	Control/ Protection	Payloads
Basic Experiments	1. High voltage, high frequency insulation systems 2. Corona Effects	(Same)	(Same)	1. (Same) 2. Gaseous insulation systems (e.g., SF6) Incl. cooling		
Device Technology	1. Superconducting-rotor* 2. Disk generator* 3. Long-life thermionics	1. Low-weight concepts	1. 3-ϕ HV,HF transmission lines	1. MOS-controlled thyristor* 2. Cooling methods		1. Single-voltage, Low-regulation RF Amplifiers at voltages less than 50 kV
Materials and Processes	Insulation Systems	(Same)	(Same)	(Same)		
Tech. Demo. (breadboards)	1. Very high voltage 2. Very high frequency	1. Low-weight devices	1. Cooling methods 2. Terminations	1. Rectifiers and inverters using MOS-controlled thyristors		
Proto types	1. VHV Generator (>60 kV) 2. VHF Generator (>5 kHz) 3. Quick Starts	1. Low weight, HV, HF 2. Quick Starts	1. 100 k Vac 3ϕ 2. 150 k Vdc 3. Quick Starts	1. 3 MW rectifier at 150 k Vdc 2. 3 MW Inverter-5 kV-150 k Vac 3. Quick Starts	1. Space-configured vacuum ckt. breaker	1. 2 MW klystrode 2. 2 MW CFA 3. High power low-voltage RF Generator 4. Quick Starts
System Integration	Demonstrate a 1-10 MW Channel <——————————————————> with Spacecraft features (including Quick Starts)					

*Existing Program

M2-011-88

and results will be available to support subsequent programs. The following sections briefly discuss the scope of the work that might be accomplished under this preliminary master plan.

6.1 Basic Experiments. Since many of the systems operate at the 100 to 150 kV level, both ac and dc, we need to review basic selections of insulation systems for applicability to the space environment. Although systems have been flown at the 10 to 12 kV level (primarily TWTs), the 100 kV level proposed here represents an order of magnitude increase. Solid insulation is of primary interest for the generators, transformers and transmission lines, but for the inverters and rectifiers, gaseous insulation becomes of high importance. Since we concluded that these high voltage systems cannot be exposed to the space plasma, it will be necessary to enclose these devices. The selection of insulating gas pressure will have a major effect on the weight of the enclosing shells. Likewise, cooling the equipment enclosed within these shells becomes a major area for investigation.

6.2 Device Technology. We need to develop device technology for the following items:

6.2.1 Generators. We need to continue current efforts in developing a superconducting rotor generator and a disk generator. In particular, we should start to develop either a very high voltage generator (>60 kV) or a very high frequency generator (>2 kHz).

6.2.2 Transformers. Initiate development of low weight, high voltage transformers both at small unit sizes of 1 to 3 MW, and at the 50 MW level. Frequency ranges of 400 to 10,000 Hz need to be addressed. Cryo-cooled transformers may be of interest.

6.2.3 Transmission Lines. Initiate the development of three-phase high voltage, high frequency lines.

6.2.4 Power Conditioning. Continue the development on the MOS-controlled thyristors (or equal) now under way at General Electric. Rectifiers and inverters need to be developed in the voltage ranges discussed under Section 5. Cooling methods need to be established, and the effect of "quick starts" evaluated.

6.2.5 Loads. Single voltage low regulation requirement RF amplifiers need to be demonstrated at the 2 MW level. If such devices can be designed for lower voltages than the 140 kV described herein, so much the better. Advanced low voltage (but up to 500 v) semiconductor RF generators need further development.

6.3 Materials and Processes. For all the devices described, advances in materials and processes are needed in high voltage insulation systems, evaluation of low temperature standby conditions, and evaluation of thermal shock during "quick start" conditions.

6.4 Technical Demonstration (Breadboards). We suggest demonstration at the breadboard level for the following items:

6.4.1 Transmission Lines. Insulation systems, terminations, cooling systems.

6.4.2 Power Conditioning. Rectifier and inverter models using techniques and devices listed above.

6.5 Prototypes. Prototypes are suggested for the following:

6.5.1 Generators. Complete the testing of the 20 MW superconducting rotor generator at AFWAL. Test the 20 MW disk generator now under design contract. Build and test a VHV generator (60kv) at the 5 to 10 MW level. Build and test a high frequency generator (>2kHz) at the 5 to 10 MW level. Demonstrate long-life thermionic diode capability. Demonstrate a unitized fuel cell/low voltage RF module. Demonstrate the "quick start" mode of operation an all prototypes.

6.5.2 Transformers. Build and test lightweight, HV/HF modules at the 3 to 5 MW level. Demonstrate the "quick start" mode.

6.5.3 Transmission Lines. Build and test a 100 kV ac, three phase line at several frequencies, under simulated space conditions. Build and test a 150 kV dc line, also under simulated space conditions. Demonstrate the "quick start"mode.

6.5.4 Power Conditioning. Build and test 3 to 5 MW rectifier and inverter modules at the voltage levels described in the various systems in this study. Utilize advanced MOS-controlled thyristors (or equal). Demonstrate the "quick start" mode.

6.5.5 Loads. Demonstrate a 2 MW (RF) klystrode and/or crossed-field amplifier under simulated space conditions. Demonstrate the "quick start" mode.

6.6 System Planning and Integration. Demonstrate at least one complete channel (at about the 10 MW level) under simulated space conditions. Include the standby, alert, and "quick start" modes of operation.

7. CONCLUSIONS

We conclude that there are no insurmountable obstacles to the building of power systems of the magnitude described herein. While early mechanizations of these concepts may be slightly higher in weight than envisioned, straightforward research and development will lead to lighter and more reliable systems. We recommend the development efforts described in Section 6 and we should start using one or more of the electrical systems described soon.

8. LIST OF REFERENCES

NUMBER	TITLE	NUMBER
1.	Integrated Spacecraft Total Energy System Analysis (U)	TRW Report No. 41808-6013-SX-00 (S) October 1985
2.	Space Power Architecture Study Task 1-Requirements	TRW Report No. 48083-IR-01
3.	Space Power Architecture Study Task 2-Power Sources	TRW Report No. 48083-IR-02 January 1987
4.	Reference Data for Radio Engineers, Third Edition, P179	FTR Corp.
5.	High Voltage System Performance in Low Earth Orbit Plasma Environments, Volume 2. SDI Space Power System Environmental Interactions Final Report for Contract NAS3-24659.	TRW Report No. 46870-6006-UT-00 October 1986

APPENDIX

RF SOURCES

Prepared By

A.S. Gilmour, Jr.

for

TRW, Inc.

PO No. R934660C6 M

APPENDIX
RF SOURCES

Extremely high RF power may be required for some systems in space. In many cases, the source of this power is considered to be part of the power conditioning system. Projected average power requirements range from megawatts for extended periods of time to hundreds of megawatts or more for relatively short time periods. Operating frequencies being considered are in the 400 to 500 megahertz range.

The selection of the best RF source for each application has not been made. In this section, the most likely candidates are discussed. These are:

Conventional gridded tubes	Crossed-field devices
Klystrodes	Klystrons

For each candidate basic operating principles are discussed, then present and projected limits to operating characteristics are pointed out.

Because cathodes and collectors are common to many of the candidate devices, sections have been devoted to those subjects.

A.1.1 Cathodes

With the obvious exception of solid state devices, all of the proposed RF sources are vacuum devices. All use either thermionic or secondary emission cathodes as electron sources. The emission capabilities of these cathodes vary widely. Secondary emission cathodes can produce a few tens of A/cm^2. Historically, average emission densities from thermionic cathodes have been limited to few A/cm^2 but over ten A/cm^2 has been demonstrated, and a capability of over several tens of A/cm^2 is predicted for short lifetime applications.

A.1.2 Thermionic Cathodes [1, 2, 3]

Thermionic cathodes are normally heated to a temperature in the 1000 to 2000° C range. At this temperature a sufficient number of electrons within the cathode are energetic enough to overcome the work function of

the cathode surface and escape into vacuum. The two thermionic cathode types most commonly used in high power RF sources are thoriated tungsten and dispenser cathodes.

In thoriated tungsten cathodes, a small percentage of thoria is mixed with the tungsten. During operation, thorium diffuses to the surface of the tungsten and so the work function of the surface is reduced from that of tungsten (about 4.6 eV) to that of thorium (about 3.5 eV). As a result, significant emission can be obtained at reasonable temperatures. Note here that the cathode surface is sometimes carburized to enhance performance.

Thoriated tungsten cathodes are usually directly heated, that is, the cathode is usually in the form of a filament through which sufficient current is passed to produce the desired temperature as the result of ohmic heating.

There are two basic configurations for dispenser cathodes. In one, referred to as an impregnated dispenser cathode and illustrated in Figure A-1, a porous tungsten cathode pellet is impregnated with emissive material typically containing barium, calcium, and aluminum. When the pellet is heated to the operating temperature (usually >1000°C), emissive material diffuses to the surface of the tungsten and forms an emitting layer.

The cathode illustrated in Figure A-1 is known as the B cathode and has been in widespread use for almost 30 years. In the B cathode, the molar ratio of the impregnant composition is 5 BaO, 3 CaO, and 2 Al_2O_3. In another similar cathode known as the S cathode, the molar ratio is 4 BaO, 1 CaO, 1 Al_2O_3. The work functions of these cathodes are about 2.1 eV.

The B and S cathodes are life limited at high emission current densities, because their high operating temperatures cause rapid barium evaporation and a decrease with time in surface coverage by the emissive layer.

In the second basic configuration of the dispenser cathode, referred to as a cavity reservoir cathode, the emissive material is contained in a reservoir. In a recent version called a controlled porosity dispenser cathode (CPD cathode), the emissive material is mixed with tungsten grains.

When heated to the operating temperature (usually >1000°C), emissive material diffuses through a thin tungsten foil with a uniform array of laser drilled holes.

Other versions of the cavity reservoir dispenser use a thin porous tungsten element in place of the tungsten foil. In the oldest and original version of the dispenser cathode, known as the L cathode, the reservoir was filled with barium carbonate. This cathode had the disadvantage that carbon dioxide released during cathode activation had to diffuse through the tungsten. This resulted in an exceedingly long processing time.

In a similar but much improved cathode, known as the MK cathode, the reservoir contains barium oxide and tungsten wool.

In the various cathodes discussed to this point, the work functions are in the 2.0 to 2.1 eV range. In practice, an operating temperature of 1100°C or higher is normally required for acceptable performance. This high temperature results in a relatively limited life.

The work function of any of these cathodes can be reduced to approximately 1.8 eV by the use of osmium, iridium, ruthenium or rhenium as an enhancing metal. This permits a reduction in cathode temperature of about 100°C and an increase in life by an order of magnitude for the same emission current density.

There are a number of ways in which the enhancing metal can be used. In the M cathode, the surface of a B cathode is coated with several thousand A of an osmium-ruthenium alloy. In the CD cathode, tungsten and osmium are co-deposited on the surface of a B cathode. In the mixed metal (MM) cathode, the enhancing material is dispersed throughout the tungsten matrix. The CPD and MK reservoir cathodes can be overcoated with enhancing metal in the same way that the M and CD cathodes are. Finally, note the use of scandium oxide in the emissive mix of a B cathode is claimed to produce emission characteristics similar to those resulting from the use of osmium, etc.

Figures A-2 and A-3 are comparisons of the performance characteristics of various cathodes. Perhaps the most significant aspect of these figures is that emission densities of at least several A/cm^2 are possible for lifetimes of 5 to 10 years.

In applications of cathodes where long life is not required, an extremely high emission density may be obtained for a relatively short period of time. Figure A-3 indicates that as much as 20 A/cm^2 may be achievable for a period of 1000 hrs. An extrapolation (if valid) to 100 A/cm^2 would imply that a life of a few tens of hours might be possible.

In the life prediction model developed by Longo et al [4], it is suggested that at high current densities and correspondingly high cathode temperatures, the rate of barium evaporation from a dispenser cathode surface will exceed the rate of supply. As a result, the fraction of the cathode surface covered by barium will decrease as indicated Figure A-4. Thus, for an M cathode, this model predicts that at least tens of A/cm^2 may be achievable.

By operating a cathode at a high emission density, the area and mass of the cathode assembly can be minimized. As a result, full emission can be achieved in a very short time period with the appropriate design of the cathode assembly. One example of a very-fast-warm-up cathode assembly is given in Figure A-5. The thoriated tungsten directly heated cathode is pulsed on in a fraction of a second by a large overvoltage. A potential difference of several hundred volts between the heater and the M-type impregnated cathode button results in rapid heating of the button by electron bombardment. A one second warm-up time is apparently possible.

In most microwave tubes, emission from the cathode surface is space-charge limited. That is, the electron cloud formed near the surface of the cathode regulates the rate of emission from the cathode. This occurs because the negative charge of the electron cloud depresses the potential so that the electric field at the cathode surface is very nearly zero, regardless of the voltage applied to the anode (within limits). This zero-field condition is an equilibrium condition. If the potential at the cathode surface tends to become positive, more electrons flow from the

cathode, thereby depressing the potential. If the potential tends to become negative, fewer electrons flow from the cathode, thereby raising the potential.

When a sufficient number of electrons is present so that emission is space charge limited, then cathode temperature, surface conditions, etc., have no effect on emission. In the absence of a magnetic field, the relationship between cathode current and anode voltage, when current is space charge limited, is given by

$$I = pV^{3/2}$$

where p is perveance and is a function only of the geometry of the cathode-anode assembly. Values of p range from 10^{-7} to 10^{-5} for most microwave tubes.

Very often, the power, P, required in the electron beam from a cathode is known. As a result, the voltage can be determined from

$$V = (P/p)^{2/5}.$$

For example, if an RF output power of one megawatt is required from a klystron or klystrode and the electronic conversion efficiency of beam power to RF power is 80 percent, then the beam power must be 1.25 megawatts. To achieve an 80 percent efficiency, the perveance must be relatively low. A value of 0.25×10^{-6} may be realistic. As a result, the voltage is readily found to be 120 kV.

While there may be ways to reduce this voltage somewhat (perhaps by as much as a factor of three of four), it will always be necessary to use a cathode-to-anode voltage of at least several tens of kilovolts at the megawatt power level. This leads directly to concern about the electrical breakdown characteristics of cathode-anode assemblies. Figure A-6 [1] contains experimental breakdown characteristics of the cathode-anode assemblies of some devices. The data points are for microwave tubes [5]. The circles are for dc operation and the triangles and Xs represent long-pulse and short-pulse operation respectively. Also shown is Kilpatrick's Criterion [6] which is often used as a guideline to the maximum electric field that can be used in a vacuum if breakdown is to be avoided.

Kilpatrick's Criterion is based on results for parallel plane electrodes while the tube results in Figure A-6 are for various electrode configurations. As a result, there are varying degrees of field enhancement that contribute to the scatter in the data. In addition, decomposition products from cathodes form surface layers of reduced work function, variable roughness and hardness, etc., that result in a reduction in breakdown voltage. Finally, devices that stand idle for extended periods of time are far more likely to breakdown than devices that are used continuously or frequently.

In view of these breakdown considerations, it will probably be necessary to operate at stress levels significantly below Kilpatrick's Criterion to achieve high reliability.

A.1.3 Secondary Emission Cathodes

When electrons bombard a surface, they may cause other electrons to be emitted from the surface. The bombarding electrons are called primary electrons and the emitted electrons are called secondary electrons. Secondary emission is of extreme importance in the cathodes on cross-field tubes where the electric and magnetic field configurations cause many primary electrons to bombard the cathode.

Often a small percentage of cathode emission is thermionic and the remainder is secondary. This is the case in magnetrons where, in a typical case, on the order of 10 percent of the total emission is thermionic and the other 90 percent is secondary. In some crossed-field amplifiers, cold cathodes are used and all of the emission is secondary. Emission is initiated by a relatively small number of free electrons that are always present (because of a small amount of thermonic emission from electrode surfaces since they are not at absolute zero; because of interactions of electrodes with background radiation, etc.). Some of these electrons are driven into the cathode by the RF fields.

The amount of secondary emission depends on the secondary emission ratio and on the impact energy and angle of incidence of the primary electrons. The secondary emission ratio for oxidized aluminum, a material commonly used in cold cathode tubes, is shown in Figure A-7. Some thermionic emission materials have extremely high secondary emission coefficients. For example, for a oxide coated cathode, it may be as high as 10.

A.2 CONVENTIONAL GRIDDED TUBES

One or more grids can be placed between the cathode and the anode of a diode to control the amplitude of the current. In a triode, a single grid is used. In a tetrode, a screen grid is placed between the control grid and anode to eliminate current induced in the grid circuit by charges in anode potential.

When the signal frequency on the control grid is high enough so that its period is short compared with the electron transit time from the cathode to the grid, electrons simply oscillate in the space between the cathode and the control grid. As a result, at high frequencies, RF current to the anode may be severely decreased or may cease altogether.

To alleviate this electron transit time problem, the control grid is moved closer to the cathode. At 3 GHz, the spacing between the cathode and control grid becomes about 100 microns, the diameter of the grid wires become about 10 microns and the diameter of the cathode, control grids and anode (planar configuration) become less than a centimeter. The average power rating is less than 100 W.

In spite of the transit-time problems which necessitate close grid-to-anode spacings, triodes and tetrodes have been built which are capable of peak powers of several megawatts and average powers of several hundred kilowatts at hundreds of megahertz. An example of one of these devices is shown in Figure A-8. The weight of 180 lb (82 kg) does not include associated RF components. In devices like that shown in Figure A-8, the high power levels are achieved by operating many linear triodes of tetrodes in parallel. The directly heated cathode of each is a long ribbon-shaped filament that is spring supported so that it retains its shape and position as temperature is varied. A copper grid block is used to suspend grid wires in close and carefully controlled proximity to the cathode.

A.3 KLYSTRODES

As frequency is increased and dimensions are reduced, a major limitation to power output of conventional gridded tubes is the power that must be dissipated by the anode. This problem is alleviated in a device known as a klystrode, which has five elements as shown in Figure A-9. These are the cathode, planar grid, anode, tailpipe and collector. The tube may be immersed in a uniform magnetic field for beam control. Superficially, the tube is similar to the tetrode except that the output circuitry is a resonant cavity.

In operation, an alternating voltage is applied between the cathode and grid. The resulting density modulated electron beam is accelerated toward the apertured anode at high potential.

Next, the beam passes through a gap, called the output gap, in the resonant cavity and induces an oscillating current and voltage in the cavity. RF power is coupled from the cavity at high power levels by direct coupling to a waveguide.

After the beam passes through the cavity, it enters the collector from the tailpipe. Some of the power remaining in the beam may be able to be recovered using a suitably designed collector. Collectors for this purpose are called multistage depressed collectors and are described in Section 5.

The gain of a klystrode is modest and the demonstrated efficiency is high as shown in Figure A-10. Shrader, et al [7] have predicted that efficiency can be increased about 10 percentage points through the use of a second cavity. The electron beam would be passed through this additional cavity prior to entering the output cavity. As is commonly done in klystrons, this additional cavity would be tuned upward in frequency from the klystrode operating frequency so that it would be inductive at the operating frequency, A a result, the voltage across the cavity gap would lag the current induced in the cavity by the electron beam. Thus, the voltage would be phased with respect to the electron bunches so that electrons between bunches would be swept into the bunches. As a result, bunching would be enhanced so that tne RF current induced in the output cavity would be increased.

The enhanced bunching and increased beam current are indicated by the computed results shown in Figure A-11. In the phase plot each line indicates the position of electrons relative to the center of an electron bunch. The effect of the inductive cavity is to squeeze the lines closer together. The corresponding RF current increase in shown by the beam current plot.

Shrader, et al [7] have projected the maximum power capabilities of klystrodes on the basis of measured performance in the 470 to 800 MHz range. The perveance assumed was 0.33X10-6. The results are shown in Figure A-12. At the 1 megawatt CW level and 450 MHz, a conversion efficiency of 75 percent is projected. The beam voltage would be 120 kV. The device is projected to be 60 in (1.5 m) long, 24 in (0.61 m) wide and 16 in (0.41 m) deep. The total weight of the device would be 250 lb (114 kg). The tube and circuitry would weight 150 lb (68 kg) and the magnet would weigh 100 lb (46 kg).

A.4 KLYSTRONS

The klystron is one of two major classes of devices normally categorized as linear-beam microwave tubes. The other is the traveling wave tube (TWT). Klystrons are capable of extremely high powers (over 1 megawatt average and nearly 1 gigawatt peak), may have high efficiency (70 percent demonstrated) but have narrow bandwidths (normally on the order of 1 percent).

In a klystron the electron beam is generated in a Pierce electron gun. The major elements of a Pierce gun are the cathode, focusing electrode, and anode shown in Figure A-13. In a Pierce gun, the electron beam from the cathode is sometimes compressed by a factor as high as 100 or more (area compression ratio) to produce the relatively high-density beam required for interaction with the RF circuit. In this way, the current density at the cathode surface can be kept at a low enough level so that long cathode life can be realized.

When long cathode life is not required, the cathode emission density can be very high (10s of A/cm^2). This leads to significant reductions in the area compression ratio, in the cathode size and mass, and to the possibility of vary fast warm-up time assemblies (see CATHODE Section).

To facilitate control of the beam in a Pierce gun, a modulating anode is sometimes used. In the modulating anode gun. the anode of the electron gun (the modulating anode) is separated from the body of the tube, a part of which is a second (final) anode. The configuration of a modulating anode gun is shown in Figure A-14.

Although the voltage range over which the modulating anode must be varied in order to vary beam current is large, the power required to drive the modulating anode is small because the current intercepted by this anode is very small. At intermediate voltage levels, perveance may be controlled with the modulating anode without severely affecting beam focusing.

A very important aspect of a modulating anode is its ability to protect the tube in the event of a gun arc. When an arc occurs between the focus electrode/cathode assembly and the modulating anode, the voltage on the modulating anode can be dropped to the cathode potential to extinguish the arc. This significantly simplifies the tube protection circuitry.

In virtually all linear-beam tubes, the electron beam is focused by a magnetic field so that it passes through the RF structure with very little interception. A typical magnetic circuit configuration for producing the desired focusing field is shown in Figure A-13.

Focusing occurs because the electron beam crosses a radial component of magnetic flux as it leaves the electron gun. The resulting rotation of the electrons in the presence of an axial component of magnetic flux results in a radial compressive force that offsets the electron space-charge forces.

The minimum magnetic flux density that can be used to focus a beam is known as the Brillouin flux density and the resulting electron beam motion is called Brillouin flow. For smooth beam formation with the Brillouin flux density, the cathode must be completely shielded from the focusing field.

In practice, Brillouin focusing is rarely used in very high power tubes because of the high sensitivity of the beam to perturbations. Instead, as shown in Figure A-13, the magnetic circuit providing the focusing field is purposely designed so that magnetic flux lines pass through the cathode. The resulting beam rotates more slowly than a

Brillouin beam and the axial focusing field is larger than the Brillouin value. Perturbations that cause a change in beam radius result in a large (compared to the Brillouin case) change in rotational velocity and a large restoring force tending to return the beam to its original radius. For a flux density two to three times the Brillouin value, the sensitivity of the beam to perturbations is reduced by an order of magnitude compared with the Brillouin case. Focusing with fields well above the Brillouin value is called confined flow focusing.

Confined flow focusing is used to prevent excessive interception of the beam by the RF circuit. The drawbacks to confined flow focusing are that the magnetic field generating structure is large and heavy and the power required for focusing, assuming a solenoid is used for generating the field, is large (compared with that for Brillouin flow).

At this point, it is appropriate to comment on the use of permanent magnets for beam focusing. When a solenoid is used for focusing, the weight of the solenoid is often larger than the weight of the microwave tube. By using permanent magnets it is possible to reduce the weight of the focusing system by an order of magnitude or more. The magnets are arranged so that they form a series of lenses that periodically focus the beam. These periodic permanent magnet (PPM) structures are in common use in applications (primarily airborne) where weight and size minimization are important. These applications are at modest power levels (hundreds of watts to tens of kilowatts).

The primary drawback to PPM focusing is that the equivalent of Brillouin focusing (for a solenoid focusing system) has normally been used and so beam interception on the RF circuit is high. This severely limits average power capability and efficiency. Recently, a confined flow version of PPM focusing applicable to low perveance ($<< 1X10^{-6}$) beams has been described by James at Varian. This technique reduces interception and permits operation at increased power levels. It appears that this technique should be investigated for possible application to very high power microwave tubes in space. Finally, there is the possibility of a hybrid focusing system in which a PPM structure is used in the small signal portion of the tube and then a solenoid is used at the output end where RF perturbations of the beam density are intense.

In the triodes, tetrodes and klystrodes discussed earlier in this report, electron flow from the cathode was controlled by one or more grids near the cathode. Operation at high frequencies degrades because the period of the RF modulating signal is comparable to , or shorter than, the transit time of electrons from the cathode to the grid.

This transit time problem is overcome in the klystron by first accelerating electrons to high velocity in the electron gun (see Figure A-13 or A-14) and then subjecting the electrons to the modulating field so that the velocities of the electrons are modulated.

As the beam drifts away from the modulating cavity, the electrons form into bunches and so the velocity modulation is converted to density (and current) modulation. If the beam containing this current modulation is passed through the gap of a resonant cavity (like that described for the klystrode) an oscillating current and voltage will be induces in that cavity.

In most klystrons, power is not coupled out of the second cavity. Instead, the voltage developed across the gap is used to enhance the modulation of the beam and the beam continues on to one or more additional cavities where further enhancement of the signal takes place. Finally, the beam is passed through an output cavity where a large fraction of the RF power on the beam is extracted.

Four or more cavities are normally used in klystrons for several reasons. First of all, by tuning all cavities to the same frequency (synchronous tuning) very high gain (Over 20 dB per amplifying stage) results. By detuning the next to last cavity (penultimate cavity) upward in frequency, the inductive effect described for the second cavity in a klystrode is achieved. The result is that bunching of the electrons in the last cavity is enhanced and output power is maximized. This is known as efficiency tuning. Finally, by stagger tuning the various cavities (broadband tuning) the bandwidth of the klystron can be increased.

The efficiency of a klystron, like that of a klystrode, depends on the quality of the bunching of electrons at the last cavity. The fundamental component of the RF current in the beam must be maximized, and the distribution of electron velocities in the bunch must be minimized. These conditions depend on the perveance of the beam and on the design of the buncher section of the RF structure (all cavities except the output cavity). The calculated dependence on perveance is illustrated in Figure A-15. Low perveance (curve 1) is a value well below $1X10^{-6}$ while high perveance (curve 2) is a value well above $1X10^{-6}$. Note that for low perveance case, a maximum efficiency of 70 percent is predicted. The limiting output gap voltage at which maximum efficiency occurs is that which reverses the trajectories of electrons.

There have been projections of efficiencies in the 80 to 90 percent range for klystrons [8 to 15]. These are all based on narrow-band operation. In several cases, one or more cavities tuned to the second harmonic frequency are used to enhance bunching. None of these investigations included the consideration of the use of multistage depressed collector (MDC) for further efficiency enhancement. In one analysis in which a MDC was considered [16] it was projected that an improvement in overall efficiency from 70 percent to the 80 to 85 percent range might be realized. If the basic interaction efficiencies in references [8 to 15] of 80 to 90 percent are realized in practice, it is not at all clear that further increased of any significance can be achieved with the MDC.

In practice, as shown in Figure A-16, an efficiency of 70 percent has been reported for a narrow-band device operating at a microperveance of 0.5. This device operated at about 3 GHz with a power output of 70 kW. At 352 MHz and a CW power output of 1 megawatt, an efficiency of 65 percent has been reported [17]. Because perveance must be relatively low for high efficiency, the electron gun voltages on high power klystrons are high. At the megawatt level, the voltage would be about the same as the klystrode that is 120 kV. An interesting approach being proposed for reducing voltage (and reducing weight at the same time) is the use of multiple beams in parallel in a single device. This is basically a renovation of the

multiple-beam klystrons (MBK) developed by the General Electric Company over 20 years ago. In the MBK, the perveance of individual beams would be low so that electron bunching would be appropriate for high efficiency. By using multiple beams, the power per beam would be reduced and so the beam voltage would be reduced. The primary advantage of the MBK over multiple klystrons would be the reduction in weight resulting from the use of single elements (such as the solenoid) rather than multiple elements.

Overall klystron dimensions (except for the collector) scale roughly in proportion to wavelength. Since wall thickness (of cavities, drift tubes, etc.) are relatively independent of size, overall klystron weight scales approximately with the square of wavelength. As a result,as indicated by Figure A-17, low frequency klystrons are large and heavy. As an example, the 352 MHz, 1-megawatt klystron mentioned in a previous paragraph weights over 2000 kg (nearly 5000 lb.). The dimensions are 4.80 m (15.8 ft) by 1.85 m (6 ft) by 1.20 m (3.9 ft). We must point out that devices specifically designed for use in space would probably be lower in weight than the ground based designs mentioned here.

A.5 MULTISTAGE DEPRESSED COLLECTORS

The electron beam leaving the gap of the RF output cavity of a klystron or klystrode contains a significant amount of power referred to as spent beam power. If the beam is collected by an electrode (collector) which is at the same potential as the anode of the electron gun (and the RF interaction structure of the tube) then the spent beam power is converted to heat as electrons impinge on the collector. If the potential of the collector can be reduced (depressed) to a value below the anode potential, then the velocity of the electrons is reduced before they are collected and some of the spend beam power is recovered.

The circuit diagram for a tube with a single-element depressed collector is given in Figure A-18. It is important to note that two separate power supplies are used. The one connected to the anode and RF structure controls the velocity of the electrons and the phase characteristics of the output power and must normally be highly regulated.

However, the current (and power) supplied is a small fraction of the total current (power) to the tube. The fraction supplied results from the current intercepted by the RF structure as the beam passes through the tube and is less than 1 percent in very-high-efficiency, well-focused devices. The remainder of the current (and power) is supplied by a separate source for which regulation is relatively unimportant because this source collects the beam after interaction with the RF circuit has been completed.

The problems with the configuration shown in Figure A-18 is that in high efficiency tubes, the spread in velocities (and energies) of electrons leaving the output cavity can be very large, because the electrons have given up so much of their energy in the interaction process. This is illustrated for a relatively high efficiency (>50 percent) UHF klystron in Figure A-19. The horizontal axis is the spent electron energy normalized with respect to the initial electron energy (before modulation). The vertical axis is the fraction of the beam current having more than a particular value of energy.

Notice in Figure A-19 that more than 25 percent of the electrons in the spent beam have given up more than 75 percent of their initial energy from the electron gun) in the interaction process. More than 75 percent of the electrons have given up more than 50 percent of their energy. Notice also from Figure A-19 that a single-element collector depressed even a small amount below the anode potential would repel electrons. These would travel in the reverse direction toward the cathode. Excessive interception on the RF circuit along with interference with the amplification process would result.

To recover a large fraction of the power in a spent beam, and, at the same time, prevent electrons from being reflected, a collector must contain electric fields shaped so that all electrons are nearly stopped, regardless of velocity, just as they strike the collector electrodes. In addition, the fields must be shaped to prevent secondary electrons from being accelerated (thus wasting energy) or leaving the collector.

The research and development collectors having the appropriate field configurations are the work of Dr. H. G. Kosmahl and his associates at the NASA Lewis Research Center in Cleveland, Ohio. The original impetus for the NASA work was the extremely high premium on efficiency resulting from the high cost of power generation and heat rejection on satellites using microwave tubes.

The NASA collectors use several electrons at a various potentials and are referred to as multistage depressed collectors (MDC). Modern collectors are fabricated with electrodes made from graphite or graphite coated copper to minimize secondary electron emission. These collectors are no larger than the conventional single element low efficiency collectors that have been used in the past.

Experience to date with MDCs is mostly on relatively low power tubes. As an example, Figure A-20 shows results for an electronic countermeasures TWT with a power capability of a few hundred watts. Without the MDC, the efficiency was in the 10 to 20 percent range (typical for very broad bandwidth TWTs). With a five-stage MDC, the efficiency increased by a factor of about three.

The application of MDCs to megawatt klystrons or klystrodes will be challenging to say the least. However, the possibility of adding 10 to 15 percent to overall efficiency along with a significant reduction in power supply regulation complexity makes it essential to at least investigate the feasibility of the use of multistage depressed collectors.

A.6 CROSSED-FIELD TUBES

In crossed-field tubes, the electrical field is perpendicular to the magnetic field, and the general motion of the electron beam is perpendicular to both fields. This is in contrast to linear beam tubes where the general direction of beam motion is aligned with the fields.

Crossed-field tubes are compact, reasonably light weight and are normally very efficient. There have been attempts to use these devices as RF power sources for linear accelerators. To date, these have been unsuccessful because of instabilities in the devices resulting from the highly reactive nature of the load.

In spite of past problems in attempting to use crossed-field devices with reactive loads, they should not be dismissed from further consideration. They may well be the lightest and most efficient devices available, and there are new developments to be described in this section that hold the promise of solving the stability problem.

Versions of crossed-field tubes that may find application are both magnetron oscillators and crossed-field amplifiers.

The basic configuration of a magnetron is shown in Figure A-21. In this case, the anode contains eight RF cavities (resonators) and is concentric with a thermionic cathode. The magnetic field is applied parallel to the cathode surface. The dashed lines indicate the RF electric field pattern at one instant in time. In the desired mode of operation shown in Figure A-23, the RF fields in adjacent cavities are 180° out of phase. This is referred to as the pi mode of operation. As a function of time, the fields oscillate and so the field pattern in Figure A-21 reverses on every half cycle of oscillation.

The motions of two electrons are indicated in Figure A-21. An electron leaving the cathode at point A enters an accelerating field and is driven back into the cathode with appreciable energy. This electron extracts energy from the RF field and the only useful purpose that it serves is to contribute to the emission process by generating secondary electrons.

An electron leaving the cathode at B enters a decelerating field and moves toward the anode. With the correct frequency of operation, this electron will remain synchronized with the decelerating field as it passes successive anode segments and will eventually strike the anode. In moving from the cathode to the anode, this electron acquires dc energy, which it gives up to the RF field. The paths of individual electrons may be traced in a relativily straight forward manner, as indicated in Figure A-21.

In an operating magnetron, a space-charge cloud of electrons surrounds the cathode, thus complicating the analysis of the trajectories. In the absence of RF fields, the electrons form a rotating sheath or hub around the cathode. When RF fields are present, those electrons in accelerating regions are forced back toward the cathode, thereby producing a depression in the space-sharge hub. In the decelerating regions, the electrons move toward the anode and produce projections on the space-charge hub.

As a result, the rotating space-charge cloud is distorted into the spoke-like pattern shown in Figure A-22. Electron current flows through the spokes from the cathode to the anode. The spoke-like cloud rotates with an anguiar velocity such that it remains synchronized with the alternating RF voltage on the anode segments. As the spokes pass the slots between anode segments, the RF fields provide a focusing action that tends to further bunch the electrons.

The mechanism by which enenrgy is extracted from the rotating spokes of electrons is identical to that described for electron bunches in a klystrode or klystron. That is, these spokes induce current flow in the Rf cavities. The current flow, in turn, produces RF electric and magnetic fields that can be coupled out of one or more cavities.

A severe problem that occurs in magnetrons having the basic configuration shown in Figures A-21 and A-22 is that various modes of oscillation other than the desired pi mode can exist. Early efforts to control this moding problem consisted of either connecting alternate anode segments together with metallic steps or else using an RF structure containing cavities with two different sizes (the rising sun structure). With either technique, the frequencies of the undesired modes were moved away from the frequency of the desired mode.

A development in the 1950s for controlling moding was the addition of a relatively large cavity surrounding the resonator structure of a magnetron. The resulting device is known as a coaxial magnetron and is illustrated in Figure A-23. Slots in the back walls of alternate cavities of the anode resonator structure tightly couple the fields in these resonators to the surrounding cavity. In the pi mode, the fields in every other cavity are in phase, and so they couple in the same direction into surrounding cavity. Thus, the surrounding coaxial helps stabilize the magnetron in the desired pi mode of operation.

The use of coaxial magnetrons to drive accelerators has been suggested. It is proposed to control the frequency of operation by injection locking; that is, by injecting a signal into the magnetron to control the signal being generated.

There are many similarities between high power, highly efficient, crossed-field amplifiers (CFAs) and the magnetrons discussed previously in this section. Both have a circular configuration with a concentric cathode. Both use an axial magnetic field. The primary difference is, as is shown in Figure A-24, that the CFA has provisions for an RF input signal. Interactions between the input signal and the cloud of electrons rotating about the cathode causes the electrons to form into spokes similar to those in a magnetron (indicated by the rectangular bunches in Figure A-24). The electrons circle about the cathode until they give up sufficient energy to reach the anode (which is also the slow-wave structure). This contributes to high efficiency and, it is believed, to improved turn on and starting. A drift region is used between the output and input so that space charge forces cause electron bunches to disperse. This removes the modulation from the rotating cloud of electrons and thus minimizes feedback from the output to the input.

Thermionic cathodes are used in some CFAs and cold cathodes are used in others. The cold-cathode technique is used primarily in high power devices ($>$ 10 kW ouput), although lower power levels are possible. With the cold-cathode technique, the initiation of emission build-up results from the presence of a relatively small density of electrons near the

cathode surface. These electrons result from various emission processes including the very low level of thermionic emission that occurs even at room temperature. For emission to buildup properly, the cathode-to-anode voltage must be correct and the RF drive must be adequate. Surprisingly, the resulting emission build up is very rapid (< 10 ns) and there is very little jitter.

Like the magnetron, a CFA is a cylindrical diode with a magnetic field applied. A typical voltage-current (V-I) characteristic is shown in Figure A-25. Because of the magnetic field, the device is essentially cut off (no anode current flows) until a relatively high voltage is applied. Factors which affect the V-I characteristic are frequency of operation, magnetic field and RF drive power.

The impedance characteristic of CFAs (and magnetrons) are of importance when considering their operation with a power supply. As Figure A-25 shows, there is a significant difference between static impedance, which is simply the operating voltage divided by the operating current, and the dynamic impedance, which is the rate of change of voltage with current. The dynamic impedance may be an order of magnitude smaller than the static impedance.

A particularly important feature of CFAs is the relatively low voltage at which they operate. For example, the anode-to-cathode voltage of a 1-megawatt device is less than 40 kV. This is a factor of two to three below that for a single-beam klystron or klystrode.

The gain of a CFA is often shown on a plot of power output vs. power input (referred to as a compression curve) like that in Figure A-26. Values of gain shown in Figure A-26 are typical, and are low compared with linear beam devices. Also note that the CFA does not exhibit any region in which operation is linear (constant gain).

Recently, a technique for improving the gain of cold cathode CFAs has been developed. Rather than having the entire RF circuit as the anode, part of the circuit at the input of the tube is on the cathode. As a result of separating the input and output circuits, the stability is

improved and gains in the neighborhood of 30 dB are achieved. Improvement in stability may cause the CFA to be more tolerant of highly reactive loads such as accelerator cavities.

Historically, alnico magnets have been used on magnetrons and CFAs and a major fraction of the tube weight has been in the magnet. Shown in Figure A-27 is the reduction in magnet size that could be achieved through the use of samarium cobalt. (This same reduction in size would, of course, occur for the other identical magnet.)

Still another possibility in cold-cathode CFAs is the placement of the magnet inside the cathode as illustrated in Figure A-28. The use of samarium cobalt in this manner has been demonstrated in low frequency CFAs [18].

In efficient crossed-field devices, the electrons are collected on the RF circuit. Thus, the RF circuit must be capable of dissipating the spent beam power. In addition, there may be a significant amount of heating of the cathode by back bombardment so that the cathode may have to be cooled.

As an example of the way in which power may be distributed in a CFA, consider the "super power" CFA for which performance characteristics are given in Figure A-29. This device generated 350 kW CW at an efficiency of 70 percent. The distribution of power in the tube is listed in Table A-1.

Table A-1. Distribution of Power in "Super Power" CW CFA (from J. Skowron, (MPTD), Raytheon Co., Workshop on High-Power, Space-Based Microwave Systems, Los Alamos, NM, March 1985.)

RF Power Generated	71.7%	350 kW*
Anode Dissipation	21.4	104.5
Cathode Dissipation	5.0	24.6
Transmission Line	1.9	9.3
Totals	100.0%	488.4 kW

*Note: The RF drive power is added to the RF power Generated for a total output power of 405 kW.

The severity of the cooling problem becomes apparent when it is realized that the total cross-sectional area of the anode segments ranges from a fraction of a square centimeter in high frequency devices to a few tens of square centimeters in low frequency devices. These relatively small areas may lead to the necessity to dissipate power densities in excess of a kW/cm2 on the anodes.

Table A-2 contains a listing of the cooling capabilities possible with various techniques. Over 10 kW/cm2 can be removed by high velocity water when nucleate boiling occurs on the surfaces being cooled. Thus, this is the cooling technique used in extremely high power applications.

Table A-2. Cooling Capability of Various Media (T = 200°C) (from J. Skowron, (MPTD), Raytheon Co., Workshop on High-Power, Space-Based Microwave Systems, Los Alamos, NM, March 1985.)

Black body radiation (T 200°C)	0.25 W/cm^2
Air, natural convection to finned forced convection	0.5-100
Organic oils, natural convection to forced convection, boiling	5-90
Water, pool boiling	125
Water, pressurized, non-boiling	155
Liquid metals, forced convection non-boiling	450
Water, high velocity, nucleate boiling	
Operational	10,000
Maximum achieved	20,000

Shown in Figure A-30 are predicted power capabilities of CW CFAs based on anode dissipation capability. The Raytheon QKS849, which used nucleate boiling to achieve an anode dissipation of 3600 W/cm^2, is used as the design reference point. Based on this power density, power outputs in excess of 1 megawatt should be possible at frequencies below about 1500 MHz.

REFERENCES

1. A. S. Gilmour, Jr., Microwave Tubes. Dedham, Mass.: Artech House 1986.

2. J. L. Cronin, "Modern Dispenser Cathodes," IEE Proc. vol. 128, pt, 1, no. 1, Feb. 1981, pp. 19-32.

3. L. R. Falce, "Dispenser Cathodes: the Current State of the Technology," Technical Digest, 1983 International Electron Devices Meeting, pp. 448-451.

4. R. T. Longo, E. A. Adler, and L. R. Falce, "Dispenser Cathode Life Predictions Model," Technical Digest, 1984 INternational Electron Devices Meeting, pp. 318-321.

5. A. Staprans, "Voltage Breakdown Limitations of Electron Guns for High Power Microwave Tubes," Proc. Second International Symposium on Insulation of Voltages in Vacuum, M. I. T., Cambridge, MA, 1966.

6. W. D. Kilpatrick, "Criterion of Vacuum Sparking Designed to Include Both RF and DC," Review of Scientific Instruments, vol. 28, no. 10, October 1957, pp. 824-826.

7. M. Shrader, D. Preist and B. Gasier, "Pre-bunched Beam Devices--Efficient Sources of UHF and Microwave Power, "Technical Digest, 1985 International Electron Devices Meeting, pp. 342-345.

8. T. G. Mihran, G. M. Brank, Jr., and G. J. Griffin, Jr., "Electron Bunching and Output Gap Interaction in Broad-Band Klystrons, "IEEE Trans. on Electron Devices, vol. ED-19, no.9, September 1972, pp. 1011-1017.

9. V. M. Piknov, V. Ye. Prokop'yev and A. N. Sandalov, "A Fast Method of Calculating Nonlinear Processed in Devices with Longitudinal Interaction," Radioteknika i Electronika, No. 4, 1985, pp. 774-780.

10. A. N. Sandalov and A. V. Terebilov, "Special Features of Bunching and Energy Exchange in Relativistic Multiresonator Klystron, "Radio Engag. and Electron. Phys., vol. 28, no. 9, 1983.

11. Ye. I. Yasil'yev, V. I. Kanavets and A. V. Terebilov, "Effect of the Velocity Distribution in a Bunch on the Kinetic Energy Extraction efficiency in a klystron, "Radio Engng. and Electron. Phys., vol. 28, no. 4, 1983.

12. A. V. Aksenchik, S. V. Kolosov, A. A. Kurayev and A. A. Paramonov, "Computer Modeling and Investigation of Most Efficient Interaction Processes in Multicavity Klystrons, "Radio Engng. and Electron. Phys., vol. 28, no. 2, 1983.

13. A. V. Aksenchik, S. V. Kolosov, A. A. Kurayev and V. P. Shestakovich, "Results of Optimization of the Efficiency of Multiresonator Klystrons, "Radio Engng. and Electrons. Phys., vol. 27, no. 12, 1982.

14. V. A. Kochetova, V. I. Kuchugurnyy, S. V. Lebedinskiy, A. V. Malykhin and D. M. Petrov, "High-efficiency Drift Klystron. Some Theoretical and Experimental Questions (Ordered Bunching, Gathered Bunch, and Convection Current Harmonics), "Radio Engng. and Electron. Phys., vol. 26, no. 1, 1981.

15. V. A. Kochetova, V. I. Kuchugurnyy, S. V. Lebedinskiy, A. V. Malykhin and D. M. Petrov, "High-efficiency Drift Klystron. Some Theoretical and Experimental Questions (optimization of the AFC, Comparison of Calculated and Experimental Characteristics), Radio Engng. and Electron. Phys., vol. 26, no.1, 1981.

16. E. J. Nalos, "High-efficiency SPS Klystron Design, "Proc. Workshop on Solar Power Satellite Microwave Power Transmission and Reception, NASA Conference Publications NASA CP-2141, p. 175, January 1980.

17. C. Bastian, G. Faillon and M. Simon, "Extremely High Power Klystrons for Particle Accelerators, "Technical Digest, 1982 International Electron Devices Meeting, pp. 190-194.

18. John F. Skowron, "The Continuous-Cathode (emitting-sole) Crossed-Field Amplifier, "Proc. IEEE, vol. 61, March 1973, pp. 330-336.

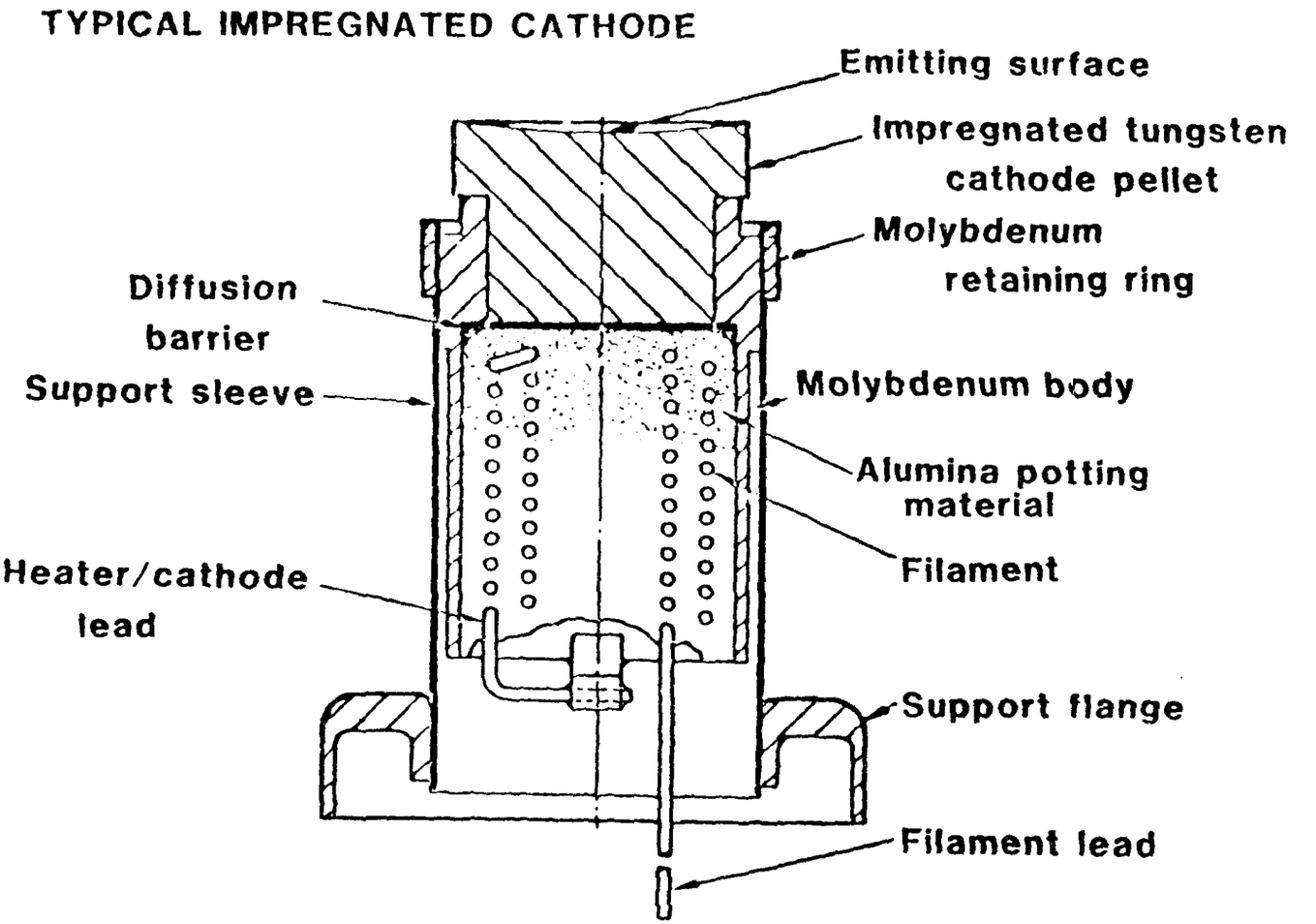

Figure A-1. Typical Impregnated Dispenser Cathode

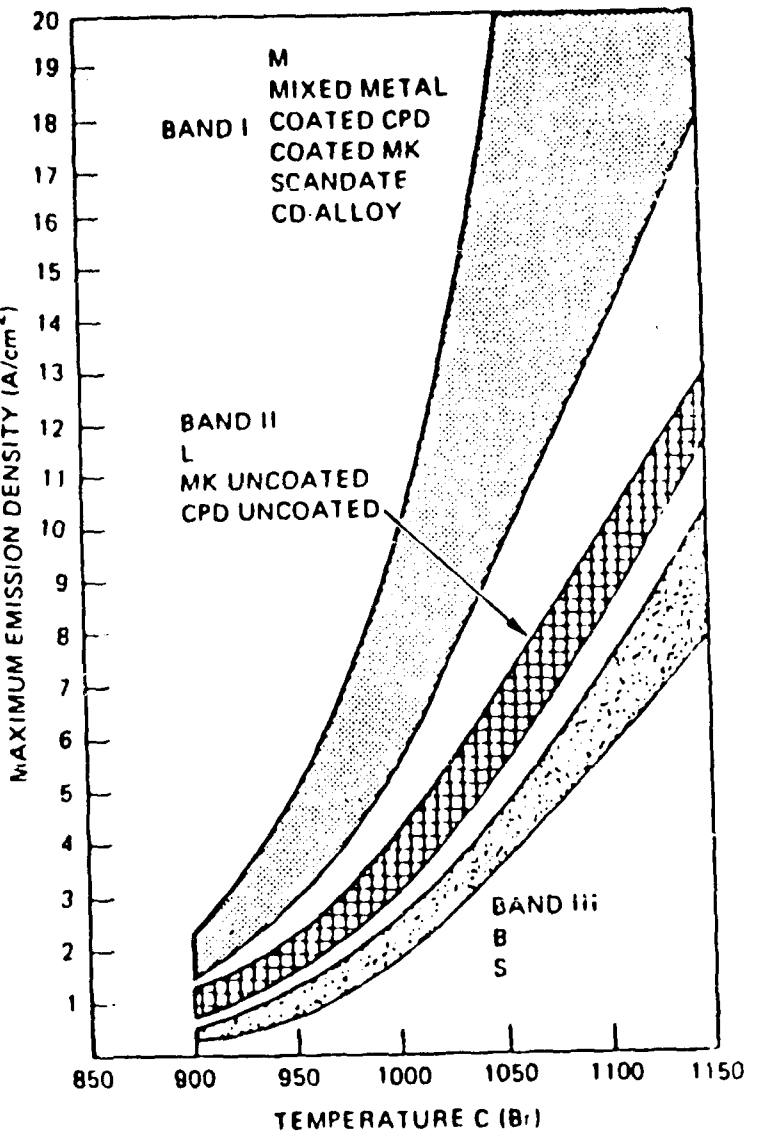

Figure A-2. Emission Density Characteristics of Various Cathodes (from L. R. Falce, Technical Digest, 1983 IEDM) c 1983 IEEE

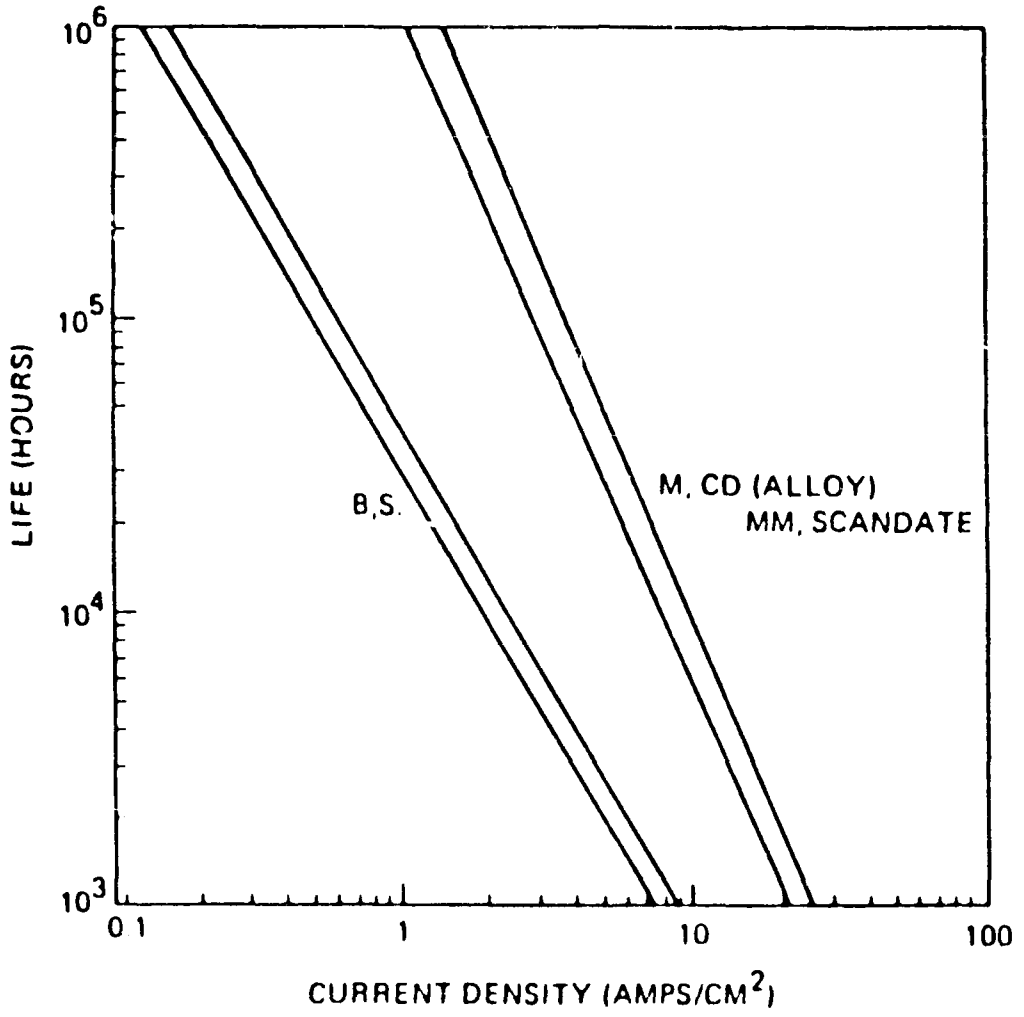

Figure A-3. Cathode Life for Impregnated Dispenser Cathodes (from L. R. Falce, Technical Digest, 1983 IEDM) c 1983 IEEE

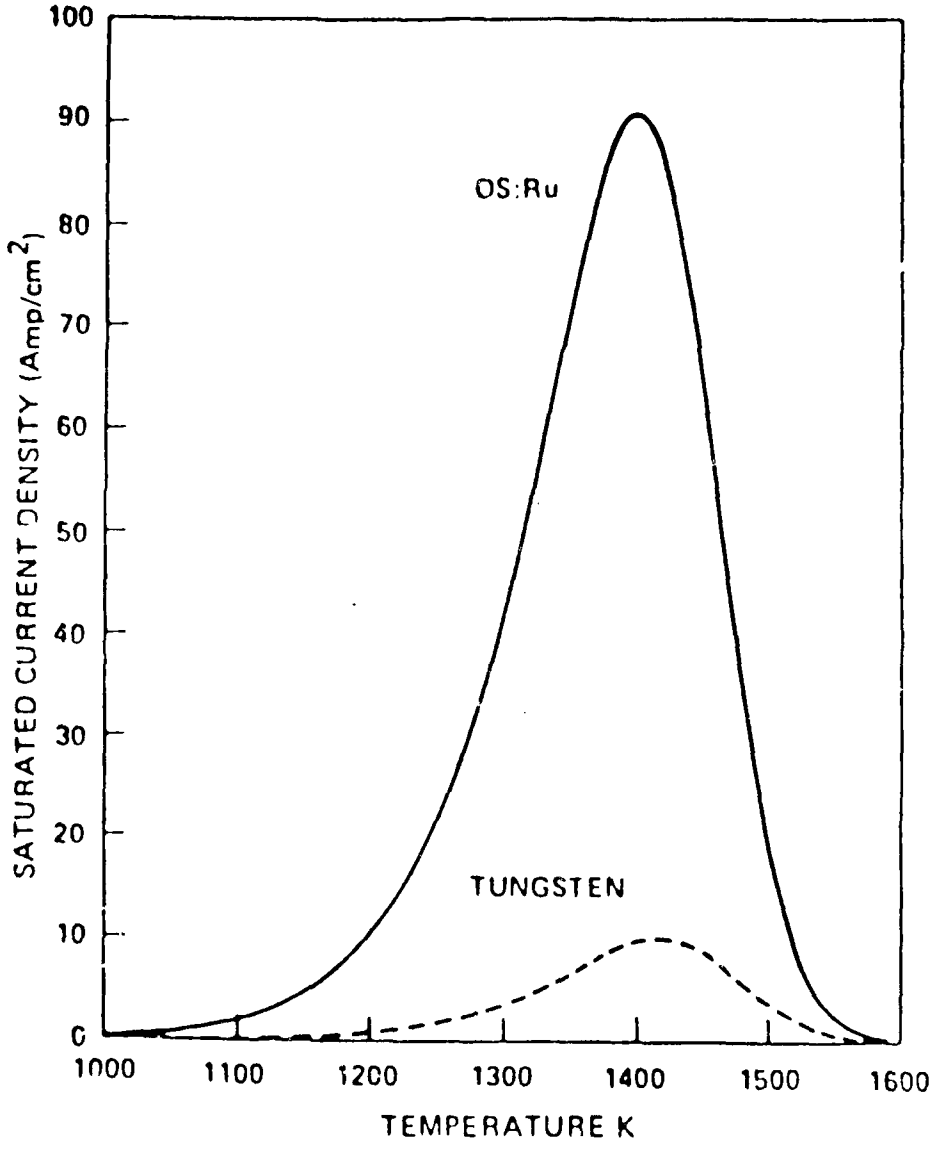

Figure A-4. Predicted Maximum Cathode Current Density as a Function of Cathode Temperature (from R. T. Longo, E. A. Adler and L. R. Falce, Technical Digest, 1984 IEDM) c 1984 IEEE

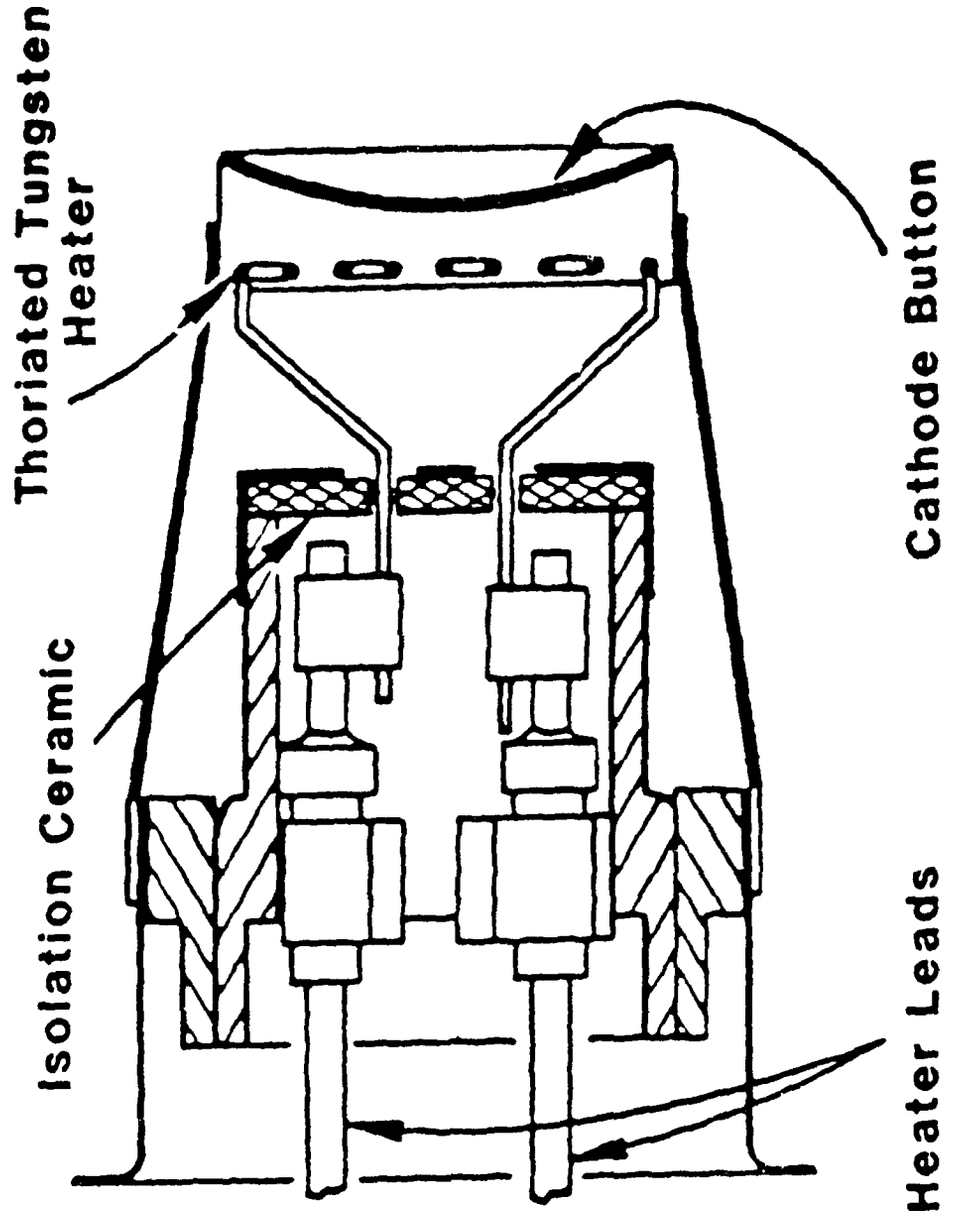

Figure A-5. Fast Warm-up Cathode Assembly (from R. C. Treseder, T. J. Grant and G. V. Miram, Technical Digest, 1983 IEDM) c 1983 IEEE

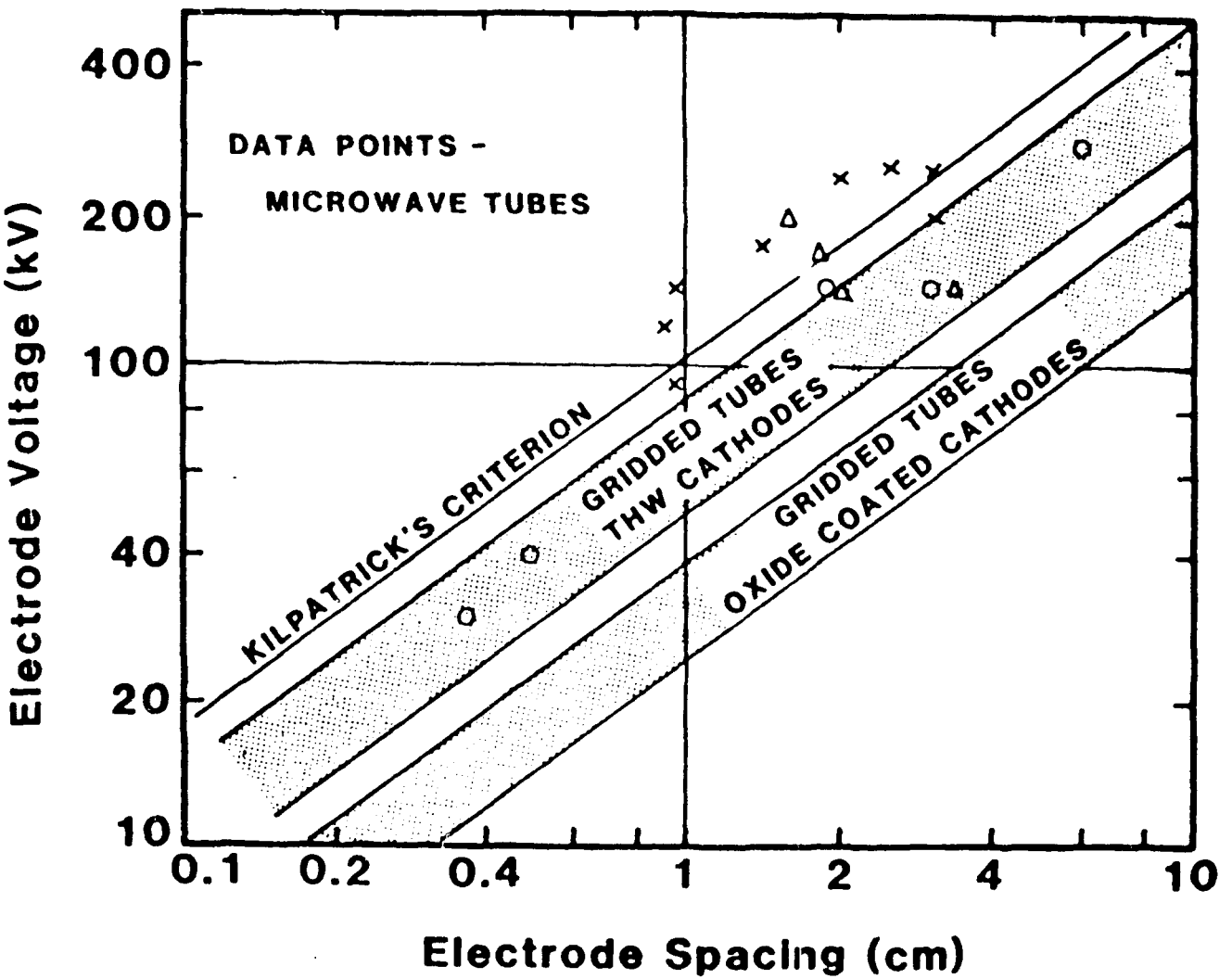

Figure A-6. Kilpatrick's Criterion and Experimental Breakdown Characteristics of Tubes

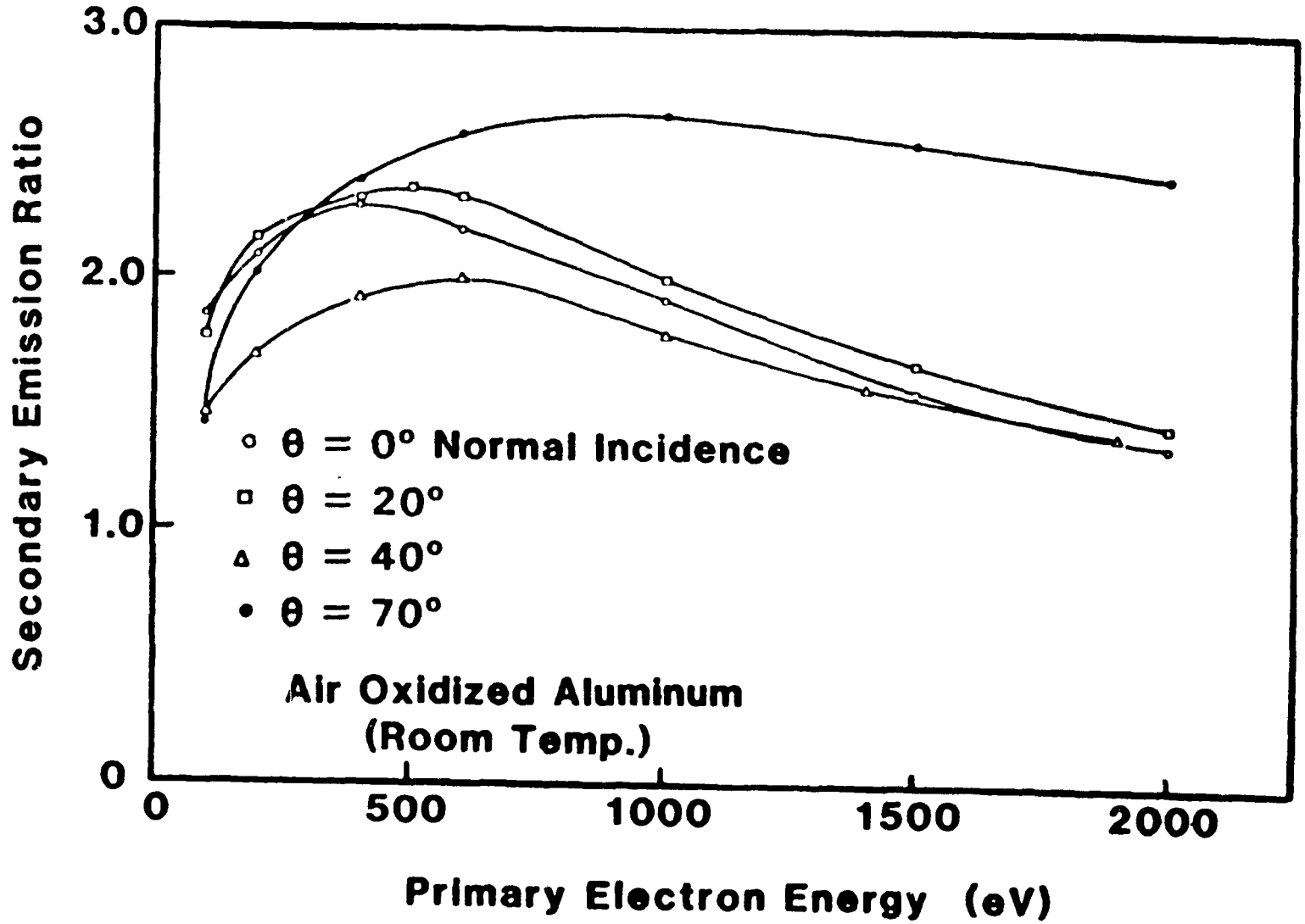

Figure A-7. Secondary Emission Ratio for Oxidized Aluminum (from John F. Skowron, Proc. IEEE, March 1973) c 1973 IEEE

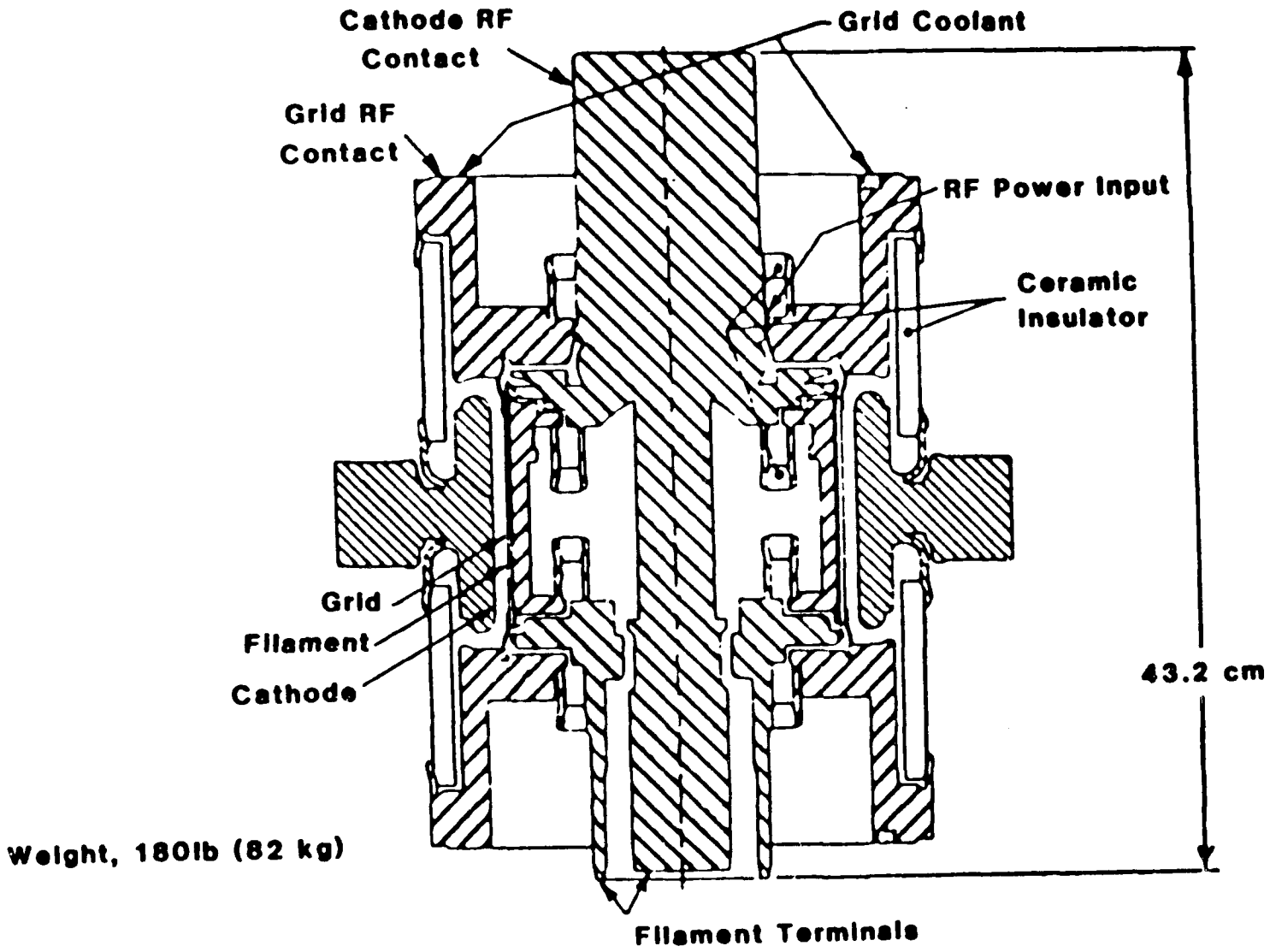

Figure A-8. Cross-Sectional View of High Power Triode
(from T. E. Yingst, et al., Proc. IEEE, March 1973.)

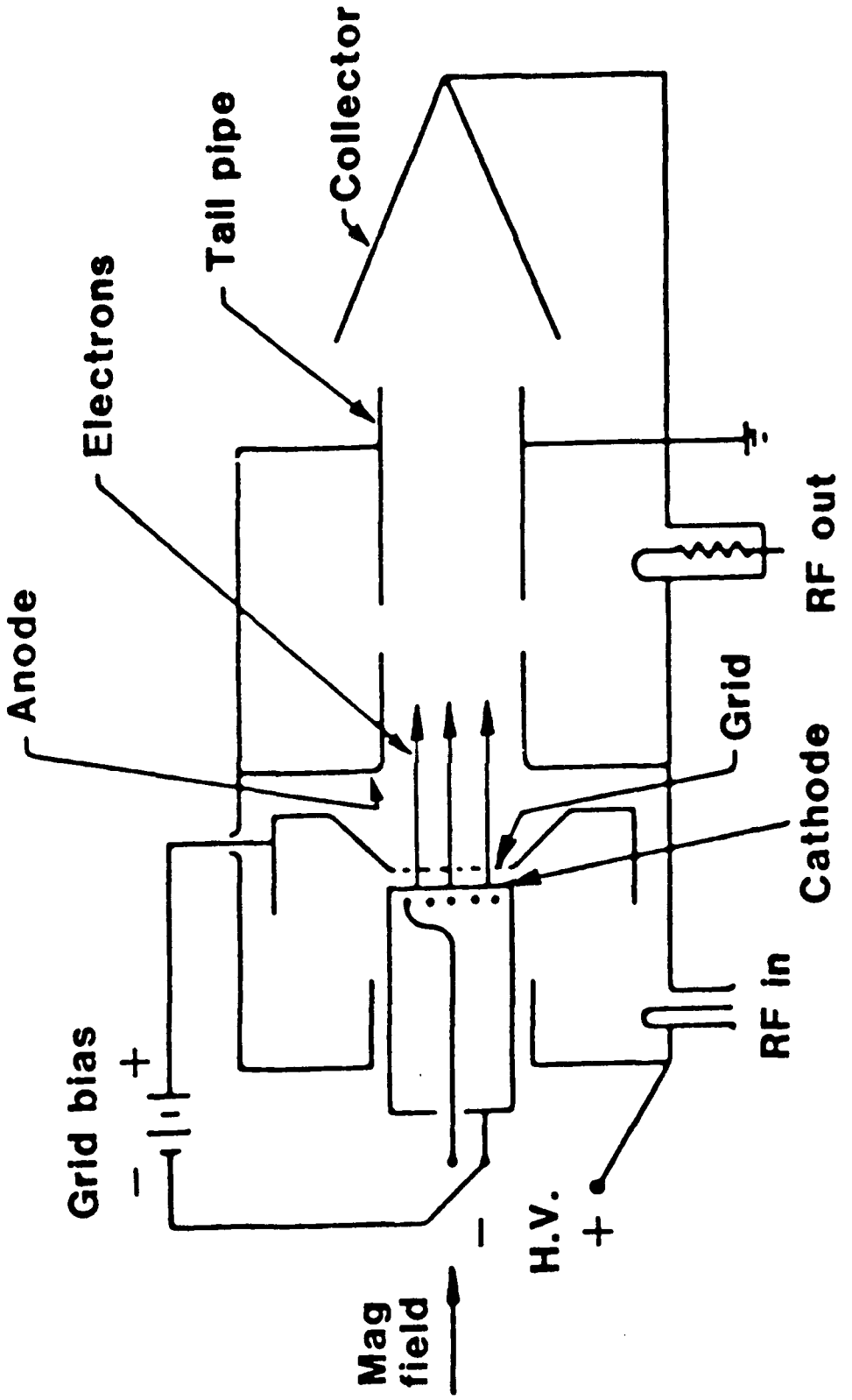

Figure A-9. Klystrode Schematic (from Donald H. Priest and Merrald B. Shrader, Proc. IEEE, Nov. 1982.) c 1982 IEEE

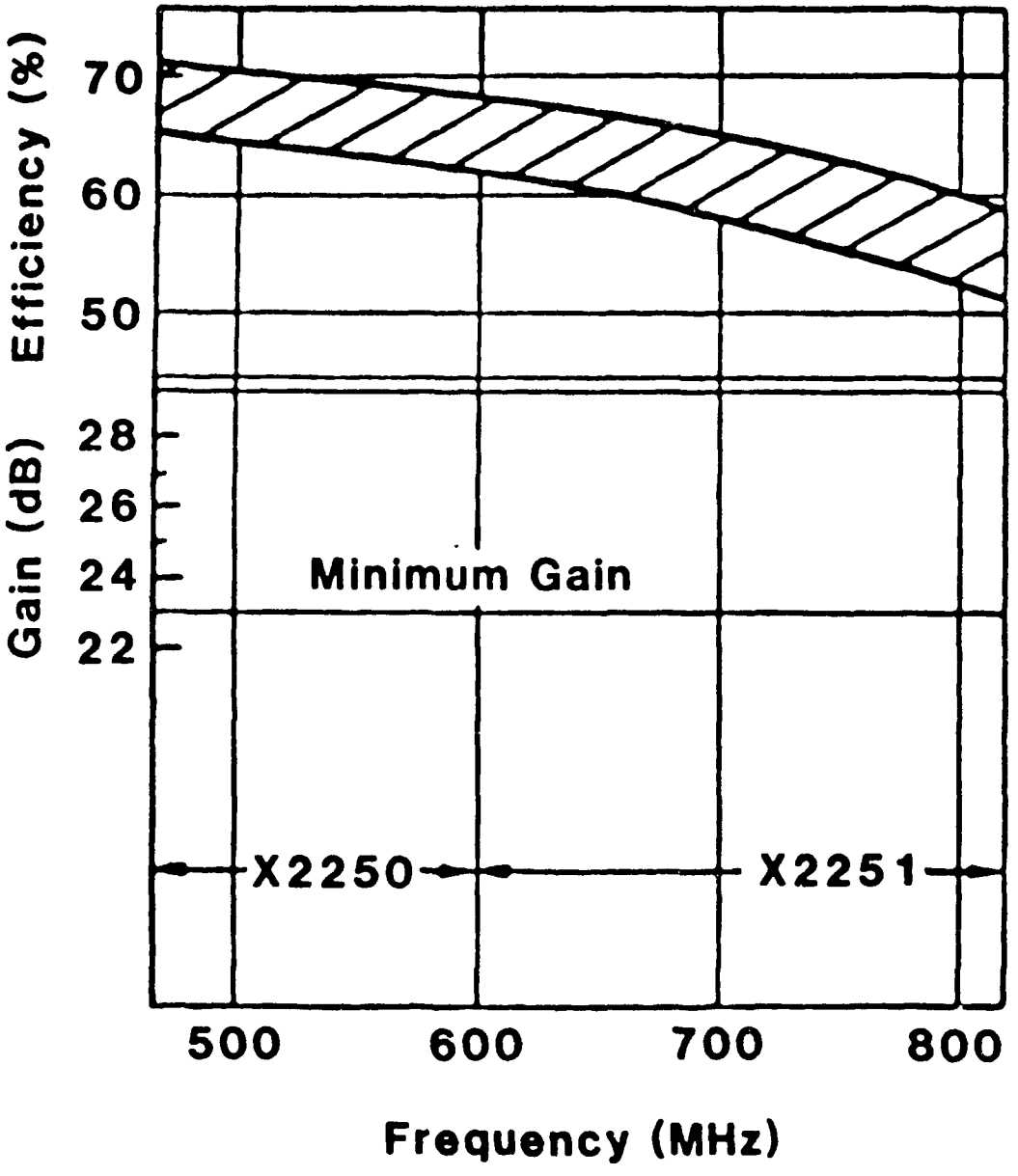

Figure A-10. Klystrode Efficiency and Power Gain versus Frequency (Courtesy Varian Eimac)

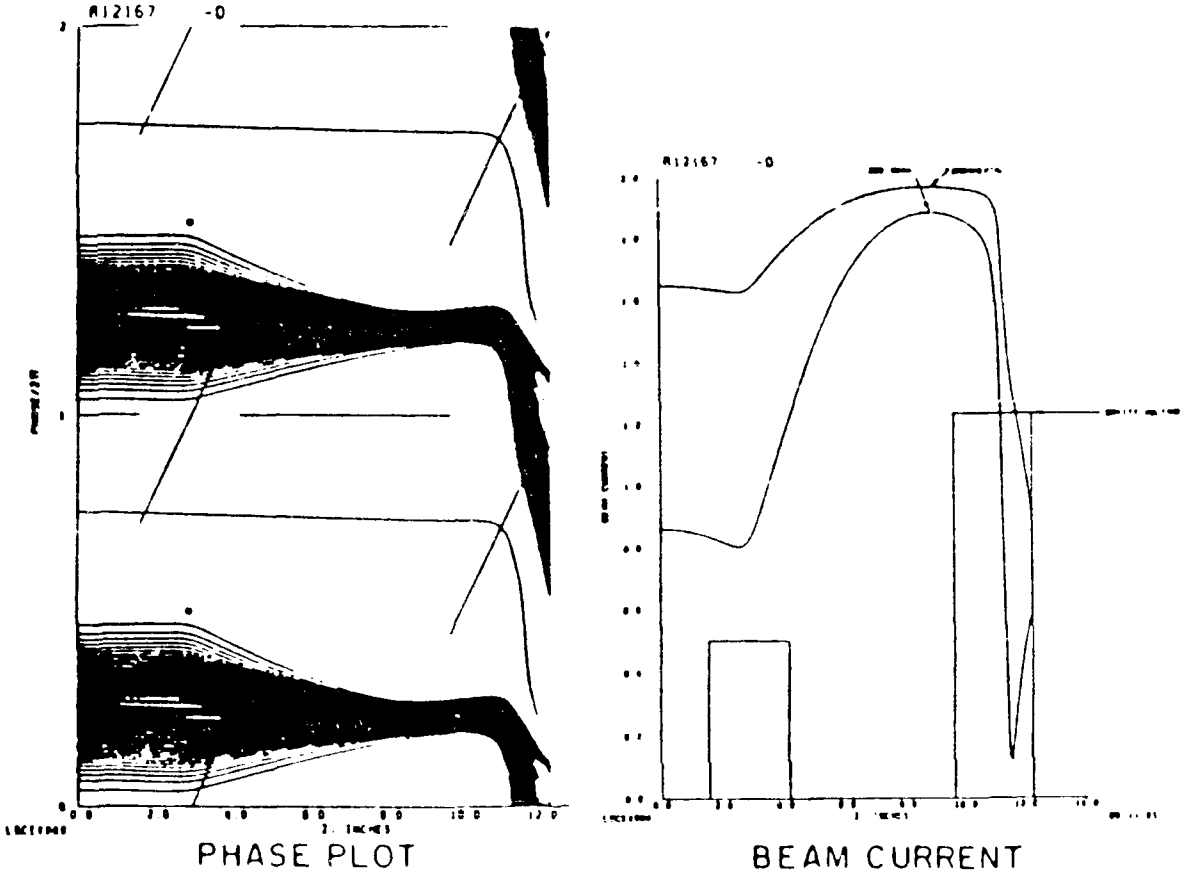

Figure A-11. Effect of Inductively Tuned Cavity on Electron Bunching (from M. Shrader, D. Preist and B. Gaiser, Technical Digest, 1985 IEDM) c 1985 IEEE

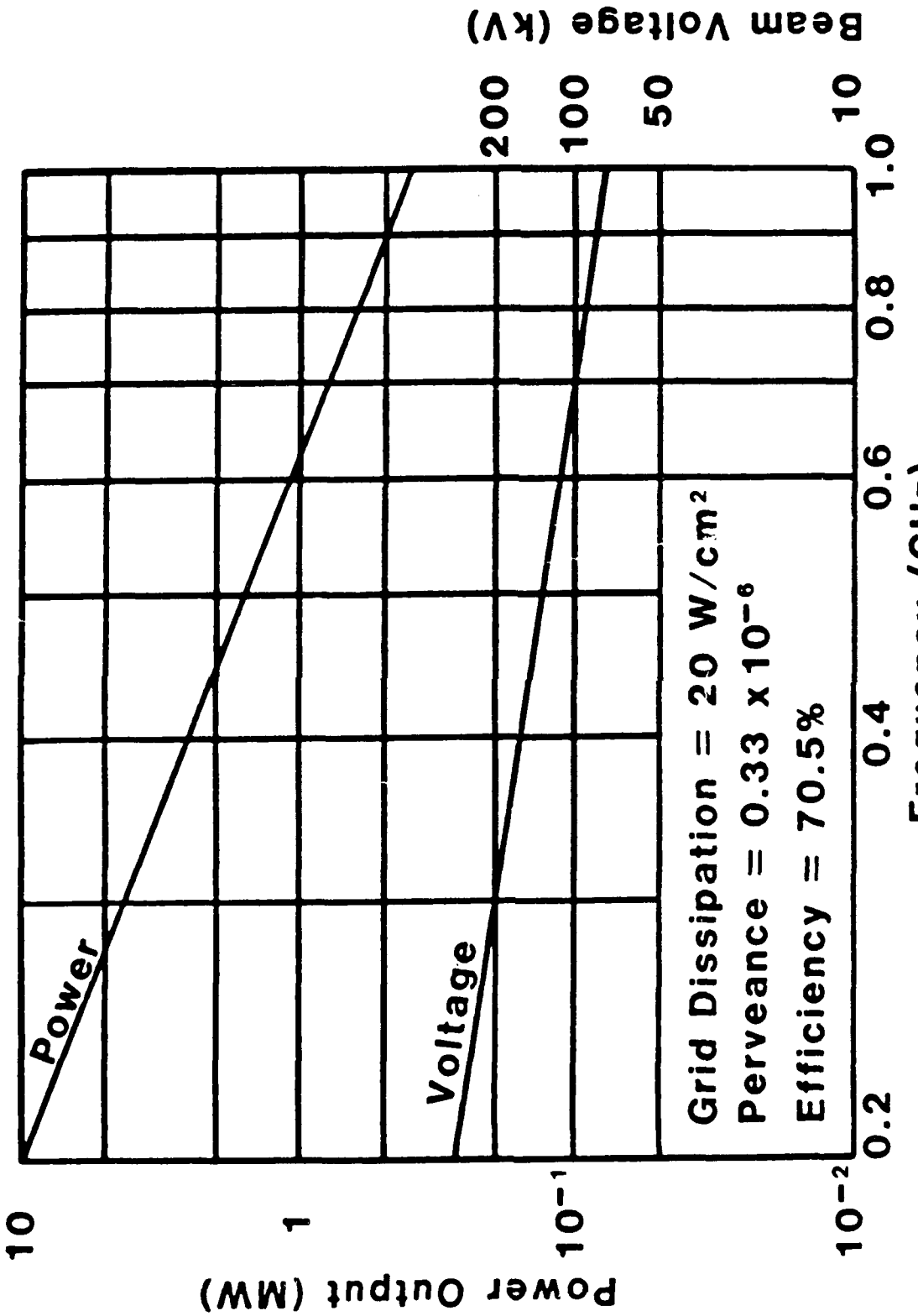

Figure A-12. Projected Klystrode Performance
(from M. S. Shrader, D. Preist and B. Gaiser,
Technical Digest 1985 IEDM) c 1985 IEEE

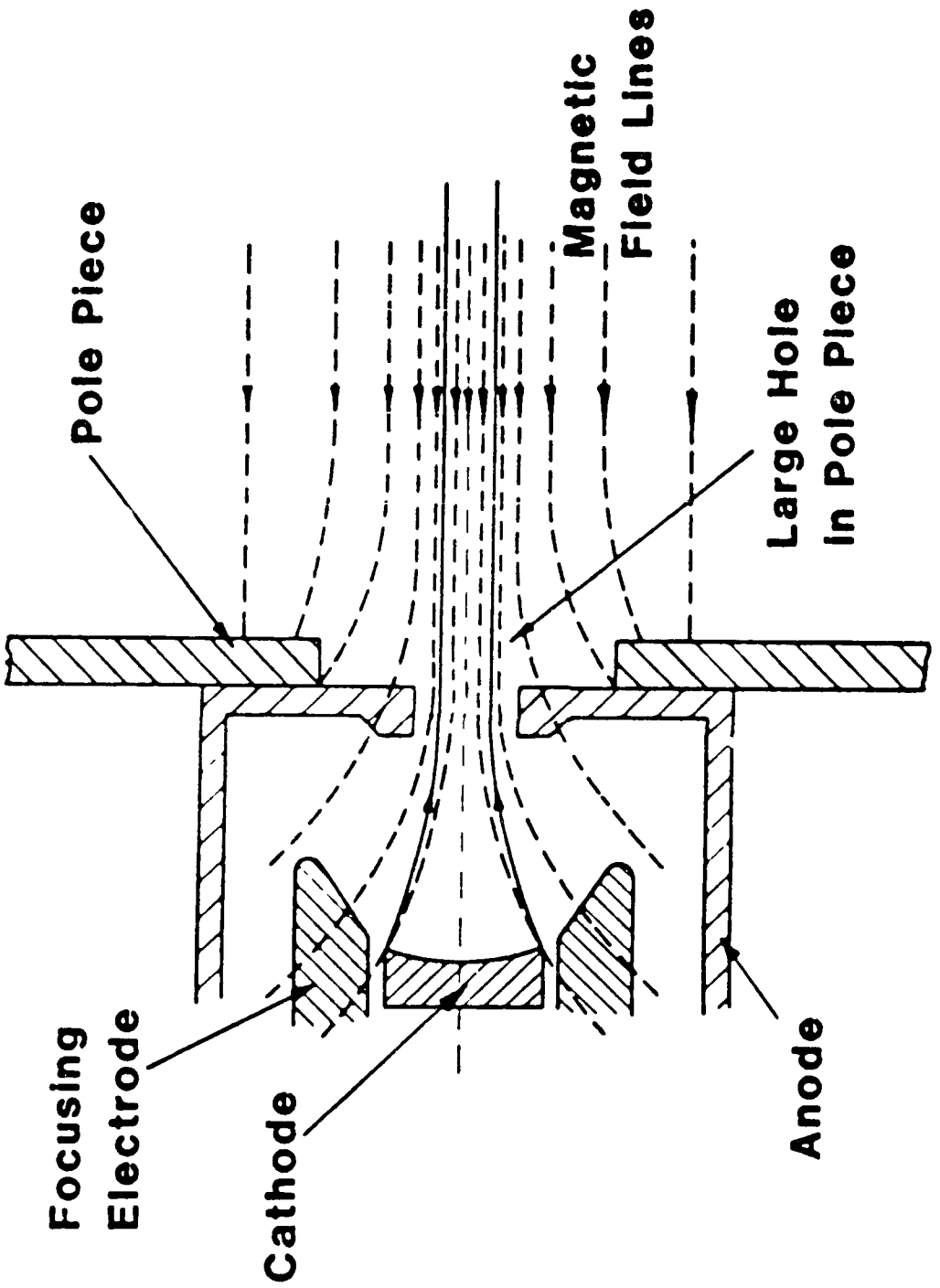

Figure A-13. Pierce Electron Gun and Magnetic Circuit Configuration for Launching a Confined Electron Beam (from Power Travelling-Wave Tubes by J. F. Gittins, Published 1965 by American Elsevier Publishing, Inc.)

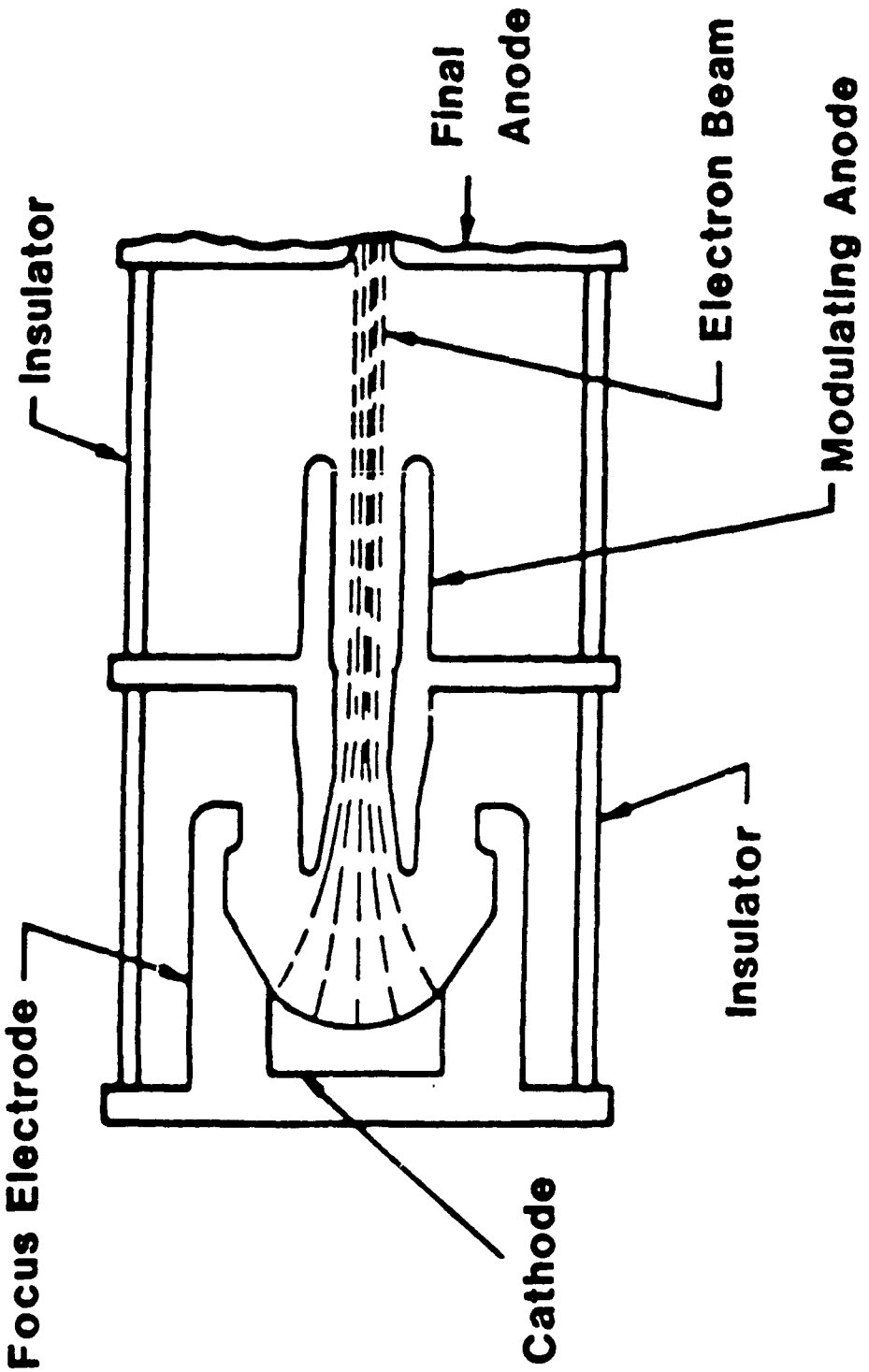

Figure A-14. Modulating Anode Gun (from Armand Straprans, et al., Proc. IEEE, March 1973.) c 1973 IEEE

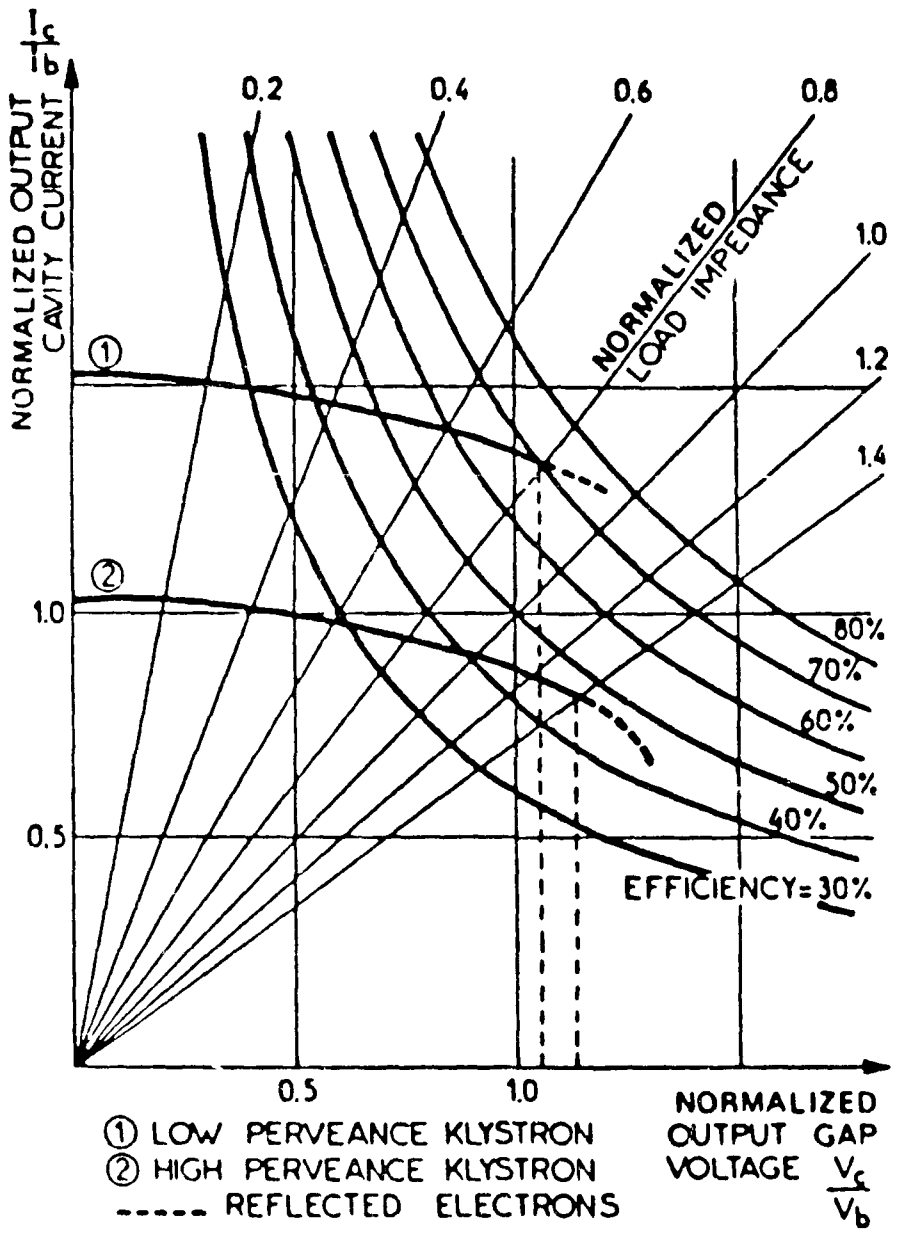

Figure A-15. Output Cavity Characteristics Curve (from C. Bastien, G. Faillon and M. Simon, Technical Digest, 1982 IEDM) c 1982 IEEE

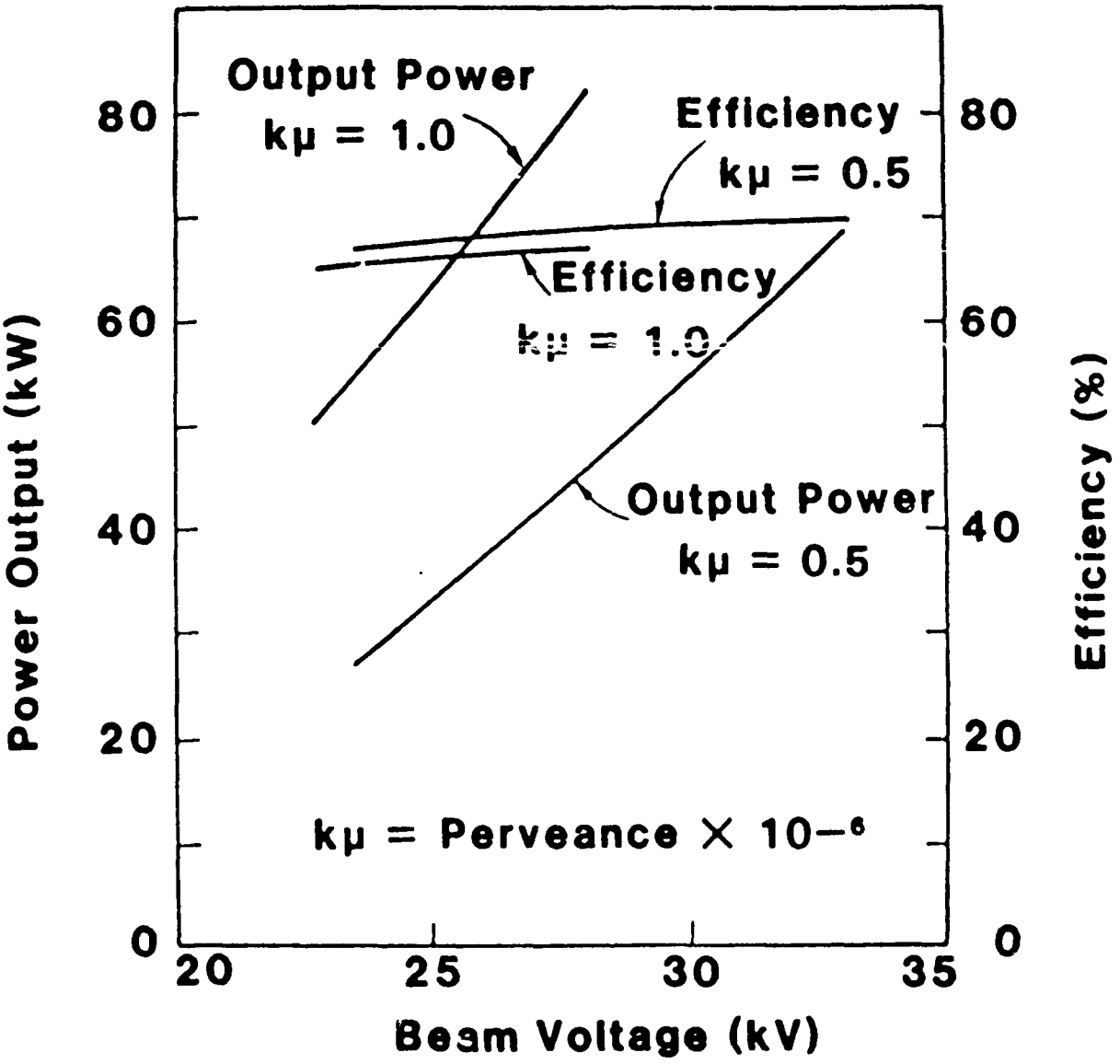

Figure A-16. Performance of X-3074B High-Efficiency Klystron (from Armand Staprans, et al., Proc. IEEE, March 1973.) c 1973 IEEE

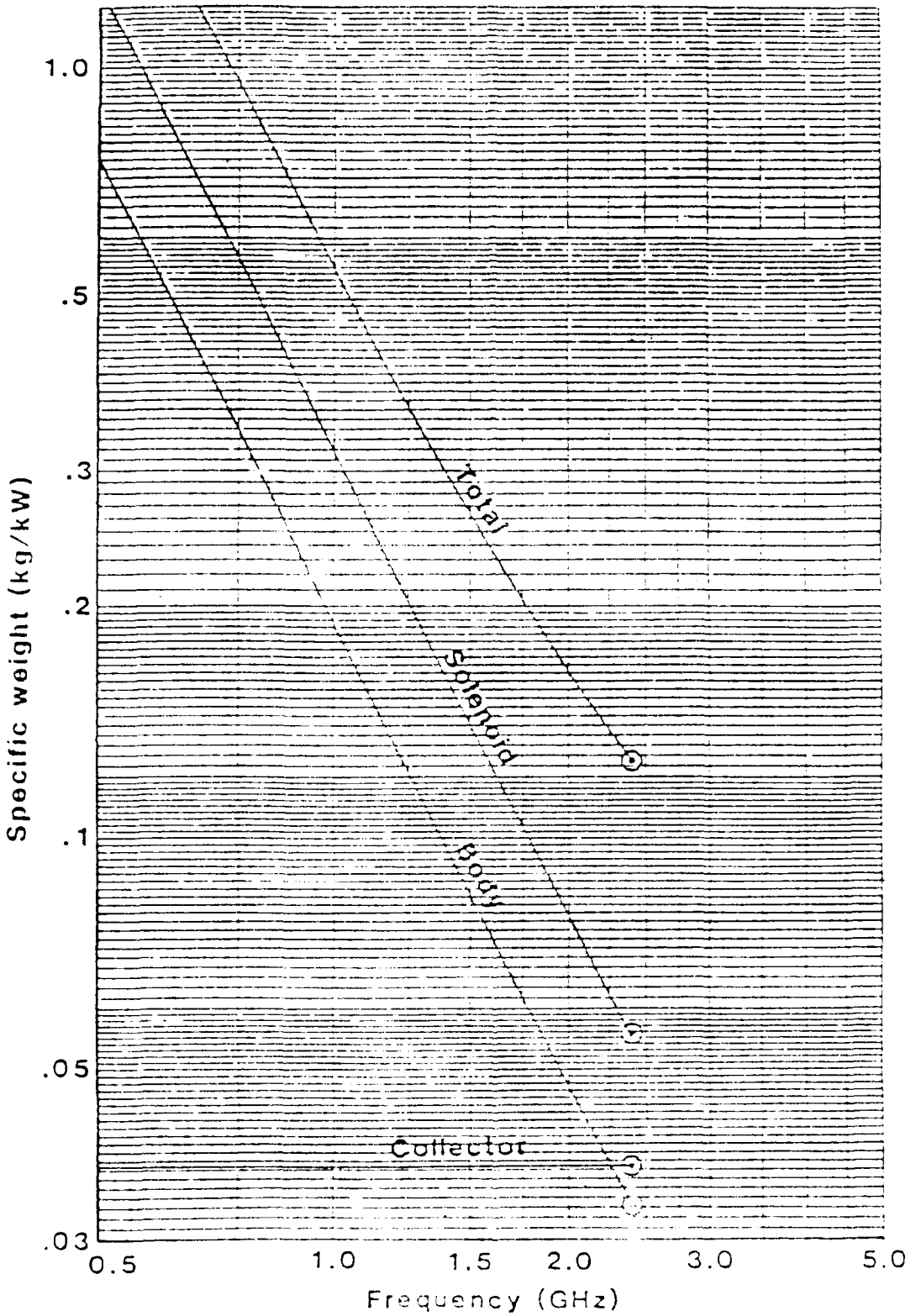

Figure A-17. Scaling of Klystron Weight with Frequency

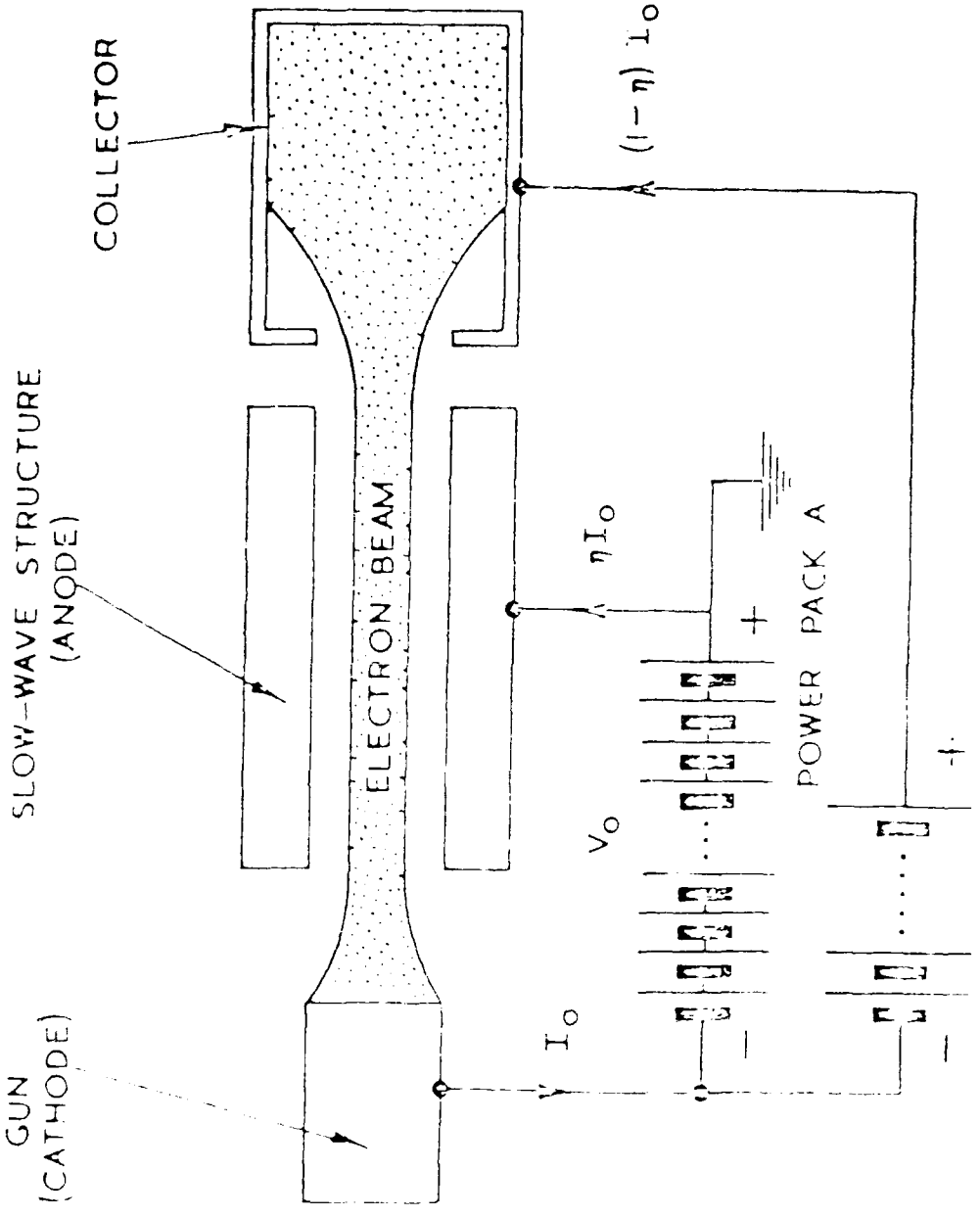

Figure A-18. Circuit for Depressed Collector Operation

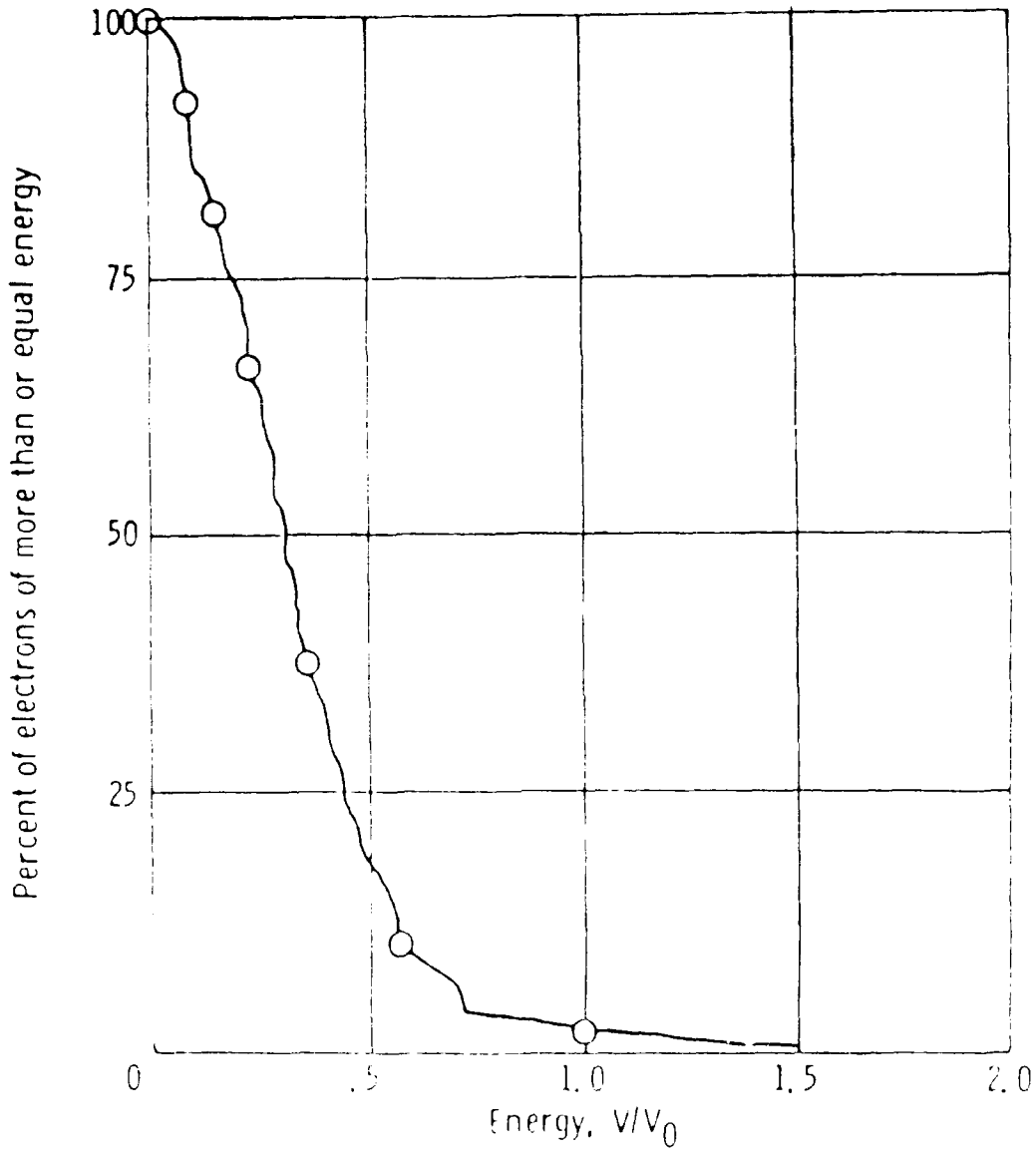

Figure A-19. Energy Distribution in the Spent Beam of a UHF Klystron (from H. G. Kosmahl, Proc. IEEE, November 1982)

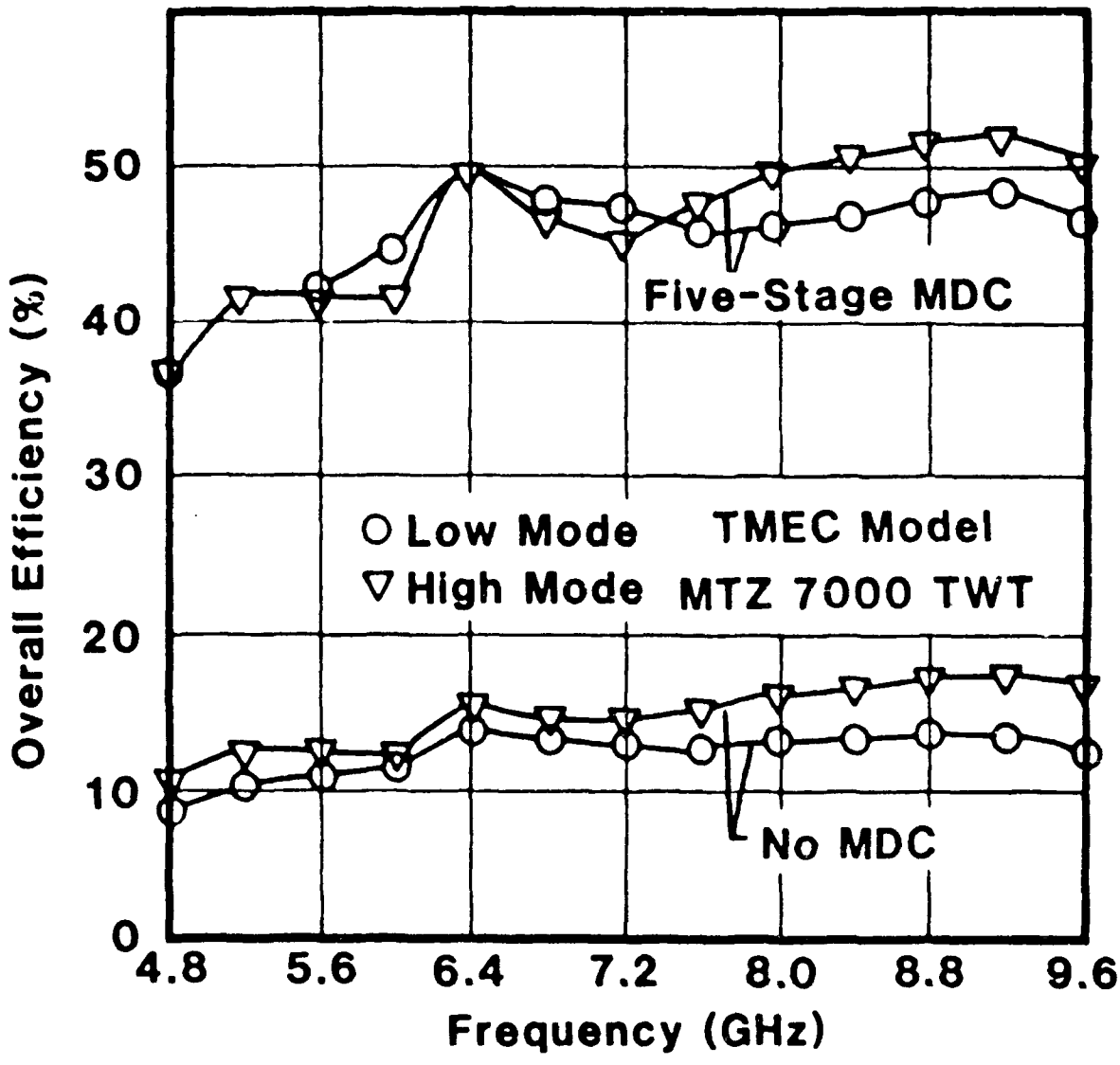

Figure A-20. Overall Efficiency of a Dual-Mode ECM Helix TWT with and without a MDC (Adapted from H. G. Kosmahl, Proc. IEEE. November 1982.)

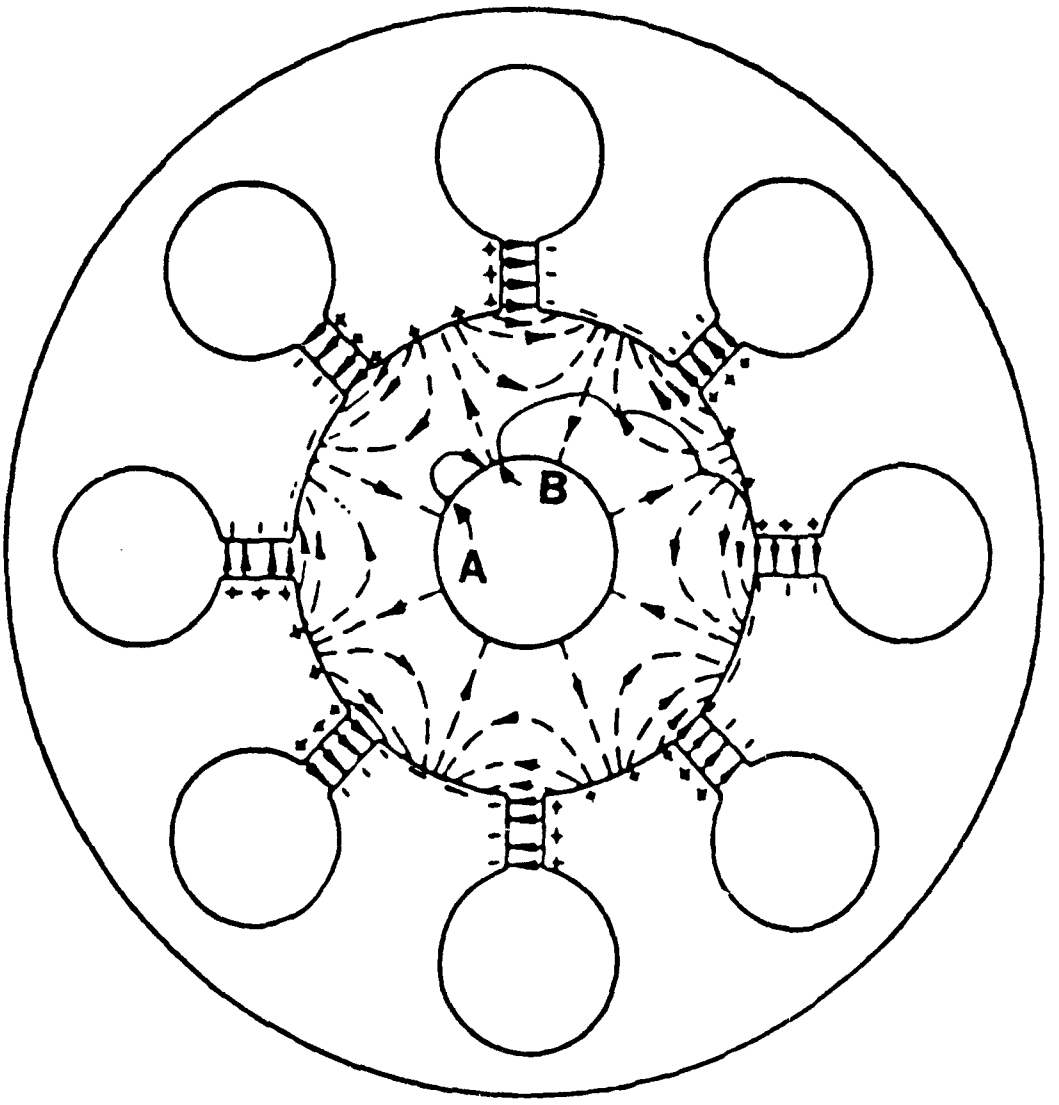

Figure A-21. Basic Configuration of Crossed-Field Tube (magnetron) (from J. Skowron, Proc. IEEE, March 1973.) c 1973 IEEE.

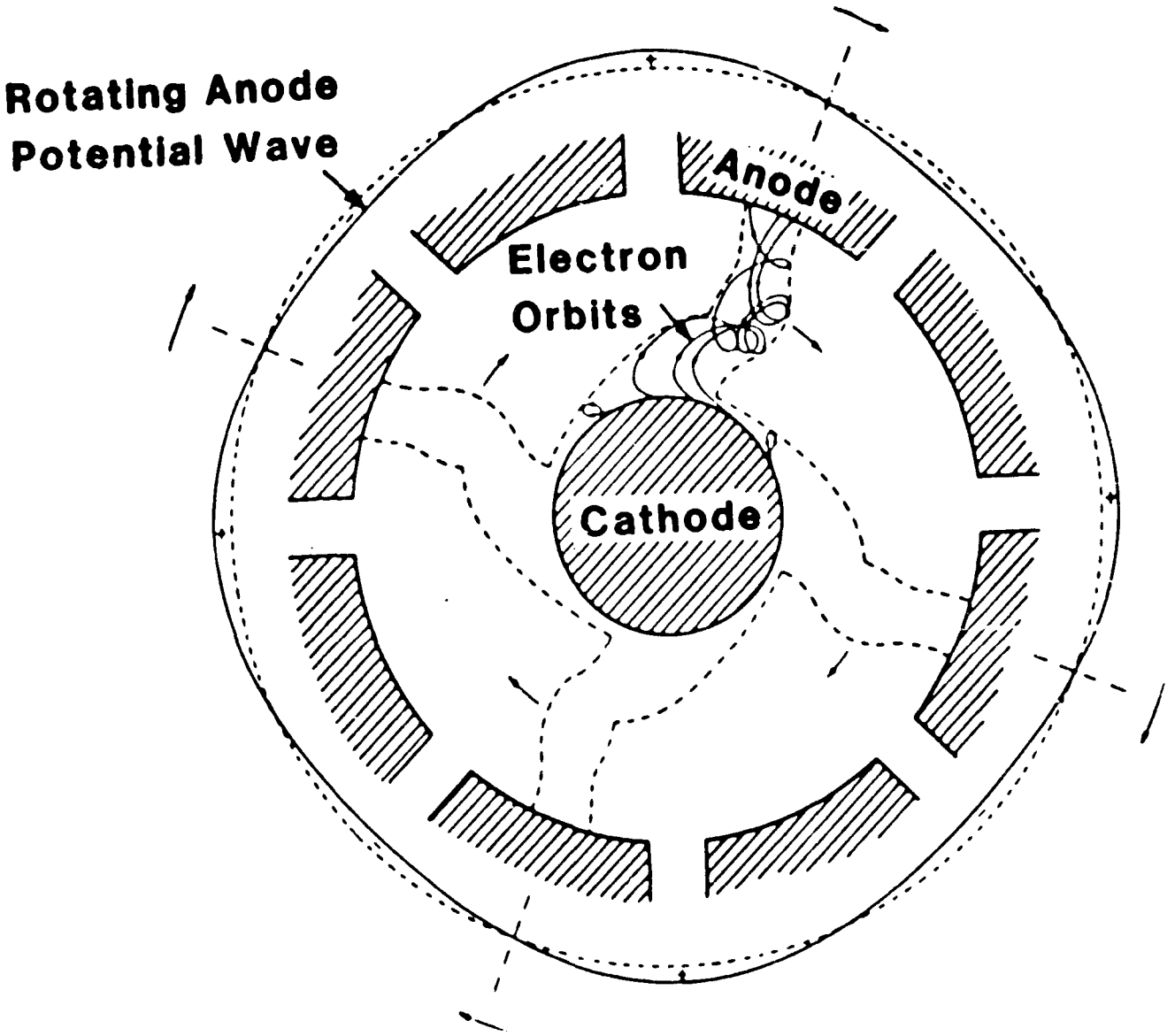

Figure A-22. Paths Followed by Electrons in a Magnetron (from Microwave Magnetrons by George B. Collins, Copyright 1948 by MCGraw-Hill, Inc.)

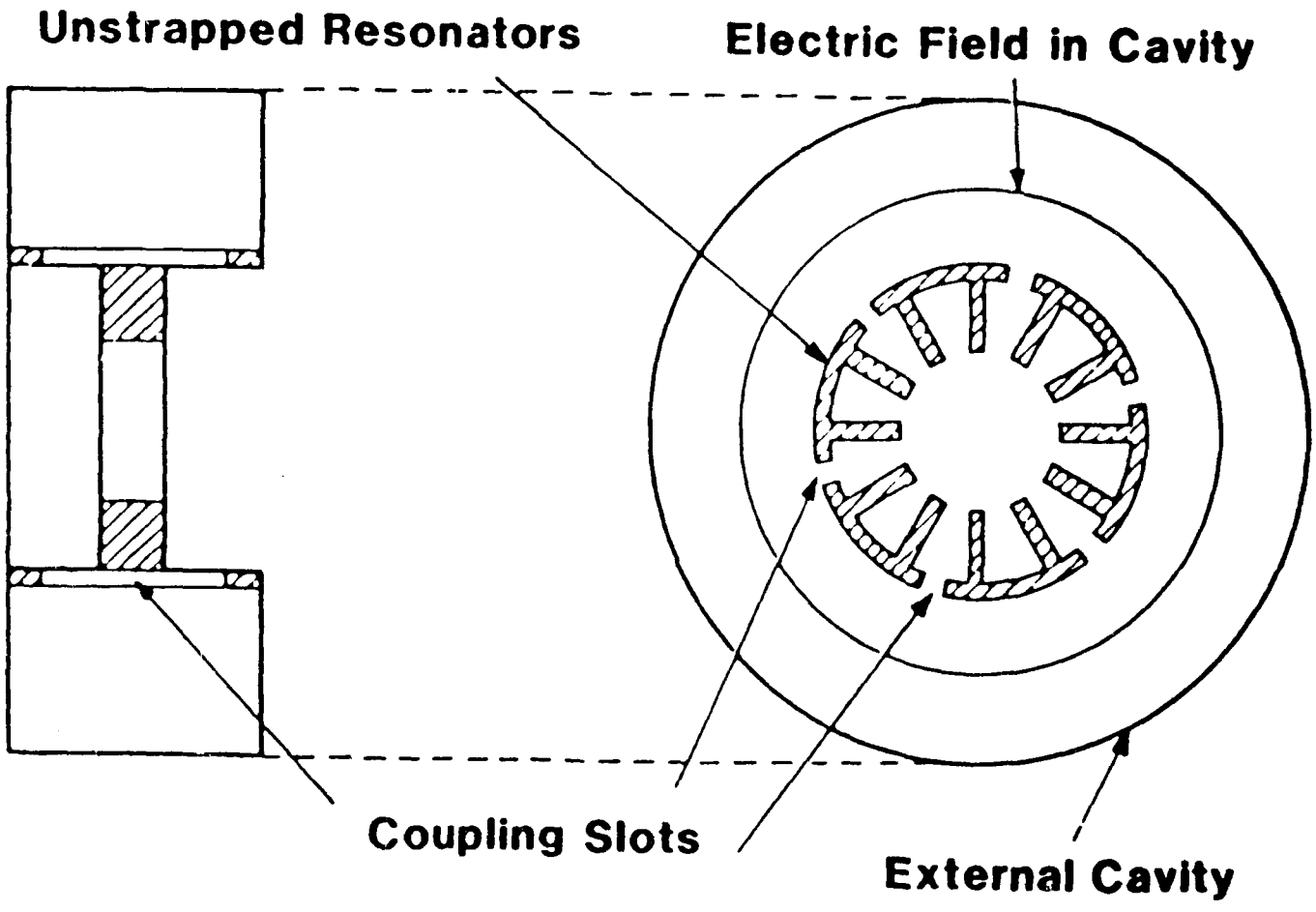

Figure A-23. Spoke-like Electron Cloud in Eight-Cavity Magnetron (from H. A. H. Boot and J. T. Randall, IEEE Trans. Electron Devices, July 1976) c 1976 IEEE

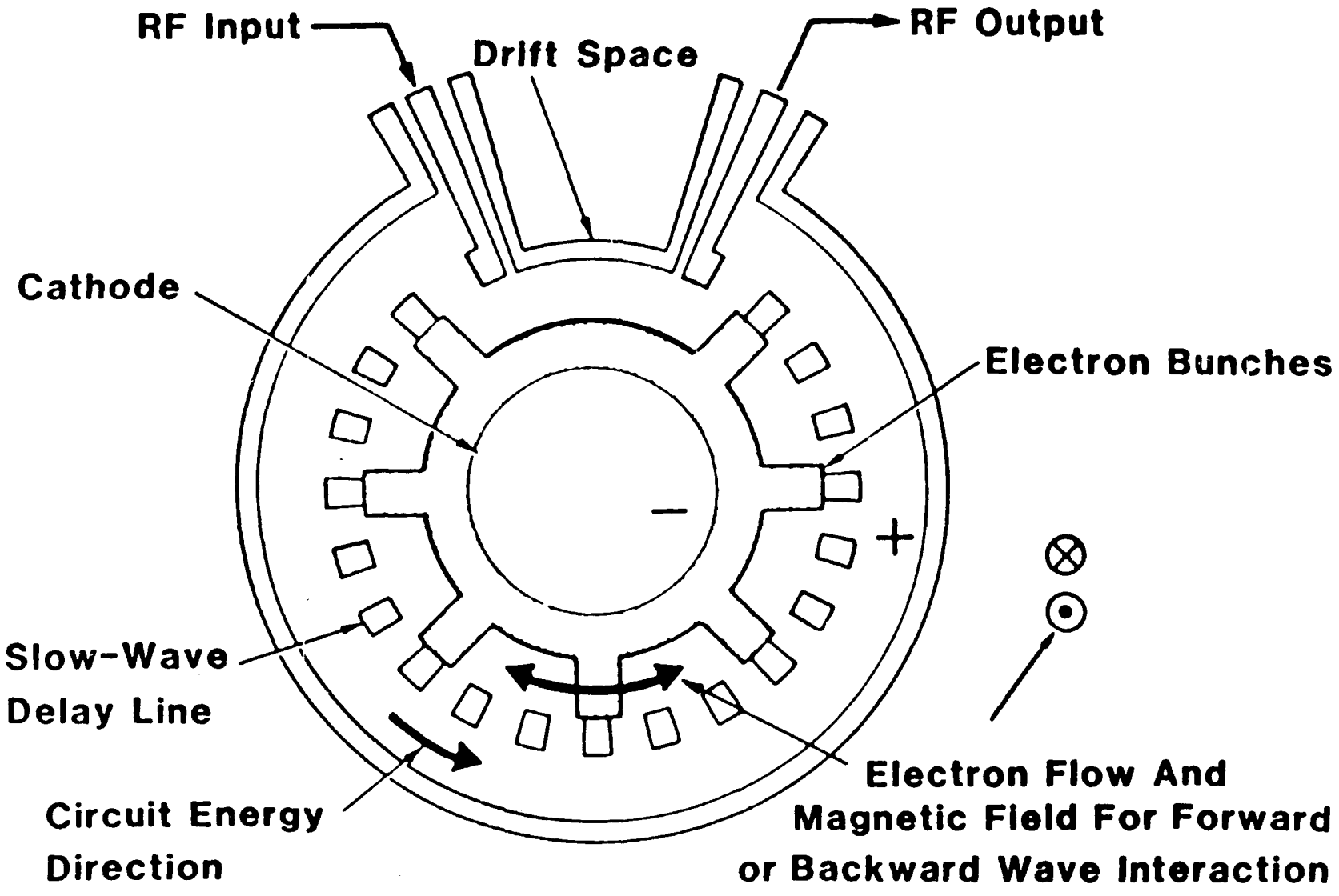

Figure A-24. Basic Configuration of Crossed-Field Amplifier (from J. Skowron, Proc. IEEE, March 1973.) c 1973 IEEE.

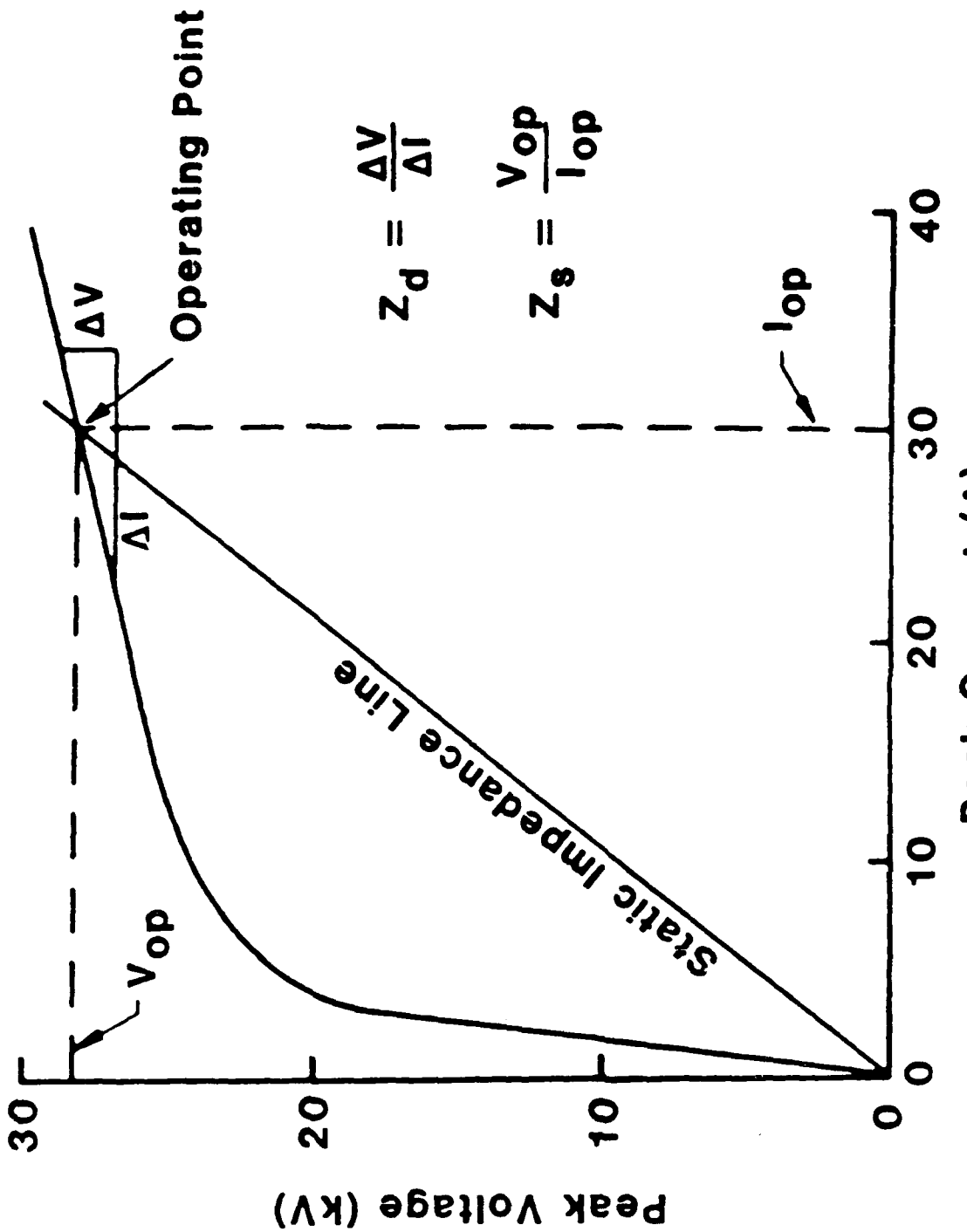

Figure A-25. Voltage-Current Characteristics of a CFA (from Microwave Tube Manual by Varian Associates, Air Force Publication Number T.O. 00-25-251, October 1979.)

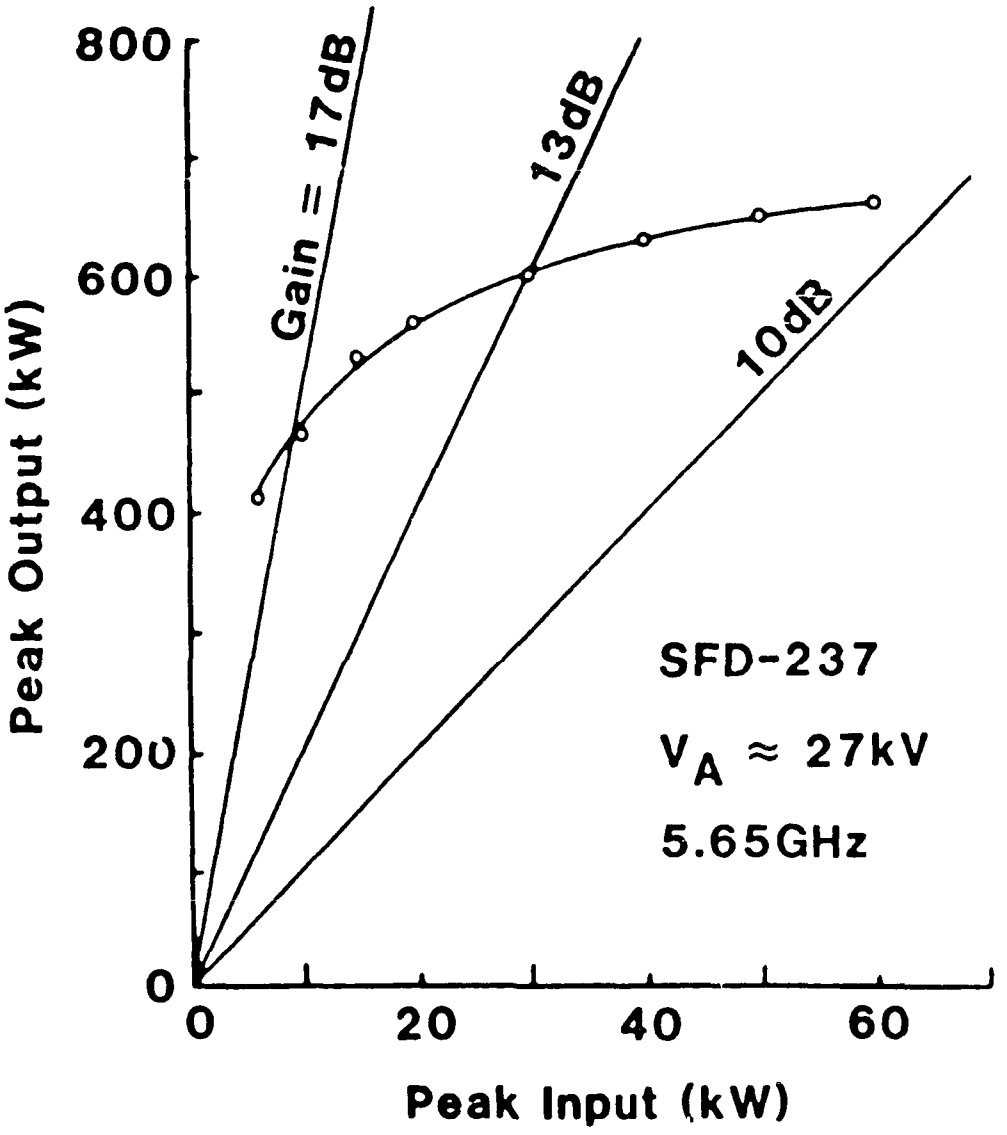

Figure A-26. Compression Curve for CFA (from Microwave Tube Manual by Varian Associates, Air Force Publication Number T.O. 00-25-251, October 1979)

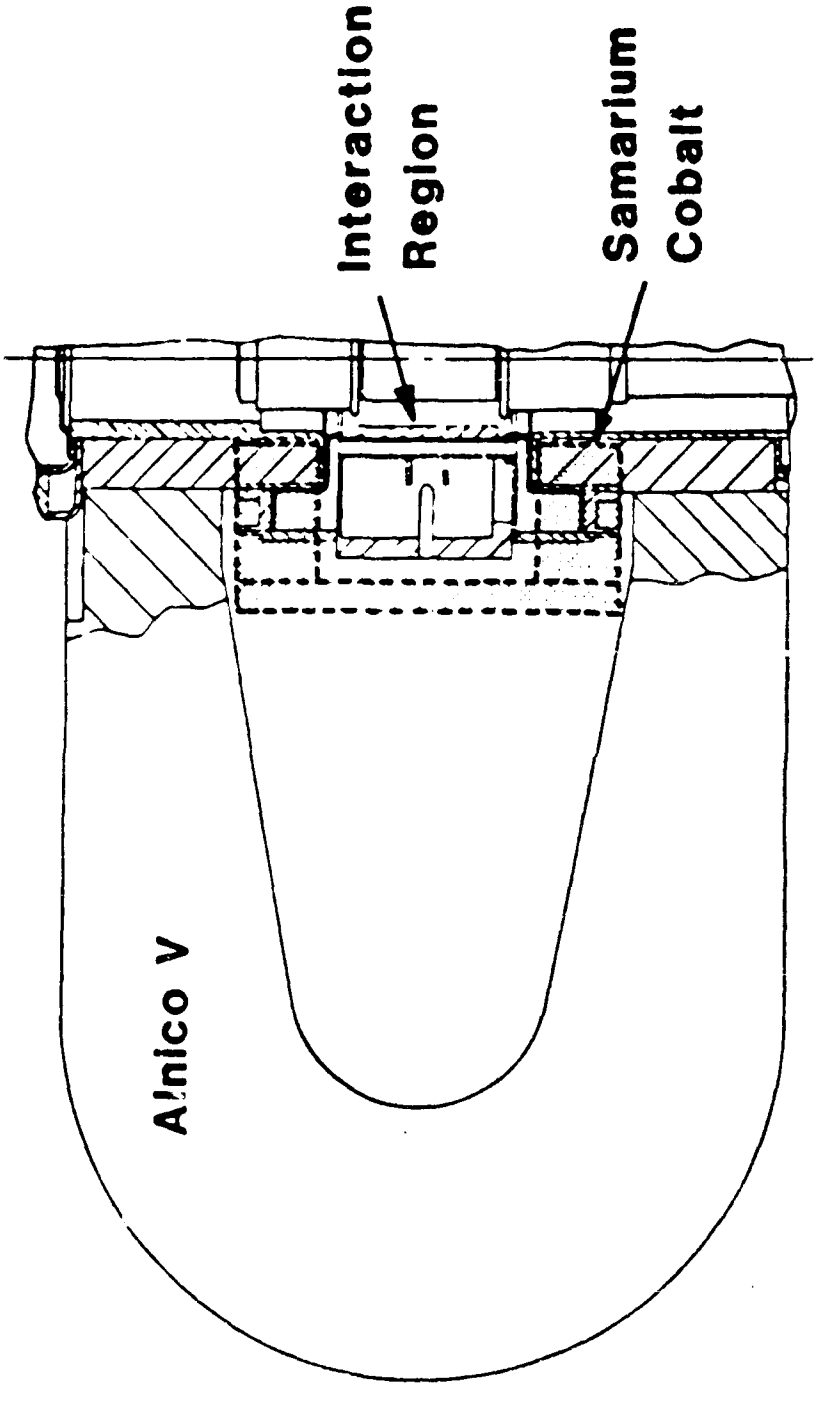

Figure A-27. Size Comparison Between Alnico V and Samarium Cobalt Magnets for a CFA (from J. Skowron, (MPTD), Raytheon Co., Workshop on High-Power, Space-Based Microwave Systems, Los Alamos, NM, March 1985.)

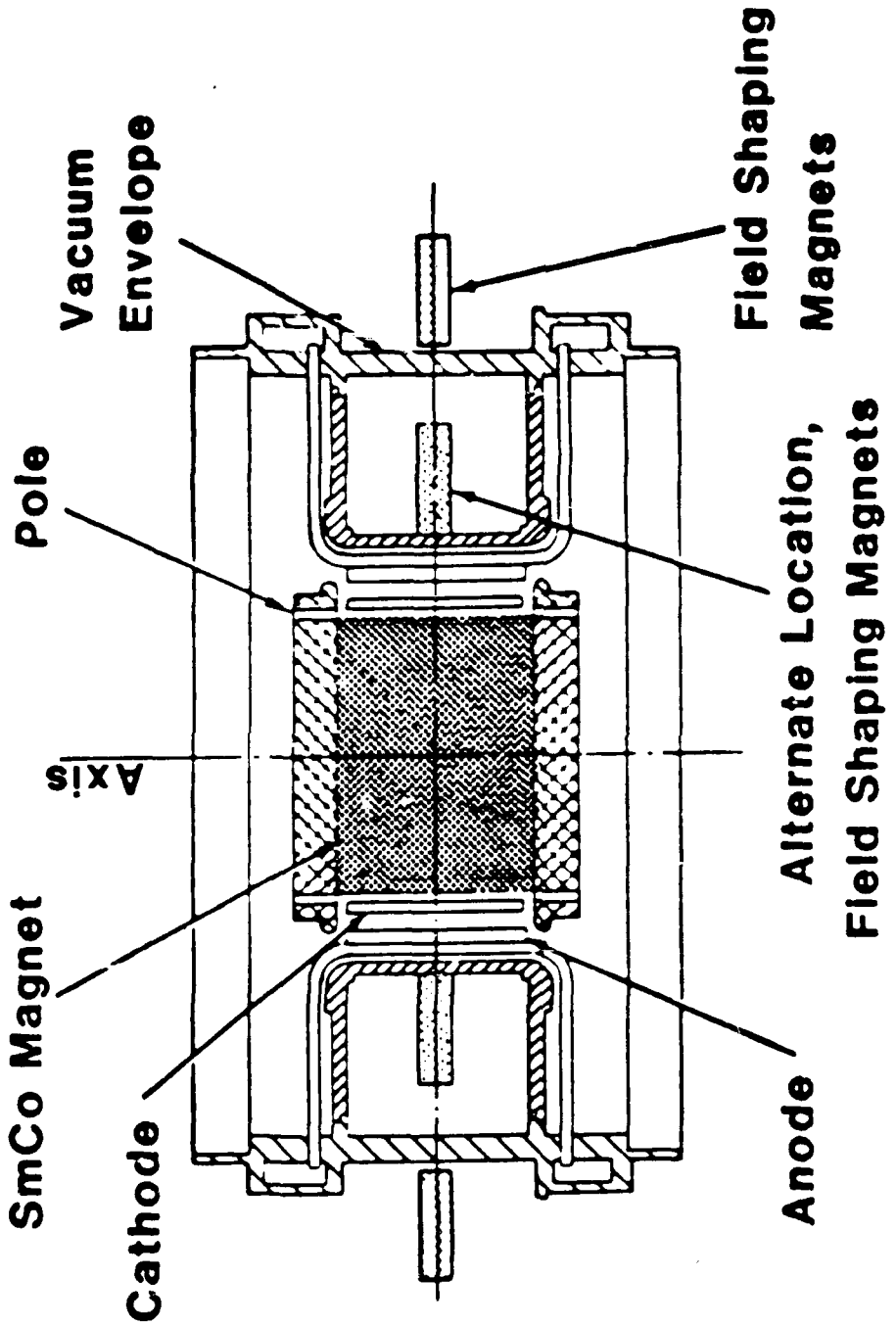

Figure A-28. Placement of Samarium Cobalt Magnet Inside the Cathode in a Cold-Cathode CFA (from J. Skowron, Proc. IEEE, March 1973.)
c 1973 IEEE

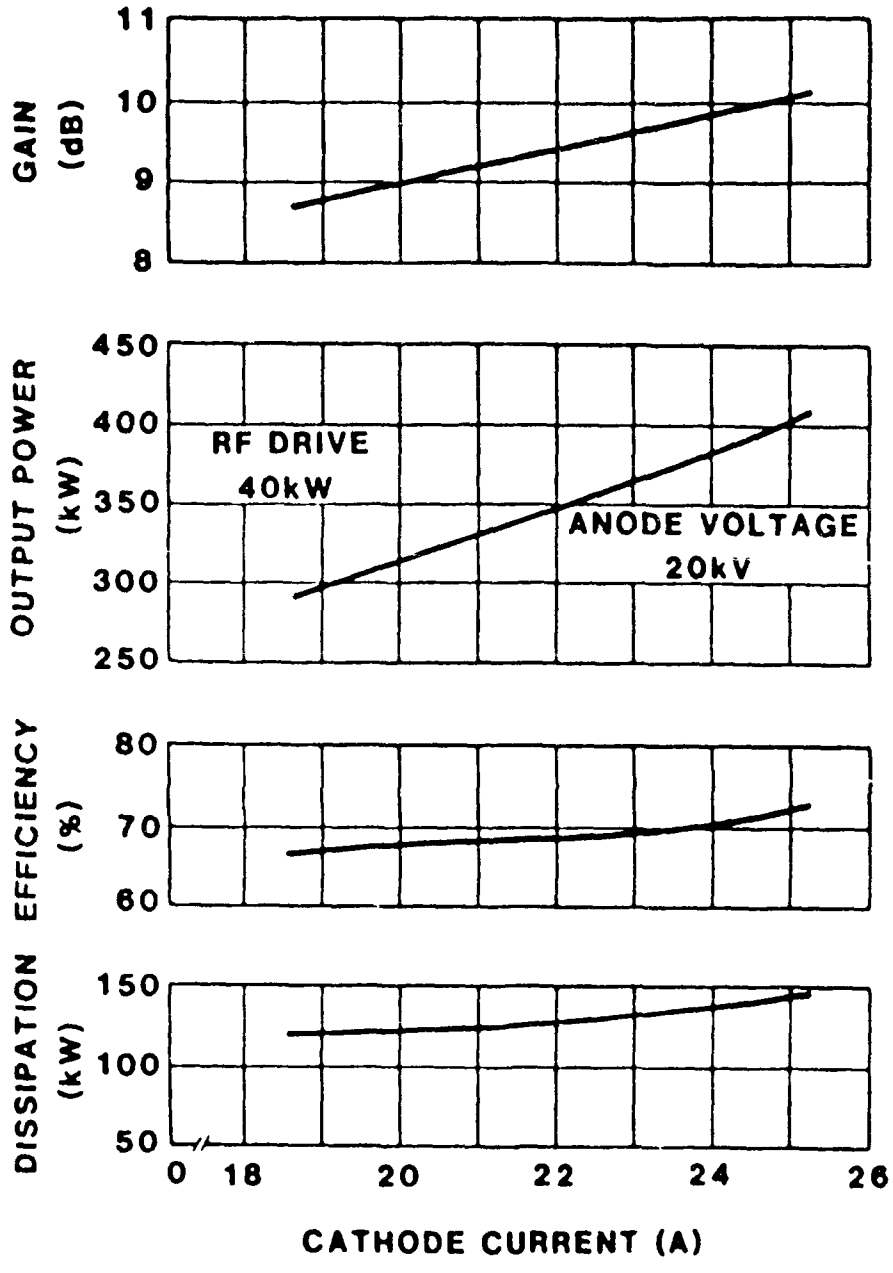

Figure A-29. Performance Characteristics of "Super Power" CW CFA (from J. Skowron, (MPTD), Raytheon Co., Workshop on High-Power, Space-Based Microwave Systems, Los Alamos, NM, March 1985.)

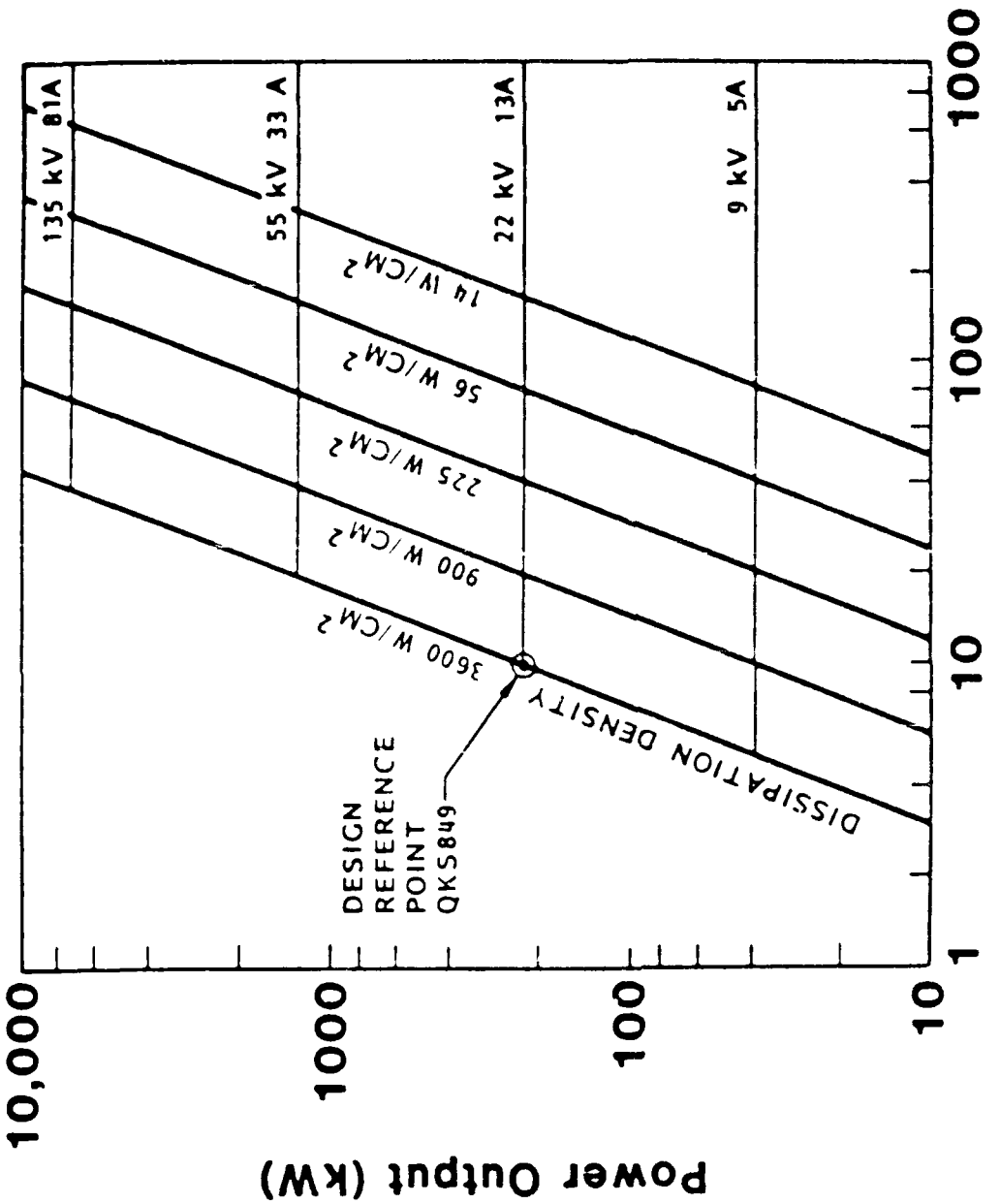

Figure A-30. Predicted Power Capabilities of CW CFAs Based on Anode Dissipation Power Densities (from J. Skowron, (MPTD), Raytheon Co., Workshop on High-Power, Space-Based Microwave Systems, Los Alamos, NM, March 1985.)